University of Alberta

Role of TG Lipases, Arylacetamide Deacetylase and Triacylglycerol Hydrolase, in Hepatitis C Virus Life Cycle

by

Mahra Nourbakhsh

A thesis submitted to the Faculty of Graduate Studies and Research
in partial fulfillment of the requirements for the degree of

Doctor of Philosophy
in
Experimental Surgery

Department of Surgery

Spring 2013
Edmonton, Alberta

Dedicated to

My Father

Dr. Majid Nourbakhsh

My Mother

Mehri Firouzi

Abstract

Hepatitis C virus (HCV) is a major cause of chronic liver disease, including liver steatosis, fibrosis, cirrhosis, and hepatocellular carcinoma. It has become apparent that the targeting of lipid droplets (LDs) by the HCV core protein and the Very Low Density Lipoprotein (VLDL) secretory pathway play important roles in the HCV lifecycle. VLDL is a triacylglycerol (TG) rich lipoprotein particle that acquires the majority of its fat cargo from the preformed TG that is stored in LDs. Therefore we hypothesize that during HCV infection the VLDL assembly/secretory process would be diverted in order to support productive viral infection. This possibility is intriguing since hepatic steatosis, characterized by hepatocellular accumulation of LDs, is a common clinical finding of HCV infection and impaired VLDL assembly/secretion characterized by hypobetalipoproteinemia is associated with chronic HCV infection.

We used Huh7.5/JFH-1 cell culture system to examine the relationship between HCV life cycle and VLDL secretory pathway. Using standard biochemical approaches, we have examined the key regulators of VLDL secretory pathway during HCV infection. In particular, the contribution of two putative TG lipases, arylacetamide deacetylase (AADAC) and triacylglycerol hydrolase (TGH) to the lipolytic mobilization of cellular TG stores for secretion with VLDL were examined. These studies demonstrate that the lipolysis of cellular TG and VLDL production were impaired in HCV infected cells during the early peak of viral infection. This was partially explained by an apparent deficiency for AADAC.

The re-introduction of AADAC to infected cells restored cellular TG lipolysis, indicating a role for HCV-mediated downregulation of AADAC in this process. Silencing of AADAC in naïve cells confirmed that endogenous AADAC indeed plays a role in the lipolysis of cellular TG stores and in the addition of lipid to nascent VLDL. TGH was absent from Huh7.5 cells and although its re-introduction to non-infected cells enhanced the mobilization of cellular TG for secretion with VLDL and VLDL production, it was not able

to restore the defective cellular TG lipolysis due to AADAC deficiency in infected cells. Finally, impaired production of HCV was observed with the AADAC knockdown cells, demonstrating a role for AADAC in the HCV lifecycle.

Acknowledgement

*I wish to thank **Dr. Norman Kneteman** and **Dr. Donna Douglas** for their supervision throughout the course of this project and preparation of this thesis.*

Special Thanks to Dr. Richard Lehner, Dr. Lorne Babiuk and Dr. Michael Houghton for their support, and critical comments.

*I wish to Thank **Mr. Jamie Lewis** and **Mr. Christopher Hao Pu**, for their assistance with the culturing of the cells and molecular biology aspects of this project.*

*I would like to thank **Mrs. Carolyn Harrison, Mrs. Chelcey Buck, Dr. Ali Alsaghir** and **Dr. Enhui Wei** for their help and great times we've had at Kneteman's lab.*

Table of Contents

List of Tables

Introduction

Paper 2

Appendix

List of Figures

Introduction

Paper 1

Paper 2

Conclusion

List of Abbreviations

AADAC	Arylacetamide Deacetylase
ACC	Acetyl CoA Carboxylase
ADRP	Adipocyte Differentiation Related Protein
AGPAT	Acylglycerol Phosphate Acyl transferase
ALF	Acute Liver Failure
ALT	Alanine Aminotransferase
AMPK	AMP-mediated Protein Kinase
Apo	Apolipoproteins
ARDS	Adult Respiratory Distress Syndrome
ATGL	Adipocyte triglyceride lipase
BSA	Bovine Serum Albumin
CE	Cholesterol Ester
CES-1	Carboxylesterase-1
CHC	Chronic Hepatitis C
Chol	Cholesterol
ChREBP	Carbohydrate Regulatory Element Binding Protein
CLD	Cytosolic Lipid Droplets
CLDN	Claudin
CM	Chylomicron
CoA	Coenzyme A
CPT	Carnitine Palmitoyl Transferase
DG	Diacylglycerol
DGAT	Diacylglycerol Acyl Transferase
DM	Diabetes Mellitus
ECM	Extracellular Matrix
EL	Extracellular loop
ER	Endoplasmic reticulum
ETR	End of Treatment Response

EVR	Early virological Response
FA	Fatty Acid
FAS	Fatty Acid Synthase
FBS	Fetal Bovine Serum
GAG	Glycose aminoglycans
GFP	Green fluorescent protein
GPAT	Glycerol phosphate Acyl Transferase
HCC	Hepatocellular Carcinoma
HCV	Hepatitis C Virus
HCVcc	HCV cell culture derived
HCVpp	HCV pseudoparticle
HIV	Human Immunodeficiency Virus
HL	Hepatic Lipase
HSC	Hepatic Stellate Cells
HSL	Hormone Sensitive Lipase
HSPG	Heparan Sulfate Proteoglycans
IDL	Intermediate Density Lipoprotein
IDU	IV Drug User
IFN	Interferon
IRES	Internal Ribosomal Entry Site
ISG	Interferon Stimulated Genes
JFH	Japanese Fulminant Hepatitis
LCS	Low Complexity Sequence
LD	Lipid Droplets
LDL	Low Density Lipoprotein
LLD	Luminal Lipid Droplets
LPAAT	Lysophosphatidic Acid Acyl transferase
LPL	Lipoprotein Lipase
LRP	LDL-receptor Related protein

LVP	Lipo-viral particle
LXR	Liver X receptor
MG	Monoacylglycerol
MGAT	Monoacylglycerol Acyl Transferase
MMP	Matrix Metalloproteinase
MODS	Multi Organ Dysfunction Syndrome
MTP	Microsomal triglyceride transfer protein
NASH	Non-Alcoholic Steatohepatitis
NAT	Nucleic Acid Test
NPC1L1	Neimann-Pick-C1-Like-1
OA	Oleic Acid
ORF	Open Reading Frame
PAP	Phosphatidic Acid Phosphatase
PDI	Protein Disulfide Isomerase
PEG	Polyethylene Glycol
PI3K	Phosphatidyl inositol -3 kinase
PKA	Protein Kinase A
PKR	Protein Kinase R
PUFA	Polyunsaturated Fatty Acid
ROS	Reactive Oxygen Species
RVR	Rapid Virological Response
RXR	Retinoid X receptor
SCAP	SREBP Cleavage Activating Protein
SIRS	Systemic Inflammatory Response Syndrome
SP	Signal Peptidase
SPP	Signal Peptide peptidase
SR-B1	Scavenger Receptor B1
SRE	Sterol Regulatory Element
SREBP	Scavenger Regulatory Element Binding Protein

SVR	Sustained Virological Response
TE	Thioesterase
TG	Triacylglycerol
TGH	Triacylglycerol hydrolase
TIMP	Tissue Inhibitor of Matrix Metalloproteinase
TIP 47	Tail Interacting Protein 47
TMD	Transmembrane domain
VCAM-1	Vascular Cells Adhesion Molecule-1
VLDL	Very Low Density Lipoprotein

Chapter 1: Introduction

A. Epidemiology, Clinical manifestation, Diagnosis and Treatment of Hepatitis C Virus

A. 1. Hepatitis C Virus, a Falaviviridae Virus

Hepatitis C virus (HCV), the major causative agent of chronic liver disease, is classified in the Hepacivirus genus within the Flaviviridae family. The Flaviviridae are a family of enveloped viruses, which have linear, single-stranded RNA genomes of positive polarity. This family is subdivided into several genera including; Flaviviruses (for example, Dengue, Yellow Fever, St. Louis Encephalitis and West Nile viruses), GB Viruses (GB agents and Hepatitis G virus), animal Pestiviruses (for example, Bovine Viral Diarrhea virus) and Hepciviruses (Hepatitis C virus).

Genetically, HCV isolates are greatly heterogeneous. In 1994, the first nomenclature system for HCV was introduced proposing the classification of HCV by phylogenetic methods into six genotypes (1). Genotypes differ in their nucleotides by 30-35%. Within HCV genotypes, a variable number of more closely related but genetically distinct subtypes (20-25% difference at the nucleotide level) can be defined (1). Since the original classification of HCV, it has been recognized that there is considerably greater diversity within some genotypes. This variability led to arbitrary classification decision that compromised the original assignment of HCV groups into genotypes and caused inconsistency with the nomenclature of HCV variants in published papers. These issues led to a new proposal for standardizing the nomenclature of currently known variants of HCV and the future assignment of newly discovered variants to subtypes and genotypes (2, 3).

A. 2. Epidemiology

According to World Health Organization (WHO) reports in 2007, about 130-170 million people were chronically infected with HCV and more than 350,000 people die from HCV-related liver disease each year. The incidence of HCV on a global scale is very difficult to estimate, because acute infection is generally asymptomatic and clinically not significant. Although HCV infection is a disease with a worldwide distribution, it is more endemic in some countries. In 2008, about 14.7% of Egyptians aged 15 - 59 were positive for HCV antibody (12.2% in female and 17.4% male) and 9.8% had active (chronic) disease (7.8%

female and 12.1% male). Parenteral therapy for schistosomiasis was considered as the prime suspect that explains the high prevalence of HCV in Egypt (4). Other endemic areas with a high prevalence of HCV are Bolivia, south-eastern of Asia, Mongolia and southern Italy (4).

In the United States, it is estimated that 2.7-3.9 million people were infected with HCV (1.3%-1.9% of US population) in 2007. In the same year, the estimated number of acute HCV was 2800 people and the estimated incidence rate of HCV (estimated number of new infection and acute clinical cases) was 17000 US residents (5). The peak prevalence of HCV in the United States of America (USA) occurred among persons aged 40–49 years, the majority of whom likely became infected in the 1970s and 1980s, when incidence was highest (6). The incidence of HCV in the USA peaked at age group of 25-39 years (5).

In Canada, recent estimates indicate that as of December 2007, approximately 242,500 Canadian had been infected with HCV (0.7% of total population) from which 7900 were estimated to be newly infected (7). The reported rates of acute hepatitis C declined from 2.5 per 100,000 population in 2004 to 1.6 per 100,000 in 2006 but since then there has been upward trend with reported rate of 2.2 per 100,000 population in 2008. The analysis of crude data revealed that this reversal of trend might be driven by increased incidence rate among females aged 15-24 and males aged 25-34 years (8).

A. 3. Transmission Routes

HCV is transmitted through contact of infectious blood to healthy non-contaminated blood. This primarily occurs through large or repeated percutaneous exposure to contaminated blood such as injection drug use, contaminated blood, blood products transfusion or contaminated organ transplantation (before availability of blood screening tests), needle accidents particularly in health care personnel and vertical transmission from infected mother to a neonate. Although very uncommon, sexual contact with infected HCV patients, sharing personal items such as razor blades and tattooing are other possible ways of transmission.

In general, the predominant method of transmission is sharing needles by injection drug users (IDUs). Midpoint prevalence estimates suggested that 64% of IDUs in Canada and 73.4% of IDUs in the USA had positive HCV antibodies in their blood (9). Incidence rate of HCV within IDUs cohort ranges from 10 to 37.3 per 100 persons per year (10-14). Eighty percent of injecting heroin addicts in Southern China acquire HCV infection in one year after starting heroin use (15). This rate is lower in the USA. In a study performed in

Baltimore, HCV prevalence quickly reached 80% within 2 years of injection drug use (16). In Chicago, 52% of addicts who began injecting more than 4 years ago, tested positive for HCV infection (17). In San Francisco, these rates were 63% and 78% in >5 and >10 years after starting drug abuse (18).

The risk of transmission of HCV by a single contaminated needle injury is about 3%, but could increase if the patient has high levels of viral load (19, 20). Transmission of HCV from infected health personnel to a patient is extremely rare. For example, when the surgeon's HCV status is unknown, the risk of HCV transmission during a single operation is 0.00018%±0.00002% (mean±SD). If the surgeon is HCV RNA positive, this risk equals 0.014%±0.002% (21).

Mother-to-infant transmission of HCV may be intrauterine, intrapartum, or postnatal. The rate of transmission from HCV RNA positive mothers to infants is about 4.3% (22). This rate is 2-4 fold greater in HIV positive (19.4%) and IDU women (8.6%) (22, 23). Although a number of studies suggest that some obstetric procedures like emergency cesarean section, amniocentesis, fetal scalp probe and rupture of membrane longer than six hours may increase the risk of vertical transmission (23, 24), the larger randomized controlled studies indicate that mode of delivery (elective versus emergency cesarean section versus vaginal delivery), amniocentesis, invasive fetal scalp probe appear not to be risk factors for transmission of HCV from mother to infant (25, 26). HCV RNA has been detected in the colostrum or breast milk of 40-51% of HCV infected mother (27, 28), but the rates of vertical transmission have been similar irrespective of breast-feeding practice in several large prospective studies conducted to date (25, 26, 29).

Before the availability of HCV screening tests, blood transfusion was one of the major routes of HCV transmission. Nowadays with a precise HCV detection test (Anti HCV EIA version 3 and Nucleic acid test) the residual risk of HCV transmission through blood (or blood product) transfusion is less than one in a million (30).

A. 4. Natural History of HCV Infection

In the majority of cases, acute HCV infection is not clinically significant but only 20-30% of individuals clear the virus spontaneously and approximately 70-80% of patients develop chronic infection, which is characterized by persistent viral replication and with substantial risk of severe chronic liver disease, fibrosis, cirrhosis and hepatocellular carcinoma (HCC) (31). In this part we will review some clinical disorders that are associated with HCV infection.

A. 4. 1. Acute HCV Infection

Acute HCV infection is defined as a new conversion from an HCV-RNA negative to an HCV-RNA positive status in blood. The acute phase is considered to be the first 6 months after exposure to HCV. During this period infection is spontaneously cleared or the individual develops chronic infection. HCV-RNA is detectable in the serum of almost all patients within 1–2 weeks after exposure (32, 33). Seroconversion (presence of anti HCV antibody) is detected after 2–6 months (window period) or later in certain risk groups such as patients with end stage renal diseases who undergo hemodialysis or HIV/HCV co-infected group (32, 33).

In the majority of cases, acute HCV infection is asymptomatic. Only 25–30% of patients develop symptoms, with a wide range of clinical presentations from flulike symptoms, fatigue and fever, to jaundice, dark urine, nausea, vomiting, loss of appetite, and right upper quadrant abdominal pain (31, 32, 34) as well as Alanine aminotransferase (ALT) levels at more than10–20 times the upper limit of normal (with or without a rise in bilirubin) (33). Presence of these symptoms accompanied by a positive HCV-RNA blood test is characteristic of acute HCV infections. If the symptoms of acute infection occur, they usually develop 6–8 weeks after HCV exposure and in most cases are self-limited (31, 32, 34). Only a slight minority of patients progress to fulminant hepatitis and acute liver failure (31, 32, 34).

A. 4. 2. Fulminant Hepatitis and Acute Liver Failure (ALF)

The term “Fulminant Hepatitis” was first introduced in 1970 to define a disorder, which is the result of severe liver injury with an onset of encephalopathy (due to inability of liver to clear ammonia and other waste products) within 8 weeks after symptoms appear in the absence of pre-existing liver disease (35). This terminology was later adjusted to acute liver failure (ALF) to accommodate other etiologies that are not inflammatory in origin (36). Hepatitis C is rarely implicated as the major cause of ALF in USA and Europe, but some cases have been reported in Japan and India (37). However an increased risk of ALF with the worst outcome has been noted in Chronic Hepatitis C (CHC) infected patients that were later infected with Hepatitis A and suggests the importance of Hepatitis A vaccination in CHC (38).

Clinical features of ALF are mostly related to decreased function of the liver. Loss of liver metabolic function such as gluconeogenesis (and hence hypoglycemia), decreases the capacity of liver for clearance of metabolic waste like ammonia (leading to encephalopathy) and lactate (leading to lactic acidosis), decreases liver synthetic capacity including synthesis of albumin (hypoalbuminemia) and coagulation factors

(coagulopathy) are some of the most important causes of mortality and morbidity in ALF. Furthermore, Systemic Inflammatory Response Syndrome (SIRS) and Multiple Organ Dysfunction Syndrome (MODS) are associated with ALF and lead to Adult Respiratory Distress Syndrome (ARDS), adrenal insufficiency and pancreatitis with high mortality rates (37). The rapidly progressive, severe multi organ dysfunction and hepatic encephalopathy associated with ALF, and other unpredictable complications, are accompanied with high mortality rates and necessitate intensive care as well as additional organ specific support. Hospitalization of patients in the intensive care unit with the addition of organ system support is used to improve the patient's condition for the possibility of hepatic regeneration or until the proper liver for emergency transplantation becomes available (37).

A. 4. 3. Chronic HCV Infection (CHC)

Approximately 75-85% (54-86% in different studies) of acutely HCV infected patients are not able to clear HCV and HCV-RNA is detectable 6 months after the first exposure (chronic HCV infection). The chronicity rate is affected by several factors including age of onset, gender, ethnicity and HIV/HCV co-morbidities. Fifty-six percent of individuals at age group 12-25 years develop chronic HCV infection, while this rate is 87% for those above 25 years old (39). Chronicity rates appear to be slightly lower in female versus male Caucasians versus African American (68% vs. 86%) (40, 41). Lower rates of spontaneous clearance of virus are expected in HIV/HCV co-infected patients (5-15%) (31, 42, 43).

Chronic HCV infection causes progressive liver damage in the majority of patients. It is mainly represented by portal mononuclear cell (lymphoid cells) infiltration, focal and bridge necrosis (fibrosis), and degenerative lobular lesion. The exact pathophysiology of the liver damage in CHC is not perfectly understood, but several possible mechanisms have been widely studied.

A. 4. 3. 1. Pathophysiology of Liver Damage in CHC: Local immune response to HCV has been considered as one of the major insults in pathophysiologic course of CHC. Aggregation of mononuclear cells (lymphocytes) in portal tracts is the main histological feature in CHC. Immunophenotyping of these lymphocytes showed significant CD4+ and CD8+ cells (44), which might be recruited by increased expression level of Vascular Cells Adhesion Molecule-1 (VCAM-1 or CD106) in sinusoidal cells (45). CD4+ cells play their general roles to orchestrate the immune response against HCV. Most of the infiltrating CD4+ in an active-CHC liver are T helper-1 (Th1), while there is a low frequency of HCV-specific CD4+ cells (Th1) in peripheral blood showing that HCV-specific CD4+ cells are

compartmentalized in the liver (46). Several studies have shown that the Th1 cytokine (IFN-γ and IL-2) were also up-regulated in the liver of these patients (46, 47). In contrast CD4+ Th2 cytokines messenger RNAs were not detected in the liver of patients with CHC but serum (peripheral) levels of Th2 cytokines (IL-10, IL-4) are dramatically increased suggesting that peripheral Th2 cells have an auto-regulatory roles that confines the Th1 response in the liver (48). The role of these Th1 cells is to activate macrophages and CD8+ cytotoxic T lymphocytes (CTL). The HCV-specific HLA I-restricted CD8+ CTL response is commonly detected in the liver of CHC patients and they act as the effector arm of adaptive immunity in HCV infection (49).

CTL cells target the hepatocytes mostly by activating death signals. Expression levels of the death ligands like perforin-granzyme B, Fas Ligand (CD95 ligand), and TRAIL are increased in these antigen-primed CTL cells (50, 51). They also secrete cytokines like TNF-α and IFN-γ, which may contribute to liver disease (52). Expression of Fas Ligand in CTL induces apoptosis in adjacent hepatocytes but this pathway did not depend on HCV antigen presentation and induces apoptosis even in non-HCV infected hepatocytes (50). Apart from this bystander killing of non-HCV infected hepatocytes, CTL cells also express TRAIL and activate TRAIL pathway which presumably only induces apoptosis in infected hepatocytes (50). Although granzyme B released by CTLs is another possible death ligand, it has been shown that hepatocytes are resistant to granzyme B mediated cell death and CTL killing of infected hepatocytes is perforin-granzyme B independent and its contribution in CHC is very unlikely (53, 54). In addition, cytokines like TNF-α secreted from CTL cells can bind to TNF-receptor 1 and induce apoptosis (50). IFN-γ secreted by CTLs or Th1 can activate Kupffer cells, which the later can kill neighboring cells via TRAIL and Fas ligand (55, 56). These death signals, TNF-α/TNF receptor-1, Fas/Fas ligand and TRAIL/TRAIL receptor-1 and -2 activate extrinsic pathway of apoptosis by induction of signaling complex which result in activation of Caspase-8 (57). Activated caspase-8 can directly recruit effector caspases (caspase-3, -6 and -7) or indirectly by cleavage of bid, which triggers mitochondrial (intrinsic) pathway by releasing cytochrome C and caspase 9 (57). Cytochrome C then sequentially activates apaf-1 and caspase 9 which the later one activates effector caspases. Caspase-3, -6 and -7 then induces cell death (57).

There is some evidence that individual HCV proteins modulate the cellular apoptotic signaling pathways, but unfortunately most of this data is generally controversial as it ascribes to a given HCV protein an anti-apoptotic or a pro-apoptotic effect. Part of these controversies can be explained by unphysiologic expression levels of HCV proteins but further could be the results of cell types (hepatoma versus hepatocytes) or absence of

quasispecies in these models. HCV core protein has been widely studied but it still remains unclear whether core protein inhibits or induces apoptosis. In some experiments core protein expression in hepatoma cells inhibited CD95-ligand induced apoptosis by prevention of cytochrome C release from mitochondria (58) while in another experiment, core expression in both hepatoma cell line or transgenic mice didn't prevent CD95-Ligand dependent apoptosis (59). Some experiments also have shown anti-apoptotic role for HCV core protein as it may interact and inhibit P53 protein (P53 induces apoptosis in cells with damaged DNA) (60, 61) or by inducing bcl-XL (an anti-apoptotic factor) (62). In contrast others have shown pro-apoptotic role for core proteins as core interacts and activates CD95 receptors (63) or P53 protein (64) or induces apoptosis through an indirect activation of bax (a pro-apoptotic factor) and cytochrome C release (65). Also HCV core has been shown to interact with mitochondria membrane and alter the transmembrane and hence induce formation of reactive oxygen species (ROS) and apoptosis (66, 67). The same conflicting results have been obtained for other HCV proteins. Envelope protein 1 and 2 (E1, E2) have shown anti-apoptotic effect by inhibiting cytochrome C and caspase-9 release from mitochondria in hepatoma cells (58). Interestingly another experiment has shown that expression of core-E1-E2 together in hepatoma cell line or transgenic mice, inhibits apoptosis, while Core or E2 expression alone induces apoptosis in the same hepatoma cell lines (68, 69). Non-structural-3 (NS3) protein has shown to have both anti-apoptotic effect by cleavage of Cardif, a downstream protein to RIG-I pathway (70) and pro-apoptotic effect by inducing caspase-8 dependent apoptosis (has been shown in hepatocytes) (71). NS4A has shown to induce the release of cytochrome C from mitochondria and the induction of apoptosis (72). NS5A has homology with anti-apoptotic factor bcl-2 and potentially can inhibit apoptosis (73) but activation of apoptosis pathways has also been shown in hepatoma cells expressing NS5A (74). In conclusion there is strong possibility that interaction of HCV proteins with apoptosis pathways may modulate the cell death and may have a role in pathogenesis of cell death in CHC, but effect of these proteins on hepatocyte apoptosis *in vivo* remains unclear.

The innate response of infected hepatocytes might also induce cell death. Activation of cytoplasmic RNA helicase RIG-I by HCV RNA, activates Cardif a cytosolic protein that localizes to the mitochondrial membrane which acts as a pro-apoptotic factor (70). In addition, activation and secretion of IFN-β through the innate response of infected hepatocytes will up-regulate the interferon-stimulated genes (ISGs) like Protein Kinase R (PKR), which phosphorylates the eIF-2α (a transcriptional factor) (75, 76). Phosphorylated form of eIF-2α has pro-apoptotic capacity (75, 76).

In response to cell death (necrosis/apoptosis), wound-healing process mediated by inflammatory cells is activated. Liver fibrosis is a part of the wound healing response to liver injury and is the characteristic feature of CHC and also has prognostic importance. It is defined as the excessive accumulation of extracellular matrix (ECM) proteins, which destructs the liver architecture and results in cirrhosis, liver failure, and portal hypertension often requires liver transplantation. In a short-term acute liver injury, hepatocytes regenerate and replace the damaged cells. This process, which is mediated by inflammatory response, is associated with a limited deposition of ECM proteins. If the liver injury persists (like CHC), the regeneration of parenchymal cells fails and more ECM protein is deposited instead of parenchymal cells (fibrosis) (77, 78).

As it was discussed above, liver injury in hepatitis C is often located around the portal triads. This process is associated with accumulation of inflammatory cells (interface hepatitis) and necrosis/apoptosis of hepatocytes (piecemeal necrosis). The regeneration process that is activated in the same location results in fibrogenesis around the portal triads (portal fibrosis). More severe and prolonged liver injury forms fibrotic bridges between portal tract to portal tract or even more importantly between portal tract and central vein (bridge fibrosis). These bizarre healing processes consequently result in excessive liver fibrosis that changes the architecture of the liver and causes cirrhosis (78).

A. 4. 3. 2. Pathogenesis of Liver Fibrosis: Liver fibrosis is associated with significant alteration of both quantity and composition of ECM (79). Excessive deposition of ECM results from both increased synthesis of ECM proteins as well as reduced degradation, which is mostly mediated by ECM-removing capacity of Matrix Metalloproteinase (MMPs) (79, 80). In acute short-term liver damage, fibrogenesis is balanced by fibrolysis. With repeated injury of sufficient severity, fibrogenesis prevails fibrolysis and causes ECM deposition. ECM proteins consist of fibril forming interstitial collagens (type I and III), sheet forming collagen (type IV), fibronectin, elastin, undulin, laminin, hyaluronic acid and proteoglycans. The level of these proteins may exceed from six to ten times normal in advanced stages of cirrhosis. The levels of MMPs secretion and activity decrease in fibrosis but the level of physiologic inhibitors of MMP (Tissue Inhibitors of MMP, TIMPs) increases (79, 80).

Myofibroblasts are the main cells that produce ECM proteins (also MMPs and TIMPs) in liver (81). These cells are either differentiated from Hepatic Stellate Cells (HSC, previously called Ito cells), which normally reside in space of Disse in a quiescent phase (82), or derived from small portal vessels (83). HSCs are the major fibrogenic cells in the pericentral area while myofibroblasts originating from portal vessels are the predominant

cells when liver injury occurs around portal tracts (83). The pathogenesis of liver fibrosis in CHC is poorly understood. Oxidative stress due to interaction of HCV proteins with Mitochondria and release of reactive oxygen species (ROS) (66, 67) from damaged hepatocytes or due to concomitant liver damage due to toxins (alcohol, acetaminophen) or steatosis can activate the HSCs and myofibroblasts cells (84). In addition apoptosis of hepatocytes (as it was discussed above) activates myofibroblasts and HSCs of liver to secrete more collagen (84). Besides aggregated inflammatory cells either lymphocytes, polymorphonuclear cells or resident macrophages (Kupffer cells) secrete cytokines which activates HSCs (85). TGF-β1 the major fibrogenic cytokine, which is secreted from Kupffer cells or almost any other cells in inflammatory or regeneration process strongly activate myofibroblasts and HSCs to deposit ECM (86). Platelet-Derived Growth Factor (PDGF) mainly secreted by Kupffer cells is another major mitogen for activated HSCs (87). Kupffer cells also release more ROS, which as it was indicated, activates HSCs (88). Activated myofibroblasts deposit ECM and release cytokines, which express cells adhesion molecules (VCAM-1) and modulate activation of lymphocyte (as it was discussed earlier). Therefore a vicious cycle, which inflammatory and fibrogenic cells stimulate each other, occurs and results in extensive deposition of ECM.

A. 4. 3. 3. Role of pre-existing or concomitant co-morbidities in acceleration of fibrosis in HCV infected patients: In chronic HCV infection apart from the direct effect of infection, other liver morbidities also play a major role in progression of liver fibrosis. Alcohol indulgence severely impacts the liver health in HCV infected cells. Chronic alcohol usage alters the population of gastrointestinal flora and inhibits intestinal motility resulting in gram-negative bacterial overgrowth (78). Lipopolysacharide released from gut flora is elevated in portal blood, which activates Kupffer cells in the liver via CD14/Toll-like recptor-4 complex (89). Activated Kupffer cells as it was indicated above activate HSCs through release of ROS, TGF-B1 and PDGF. Alcohol directly damages hepatocytes through release of ROS or indirectly through its waste product acetaldehyde (by intoxication through alcohol dehydrogenase) and causes activation of HSCs (90). Hereditary Hemochromatosis (mutation in HFE gene on chromosome 6) is an autosomal recessive disease characterized by excessive absorption of iron from intestine and deposition in tissues such as skin, gonads, pancreas and liver. Overload of iron acts as pro-oxidants and induces oxidative stress resulting in liver damage and fibrosis. Progression of liver fibrosis in these patients is devastating when they are infected with HCV. Other types of hepatitis infection can also accelerate liver damage in HCV infected patients. HAV infection mostly leads to acute liver failure in patients infected with HCV, but HBV infection accelerates the duration of progression of disease to decompensated cirrhosis. Liver steatosis (accumulation of lipid in hepatocytes) is another co-morbidity,

which is highly associated with chronic HCV infection. The mechanism of liver damage in liver steatosis is poorly understood, but a two-hit model has been proposed. HCV induces hepatic accumulation of lipids indirectly through insulin resistance and elevated serum levels of free fatty acids or directly by modulating lipid metabolism in hepatocytes resulting in hepatic steatosis. In the second hit, oxidative stress and pro-inflammatory cytokines promote hepatocyte damage (apoptosis) and recruitment of inflammatory cells leading to acceleration of fibrosis (91). The possible mechanisms of hepatic steatosis in HCV infection will be discussed in section C. 3 (HCV Assembly: Lipid Droplets and Their Role).

A. 4. 4. Compensated and Decompensated Cirrhosis

Cirrhosis is an ultimate result of liver fibrosis and is defined histopathologically based on the extent of fibrosis. It is the 12th leading cause of death in US and a major risk factor for hepatocellular carcinoma. The pathologic feature of cirrhosis consists of architectural distortion of liver due to numerous fibrotic bridge and septa with the formation of regenerative nodules. These changes decrease hepatocellular mass, and thus function and alter the portal blood flow results in portal hypertension. Although the liver function decreases and portal hypertension occurs most of the patients have varying degree of compensated liver function (compensated cirrhosis), while the minority of patients may develop more severe cirrhosis with liver decompensated for daily body supply (decompensated cirrhosis). HCV infection is the etiology of 50% of patients with cirrhosis. Regardless of underlying cause of the liver disease, the clinical course of patients with cirrhosis is usually complicated by a number of sequelae:

1) Portal Hypertension and its complications resulted in esophageal varices and bleeding (with 20-30% mortality rate), refractory ascites with possibility of sub acute bacterial peritonitis (with 25% mortality rate) and hypersplenism with thrombocytopenia and leukopenia (enhanced chance of bleeding and infection.

2) Abnormalities in synthesis of proteins such as albumin (major protein for preserving oncotic pressure), the coagulation factors (such as factors II, V, IX, X, XIII), anticoagulant factors (protein C, S and Z) and components of fibrinolytic system (such as plasminogen and antithrombin III) result in severe abnormalities in homeostasis presented with risk of bleeding and severe edema.

3) Malnutrition and indigestion of proteins and vitamins is a common feature of cirrhosis. Vitamin D and calcium malabsorbtion can accelerated the bone resorption results in osteoporosis, osteopenia and osteomalacia.

4) Reduced detoxification capacity of hepatocytes: Ammonia released by catabolism of proteins and amino acids is extremely toxic for neurons. The ammonia is generally cleared from the blood by the liver and is metabolized to urea, which is later secreted in urine. But hyperammonemia is not the only reason for hepatic encephalopathy. Neurotoxins produced by gut flora are another factor that their detoxification by hepatocytes is impaired. Hepatic encephalopathy is a serious complication and is the main criteria for diagnosis of decompensated cirrhosis. Estrogen and bilirubin are two waste products that are also cleared by liver and their accumulation in body result in failure of proper vasoconstriction and two well-known lesion; spider angioma and palmar erythema and unconjugated hyperbilirubinemia (jaundice) respectively.

5) Hepatorenal syndrome: Appearance of functional renal failure without renal pathology occurs in 10% of patients with advanced cirrhosis. The mechanism of hepatorenal syndrome is not perfectly understood, but renal vasoconstriction is the hallmark. The prognosis is variable. In type 1 of this syndrome, renal function and creatinine clearance reduce progressively and the prognosis is poor. Type 2 is more stable and the outcome is more favorable.

A. 4. 5. Hepatocellular Carcinoma (HCC)

Liver cancer is the fifth most common cancer in men and the seventh in women (92). Excluding metastatic liver cancer, Hepatocellular Carcinoma (HCC) accounts for most of the liver malignancies (92). Infection by hepatitis B virus (HBV), HCV, chronic alcoholism, aflatoxin exposure, and smoking are the major risk factors associated with appearance of HCC (92). Although the incidence for most of cancers has been stable or declining, it has increased substantially for HCC (93). HCV infection is the leading cause of HCC worldwide and it is estimated that in 2002 alone, HCV infection accounted for 155,000 liver cancer deaths worldwide (94). The trend for HCC incidence or HCC related death is highly related to the trend of HCV prevalence two or three decades earlier (93, 94). In the United States of America (USA), the incidence of HCC in person aged 50-59 has increased dramatically during the last decade (9.1% average annual rate of increase), reflecting the extensive spread of HCV infection in 1980-1990 (95). Unfortunately, the long-term prognosis of HCC is very poor and 1-year and 5-year survival rate of HCC in the USA remains less than 50% and 12% respectively (92, 95).

Presence of cirrhosis is the most important causative factor for the development of HCC. The annual risk for the development of HCC in patients with HCV-related cirrhosis depends on region (2-3% in west and 6-11% in Japan) (92) and stage of cirrhosis (with greatest risk among patients with decompensated cirrhosis) (96). It has been shown even

after eradication of virus (SVR see below), HCC can still occur in patients who developed cirrhosis. But the important question is whether there is a direct role for HCV in HCC promotion. HCC is more prevalent in cirrhosis related to HCV rather than cirrhosis related to autoimmune hepatitis. Furthermore, HCC may occur in HCV infected patients in the absence of cirrhosis. This evidence supports the direct role of HCV in cancer promotion. It is estimated that in patients with HCV infection, but without cirrhosis, the annual risk for developing HCC is 1.7%, which is much higher than the normal healthy population (96).

The mechanism of initiating and promoting HCC in HCV patients is not perfectly understood. Both genetic and epigenetic (stable changes of phenotypic traits which are not encoded in the DNA sequence) mechanisms form the molecular basis of HCC. Aberrant epigenetic states may predispose the cells to genetic changes but in contrast genetic changes may also initiate aberrant epigenetic events. Although sequence of HBV DNA are integrated into genomic DNA of HCC cells, HCV (a positive-strand RNA virus which replicates in cytoplasm) has little potential for integrating its genome to host DNA. This indicates that the mechanism by which HCV virus promotes the cancer differs substantially from the HBV models of carcinogenesis.

A. 4. 6. Extrahepatic Manifestation of Chronic HCV infection

Several extrahepatic syndromes are associated with chronic HCV infection and could be the first signal of HCV infection in some cases. Mixed cryoglobulinemia (overproduction of IgM and rheumatoid factor by over activation of lymphocyte B) resulted in serious conditions such as renal insufficiency, acute renal failure (97), leukocytoclastic vasculitis, palpable purpura with large necrotic ulceration (98, 99) and neurologic findings such as peripheral neuropathy and mononeuritis multiplex (100, 101). This abnormality is generally seen in HCV infection (98, 102-104). In addition Clonal expansion of B-cells in mixed cryoglobulinemia may act as an intermediary disorder and these cells may ultimately go under several mutations with activation of oncogenes with appearance of lymphoma (105) in particular Non-Hodgkin Lymphoma (106).

Porphyria cutanea tarda and Lichen planus are two dermatological abnormalities, which are highly associated with HCV infection (104, 107). Hypothyroidism (108, 109), Graves disease, Hashimoto thyroiditis (110, 111) are also associated with HCV infection. Insulin resistance and Diabetes Mellitus (DM) are another endocrinolopathy associated with HCV (112). Rheumatologic abnormalities associated with HCV are sialoadentis similar to idiopathic Sjogren syndrome (113), non-errosive oligoarthritis of medium and large size joints and symmetrical polyarthritis involving small joints (114). Hypertrophic and dilated cardiomyopathy (115), idiopathic pulmonary fibrosis (116), Mooren corneal ulceration

(117) and Osteosclerosis (118)have recently shown to be associated with chronic HCV infection.

A. 5. Diagnosis of HCV

HCV infection is mostly a subclinical disease, which at early stage of disease has either no obvious signs and symptoms or the signs and symptoms are not specific. Therefore the diagnosis of HCV is mostly insidious and screening of people at risk is required to detect the HCV patients in earlier stages of disease. This has several potential benefits such as more effective treatment (119), harm reduction by lifestyle modification (120) and reduction of transmission of HCV infection to other people. Since the late 1980, after discovery of HCV and introduction of diagnostic tests for screening of HCV, incidence of acute infection has declined dramatically (5). According to National Hepatitis Surveillance Program calculation, the estimated cost of screening test for HCV in the USA is $1,246 per case detected and can be reduced to $357 per case detected if risk factor for HCV transmission is incorporated on history of patients (121). This amount is comparable to the cost of a routine screening test for other diseases.

According to the latest outline by the American Association for the Study of Liver Disease (AASLD) (122) all persons including: (i) IDUs (even persons that tried once), (ii) HIV positive individuals, (iii) persons who received clotting factor concentrates before 1987 and in particular hemophiliacs, (iv) persons who have ever been on homodiyalysis, (v) recipients of transfusion or organ transplantation before 1992, (vi) persons with unexplained repeated elevated liver aminotransferase, (vii) children of HCV positive mother 12 months after birth, (viii) medical or health workers after needle accident injury or mucosal exposure to HCV positive blood, and (ix) current sexual partner of HCV positive patients should be screened for HCV. For some of the groups such as IDUs or hemophiliacs who received clotting factor the prevalence is high (~ 90%). For groups like recipient of blood before 1992 the prevalence is intermediate (~10%) and for others (needle stick exposure, sexual partners of HCV infected patients) the prevalence is low (1% to 5%) (122).

Serological tests that detect anti HCV antibody are considered as an initial screening test. Two enzyme immunoassays tests and one enhanced chemiluminescence immunoassay test have been approved by FDA for HCV screening (122, 123). These tests are >99% sensitive and specific in immunocompetent patients, and eliminate the need for confirmatory HCV antigen immunoblot assay (124, 125). The false positive rate is low and generally occurs in patients with autoimmune liver disease or hypergammaglobulinemia with no risk of HCV exposure (124). False negative results

usually occur in immunosuppression states such as HIV infection, solid organ transplantation, hypo or agammaglobulinemia and hemodialysis (126-128). In both cases of false positive or false negative, patients should be tested by HCV RNA assay tests. As a positive anti-HCV antibody achieved from the above assays cannot discriminate between active infection and resolved infection (in which HCV antibody is still present in blood), the presence of virus should be evaluated by nucleic acid tests (NATs) that detect HCV RNA in blood.

NATs use amplification of the nucleotide targets with PCR, transcription-mediated amplification (TMA) and signal amplification methods such as a branched DNA (bDNA). There are two types of NATs; qualitative and quantitative. Qualitative assays are generally more sensitive (123), while quantitative assays (except to one test "Cobas Taqman HCV test of Roche Molecular System") are less sensitive and a negative result does not completely exclude hepatitis C (123). The benefit of quantitative tests is that they are extremely useful before and during treatment to evaluate the response to therapy and decision-making about continuing treatment (122, 123). After confirming the presence of HCV infection by NATs determining genotypes is the next test that should be performed. It is not only useful for epidemiological studies but also is crucial in clinical management of the disease as treatment response is genotype dependent. Dose and duration of treatment is various from one genotype to the other genotypes (129-131).

A. 6. Therapeutic Approach To the Patients with HCV Infection

A. 6. 1. Treatment objectives and outcomes

The ultimate goal of therapy in HCV infection is to permanently eradicate hepatitis C virus in order to prevent irreversible liver damage and complications, such as cirrhosis, and reduce the risk of HCC. Several types of virological response to therapy may occur based on their timing relative to initiation of treatment (122):

Sustained Virological Response (SVR) is defined as the absence of HCV RNA in serum by a sensitive PCR assay 24 weeks following discontinuation of therapy. Although it is regarded as virological cure, liver cancer still could be detected several years after SVR especially if cirrhosis had existed during treatment (132).

End of Treatment Response (ETR) is defined as undetectable levels of HCV in serum by a sensitive PCR assay 24 weeks (genotypes 2 and 3) or 48 weeks (genotype 1) after initiation of antiviral treatment. Although it shows effective treatment and therapy can be

discontinued, it doesn't predict definite SVR and virological relapse can occur after discontinuation of treatment.

Rapid Virological Response (RVR) predicts a high likelihood of achieving SVR and is defined as absence of HCV RNA at week 4 of treatment, using a test with sensitivity lower than 50 IU/ml. Absence of RVR doesn't mean that SVR is not achievable (poor negative predictive value). Ninety-one percent of persons with genotype 1 who achieved RVR with routine anti HCV treatment (Pegasys and ribavirin, see below) reached SVR (133).

Early Virological Response (EVR) is defined as more than 2 Log decrease in viral load when it is compared with baseline viral load, 12 weeks after initiation of therapy. Failure of EVR is the strongest predictor of not achieving SVR (131, 134), and treatment can be discontinued especially in patients with genotype 1 infection (134). Ninety-seven to 100% of treatment naïve patients with genotype 1 who didn't reach to EVR didn't achieve SVR (134). The clinical utility of EVR is less useful in patients with HCV genotypes 2 and 3 as majority of these patients clear virus by 12 weeks in response to therapy. Achieving EVR is less accurate in predicting SVR (less positive predictive value) (134).

Virological Breakthrough occurs if the HCV RNA reappears in serum while patient is still on therapy.

Virological Relapse refers to reappearance of HCV RNA after achieving ETR and discontinuation of therapy.

Non-responders are the patients who failed to clear virus after 24 weeks of therapy. If the HCV RNA level decreases more than two logs but is not completely eradicated from serum after 24 weeks of treatment, the patient is defined as **Partial Responder** and if it decreases less than 2 logs, the patient is **Null Responder.**

A. 6. 2. The antiviral treatment for HCV infection; Pegylated Interferon-α (Peg-IFN) and Ribavirin

Pegylated interferon-α (Peg-IFN) in conjunction with weight based Ribavirin (RBV) was considered the recommended therapy of HCV infection for many years (129-131). Appearance of protease inhibitors (PIs) such as Boceprevir and Telaprevir (see the following) and other direct acting antiviral (DAA) therapies have moved the standard of treatment toward combination therapies with these agents. Although interferon-α is still considered as the mainstay of HCV treatment, high cost and numerous side effects have encouraged the clinician to pursue an interferon-free regimen exploiting combination of

new DAA. This approach is still at early stages of evaluation, but since numerous DAAs will be available in the next several years, it is assumed achievable in a near future.

A. 6. 2. 1. Interferon-α compounds for treatment of HCV and major side effects: Peg-Intron (Shering Plough Corp) and Pegasys (Hoffmann-LaRoche) pegylated interferon-αs have been licensed for clinical use in US. The addition of Polyethylene Glycol (PEG) to interferone has several benefits. It slows the absorption from the injection site and provides prolonged stable serum concentration, reduces the renal clearance and enhances the bioavailability of the drug and reduces immunogenicity by masking the interferon molecule (135). Peg-Intron is a pegylated interferon-α2b with a 12 kilo Dalton (kDa) linear polyethylene glycol (PEG) and Pegasys is a pegylated interferon-α2a, which is pegylated by 40 kDa branched PEG (135). In general, pegylation of interferon-α increases the plasma half life the drug from two to three hours to 30-45 hours in Peg-Intron and to 80-90 hours in Pegasys (135). The dose of PEG-Intron is 1.5 µg/kg/week, which is given subcutaneously (130). It is safe to be used in children (122, 130). Usual dose of Pegasys is 180 µg/week subcutaneously (129, 131) and has not been approved for use in children (122). The most common side effect of interferon is an acute influenza-like syndrome with symptoms including fever, chills, myalgia, arthralgia, fatigue, headache, nausea, vomiting and diarrhea. Other major side effects are Myelosuppression with anemia, granulocytopenia and thrombocytopenia, psychiatric adverse effects ranging from irritability and major depressive disorder to psychosis and suicidal behavior, dermatologic reactions such as dermatitis, alopecia universalis and pruritus, endocrinologic abnormalities such as thyroid dysfunction, insulin resistance and diabetes mellitus, declined male sexual function and metabolic abnormalities such as rise in very low density lipoprotein (VLDL) triglyceride and reduced high density lipoprotein (HDL). Some of these adverse effects can be medically managed but in some cases it may require dose reduction or even discontinuation of Peg-IFN. IFN-based therapy also exacerbates co-morbid autoimmune diseases such as thyroid disease, type 1 diabetes, systemic lupus erythematosus, hemolytic anemia and immune-mediated thrombocytopenia. In rare cases, pulmonary toxicity and pneumonitis, Retinopathy, including retinal hemorrhages, cotton wool spots, papilledema, optic neuropathy and, more rarely, retinal artery or vein obstruction, hearing loss and tinnitus have been reported in IFN-based therapy (136).

A. 6. 2. 2. Ribavirin for the treatment of HCV and major side effects: Ribavirin is a purine nucleoside analog with altered base and sugar. The antiviral mechanism of ribavirin is not completely understood but mono-phosphate form of ribavirin inhibits inosine 5-phosphate dehydrogenase the rate limiting enzyme for the *de novo*

biosynthesis of GTP. Tri-phosphate from of ribavirin competitively inhibits the GTP-dependent 5′ capping of viral RNA. Due to its similarity to purine nucleosides, ribavirin is incorporated into HCV RNA, as a base analog of either adenine or guanine and it pairs with pyrimidines (either uracil or cytosine), inducing lethal mutations in RNA-dependent replication of HCV genome. The optimal dose of ribavirin administrated with Pegasys is 1000 mg/day for those who weigh ≤ 75 kg and 1200 mg/day for patients who weigh > 75 kg. The recommended dose for combination of ribavirin with Peg-Intron is 800 mg/day, although in patients with HCV genotype 1 the weight-based ribavirin showed better SVR (800 mg/day for patients <65 kg, 1000 mg/day for patients weigh 65-85 kg, 1200 mg/day for those who weigh 85-105 kg and 1400 mg/day for patients > 105 kg) (122). The most life important life-threatening side effect of systemic ribavirin is dose-dependent reversible hemolytic anemia. Dose reduction is recommended if the hemoglobin (Hb) level falls below 10 g/dl in patients with no cardiac risk factor and ribavirin should be interrupted if Hb level drops below 8.5 g/dl. Ribavirin is also highly teratogenic (FDA pregnancy category X) and is contraindicated in pregnancy or in males whose their female partners are pregnant. Pregnancy should be ruled out before initiation of treatment. Men and women of childbearing age must use two effective contraception methods during treatment and should continue using contraception up to six months after drug discontinuation (122).

A. 6. 2. 3. Duration, follow up and termination of the combined treatment: The duration of treatment is genotype dependent (24 weeks for genotypes 2 and 3 versus 48 weeks for genotypes 1 and 4). Twelve weeks after initiation of the combination therapy (Peg-IFN and ribavirin), HCV RNA level should be tested. Ninety-seven to 100% of treatment naïve patients with HCV genotype 1 infection who their HCV RNA level didn't decline by ≥ 2 Logs (early virological response has not reached) failed to achieve SVR, thus treatment can be stopped without compromising the chance of achieving SVR. This is less helpful in genotype 2 and 3 since majority of the individuals clear virus by week 12. HCV RNA level is tested again 24 weeks after initiation of the treatment and if a patient failed to clear the virus (non-responder) treatment could be discontinued. If the patients cleared the virus treatment can be stopped in genotypes 2 and 3 patients (end of treatment response, ETR) and should continue for another 24 weeks in genotypes 1 and 4 patients. In genotypes 5 and 6 patients the guideline is not perfectly clear due to the lack of proper study, but treatment for 48 weeks is preferable to 24 weeks in genotype 6. To confirm the SVR, absence of HCV RNA should be tested 24 weeks after finishing the treatment (122).

A. 6. 2. 4. Treatment of acute HCV infection: Treatment of acute hepatitis C reduces the risk of developing chronic infection. The SVR rate was between 83-100% in patients who received standard interferon, 5-10 million units/day for 12 weeks. The optimal time for initiation of treatment has been evaluated in several studies and collectively the data supports to delay the treatment to 8-12 weeks after diagnosis rather than starting immediately. Although excellent comparable results were achieved using standard non-pegylated interferon, pegylated types are favored due to greater ease of administration. Although there is no recommended dose of Peg-IFN for treatment of acute HCV infection, several case series reported higher SVR rates in patients who received dose higher than 1.2 μg/kg/week of Peg-Intron. Similarly there is not enough data to support or reject the addition of ribavirin to this regimen and the decision should be made on a case-by case basis. In addition duration of therapy is controversial and although in a study of 102 patients who received Peg-Intron, compared to patients who received treatment for 8 and 12 weeks, those who received the treatment for 24 weeks showed better SVR rate (91% in 24 weeks patients versus 82% and 68% in 12 weeks and eight weeks patients respectively), there are concerns about the overall validity of these results. So currently the recommendation is to treat the patients for at least 12 weeks, and 24 weeks may be considered especially in patients with genotype 1 (122, 137).

A. 6. 3. Direct-Acting Antiviral Agents for HCV Therapies

The development of HCV cell culture system and introduction of animal model have improved our understanding of HCV life cycles in recent years and has led to identification of several potential targets for direct-acting antiviral (DAA) drugs. Recently two of these drugs, Telaprevir (Vertex/Janssen) and Boceprevir (Merck) have been approved as anti HCV viral agent in US and Europe. Several other agents are at various stages of clinical trials to achieve FDA approval for clinical applications. Introduction of these agents can offer hope for patients that are non-or partial responders and in relapsers when they were treated with standard Peg-IFN and ribavirin. In addition, these new drugs are much less toxic than Peg-IFN and can be better tolerated. In the following section some of these drugs will be introduced and discussed.

A. 6. 3. 1. NS3/4A Protease Inhibitors: The 9.6 Kb positive strand RNA genome of HCV encodes a long polyprotein, which is later processed to 3 structural (core, E1 and E2) and 7 non-structural proteins (P7, NS2, NS3, NS4A, NS4B, NS5A and NS5B). Viral NS3/4A is a serine protease that mediates cleavage of non-structural proteins downstream to NS3 (see NS3/4A protein), therefore it is considered as an excellent targets for development of inhibitors. The inhibitors in this group of drugs are divided to two classes: 1) macrocyclic inhibitors and 2) linear tetrapeptide α-ketoamide derivatives (138).

The first drug in this group which showed substantial antiviral therapy, introduced by Boehringer Ingelheim was a macrocyclic inhibitor named Ciluprevir (BILN 2061). It was later discontinued due to severe side effect, cardiotoxicity (139). Telaprevir (VX-950, Vertex Pharmaceuticals) and Boceprevir (SCH50, Merck) were the first generation of NS3/4A inhibitors that received license by FDA. Telaprevir is a α-ketoamide inhibitor and was studied in three phase III trials. The ADVANCED study was preformed in order to evaluate the Telaprevir-based regimens. The patients were randomly allocated into three groups. In the first and second groups, patients received a combination of Peg-IFN and Ribavirin (PR) plus Telaprevir for eight or 12 weeks. The third group received standard PR for eight to 12 weeks. In all groups the treatment was continued for up to 48 weeks with PR. The first two groups had 57% and 58% RVR respectively compared to only 8% in PR group. The SVR rates were 69% and 75% respectively versus 44% in PR alone (140).

The REALIZE study was performed on HCV genotype 1 infected patients who had previously failed on standard PR therapy. The patients were treated with combination of Telaprevir for 12 weeks and PR up to full 48 weeks or standard PR for 48 weeks. The SVR rates in the Telaprevir arms were 31%, 57% and 86% in non-responders, partial responders and relapsers respectively versus 5%, 15% and 24% in the same groups in PR arm (141). The ILLUMINATE trial was preformed in treatment naïve patients and was assessing response-guided therapy. The most common side effects of Telaprevir were anemia and fatigue (141). Boceprevir is also a α-ketoamide this is generally used with HCV genotype 1 infection. Boceprevir was evaluated on treatment naïve infected patients in HCV-SPRINT phase III clinical trial. Patients were treated for 4 weeks with standard PR regimen and then were randomized into three arms: Boceprevir + Placebo for additional 44 weeks, PR+ Boceprevir for additional 44 weeks and PR+ Boceprevir for additional 24 weeks if the virus was undetectable before week 8. The SVR rates were 40%, 68% and 67% in non-Black patients and 23%, 53% and 42% in Black patents respectively (142). In RESPOND-2 clinical trial, Boceprevir was used in previously treated patients but in this trial null responders were excluded. The patients who received 4 weeks of PR followed by 44 weeks of Boceprevir and PR combination achieved 59% SVR versus 21% in those that were treated by PR for 44 weeks (143). These superior outcomes in clinical trials plus absence of serious toxicity resulted in FDA approval for these two agents and they are now clinically used specifically in patients who were failed on standard PR regimen.

The second group of first generation NS3/4A inhibitors is mostly in phase II clinical trials. TMC435 has shown outstanding results with very acceptable tolerability. In a phase II

clinical trial, TMC435 combination therapy with PR was used in genotype 1 patients who had failed on standard PR regimen before. HCV RNA was undetectable (25 IU/ml) in 94% of relapsers, 89% of partial responders and 87% of non-responders (144). BI 201335 is currently in phase III and when it was used in combination with PR for 24 weeks in treatment naïve genotype 1 patients, resulted in 83% SVR rate (145). The other drugs in this group are BMS-650032, ACH-1625, Danoprevir and Vaneprevir (MK-7009), which are in various phase of clinical trials and have shown potent antiviral activity and favorable tolerability.

One of the difficulties with both groups of first generation drugs is their low genetic barrier to resistance and extensive cross-resistance between different compounds (144). MK-5172 and ACH-2684 are second-generation drugs in this group with promising antiviral activity and improved resistance profile (138). A list of newer drugs in this group has been shown in table 1-1 (138).

Table 1-1. List of new NS3/4A protease inhibitors in trial (138)

Drug name	Company	Structure	Study Phase
Danoprevir (RG 7227)	InterMune/Roche	Macrocyclic	Phase 2
TMC435	Tibotec/Medivir	Macrocyclic	Phase 2
Vaniprevir (MK-7009)	Merck	Macrocyclic	Phase 2
BI 201335	Boehringer Ingelheim	Linear Ketoamide	Phase 2
BMS-650032	Bristol-Myers Squibb		Phase 2
GS-9256	Gilead		Phase 2
ABT-450	Abbott/Enanta		Phase 2
Narlaprevir (SCH900518)	Merck	Linear Ketoamide	On hold
PHX 1766	Phenomix		Phase 1
ACH-1625	Achillion		Phase 1
IDX320	Idenix	Macrocyclic	On hold
MK-5172	Merck	Macrocyclic	Phase 1
VX-985	Vertex		Phase 1
GS-9451	Gilead		Phase 1

A. 6. 3. 2. NS5B Polymerase Inhibitors: Non-structural protein 5B (NS5B) is an RNA-dependent RNA polymerase (RdRp), which replicates the HCV genome, and it is essential for HCV life cycle. A list of NS5B RdRp polymerase inhibitor in various stages of trial has been shown in table 1-2. NS5B polymerase inhibitors are classified to two groups:

1) Nucleoside or nucleotide analogues mimic the structure of natural substrate of RdRp and incorporated into newly synthesized RNA and act as chain terminator. One benefit of

this type of drug is its similar efficacy against all the HCV genotypes as the active center of NS5B is highly conserved amongst different genotypes (138). Among the nucleos(t)ide analogue RG 7128 (cytosine analogue) is the most promising and advanced one and in combination with Peg-IFN and ribavirin in treatment-naïve genotype 1 and 4 patients it has shown EVR rate of >80% and viral suppression in 91% of patients at 24 weeks. No viral breakthrough due to the selection of resistant HCV variant was observed with this drug. PSI-7977 (uridine analogue) has also shown promising effect (100% RVR in genotype 2 and 3 in combination with PR) and has been well tolerated in short-term therapy. These two drugs are now in phase III trial. Development of Valopicitabine and R1626 was halted due to modest antiviral activity and high level of resistance in Valopicitabin and serious adverse effects in both cases (138).

2) Allosteric non-nucleoside inhibitors analogues bind to different enzyme sites (Site 1 to 4) and induce conformational change in NS5B and change its RdRp activity (138). The HCV RdRp has the shape of a right hand. Site-1 inhibitors (thumb-domain 1/benzimidazole site) exhibit low to medium antiviral activity in phase 1 clinical trials. The only drug from this group that remained in clinical trial is BI207127. The development of BILB 1941 and MK-3281 was halted because of severe gastrointestinal side effects. Site-2 inhibitors (thumb-domain 2/thiophene site) have shown medium antiviral activity in phase 1 clinical trials. In this group, Filibuvir (PF-0086854, Pfizer) and VX-222 (Vertex) showed medium antiviral activity and now are in phase II of development. VX-222 has progressed to phase 2 of the development. Site-3 inhibitors (palm-domain 1/benzothiadiazine site) have shown more promising results and all of the drugs in this group are now in phase 2 of development. In this group ANA598 in combination with Pegasys and ribavirin has shown 75% clearance of HCV at treatment week 12. Site-4 inhibitors (palm-domain 2/benzofuran site) are currently in various phases of development. HCV-796 (Nesbuvir) showed low antiviral activity against genotype 1 in patients and resulted in selection of resistant variant and viral breakthrough in several patients. Its development was stopped due to elevation of liver enzyme in patients. GS-9190 (Tegobuvir) with low activity against HCV genotype 1 has recently entered to phase-2 clinical trials as a potential drug for combination therapy. IDX 375 is still in phase-1 of development [reviewed in (138)].

A. 6. 3. 3. NS5A inhibitors: Non-structural protein 5A is crucial for the regulation of HCV replication and assembly. BMS-790052 (Daclatasvir) is a potent NS5A inhibitor that entered into phase II trial and has shown RVR rate of 83-92% when it was combined with Peg-IFN and Ribavirin. However, genetic barrier of this drug is low and selected mutants

have good *in vitro* and *in vivo* fitness. Other drugs in this group, BMS-824393, PPI-461 and AZD7295 are in early phase of clinical development (138).

A. 6. 3. 4. Other antiviral agents: Cyclophilin is a human cell protein which is involved in protein folding and function as a regulator for NS proteins which are involved in replication complex especially NS5B RNA polymerase (146). Alisporivir (Debio 025, Debiopharm/Novartis), a Cyclophilin inhibitor lacking anti-calcineurin activities (no immunosuppressive effect), is currently at phase II of clinical trial. A combination therapy with Peg-IFN and ribavirin has shown 69% and 76% SVR rate (138) that were higher than Peg-IFN and Ribavirin standard therapy (55%). The resistance selection was observed but the mutants were poorly fit, therefore no viral breakthrough has been reported so far. SCY-635 (Scynexis) and NIM811 (Novartis) are two other cyclophilin inhibitors which NIM811 development was discontinued (138).

Table 1-2. List of new NS5B RNA dependent RNA polymerase inhibitors in trial (138)

Drug name	Company	Target/active drug	Study Phase
Nucleos(t)ide NS5B polymerase Inhibitor			
Valopicitabin (NM283)	Idenix/Novartis	Active site/NM107	Stopped
RG7128	Roche/Pharmasset	Active site/PSI-6130	Phase 2
IDX 184	Idenix	Active site	On hold
RI626	Roche	Active site/RI579	Stopped
PSI-7977	Pharmasset	Active site	Phase 2
PSI-938	Pharmasset	Active site	Phase 2
Non-nucleoside NS5B polymerase Inhibitor			
BILB 1941	Boehringer Ingelheim	NNI site I/thumb 1	Stopped
BI 207127	Boehringer Ingelheim	NNI site I/thumb 1	Phase 2
MK-3281	Merck	NNI site I/thumb 1	Stopped
Filibuvir (PF-00868554)	Pfizer	NNI site 2/thumb 2	Phase 2
VX-916	Vertex	NNI site 2/thumb 2	On hold
VX-222	Vertex	NNI site 2/thumb 2	Phase 2
VX-759	Vertex	NNI site 2/thumb 2	Phase 1
ANA598	Anadys	NNI site 3/palm 1	Phase 2
ABT-333	Abbott	NNI site 3/palm 1	Phase 2
ABT-072	Abbott	NNI site 3/palm 1	Phase 2
Nesbuvir (HCV-796)	ViroPharma/Wyeth	NNI site 4/palm 2	Stopped
Tegobuvir (GS-9190)	Gilead	NNI site 4/palm 2	Phase 2
IDX375	Idenix	NNI site 4/palm 2	Phase 1

Silibinin is one of the flavonolignans contained in Silymarin (extract of milk thistle) that has reported to act like a direct non-nucleoside inhibitor of HCV RdRp (147). Oral administration of this drug is not effective in HCV treatment but intravenous injection of Silibinin results in substantial decline in HCV RNA levels and can be used as a rescue approach in patients who did not respond to Peg-IFN and ribavirin therapy (138). Nitazoxanide (Alinia, Romark) is a thizaolide with an anti-HCV effect. The antiviral mechanism of action of Nitazoxanide is still unknown. A phase-2 study of 500 mg

Nitazoxanide twice a day for 12 weeks followed by combination of Peg-IFN-α2a and Ribavirin and Nitazoxanide for 36 weeks yielded 79% SVR rate in genotype-4 but it was not siginificantly effective in genotype-1 patients (SVR rate of 44%) (148). Another drug at phase-2 of clinical trial, Celgosivir (Migenix) is an inhibitor of α-glycosidase-1, an enzyme that is required for viral assembly, release and infectivity (138).

A. 6. 3. 5. New Interferons: Albinterferon-α2b (Joulferon) from HGS/Novartis is a recombinant Interferon-α-2b fused with human albumin (which decreases renal clearance of the drug), which can be administered every two weeks. The clinical trials that were done with this drug did not show any superiority of this interferon to Peg-IFN and there were concerns by the regulatory authorities regarding the benefit/risk ratio. Further development of this drug was halted. Locteron (BLX-883, Biolex) is a sustained release formulation of interferon-α2b with much less flu-like symptoms is in phase II of clinical trial and the SVR rate has to be determined. PEG-rIL-29 (ZymoGenetic/BMS) is a pegylated interferon-λ, with a more limited distribution than interferon-α and is currently at phase-1 of development (138).

B. Hepatitis C Virion Structure and Proteins

Despite multiple efforts to visualize the structure of HCV, it has not been completely visualized yet, but according to the chemical and physical properties and current data, it is hypothesized that the virion particles are about 40-70 nm in diameter (149). The virion contains an icosahedral nucleocapsid that is formed by core protein and covers the 9.6 kb positive single-strand RNA. Outside the nucleocapsid, HCV is surrounded by a double-layered lipid membrane (envelop) derived from host cells. Inside this membrane, envelop glycoprotein E1 and E2 reside and form a heterodimer (150). Despite this simple structure, HCV circulates in blood in various forms, as virions bound to immunoglobulins, free virions and is associated with very low-density lipoprotein (VLDL) and low-density lipoprotein (LDL) (149).

The 9.6 kb HCV RNA is formed by: (i) 5′-untranslated region (5′-UTR) that contains Internal Ribosomal Entry Site (IRES), (ii) an open reading frame (ORF) which encodes a polyprotein containing about 3000 amino acids, and (iii) a 3′-UTR region with secondary structure which is necessary for RNA replication. The polyprotein is processed into 10 mature structural and non-structural (NS) proteins by host and viral proteases (150).

B. 1. Structure and function of 5′-UTR side of HCV RNA (IRES Domains)

Translation of eukaryotic messenger RNA is a protein-mediated process, which requires 5′-methyl-capped mRNA and eukaryotic initiation factors (eIF). Initially the 5′-methyl-cap structure on RNA is recognized by eIF4 complex that is formed by eIF4A, eIF4B, eIF4E and eIF4G. The eIF4A is a DEAD box RNA helicase that resolves secondary structure of mRNA and helps the pre-initiation complex (see follow) scan the mRNA and find the start codon. The eIF4B is a co-factor for eIF4A and also contains two binding subunits, one for attachment to mRNA and the other for 18S subunit of 40S ribosome on pre-initiation complex, that is involved in recruitment of pre-initiation complex to mRNA. When it is phosphorylated, it promotes formation and attachment of pre-initiation complex. The eIF4E is the component of eIF4 complex that recognizes the 5′-methyl-cap structure on RNA. The eIF4G acts as a scaffolding protein and binds to poly-A-tail of mRNA through poly-A binding protein (151, 152).

The attachment of eIF4 complex to mRNA, recruits the 43S pre-initiation complex to form and attach to mRNA. The 43S pre-initiation complex includes, 40S small ribosomal subunit, eIF1, eIF1A, eIF3 and the eIF2/GTP/Methionine-charged initiator tRNA (ternary complex). The eIF1, IA and 3 are implicated in preventing the attachment of 60S large

ribosomal subunit to 40S small subunit before it is ready to commence elongation. The ternary complex contains methionine charged tRNA (correspondent to AUG start codon) and eIF2-bound GTP, which the release of energy in its phosphate bound detaches the eIF3 and eIF2/GDP. Both prevent the attachment of 60S ribosome. In this process, attachment of ternary complex to the start codon during the scanning of mRNA by per-initiation complex releases the eIF1 from 40S ribosome. The eIF1 is an inhibitory factor, which prevents the hydrolysis of eIF2-bound GTP and therefore its detachment triggers eIF5-mediated hydrolysis of eIF2-bound GTP. As it was indicated the energy released from this process detaches eIF-3 and eIF2-GDP and allows the attachment of 60S ribosome to mRNA (151, 152).

Hepatitis C virus RNA does not contain 5′-methyl-cap and the initiation pathway is different than eukaryotic mRNA(151, 152). On HCV RNA, a secondary structure forms the Internal Ribosomal Entry Site (IRES) at the 5′-UTR side, which mediates translation initiation. HCV IRES-mediated translation initiation doesn't require 5'-cap structure and scanning process to find the codon at p-site and is not mediated or controlled by external eIF4 complex. Instead the IRES structure bypasses the formation of eIF4 complex and interacts directly with the 40S subunits. This interaction promotes attachment of eIF3 and ternary complex to form a 48S ribosome particle already attached to the tRNA. This will activate the eIF-5 mediated hydrolysis of eIF2-bound GTP on ternary complex. The subsequent process is similar to eukaryotic mRNA translation (153-155).

The secondary structure of HCV RNA is conserved among some viruses in the Flaviviridae family (155-158). The IRES elements span from nucleotide 40 on 5′-UTR to nucleotide 372 of the viral genome (AUG start codon, 342-344) (159-161) [see figure 1-1(162)]. This secondary structure contains two major domains (domains II and III) and one accessory domain (domain IV) around AUG start codon. Domain I and II are able to form stem-loop structure, and domain IV has the potential to make a small stem-loop (163). Domain III contains 5 branching hairpin stem-loops (a, c, d, e and f) (163). Stem loop IIIc, two very conserved areas on stem loop IIId ($U_{264}UGGGU_{269}$) and stem loop IIIe ($G_{295}AUA_{298}$), are specifically important for attachment to 40S ribosome (164). The specific interaction of these stem loops with the IIIf is extremely important for the attachment of IIIf to 40S ribosome. This interaction forms a binary complex with the AUG start codon already placed in the ribosomal P-site (165). Domains IIIa and b provide a platform for the attachment of eIF3 (166). Domain II contains two stem loops (IIa and b) from which IIb is attached to 40S subunit. This interaction is not important for the recruitment or attachment of eIF3 and ternary complex (154, 155) and is mostly downstream to formation of 48S complex; however, it is essential for conformation

change in 40S ribosome that results in opening of the mRNA entry channel to accommodate HCV open reading frame (167, 168). In addition, domain II has an important role for efficient subunit joining and formation of 80S ribosome for elongation process (169).

Regulation of IRES dependent translation of HCV RNA is most likely mediated by viral factors rather than host factors. Core protein has been proposed to inhibit HCV RNA translation possibly by binding to $U_{264}UGGGU_{269}$ area of stem-loop IIId (170). The amino acids 34-44 on core have been shown to interact with IRES (171). Some reports have proposed that RNA-RNA interaction may inhibit HCV RNA translation (172).

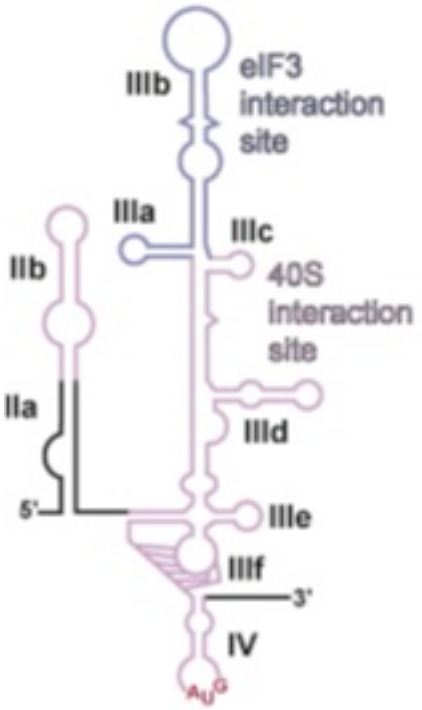

Figure 1-1. Secondary structure of the HCV IRES RNA with individual domains (II–IV) indicated. The 40S subunit is in pink, eIF3 and the ternary complex in blue and AUG start codon in red. Taken from (162) with permission.

B. 2. Translation of HCV ORF and polyprotein processing

As it was discussed earlier, the translation of HCV-ORF produces a polyprotein with about 3011 amino acids, which is processed to 10 mature structural (core, E1 and E2) and non-structural (P7, NS2, NS3, NS4A, NS4B, NS5A and NS5B) proteins by cellular and viral proteases (Figure 1-2). The hydrophobic amino acid residues between positions

173-191 are recognized as a signal peptide, which direct the polyprotein chain to the ER membrane and induce the downstream E1 region into the ER lumen. The ER membrane protein complex, signal peptidase (SP) cuts the bounds between amino acids 193-194 (core-E1), 383-384 (E1-E2), 746-747 (E2-P7) and 809-810 (P7-NS2) and releases core (P23), E1, E2, P7 proteins. Core is later processed more and the signal peptide attached to its C-terminal is separated by signal peptide peptidase (SPP) to form mature core (P21). NS2-3 and NS3-4A viral proteases further process the polyprotein by cutting the bounds between amino acids 1026-1027 (NS2-NS3), 1657-1658 (NS3-NS4A), 1711-1712 (NS4A-NS4B), 1972-1973 (NS4B-NS5A), 2420-2421 (NS5A-NS5B) and release NS2, NS3, NS4A, NS4B, NS5A and NS5B proteins (150).

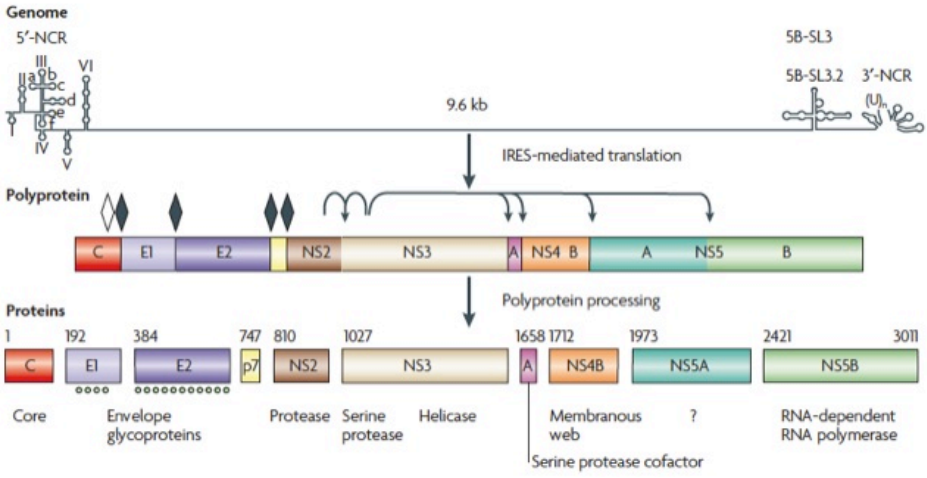

Figure 1-2. The 9.6-kb positive-strand RNA genome is schematically depicted at the top. Simplified RNA secondary structures in the 5'- and 3'-non-coding regions (NCRs) and the core gene, as well as the NS5B stem-loop 3 cis-acting replication element (5B-SL3) are shown. Internal ribosome entry site (IRES)-mediated translation yields a polyprotein precursor that is processed into the mature structural and non-structural proteins. Amino-acid numbers are shown above each protein Solid diamonds denote cleavage sites of the HCV polyprotein precursor by the endoplasmic reticulum signal peptidase. The open diamond indicates further C-terminal processing of the core protein by signal peptide peptidase. Arrows indicate cleavages by the HCV NS2–3 and NS3–4A proteases. Dots in E1 and E2 indicate the glycosylation of the envelope proteins (4 and 11 N-linked glycans, respectively, in the HCV H strain). Taken from (173) with permission.

B. 2. 1. Core Protein

Immature complete core protein (P23) is primarily released from N-terminus of the polyprotein precursor by signal peptidase cleavage at Alanine-191 (174). This P23 core contains hydrophobic residues of signal peptide at its C-terminus, which anchors it to the ER membrane (174). Further cleavage of P23 by signal peptide peptidase at cytosolic side of ER, dissociates the mature form of core (P21) (174). This process occurs somewhere between amino acids 173-182 (175) (the exact cleavage site is unknown) and is necessary for the transport of core into the lipid droplets (see below) (176). It has been shown, that cleavage by SP and formation of P23 is a prerequisite for cleavage by SPP and formation of P21 (176, 177).

Core is a polymeric protein (178, 179). Based on hydrophobicity of amino acids, P21 can be divided into two domains. N-terminal domain I (D1) consists of 117 amino acids with highly conserved pattern of basic amino acids which have a relatively positive charge at physiologic pH and are believed to attach to the negative phosphate backbone of RNA (180-182). The domain II (D2) region begins at amino acid 118 and is believed to attach to the surface of ER membrane (and lipid droplets membrane) as deletion of D2 abrogates the attachment of core to lipid droplets (183, 184).

The structure of core protein mediates encapsidation of viral RNA and formation of viral nucleocapsid. It has been shown that core protein is capable of assembling to a nucleocapsid like particle in the presence of RNA (185); however, only the D1 has the necessary structural element for this assembly (185). D1 region contains three conserved clusters of highly basic amino acids (Arginine and Lysine) with positive charge that are located from amino acids 6-23, 39-74 and 101-117 (186). The 10 arginine and lysine residues located between 39-62 are highly conserved and can be a specific location for attachment to RNA (186). Truncations of either cluster 1 (amino acids 6-23 contains seven basic amino acids) or part of cluster 2 (39-64 contains 10 basic amino acids) abolishes the ability of core to assemble the RNA into a nucleocapsid particle (180, 182) and when their residues are mutated with alanine (non basic non-charged amino acids), this ability diminishes as more basic residues are mutated. In contrast, the non-basic residues are dispensable for interaction with RNA and assembly of nucleocapsid (180).

While the notion that core binds to RNA is well established, several groups have investigated whether HCV preferentially binds to its genomic RNA over host RNA or whether there is a specific sequence of RNA which interacts with core. Due to the RNA secondary structure, core can effectively bind to rRNA (187), tRNA (185) and genomic RNA (181, 185) and fails to assemble into a nucleocapsid like structure when it is

incubated with linear or denatured RNA (185). Indeed core binds tightly to 5′-UTR of HCV RNA (with extensive secondary structure) and this interaction suppress the translation of the RNA(188). But how does core specifically package HCV genomic RNA? One possibility is that HCV core has higher affinity for its genomic RNA. This possibility is still controversial as one group has shown evidence in favor of this hypothesis (181) and another group has reported that core doesn't have enough specificity in its binding to genomic RNA (187). On other possibility is that assembly occurs in a microenvironment, which only a single species of RNA (it is HCV RNA) is present. The possibility that nucleocapsid assembly takes place in a vicinity of lipid droplets (where HCV core resides) and the replication complex (where new HCV RNA is synthesized) has been extensively tested recently and will be discussed later.

The D2 contains two amphipathic α-helices (H1 and H2) and putatively is responsible for core attachment to LDs (189). The structure and interaction of D2 with LDs will be discussed separately (see C. 3. 4. 3 Role of Lipid Droplets in HCV Assembly). Apart from attachment to LDs, D2 is also important for proper folding of D1. Indeed D1 lacks stable secondary structure and shows a random coil without D2, therefore lack of D2 or any defects in proper D2 folding may create misfolded D1 protein and degradation (190). This lack of stable secondary structure in D1 has been one of the focuses of several researchers trying to link this property of D1 to the ability of core protein interacting with a wide variety of proteins and cellular pathways. They have proposed that D1 might be related to intrinsically unstructured proteins (IUP), a family of proteins, which lacks stable secondary and tertiary structure, and they obtain a specific conformational change based on the protein they are interacting with or based on physiologic or environmental conditions. Based on amino acid similarity with other intrinsically unstructured proteins, charged hydrophobicity and circular dichroism, it has been proposed that the first 82 amino acids (C82) is in the region of intrinsically unstructured proteins and forms a random coil lacking apparent secondary structure (191). In another attempt, the possibility of change in C82 structure in various environmental conditions was investigated and was shown that changing pH or addition of salt or detergent didn't alter the C82 structure (192). But 2,2,2-trifluro-ethanol that produce a hydrophobic environment similar to the one found in membrane or during interaction with another proteins, induces α-helical structure in C82 (192). Although this hypothesis looks appealing, but the nature of core interaction with other proteins still remains unknown.

Dimerization (and probably polymerization) of core is important for nucleocapsid formation. Mutation analysis in Huh7.5/JFH1 system has revealed a very interesting disulfide bound core dimerization site at Cys-128(193). The Cys-128 residue belongs to

the hydrophilic side of helix I of D2 (see below), which is expected to interact with the membrane interface hydrophilic plane. This interesting site is not only a core dimerization site, but also is expected to be critical for proper configuration of D1 and D2 of core protein in HCV nucleocapsid structure. D1 should be located at the inner surface of the capsid to interact with RNA and D2 at the outer surface of capsid close to lipid membrane surface where it interacts with lipid bilayer originating from host cell. The mutation of Cys-128 completely abolishes this configuration. Yet when the cell is infected by HCV, and the nucleocapsid is released from endosome, this disulfide bond can be easily cleaved under cytoplasmic reducing conditions, which disassembles nucleocapsid and releases the RNA (193).

As it was indicated earlier, core is primarily found in the cytoplasmic compartment of ER membrane and LDs. But core or part of core has been located in nucleus and mitochondrial outer membrane as well (194, 195), which may be necessary for the regulation of cellular events such as growth, carcinogenesis, bioenergetics, apoptosis, etc. Presence of core protein in nucleus was initially reported in the hepatocytes of a chronically HCV infected cells (196). Truncated form of core has been found at nucleus of tumor cells in HCV related HCC (196, 197). By expressing HCV core, it was shown that the truncated form of core (D2 was removed) is localized in the nucleus (198), while full length core was localized in cytosol (198-200) but when expression levels were high it could be detected in nucleus as well (199). Using Huh7.5/JFH-1 cell culture system, core protein has been found in nucleus at early stage of infection but exported out rapidly (197). To enter and exit nucleus, core is assumed to contain nuclear localization signal (NLS) and nuclear export signal (NES). Indeed, three NLS sites have been proposed and identified in amino acids 5-13, 38-43 and 58-71 all at D1 region (197). Recently, it has shown that core protein contains a functional NES region in the amino acids (109-133), which may facilitate its export from the nucleus (197). It is not clear how a membrane-bound protein is able to transfer to nucleus. In addition, the in-vivo existence of truncated form (which is not bound to a membrane) is still debated. The possibility that core or a part of core translocates to nucleus and directly or indirectly regulates events, which are involved in carcinogenesis or expression of protein, can be speculated although no solid evidence is still available.

In addition, core protein (and NS3/4A) can be partially localized to the outer membrane of mitochondria and particularly at contact points between mitochondrial outer membrane and ER (defined as mitochondria-associated membrane) (195). The mechanism responsible for translocation of core (and NS3/4A) from ER to mitochondrial outer membrane is not clear; it is possible that it occurs during transient fusion of different

membranous sub-compartment (195). This translocation of core (and NS3/4A) may contribute to mitochondrial dysfunction and elevated ROS production associated with HCV infection (201). HCV protein expression is associated with inhibition of complex I (NADH dehydrogenase also called NADH/ubiquinone oxidoreductase), reduced mitochondrial transmembrane potential and the oxidative phosphorylation efficiency and generation of ROS (201). These changes are correlated with enhanced Ca^{2+} influx into the mitochondria. Indeed Ca^{2+} transport imbalance might trigger all the effects discussed above. Enhanced entrance of Ca^{2+} into mitochondria increases the positive charge and decreases mitochondrial transmembrane potential and reduces the energy transferred to ATP synthase from proton influx. In addition, high levels of mitochondrial Ca^{2+} inhibit complex I directly or indirectly (by activation of nitric oxide synthase and thereby releasing $NO^{\cdot}$) and enhance ROS production. Under physiologic conditions, Ca^{2+} concentration inside cells is kept very low, as Ca^{2+} is able to activate variety of signal transduction pathways. Ca^{2+} is generally stored and sequestrated inside the ER by action of ER calcium channels. At the mitochondria associated membrane, release of Ca^{2+} enable other calcium channels (calcium uniporter and voltage dependent calcium channels) on internal mitochondria membrane to open and Ca^{2+} flux into the mitochondrial matrix. It has been shown that mitochondrial alteration (Mitochondrial Ca^{2+} overload, inhibition of complex one and dissipation of mitochondrial transmembrane potential) elicited by HCV protein expression is completely prevented if cells are incubated with ER calcium channel inhibitor (201). Impaired oxidative phosphorylation pathway during HCV infection shifts the production of ATP to glycolysis to compensate the imbalance of energy production and possibility of ROS formation. Indeed, substitution of glucose with galactose in media (to force the cells to rely only on glycolysis), resulted in significant reduction in ATP contents of the cells expressing core(202). High Ca^{2+} concentration, ROS and reactive nitrogen species are able to induce opening of mitochondrial permeability transition pore and release cytochrome c and pro-apoptotic factors, which initiate apoptosis (201). Although it is proposed that low ROS production level is in favor of HCV life cycle and is not extremely harmful for cells, it may lead to accumulation of DNA mutation and ultimately HCC (as it was discussed earlier). The ROS production is important in pathogenesis of HCV related liver disease as it promotes liver fibrogenesis through activation of hepatic stellate cells cells (see Pathophysiology of liver fibrosis) and also act as the second hit in pathogenesis of accelerated liver fibrosis in a liver with steatosis (a common feature of HCV infected liver).

HCV core is also believed to be important for formation of HCV-related steatosis. Several mechanisms have been suggested and it will be discussed later.

B. 2. 2. Envelope Protein 1 and 2 (E1 and E2)

Two envelope proteins (E1 and E2) are membrane type of glycoproteins, which are released from the polyprotein by host signal peptidase. The heavily glycosylated E1 and E2 are about 35 kDa and 70 kDa respectively (203, 204) and are composed of a large N-terminal ectodomain and a small [<30 amino acid (aa)] C-terminal transmembrane domain (TMD) contains hydrophobic residue, which anchor them to the membrane (205). E1 and E2 form non-covalent heterodimers and are involved in virus entry (206). E2 plays a major role in the interaction between virus and its major cellular receptors (see HCV entry), while the role of E1 is less clear but is believed to be a class II virus membrane fusion protein (206).

TMD in E1 and E2 is composed of two hydrophobic membrane-spanning stretches (residue 354-379 and 718-742 in E1 and E2 respectively) separated by a short segment containing at least one fully conserved positively charged amino acid (205, 207, 208). The hydrophobic stretches are important for α-helix-α-helix interaction and formation of E1-E2 heterodimer and alanine mutations in these areas abolish the formation of heterodimers (207). The signal sequence of E1 and E2 are present at the C-terminus of the immature form of capsid (P23) and second half of the hydrophobic stretch in TMD structure of E1 (209). Membrane topology of TMD in E1 and E2 has been recently studied. When E1 and E2 are expressed alone or in conjunction, TMDs exhibit a single membrane spanning topology. In contrast, the downstream of signal sequence in E1 and E2 has to be cleaved by signal peptidase at the luminal side of ER, TMDs form a hairpin topology with charged residues in the middle and facing cytosol. It has been shown, after cleavage of signal sequence by SP, a change in the orientation of second stretch of hydrophobic residues occurs leading to a single TMD topology (210).

N-terminal ectodomain of E2 (specifically residues 480-493, 528-535 and 544-551) interacts with cellular receptors (specially CD81, see follow) that are involved in HCV entry (211-213). In addition several highly conserved individual amino acid residues (Tryptophan 420 and 529, Tyrosine 527, Glycine 530 and Aspartic Acid 535) are critical for interaction between E2 and CD81 (213). Furthermore, mutation between amino acids 612-620 and antibody directed to amino acids 412-423 and 432-447 abolishes CD81 binding (214). Hypervariable region-1 (HVR-1) on E2 is an important feature of hepatitis C and assists the virus to escape from host immune responses (215). In spite of the high sequence variability, structural conformation of this segment is highly conserved. This area is involved in virus interaction with another host receptor scavenger receptor class B type I (SR-BI) in vitro, although this role in vivo remains to be confirmed (216).

E1 is thought to act like a Class II membrane fusion protein. Class II membrane fusion proteins have been widely studied in Flaviviridae viruses and have important roles for the fusion of endosomal membrane (contain virus) and viral lipid envelope. During pre-fusion period, E2 ectodomain covers the E1 ectodomain and prevents the membrane fusion. In endosome, low pH dissociates E1 from E2 and releases the E1 to form E1-trimer. Also low pH triggers the viral membrane to form a loop toward the endosomal membrane. The E1-trimers attach to the endosomal membrane and pull the membranes toward each other until they fuse (217, 218).

N-Glycosylation of E1 and E2 is a post-translational modification that maturates the envelope proteins. The addition of N-linked oligosaccharides is mediated by oligosaccharyltransferase which transfers a pre-synthesized $Glucose_3$-$Mannose_9$-Glucose-$Nacetylglycosamine_2$ from a membrane-associated donor, oligosaccharide-pyrophosphodolichol (219), to Aspargine residue in a tri-peptide sequence Aspargine-X-(Serine/Threonine), where X is any amino acid except for Proline. Although this sequence is preliminary for N-glycosylation, not all the potential sites are glycosylated (220). Four and eleven glycosylation sites have been defined in E1 and E2 respectively. These glycosylation may play a role in the HCV life cycle as deletion and mutation of some the glycosylation site alters the infectivity of HCV (220-222).

B. 2. 3. P7 Protein

The HCV P7 protein is s small (6.7 kDa) hydrophobic protein and is believed to be an ion channel as it is capable of mediating cation flow across artificial membranes (204, 223). P7 channel activity is mostly potassium and sodium-selective and presence of calcium modifies this selectivity (224). These properties are very similar to characteristics reported for a group of proteins called viroporins (225). Viroporins are viral encoded proteins comprised of 60-120 amino acids that interact with membrane and modify the membrane permeability to ions or other molecules (225, 226). The mature form of P7 is liberated by cleavage between E2-P7 and P7-NS2, which is mediated by SP. In contrast to most of cleavages in polyprotein precursor, cleavages at E2-P7 and P7-NS2 sites are delayed resulting in the formation of a E2-P7-NS2 precursor protein (227-229). In addition cleavage at P7-NS2 site is complete and occurs first while the cleavage at E2-P7 site is incomplete resulting in formation of E2 and stable E2-P7 precursors (227, 228). Presence of both E2 and stable E2-P7 species suggests that it may regulate the generation of P7 monomer and later oligomer complex (230). After cleavage from polyprotein, P7 is localized on ER membrane (231) and the initial results indicating the presence of P7-GFP on mitochondrial membrane (232) was later shown to be the result of addition of GFP or tags (233).

Structurally P7 monomer is formed by 63 amino acids. It is composed of two hydrophobic TMDs (spanning amino acids 19-32 and 36-58), separated by a short cytoplasmic positively charged loop formed by a dibasic motif (Arginine-33 and Lysine-35), positioning the N and C-terminus of the protein toward the ER lumen (232, 234). An α-helix is attached to the N-terminal side of TMD-1 through a short turn formed by Histidine-17 (235). Early electron microscopy studies suggested a hexameric or heptameric flower-shaped structure for P7, with a lumen of about 3-5 nm and six protruding petals oriented towards ER lumen. For formation of this hexamer, the C-terminus of TMD-2 is thought to interact with adjacent TMD-1 and N-terminal helix (236). Amino acids in N-terminal helix are oriented toward the hexamer channel pore and would most likely mediate the channel gate or drug-binding site (236). It is believed that P7 opening and closure is pH dependent and based on the ability of its side chain to gain and lose protons, Histidine-17 (at the junction of α-helix and TMD-1) is suggested to be the key residue for pH-based controlling of the gate (237). The Alanine mutation at this residue, significantly reduce the P7 function (235). The hydrophilic positively charged cytosolic loop is highly conserved among various genotypes and contains Arginine-33 and Lysine-35. This loop is believed to contain the membranotropic region, which induces change in membrane and, also in the presence of phospholipids, exhibit a high tendency to oligomerize (232). Mutation at these sites abrogates ion channel function without effect on localization of protein (232, 238, 239). Mutation of the Arginine-33 and Lysine-35 with Alanine, blocks the HCV particles production in culture and replication in chimpanzees (238). In addition, the hexamer model predicted that Arginine and Lysine side-chains protrude into the lumen of hexamer perhaps forming a gate for controlling the lumen (236).

Whether P7 acts as an ion channel or not and the exact role of P7 in HCV life cycle is not perfectly understood. Based on the current knowledge, P7 is dispensable for HCV RNA replication or HCV entry as both of these processes can occur in the absence of P7 efficiently (238, 240). In contrast, the presence of active P7 is mandatory for HCV assembly through its interaction with NS2 (see C. 3. 4. 3 Role of Lipid Droplets in HCV Assembly). Partial or complete deletion of P7 or different point mutations reduces and/or ablates the production of infectious virus particles (241). In addition it also profoundly changes the ratio between cell-associated infectious particles and released particles indicating that both assembly and release of viral particles requires P7 (242). It has been proposed that as an ion channel, P7 prevents formation of pH gradient between several compartments that are required for virus production. The role of P7 in maintaining acidification has been demonstrated as P7-containing vesicles equilibrates pH more rapidly than vesicles lacking P7, when sudden pH shifts occurs (243). E1 and E2 glycoproteins are sensitive to acidic pH and especially E2 membrane may adopt

fusogenic conformation prematurely at acidic pH. Therefore P7 possibly protects E1 and E2 from pH changes during assembly and release of particles (236). The role of P7 in virion assembly will be discussed later.

B. 2. 4. Non-Structural Protein-2 (NS2)

NS2 is a 23-kDa non-glycosylated integral membrane protein, extended from amino acid 810 to 1026 on polyprotein (244, 245). It is liberated on the N-terminal side from adjacent P7 by host signal peptidase and on the C-terminal side from NS3 by NS2/3 protease activity (246). The protein is divided into two domains: N-terminal membrane-binding domain (residue 1-94) that is not required for protease activity and C-terminal domain (residues 95-217) with the 181 N-terminal amino acids of NS3 forms the NS2/3 protease (247, 248). After release from polyprotein, NS2 protein is localized to ER membrane (249).

The N-terminal membrane-binding domain of NS2 protein is highly hydrophobic and is believed to contain three transmembrane domains (TMDs) that anchor the NS2 to ER membrane(249) (figure 1-3). The exact topology of these three TMDs is not perfectly understood, but based on physicochemical properties of N-terminal residues, a model has been proposed (249). Based on this model, the first TMD (residue 1-23) clearly forms an α-helical membrane-spanning TMD. Due to the presence of charged and polar amino acids, transmembrane orientation of the amphipathic α-helix in TMD-2 (residue 27-49) is only possible if interaction with a complementary TMD neutralizes these charged residues. This interaction is believed to be partly with TMD-3 and in some extent TMD-1. TMD-3 (residues 72-94) is believed to form three α-helices, all are required for membrane targeting. TMD-3 is believed to interact with E1 and E2. The TMD-1 and -2 and TMD-2 and -3 are connected to each other through a small cytosolic loop (residues 24-26) and a luminal segment (residue 50-71) respectively (249). In general as we will discuss later, the presence of the membrane-binding domain is required for early steps of virion assembly.

The NS2 protease domain has two parts. The N-terminal side part contains two antiparallel α-helices (H1 and H2) and a turn loop that connects the H1 and H2. The C-terminal region contains an extended linker and a four-stranded antiparallel β-sheet (250). Although the first 181 N-terminal amino acids of NS3 are mandatory for NS2 protease activity, this does not contain the NS3 catalytic activity (244, 248). Therefore, catalytic activity of this residue is referred as NS2/3.

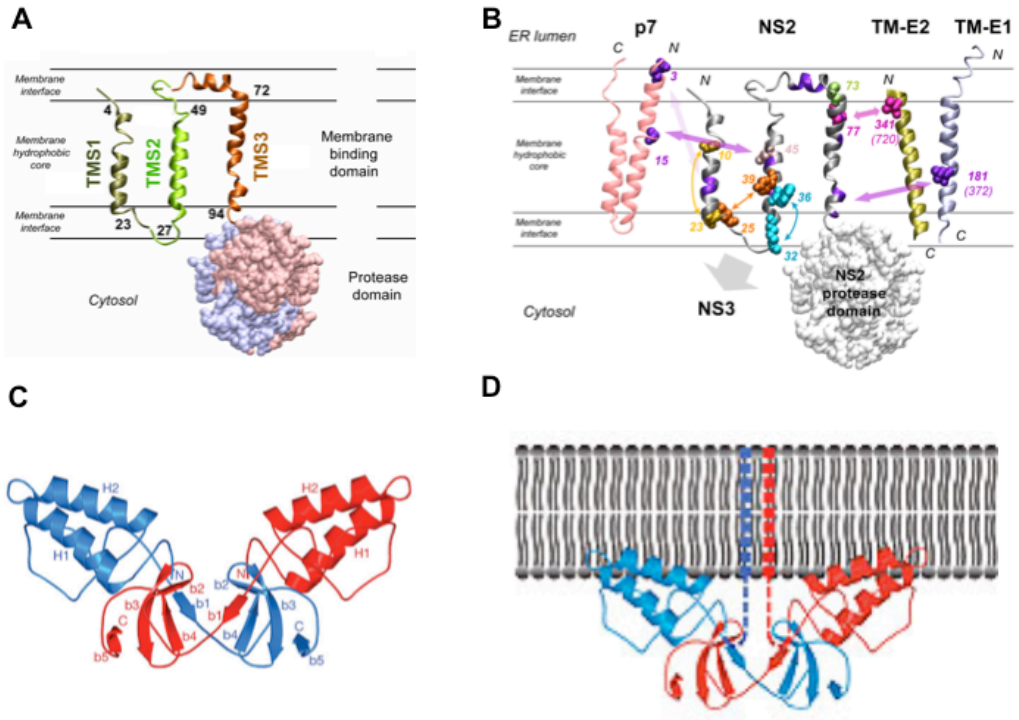

Figure 1-3. A. Model of NS2 membrane topology. TMS 1, 2 and 3 are shown in ribbon representation and colored bronze, green and copper, respectively. The TMS are tentatively positioned in the membrane and the limits of transmembrane helices are given (TMS1, 4–23; TMS2, 27–49; and TMS3, 72–94). **B**. Summary of interactions within NS2 and with HCV proteins as deduced from the genetic analysis. The structural models of NS2, p7, the transmembrane domain of E1 (TM-E1) and E2 (TM-E2) are represented as ribbon. **C.** Ribbon diagram showing the NS2 dimer with one monomer in blue, the other in red. The N and C termini, and secondary structure elements of each monomer, are indicated. **D.** Ribbon diagram of the NS2 dimer positioned relative to the membrane. Taken from (249) and (250) with permission.

NS2 is a cysteine protease with classic triads of Cysteine, Histidine and Glutamate in catalytic pocket (250). As the NS2/3 activity is Zinc-dependent, it was classified as a zinc metalloprotease, but later it was shown that zinc is only important for proper positioning of residues involved in catalytic activity and indeed NS2/3 is not a metalloproteinase (244, 251). Cysteine-97, -99 and -145 and Histdine-149 in the N-terminal region of NS3 (not NS2), participates in coordination of zinc molecule and mutation in these sites abolishes both NS2/3 and NS3 catalytic activity, probably by disrupting the proper folding of these

proteins (244, 252, 253). This suggests that N-terminal residue of NS3 might be required for NS2/3 proper configuration and zinc might regulate this process.

Crystal structure of NS2 has been revealed and it has been shown that NS2 is a dimer and the cleavage between NS2 and NS3 is performed by dimers of NS2 (and the attached NS3) encoded by adjacent polyprotein chains. The N-terminal region of one monomer interacts with a C-terminal region of the other monomer to form a dimer that resembles a butterfly in which the N-terminal regions of the two monomers lie relatively close to each other and C-terminal regions are positioned at opposite sides (figure 1-3). The residues that are critical for dimerization are Methionine-170, Isoleucine-175 and -201, Aspartate-186 and Valine-162. The catalytic triad is formed by Histidine-143, Glutamate-163 from one monomer and Cysteine-184 from the second monomer all located at the linker. The sulfur atom on Cysteine-184 mediates the nucleophilic attack required for protease activity of NS2/3 protease. Two other highly conserved amino acids are also critical for catalytic acid, Proline-164 that bends the peptide backbone of adjacent Glutamate-163 to contact the side chain of Histidine-143 and Leucine-217 that serves as part of oxyanion hole. As it was discussed above, the N-terminal of NS3 also has a role for proper folding for NS2 and correct geometry of catalytic site and zinc play an important role in this process.

Although NS2/3 activity solely liberates the NS2, the role of NS2 protein is not completely known. What is the advantage for the virus to encode two distinct proteases?

Several roles have been implicated for NS2. One of the unique features of NS2/3 is that the release of NS2 inhibits NS2/3 protease activity and consequently NS3 release. Therefore it has been proposed that the presence of NS2 may regulate the release of NS3, which is the major protease for polyprotein processing (254). In addition, NS2/3 activity (not NS2 alone) has been shown to be important for the hyperphosphorylation of NS5A (P58, see NS5A); therefore, by modulating NS2/3 activity, NS2 might control the formation of P58 (255). Furthermore, NS2 exerts an inhibitory effect on a variety of promoters involved in gene expression such as INF-β, CXCL10/IP-10. The amino-terminal (amino acid 1-130) is sufficient to cause this effect (256). This aspect of function needs more confirmation. Another possible role is that NS2 may inhibit apoptosis by preventing cytochrome C release from mitochondria. Furthermore, it has been shown that NS2 expression also sequesters a cell death activator CIDE-B and thereby prevents the formation of CIDE-B dimer, a mandatory process for its localization on mitochondria and activation of apoptosis (257). Finally, expression of NS2 protein in Huh-7 (transient) and

HeLa (stable) found to associate with 40-50% decrease in cell growth and cell cycle arrest in S-phase (258).

Recently an important role has been found for NS2 and it has been shown that it may orchestrate the assembly of the virus. This role explains the main reason for presence of NS2 and will be discussed later (see C. 3. 4. 3 Role of Lipid Droplets in HCV Assembly).

B. 2. 5. Non-Structural Protein-3 and 4A (NS3 and NS4A)

NS3 protein is a 70 kDa multifunctional protein composed of 631 amino acids with protease activity (resides 1-188) and RNA helicase activity of the DExH family (residues 189-631). NS3 form a non-covalent complex with its cofactor NS4A that directs the localization of NS3 and modulates its enzymatic activity. The NS3 protease is responsible for the cleavage of non-structural proteins downstream to NS2-NS3. The first cleavage occurs in cis at NS3/NS4A site followed by trans cleavages at NS5A/NS5B, NS4A/NS4B and finally NS4B/NS5A sites. The biological function of RNA helicase is not clear yet, but RNA folding/remodeling, enhancement of polymerase processing (see NS5B) and genome encapsidation have been proposed (204, 240, 259).

NS3 protease is a serine protease and its protease domain is very similar to trypsin/chemotrypsin protease family with two β-barrel subdomains that are flanked by two short α-helices (252, 260). The first α-helix (α_0, residue 12-23) is mostly hydrophobic and interacts in plane with cytosolic leaflet of the ER membrane (261) and is followed by the first β-barrel subdomain that is formed by eight strands of β-sheets from which one is from NS4A (262). The second β- barrel subdomain (residue 93-180) is formed by six strands and is followed by the second α-helix that is highly conserved (262). The active site is composed of a classic catalytic triad, formed by Serine, Histidine and Aspartate at positions 139, 57 and 81 respectively (263, 264) and an oxyanion hole formed by backbone amide of Glycine-137 and Serine-139. Structure of NS3 (and also NS2/3 as it was discussed earlier) is stabilized by Zinc ion that is coordinated with Cysteine-97, -99, -145 and Histidine-149 (Zinc binding site) (264). The catalytic site can accommodate 10 residues and the consensus cleavage sequence Aspartate/Glutamate-X-X-X-X-Cysteine/Threonine | Serine/Alanine-X-X-X is required for cleavage at "|" sign (264, 265). However it has been shown that this is a complex scenario as vast numbers of host proteins display this consensus sequence and only a few are cleaved by NS3. On the other hand, the identified cellular substrates such as mitochondrial antiviral signaling protein (MAVS), T-cell protein tyrosine phosphatase (TC-PTP), TIR domain-containing adaptor inducing IFN-β (TRIF) do not show the classic canonical cleavage site [reviewed in (265)].

By revealing the structure of the NS3 protease, pharmaceutical companies have designed molecule that inhibits the catalytic action of NS3 (see direct acting antiviral drugs). Most of these inhibitors are competitive with the substrate and targets substrate-binding sites. As it was discussed earlier, two groups of NS3 inhibitor are developed or currently under development; macrocyclic compounds and linear ketoamide. Electrophilic α-ketoamide group at the scissile bond can react with Serine-139 to from a covalent bond that is reversible (266, 267). The major obstacle for the development of an ideal NS3 inhibitor is the appearance of a drug-resistant mutant. As it will be discussed, the NS5B RNA polymerase activity has low proofreading activity and introduces mutants that can actively survive. Mutants capable of surviving and replicating efficiently in the presence of the inhibitor will then be rapidly selected. By studying these mutants, numerous positions of NS3 protease contributing resistance to inhibitors are found. Many of these residues are quite far from the substrate-binding pocket (264). How these mutations, far from the active site, introduce resistance to an inhibitor, which interacts with catalytic site, has been recently hypothesized as the "substrate envelope hypothesis" (268-270). According to this hypothesis, the inhibitor envelope (the area that the inhibitor attaches to the enzyme) exceeds substrate envelope (the area where the envelope attaches to the enzyme). Therefore mutation in the areas that specifically are in the domain of the inhibitor envelope may influence the attachment efficiency of the inhibitor without any significant effect on the substrate attachment. Recently it has shown that many amino acid residues involved in drug resistance do not interact directly with the substrate while they are mostly in the area of inhibitor envelope. These data confirm the "substrate envelope hypothesis" for NS3 protease (270).

The NS4A protein is a 6 kDa polypeptide containing 54 amino acids. It acts as a cofactor for NS3 protease activity by mediating the proper folding of the protein and also the membrane association of NS3/4A complex (271). It contains 4 distinct areas. N-terminal hydrophobic domain (amino acids 1-21) forms an α-helix with high number of hydrophobic residues that is inserted to anchor the NS3/4A to ER membrane (262). The central portion (residues 22-32) forms a β-strand that interacts with two β-strands from the first β-barrel of NS3 protease and is critical for the cofactor effect of NS4A. The cofactor function of the central part of NS4A is largely due to its effect on proper orientation of catalytic triad. These areas are followed by a kink (residues 33-39) and a highly conserved C-terminal region. The C-terminal acidic residue has been shown to act as a dynamic regulator of NS3/4A interaction, and also NS5A hyperphosphorylation (262).

The C-terminal part of NS3 (NS3 helicase, NS3h) is a member of the superfamily-2 DExH/D-box helicase. Its action is essential for HCV RNA replication and also plays a

role in viral assembly, although its precise function in viral life cycle remains elusive. NS3 helicase binds to and unwinds both DNA and RNA in vitro expending ATP for this action and requiring Mg^{2+}. As it was indicated, the exact biological function of NS3 helicase in HCV life cycle is not clear, but it is essential for RNA replication, which makes the idea of developing inhibitors very appealing. Unfortunately, NS3 helicase lacks specificity and it does not recognize specific RNA sequences. In addition, NS3 helicase interacts more actively with DNA rather than RNA. Therefore it may be difficult to find molecules that bind to NS3 specifically that doesn't inhibit other helicases. Indeed no inhibitors of NS3 helicase have entered clinical trials yet (272, 273).

B. 2. 6. Non-Structural Protein-4B (NS4B)

NS4B is a 27 kDa membrane polypeptide with 261 amino acids with high hydrophobic characteristics(204, 259). This hydrophobic character and the association of NS4B with membrane make this protein extremely difficult to study and in fact among the HCV proteins, NS4B is the least characterized. This protein is liberated from polyprotein by NS3 protease activity (204, 259). As it was discussed earlier, the polyprotein processing occurs in a stepwise order with NS4A-NS4B and NS4B-NS5A cleavages being cleaved last (204, 259).

After cleavage from polyprotein, NS4B is co-localized with other non-structural protein in a specific structure on ER called membranous web (274, 275). Majority of the protein structure is faced toward the cytosol (275). Structurally, presence of at least two TMDs has been confirmed, although based on characteristics of amino acid residues, it is believed that NS4B contains 4 TMDs (276). On the N-terminal side of TMDs, two amphipathic helices (residues 6-29 and 42-66) and on the C-terminal one amphipathic helix (residues 229-253) are formed (277, 278). Alanine mutations at these sites abolish the membrane association of NS4B and formation of membranous web(278). Membranous web is aggregates of ER membrane vesicles that is formed after infection by the majority of plus-strand RNA virus (such as HCV) and is believed to provide a lipid raft around replication complex and protect the HCV RNA from degradation by cellular nucleases (279). The presence of membranous web was detected initially by electron microscopy during HCV replication, and was shown to be NS4B dependent (279, 280). Expression of NS4B alone can induce membrane alteration seen for membranous web formation (276, 280). Therefore, it is now confirmed that NS4B is mandatory for this process and its highly hydrophobic structure and tight association with ER membrane also confirms this role. How NS4B morphologically alters the ER membrane for membranous web formation remains to be elucidated, but it has been hypothesized that this process requires energy further validated by the presence of ATP-binding consensus

in the NS4B sequence (281). In addition it has been shown that NS4B can recognize the 3'- terminus of newly formed minus-strand HCV RNA and possibly act as a scaffold that hold the minus-strand RNA for formation of plus-strand genomic RNA of HCV (281). These rationales provide more support for the specific role of NS4B in HCV replication and replication complex formation.

Other roles have recently been suggested for NS4B such as anti-apoptotic effect (and hence development of HCC) (282) and modulation of NS5B polymerase activity(283), but they are less well supported.

B. 2. 7. Non-Structural Protein-5A (NS5A)

NS5A is released from polyprotein by NS3 protease, is a phosphoprotein formed by 447 amino acids (284). This protein exists in two forms during HCV life cycle; a basally phosphorylated form (P56, 56 kDa) and a hyperphosphorylated form (P58, 58 kDa) (285). It is similar to a core protein in which it is involved in multiple cell processes resulting in pathologic sequelae. This protein is part of the replication complex and is crucial for initial assembly of nucleocapsid. As it will be discussed later, the interaction between core and NS5A keeps the lipid droplets in the vicinity of the replication complex, which is required for encapsidation of newly synthesized HCV RNA (C. 3. 4. 3 Role of Lipid Droplets in HCV Assembly). Structurally, NS5A is organized into three domains, which are separated by two series of low complexity sequence (LCS) blocks of repetitive amino acids; LCS1 and LCS2 (284) (Figure 1-4).

Domain 1 (amino acids 1-213) is crucial for attachment to the newly synthesized HCV RNA (286). This domain is further divided to the amphipathic N-terminal helix (AH1), Subdomains 1A and 1B. The AH subdomain (amino acid 1-30) is highly conserved and is absolutely required for membrane localization of NS5A protein. Deletion of this segment abolishes the ER-localization of NS5A and results in predominant nuclear localization of NS5A (287). The nuclear localization of truncated NS5A can be explained by the presence of nuclear localization signal within domain 3, which becomes functional after removal of naturally occurring AH subdomain (288). It appears that the presence of hydrophobic residues in this segment is critical for membrane association of NS5A as disrupting the hydrophobic face by introducing charged amino acids completely abolishes the ER membrane localization of NS5A. Interestingly, these mutations are also associated with significant reduction of HCV RNA replication, suggesting the importance of ER membrane association of NS5A for RNA replication (287). This is consistent in regards to the presence of NS5A in the replication complex (an ER membrane dependent process). Subdomain 1A (amino acid residue 36-100) resides on the N-terminal side of

domain 1 and consists of three anti-parallel β-sheets (B1-B3) followed by an α-helix H2 (AH2) (284, 287). Subdomain 1A actively participates in zinc coordination, which is required for the proper folding of NS5A (287). Four cysteine residues (cysteine-39, -57, -59 and 80) are involved in zinc coordination (287). AH2 and a second stretch of random coil connect subdomains 1A to 1B(284). Subdomain 1B (101-198) consists of six anti-parallel β-sheets (B4-B9) which participate in the structural architecture that is required for attachment of HCV RNA. Structural analysis has suggested dimeric form of NS5A via the contact near the N-terminal ends (Domain 1). The dimeric model of domain I has been suggested. In this model AH1 anchors the two monomers to the membrane and positions the interface between two monomers and the two subdomain 1A close to the membrane. The two domains are facing away from the membrane forming a claw-like structure with domain 1B as two arms. The deep portion of the groove between these two arms is highly basic which is an attractive pocket for RNA-binding. The arms extending out of this groove are mostly acidic and might prevent RNA from exiting in the groove. A model of this dimer has been shown in figure 1- 4 [Reviewed in (289)].

Domain 2 (residues 250-342) structure has not been resolved yet. Presence of low content of hydrophobic amino acids and high content of acidic residues, is in a favor of an extended conformation, therefore it is thought that domain 2 might act as IUPs (290-292). This is consistent with a tendency of NS5A to interact with various cellular protein and pathways. A stretch of 40 amino acids from residues 236-275 mostly on N-terminal of domain 2 have been identified as Interferon Sensitivity Determining Region (ISDR). This area has been shown to prevent the interferon response through inhibition of interferon-inducing Protein Kinase RNA-associated (PKR) (293-295). PKR is an IFN-induced gene product that is essentially activated by binding to dsRNA (produced during RNA virus genome replication) and phosphorylates the eIF-2α, a translation initiation factor required for HCV RNA translation. Phosphorylation of eIF-2α reduces its activity and hence HCV RNA translation (296). Mutants are more sensitive to IFN therapy (293-295). Although the residues on domain 2 of NS5A are less conserved among the various genotypes and majority of domain 2 is dispensable for RNA replication, ten residues are critical and mutations produce lethal or near lethal phenotype. Six of these ten residues are highly conserved (297).

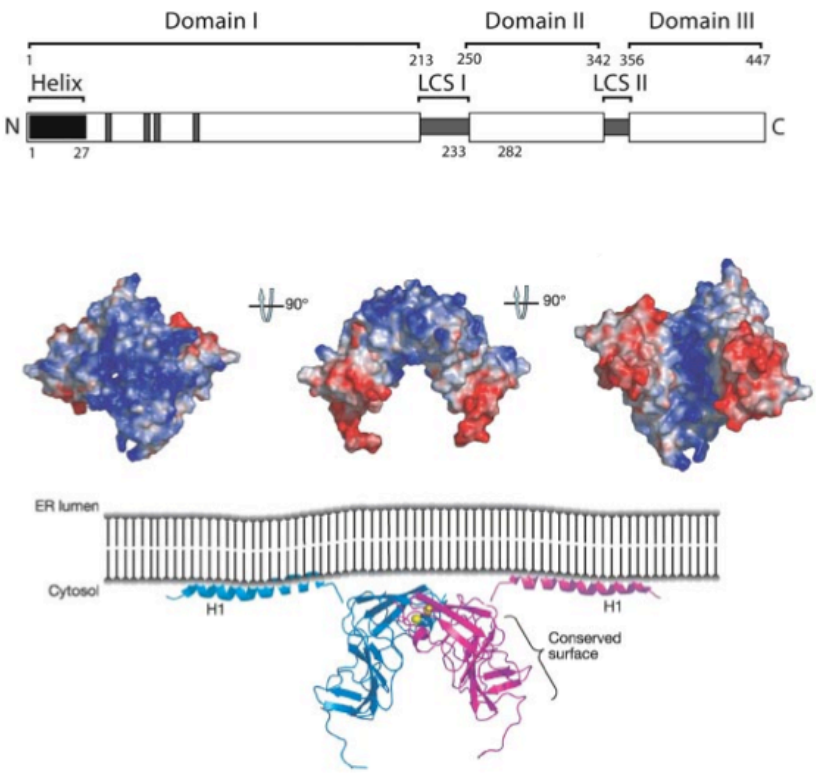

Figure 1-4. A. Schematic representation of the hepatitis C virus NS5A protein. NS5A has been proposed to consist of three domains (labeled domains I, II, and III) with domains separated by low-complexity sequences (labeled LCS I and II). **B.** Surface potential plots of the domain I dimer. **C.** Model of NS5A position relative to the ER membrane. Taken from (289) and (297) with permission.

Domain III (residue 356-447) has been shown to be dispensable for RNA replication but plays a critical role in assembly of infectious virion. Except in the N-terminal region (359-378) where some extended α-helix is predicted similar to domain 2, domain 3 acts as intrinsically unfolded protein (IUP)(298). Domain 3 interacts with core protein to couple the replication process with initial phase of virion assembly. Two clusters of highly conserved serine residues (cluster 3A and 3B) are found on domain 3 which are involved in basal phosphorylation of NS5A (P56) (299). Cluster 3A contains 4 serine residues at positions 2384, 2388, 2399 and 2391 (according to the position within the original JFH-1 polyprotein) and cluster B, contains three serine residues at positions 2428, 2430 and 2433 (299). Apart from phosphorylation sites, the residues in cluster 3B are important for interaction with core. Mutation in at least two positions results in reduction of co-localization with core around LDs and also release of virion, without any impact on replication (299).

In addition to participation in the primary stage of virion assembly, NS5A plays several other important roles in HCV life cycle. As it was discussed above, phosphorylation of NS5A in serine clusters of 3A and 3B form the basally phosphorylated NS5A (P56). Another serine cluster (Cluster 1) is located in the area of domain 1. This cluster contains serines 2194, 2197, 2200, 2201, 2202, 2204 and 2207 and is considered as the hyperphosphorylation site (299). The tight regulation of ratio between P56/P58 is important for HCV RNA replication as lower ratio (higher P58) may arrest HCV RNA replication (300, 301). NS5A can modulate the cell growth. This modulation is mediated through mitogen-activated protein kinase (MAPK) signaling pathway. One of the effects of MAPK signaling pathway is to pass the cells through the restriction point in G1 phase. Down-regulation of MAPK signal by NS5A perturbs the cell cycle in order to facilitate maximal virus replication (302, 303). NS5A also inhibits apoptosis. NS5A attaches and blocks TNF receptor type 1-associated DEATH domain protein (TRADD) and TNF receptor associated factor-2 (TRAF2) and therefore TNF- dependent activation of caspases (304, 305). In addition, a sequence within the ISDR shares homology with the BH domains of anti apoptotic members of Bcl2 family and thus are able to divert two members of Bcl2 family Bax and Bad from the mitochondria to the nucleus and cytosol respectively, resulting in their anti-apoptotic action (306). NS5A is also able to bind to and sequester p53 (307). NS5A also perturbs the Phosphatidylinositol 3-kinase (PI3K) pathway which results in activation of Akt, a master control switch that inhibits several pro-apoptotic factors such as Bcl2 family (308, 309). The anti-apoptotic effect of NS5A and growth arrest may cause accumulation of mutation in cells (which were naturally targeted for death through apoptosis) and formation of HCC.

B. 2. 8. Non-Structural Protein-5B (NS5B) and Replication Complex

Like other positive-strand RNA viruses, HCV copies a complementary negative-strand RNA from its positive strand that is then used as the template for the synthesis of the genomic positive-strand progeny RNA molecules (RNA-dependent RNA polymerase activity, RdRp) (310). A complex of proteins encoded by both viral and host polypeptides (replication complex) are responsible for the replication of HCV RNA, from which non-structural protein 5B (NS5B) is the catalytic subunit (RdRp unit). NS5B is a 66 kDa membrane-associated protein, which contains 591 amino acids (311). It is a compact globular protein (heart shaped) with dimensions of 67×63×68 Å(312). Similar to other known polymerases such as DNA-dependent RNA polymerases, reverse transcriptase (RNA-dependent DNA polymerase) and DNA-dependent DNA polymerases, NS5B has a basic right hand-like structure with fingers, thumb and palm domains (312, 313). Functionally, NS5B contains six conserved motifs, designated A-F from which motifs A, B and C are more important (312-314). The presence of the hallmark Gly-Asp-Asp and

Asp-X_4-Asp sequences on motif A and C are required for RdRp activity (314). NS5B exhibits a common two-metal mechanism of catalysis, which involves two conserved Aspartic residues (one on motif A, and one on motif C and two divalent ions (mostly Mn^{2+} or Mg^{2+}) for the formation of di-ester bonds (314, 315). NS5B reads the template in the 3' to 5' direction and synthesizes the daughter RNA in the 5' to 3' direction (316). The initiation of RNA synthesis is primer-independent and requires an RNA template with a specific initiation nucleotide, an initial ribonucleoside triphosphate ($rNTP_i$) and a second rNTP ($rNTP_i$+1)(316). The first phosphodiester bond is formed between these two nucleotides.

The finger domain is formed from extensive mixture of α-helices and β-sheets and can be further divided into two distinct areas: 1) region proximal to palm that is mostly formed by α-helices (α-fingers) and 2) region distal to palm that contains mostly β-sheets (β-fingers or fingertips) (314, 317). The fingertip domain is formed by four β-sheets (β_1 to β_4), an α-helix (α_1) and a pseudo β-sheet of the N-terminal region. Most of the polymerases are U-shaped but due to the presence of two long loops that connect the fingers to thumb domain (two arms of U), NS5B forms a closed heart-shaped structure. The first longer loop (residue 11-45) is a two-turn helix, emanates from fingertips and reaches to the back of the thumb domain and locked into a dimple at the top corner of thumb domain. The second loop reaches to the front of the thumb, inferior to longer loops (314, 317). At the bottom of the second loop there is a hole for entry of the nucleotides (314, 317). The fingertip surface facing to the hole has a positive charged-belt formed by a line of basic residues (Arg-48, Lys-51, 141 and 155 and Arg-158) extending from outside surface of protein to the inside of protein and is suitable for absorbing highly negative phosphate backbone of rNTPs (312). The α-finger region is located proximal to palm and is formed by nine α helices (αA to αI) (312, 314, 317). Between the α-fingers and fingertips, there is an U-shaped valley, which in conjunction with a concave wall created by αC, αD and αE, forms a line of basic residues (Lys-90, 98, 106, 172 and Arg-109, 168) (312). Also, around the interface of α-fingers and the palm exists a long shallow trench composed of the αF helix and the N-terminal of edge of αJ helix fits the phosphodiester backbone of ribose moieties (312). These areas constitute the template tunnel and should be a good acceptor of RNA template (312). In addition, positive electrostatic surface formed by Lys-90, 106 and Arg-109 faces the phosphodiester backbone of the daughter RNA and is the first structural motif that holds the daughter strands in place close to template (312).

The palm domain is the catalytic domain and is composed of the highly conserved motif (motifs A, B and C) of RNA-dependent polymerases (318). It is composed of three

antiparallel β-sheets (β_6, β_7 and β_3) and three α-helices (αJ, αK and αG) (312, 314, 317). Based on the crystal structure, motifs A-E are also located in the palm with catalytic motifs A, B and C corresponding to β_3 (residue 213-228), αJ (282-302) and β_2/β_3 (310-324) respectively (312). As it was indicated above, the catalytic domain of NS5B supports a "two metal ion" mechanism. In this mechanism, carboxylate group of Asp-220 on motif A and Asp-318 and -319 on motif C anchor a pair of divalent ions (312). The first metal ion reduces the affinity of accepting proton by 3' hydroxyl group of first rNTP. This facilitates the 3' O^- attack on the α-phosphate backbone of the second rNTP. The second divalent ion assists the departure of pyrophosphate from α-phosphate. Presence of Asp-225 close to the second hydroxyl group of rNTP contributes to selectivity of rNTPs instead of dNTPs (which don't contain second hydroxyl group) (312). Motif B, an α-helix, packs adjacent to the catalytic site with motif D, supports the proper structure of the site and is important for proper positioning of rNTPs and RNA template. Indeed, carbonyl oxygen atoms of the peptide backbone of Gly-283, Leu-285 are located at the hydrogen-binding distance of the hydroxyl group of both $rNTP_i$ and $rNTP_i$+1 (312). The hydroxyl group of next nucleotide on template is also located close to the OH group of Ser-288 and Tyr-191 and forms a hydrogen bond(312). Motif E forms part of antiparallel three strands of β-sheets, with a turn projecting toward the active site and must be important for the proper positioning of the first rNTP (312).

The thumb domain is composed of seven α-helices and two-stranded antiparallel β-loops with a U-turn (β-hairpin) (314, 317). This β-hairpin is believe to be important for correct positioning of 3'-terminus of template and prevents the slipping of RNA through the active site.

The c-terminal part of NS5B is believed to be a tail-anchored protein (319, 320). These features include posttranslational targeting into membranes through hydrophobic C-terminal, integral membrane association and cytosolic orientation of the protein (319). Twenty one amino acids near the C-terminus mediate the attachment of NS5B into ER-membrane and is required for NS5B activity (319, 321).

Following viral entry, the genomic RNA of the virus is released and utilized to produce the HCV proteins. Some of these proteins are required for RNA replication. Similar to other positive strand RNA viruses, HCV induces extensive membrane alteration to form a membranous web. Formation of the membranous web is triggered by the presence of NS4B, even in the absence of other viral proteins (280). The role of double layered membranes in the membranous web complex is not perfectly known, but it may include: 1) a raft for organization of replication complex (322), 2) the compartmentalization and

condensation of factors that are required for the replication (323), 3) providing lipids important for replication (324) and 4) protection of the viral RNA from RNA interference or host defense. Within the membranous web, a complex of host and viral proteins exist. The presence of NS3, NS4A, NS4B, NS5A and NS5B was confirmed (279, 280). In addition, replicating HCV RNA (both template and daughter RNA) forms the HCV replication complex with the above proteins (279, 280). The membrane of replication complex is derived from ER membrane and is rich in sphingomyelin and cholesterol (274, 325). Various host proteins are also present in membranous web. The presence of some of these proteins may be related to the origin of the membranous web (ER-membrane), which may not play a direct role in HCV replication, but are required for HCV replication.

Proteins located in lipid rafts of replication complex are crucial for recruitment of non-structural protein into RC. For example F-box/leucine-rich repeat protein-2 (FBL-2) is mandatory for HCV replication and is believed to recruit the NS5A into replication complex. Prenylation (geranylgeranylation) of FBL-2 is required for its interaction with NS5A and in the absence of this process (using HMG-CoA Reductase inhibitor), the interaction between NS5A and FBL-2 is prevented resulting in impaired HCV replication (326). Human vesicle-associated membrane protein-associated protein A (VAPA or hVAP-33), a SNARE-like protein, is required for the localization of NS5B into the replication complex. It is present in the lipid raft and its inhibition or down-regulation results in relocation of NS5B from the replication complex to the ER membrane (327, 328).

Apart from NS4B, the alteration of membrane for formation of membranous web depends on another key factor, phosphatidylinositol 4-kinase IIIα (PI4K-IIIα)(329). NS5A recruits and stimulates PI4K-IIIα to enrich the membrane compartment with phosphatidyl inositol-4 phosphate (PI4P) (329). This may induce membrane alteration. In addition, PI4P facilitates the recruitment of some other proteins such as oxysterol-binding protein-1 (OSBP-1) that is required for HCV replication and release (330). The OSBP-1 provides a sterol-rich environment in the replication complex.

In addition to these host proteins, FK506-binding protein-8 (FKBP8) is a propyl isomerase that is involved in the formation of the replication complex by interacting with NS5A and HSP90 (331). Propyl isomerases are a family of proteins that has an important role in proper folding of proteins. In this regard, Cyclophilin A and B (both proteins with propyl isomerase activity) have critical roles in the replication complex by assisting NS5B folding that affects its ability to interact with RNA template (146, 332). The importance of

Cyclophilin A and B for HCV replication renders them a worthy target for anti-HCV therapy (see A. 6. 3. 4. Other drugs with antiviral activity that target host).

The positive strand RNA in the replication complex is copied into a negative strand that is utilized for the synthesis of excess positive genomic RNA. This newly synthesized RNA can be utilized in the formation of more negative strands, translocation to ribosomes and generation of more viral proteins or assembly into new virions. NS5A that have intrinsic RNA attachment ability may be involved in translocation of this newly synthesized RNA into the surface of cytosolic LDs where the core is present and nucleocapsid is assembled (333)(see C. 3. 4. 3. Role of Lipid Droplets in HCV assembly).

C. Hepatitis C Virus Life Cycle

Various aspects of HCV life cycle are in close relationship to lipoprotein and lipid metabolism. In circulation, HCV is associated with lipoproteins and this association reflects their infectivity (334-336). Lipoprotein receptors such as Low Density Lipoprotein Receptor (LDL-R) (337-340), Scavenger Receptor BI (SR-BI) (341-344) and Heparan Sulfate Proteoglycans (HSPG) (345-347) are among the receptors that are believed to mediate HCV entry. Lipoprotein Lipase (LPL) has been shown to enhance the attachment of HCV to cells, possibly by acting as an adaptor molecule between virion and HSPG (348). Inside the cells, it is now well known that cytosolic lipid droplets (LDs), formed by accumulation of neutral lipids and in particular TG, are essential organelles for virion assembly (349, 350). In addition, intrahepatic accumulation of TG (steatosis) is one of the hallmarks of chronic HCV infection that intensifies the liver fibrosis and plays an important role in pathogenicity of HCV (351). Very Low Density Lipoprotein (VLDL) secretion pathway is now agreed to be the major path for HCV egress. In this section, the HCV life cycle will be explained in conjunction with lipid metabolism.

C. 1. Circulation of HCV in Peripheral Blood; HCV RNA-Containing Particles and Lipoprotein Circulation

Analysis of blood from chronically HCV infected patients has shown that the buoyant density of HCV RNA-containing particles covers a range from <1.06 g/ml to values more than 1.30 g/ml (352-354). This vast range of densities, suggests the circulating HCV particles are not uniform and another component associates with HCV in circulation. Several early reports attributed these variations in density to the presence of anti-HCV antibodies (353, 355-357), but the same pattern of variation was observed in HCV infected congenitally immunodeficient patients with no or very low serum antibodies to the virus (358). In addition, the variation in densities of HCV RNA-containing particles can be observed in HCV cell culture (HCVcc) as well. The unusually low densities in some of the HCV RNA-containing particles suggest association of the virus with lipoproteins. The interaction of HCV with lipoproteins was supported through capturing HCV particles in low-density materials with anti-apolipoprotein B-100 (334, 335).

C. 1. 1. Lipoproteins and Their Structures

C. 1. 1. 1. Lipoprotein Components and Structure: Lipids are generally hydrophobic or amphiphilic small molecules that are essential for life and have multiple functions in the body such as energy production, incorporation into the membrane as structural blocks, forming backbones of vitamins and hormones and bile acids, etc. Amphiphilic structure of

some lipids such as Phospholipid (PL), Cholesterol (Chol), Monoacylglycerol (MG) and Diacylglycerol (DG) allows them to form a micelle in a liquid phase with the polar head toward the liquid and the non-polar head facing to the lumen of the vesicle. But the majority of lipids, in particular lipid esters such as Triacylglycerol (TG) and Cholesterol Esters (CE), are hydrophobic water-insoluble compounds and are not able to circulate in the peripheral blood as nascent free molecules, thus they form very unique structures named lipoproteins. Lipoproteins are spherical aggregates of lipids, which have a hydrophobic-core formed by TG and CE and a monolayer of lipid coat formed by amphiphilic lipids such as Chol and PL. A group of specific proteins called apolipoproteins (apo) reside on lipoprotein coats, which dictate the fate of lipoproteins (359-361).

In humans, different subtypes of lipoproteins exist. These lipoproteins can be classified into three distinct subclasses: 1-Chylomicron (CM) and Chylomicron remnant, 2-Very Low Density Lipoproteins (VLDL) and its derivatives such as VLDL remnant (also named Intermediate Density Lipoprotein; IDL) and Low Density Lipoproteins (LDL) and 3-High Density Lipoproteins (HDL). The size and density of these lipoprotein classes partially correlate to their TG and the protein contents. The lipoproteins with a higher ratio of TG contents to weight have lower densities and larger size. Table 1-3 summarizes the characteristics of lipoproteins (359-361).

Table 1-3. Characteristics of Lipoproteins

				Apolipoprotein		Composition (% by weight)				
	Source	Density (g/ml)	Diameter (nm)	Major	Others	TG	PL	Chol	CE	Protein
Chylomicron	Intestine	0.93	75 to 1200	apoB48	E, A-I, A-IV C-I, C-II, C-III	80 to 95	3 to 6	1 to 3	2 to 4	1 to 2
VLDL	Liver	0.930 to 1.006	30 to 80	apoB100	E, A-I, A-II, A-V C-1, C-II, C-III	45 to 65	15 to 20	4 to 8	16 to 22	6 to 10
VLDL remnant	Product of VLDL Metabolism	1.006 to 1.019	25 to 35	apoB100	E, C-I, C-II, C-III	-	-	-	-	-
LDL	Product of VLDL Metabolism	1.019 to 1.063	18 to 25	apoB100	-	4 to 8	18 to 24	6 to 8	45 to 50	18 to 22
HDL	Liver	1.063 to 1.21	5 to 12	apoA-I	E, A-II, A-IV, C-III	2 to 7	26 to 32	3 to 5	15 to 20	45 to 55

C. 1. 1. 2. Chylomicron (Exogenous) Lipid Pathway and VLDL (Endogenous) Lipid Pathway: CMs are the largest lipoproteins, together with VLDL, carry the majority of TG (TG-rich Lipoproteins) [herein and after reviewed in (361) and (362)]. CM is produced and assembled in enterocytes from dietary lipids absorbed by small intestine and secreted to

the lymph vessels and reach circulation through the thoracic duct. It is responsible for post-prandial transporting of dietary lipids to the peripheral tissue in particular adipose tissue (Exogenous Lipid Pathway). The apolipoproteins in newly synthesized CM before blood circulation are apoB48, apoA-I and apoA-IV. ApoB48 (48% of ApoB100 mass), a 241 kDa protein, is the major structural apolipoprotein of CM. Both apoB100 (see VLDL) and apoB48 are the products of APOB gene, but apoB48 is produced uniquely in enterocytes when the stop codon is generated in the middle of mRNA (at residue 2153) by RNA editing. ApoA-I (29 kDa) and ApoA-IV (46 kDa) are secreted along with chylomicrons from the enterocytes (or free ApoA-I from liver), but are later transferred into HDL. These apolipoproteins have a major role in HDL-mediated reverse cholesterol transport, a process in which cholesterol is transferred from peripheral tissues back to the liver. As soon as they appear in blood circulation, other sets of apolipoprotein (apoC proteins) are transferred from HDL to CM. Three subclasses of apoC are generated by three distinct genes (APOC-I, APOC-II and APOC-III) in the liver and are secreted into blood. During fasting, these proteins reside on the HDL structure, but are transferred to VLDL and CM when these lipoproteins are available to circulate. When CM reaches peripheral tissue, Lipoprotein Lipase (LPL), attached to the endothelial surface of peripheral tissue vasculature, hydrolyzes TG contents of CM to glycerol and fatty acid for uptake by the adjacent cells. This process is activated by apoC-II (as the co factor for LPL) and is inhibited by apoC-III (as the inhibitor for LPL). The process of TG breakdown reduces the size and TG content of CM. As the size decreases, apoA-I, A-IV and C-II are peeled off from the surface along with some surface phospholipids and cholesterols. Loss of apoC-II prevents more hydrolysis of TG by LPL. The remainder molecule is called CM remnant and is absorbed by the liver through a pathway mediated by LDL receptor (LDL-R), LDL-R related protein (LRP) or heparin sulfate proteoglycans (HSPG) (see the C. 1. 1. 3 remnant clearance) [Reviewed in (361) and (362)].

VLDL, the second most TG-rich lipoprotein, is secreted exclusively by liver and transports endogenous lipids to peripheral tissue (Endogenous Lipid Pathway). In contrast to chylomicron, which is synthesized post-prandial, synthesis of VLDL is continuous and is regulated by a complex mechanism. Several possible sources can supply TG content of VLDL: 1) Hepatic uptake of VLDL or CM remnants, 2) Fatty acid released from adipocytes and incorporation to TG and 3) De novo hepatic TG synthesis. The secretion pathway for VLDL will be discussed later in detail. VLDL biology is very similar to CM; they share many features in their catabolism and uptake. VLDL contains apoB100, (550 kDa) a major structural protein synthesized by APOB gene exclusively in the liver, apoCs and apoEs. As the VLDL reaches the endothelial surface of peripheral tissue vasculature, LPL hydrolyzes TG to fatty acid and glycerol in a similar fashion to CM with apoC-II as

the co-factor. As VLDL loses more TG, apoC-II is separated and the VLDL remnant is formed. VLDL remnant, also known as “intermediate density lipoprotein” (IDL), contains apoB100 and apoC and can be cleared by the liver or sequestered in space of Disse and metabolized further by hepatic lipase. By hydrolyzing more TG, apoE is dissociated from IDL and LDL is formed. LDL contains high level of Chol and CE [Reviewed in (361) and (362)].

C. 1. 1. 3. Remnant Clearance: Conceptually, VLDL and CM remnant are formed when the VLDL and CM are substantially modified by LPL to become more TG and apoC-depleted and apoE-enriched, but is more relevant in defining core remnant rather than surface remnant. Two distinct types of remnants are derived from CM and VLDL: core remnant and surface remnant. Surface remnant is formed when excess of surface material is peeled off from the lipoprotein surface. This remnant is discoidal in shape and contains mostly PL and apolipoprotein complex of apoA-I, A-IV and C-II (similar to prebeta-2 HDL in reverse cholesterol transport) (363, 364). As it was discussed above, separation of apoC-II from VLDL and CM prevents further lipid hydrolysis (361, 362). The process of CM and VLDL remnant formation and uptake is quite similar, but in contrast to CM, which is not converted to a particle with a density more than 1.006 g/ml, VLDL is converted to a smaller size lipoprotein (LDL) with density higher than 1.006 g/ml (364). Both CM and VLDL remnant clearance occur primarily via the liver (365-367). Peripheral tissues such as kidney, lung, adrenal gland, adipose tissue and bone marrow take up small amounts of remnant (365, 368, 369). The presence of fenestrated endothelial cells lining the liver sinusoids function as a sieve, which filtrates and sequesters remnant particles with an appropriate size into the space of Disse (370, 371). In space of Disse, several receptors are able to bind to the remnants and are important in their clearance by hepatocytes.

LDL receptor (LDL-R) is the major receptor for remnant uptake. ApoB100 is the natural ligand for LDL-R, but the residues that are critical for LDL-R attachment (3359-3369) are not present in apoB48 structure (stop codon at residue 2153 is created by RNA editing) (372, 373). LDL-R has the ability to attach to apoE as well. ApoE is secreted by the liver as a free apolipoprotein or in conjunction with VLDL. It also resides on HDL surface during fasting and is transferred to CM. Three isoforms of apoE exist (apoE-II, E-III and E-IV) and all are essential for CM (or VLDL) remnant uptake. ApoE-III and E-IV bind to LDL-R with a high affinity while apoE-II binds with a lower affinity. But apoE-II is able to bind to HSPG as well which indicates there is more than one pathway for clearing the remnant. By attachment to LDL receptors, remnant particles are cleared by clathrin-based endocytosis in association with the receptor [Reviewed in (364)].

LDL Receptor-Related Protein (LRP) is another receptor and mediates the clearance of remnant particles by hepatocytes. This receptor has an extensive homology to LDL-R but has larger structure due to the presence of 31 LA repeats rather than seven in LDL-R (ligand binding motif, see C. 2. 7. Low Density Lipoprotein Receptor) (374). LRP is not able to bind to apoB but is capable of binding to two apoE and can mediate the endocytosis of ligands attached to them [Table in(364)].

Cell-surface proteoglycans (glycosaminoglycans) such as heparin sulfate proteoglycan (HSPG) have also been shown to attach to remnant particles. It is suggested that HSPG is the initial binding site of remnant. ApoB100, apoE, hepatic lipase (HL) and LPL are known to attach to HSPG. Although internalization of HSPG may concomitantly remove the attached remnant, this process is extremely slow and is not considered the prominent process for removal of the remnant. Instead apoB100, apoE, HL and LPL may anchor the remnant particles to HSPG and may serve to concentrate the remnant lipoprotein on the cell surface and increase their availability for LDL-R or LRP. They may trap the remnant particles in the space of Disse for more lipolytic processing by HL until they can be taken up or converted to LDL (in VLDL case) [Reviewed in (364)].

LPL also has been shown to have an important role in remnant clearance. LPL can bind to apoE (and in lower extent to apoB) in one hand and to all LDL-R family (in particular LRP and with less affinity to LDL-R). LPL acts as an adaptor molecule that significantly augments the remnant uptake by the liver. This process is not dependent on LPL catalytic activity as it occurs even with presence of LPL inhibitors. Furthermore, several studies have indicated that LPL binding to the hepatocyte cell surface at space of Disse may be facilitated by HSPG. It is suggested that LPL-lipoprotein complex binds to HSPG and this enhances the concentration of lipoprotein on cell surface for interaction with receptors (LDL-R and LRP). The same interaction between lipoprotein remnant and HL is known. Hepatic lipase is able to enhance the LRP-mediated uptake of lipoprotein remnant. In addition, they are able to attach to HSPG; therefore, a similar role for HL in relation to LPL occurs in the absence of its catalytic (lipase) activity [Reviewed in (364)].

In summary, CM (and VLDL) remnant is taken up either directly by LDL-R after achieving apoE or acquiring additional apoE (from locally secreted apoE in space of Disse) and taken up by LRP. The LDL-R mediated uptake is the fastest and major remnant uptake pathway while LRP mediated uptake is slower. A third pathway has been explained in which remnant particles are sequestered by HSPG (through apoE) and following interaction with hepatic lipase, the particles are transferred to LDL-R or LRP. It is also proposed that in the absence of apoE, remnant particles are attached to hepatic lipase

through apoB and are absorbed by LRP since hepatic lipase can act as ligand for LRP (364).

C. 1. 2. Characteristics of high and low-density HCV RNA containing particles

As we have already discussed, HCV is an envelope virus with a lipid coat covering the nucleocapsid (formed by RNA and core protein) and envelop proteins (E1 and E2) in the lipid coat. Several lines of evidence suggest that apart from this general structure, naked nucleocapsid of HCV (with no lipid layers) also exists in human blood in high-density fractions (>1.27 g/ml). First, it has been shown that the HCV–containing particles with buoyant density of about 1.27 to 1.34 g/ml are precipitated by anti-core antibody (355, 356, 375). These particles have been observed by electron microscopy and appear to have a wide range of sizes from 38-62 nm in diameter with majority in the range of 38-43 nm (376, 377). Second, these particles have very similar characteristics to the HCV-RNA containing particles from very low-density fractions that were treated with detergent (to remove the lipid coat) (378). Third, the detection of core protein in glomerulus of patients with HCV related-membranous glomerulonephritis in the absence of E1 and E2 suggests the presence of naked nucleocapsid in human blood (379). Thus, it seems that the majority of HCV in high buoyant densities represent naked nucleocapsid. In comparison to HCV particles with low buoyant density (<1.06 g/ml), these particles are poorly infectious. The infectivity titer of human plasma increases 10^6 times from density of 1.219 g/ml to density below 1.086 g/ml (336).

As it was indicated before, precipitation of low-density HCV RNA containing particles with apoB antibody, suggests the association of these particles with TG-rich lipoproteins (in particular VLDL) (334, 335). Therefore, the low-density HCV particles are referred as lipo-viro-particles (LVP) (380). These particles predominantly have densities less than 1.086 and contain HCV nucleocapsid, E1, E2 and also apoB, apoE and apoC-1 and C-II and are rich in TG (380). They appear as a large spherical structure up to 100nm in diameter (380) and it seems that HCV envelope protein is exposed on the surface of LVP as it is recognized by anti-envelop antibodies under non-denaturing conditions (381). ApoB100 is the first protein that was discovered in LVP structure as these particles can be precipitated by anti-apoB100 (334, 335). Interestingly, the presence of apoB48 has also been reported in these particles (381). In humans, the apoB48 is exclusively secreted by enterocytes in the context of CM and it is non-exchangeable apolipoprotein. It has been proposed that enterocytes might be another site for assembly and maturation of HCV (381). Although the presence of non-structural proteins in enterocytes of chronically infected patients supports this finding (382), it is not yet clear how apoB48 incorporates

into LVP structure and if enterocytes play any major role in HCV assembly. Presence of apoE in LVP is correlated with infectivity of the particles. It has been shown that particles with higher infectivity rate contain more apoE (383). This finding can be explained by the importance of apoE for uptake of lipoproteins (as it was discussed) and shows the possible interaction between LVPs and lipoprotein receptors for HCV cell entry (see the following).

In comparison to HCV isolated from patient sera, HCVcc particles have a higher average density (1.1 g/ml) and lower infectivity rate. After infection of a chimpanzee or cultured human hepatocytes with HCVcc, viral particles isolated from animal or cultured human hepatocytes have a lower average density and higher infectivity rate comparable to HCV isolated from patients sera(384). This result is very important as it shows that the variation in density and infectivity may arise from the host cells and suggest that association of HCV with lipoprotein may take place during assembly of virus. In contrast to HCV isolated from patient sera, the association of apoB100 with HCVcc was sporadic (385).

In summary, association of HCV RNA containing particles with TG-rich lipoprotein (in particular VLDL) suggests that these particles may have a very similar biology to TG-rich lipoprotein. In addition, hepatocytes are the major cells for synthesis and assembly of VLDL and HCV and also are a repository site for VLDL remnant and HCV. Therefore, it is tempting to speculate that HCV entry, assembly and release are dependent on lipoprotein metabolism.

C. 2. HCV Cell Entry; Cellular Receptors and Role of Lipoproteins

Based on our current knowledge of HCV life cycle, the cell entry is a multi-step process that requires various receptors or molecules. Several membranous proteins, such as tetraspanin CD81, Scavenger Receptor BI (SR-BI), tight junction molecules Claudin-1 and Occludin have been shown to be important for HCV cell entry. In addition, Dendritic Cells (DC)-specific intracellular adhesion molecule-3-grabbing non-integrin (DC-SIGN), Liver Specific (L)-SIGN and Glyscosaminoglycans such as HSPG play a role in attachment and entry. These receptors and molecules determine the target cells for the virus and are responsible for hepatotropism of HCV. HCV envelope proteins (E1 and E2) and particularly E2 are the ligands for some of these receptors (see E1 and E2). In addition, as we discussed earlier, one of the unique features of HCV is its association with betalipoprotein (in particular VLDL) in patient sera that contains apoB100 and apoE (LVPs). Only a minority of circulating HCV in patient sera has properties similar to

canonical virus; therefore, lipoproteins and their receptors (LDL receptors) should play important roles in viral cell entry. After attachment to these receptors, HCV enters the cell by clathrin-mediated endocytosis. The discussion on these receptors follows.

C. 2. 1. Tetraspanin CD81

CD81 is an integral protein belonging to the Tetraspanin family. It contains four TMDs and the N- and C-terminus are located intracellularly. Positioning of TMDs forms a large extracellular loop (LEL), a small extracellular loop (SEL) and a very small intracellular loop. The LEL contains two disulfide bonds (386), which are required for proper folding of the receptor and interaction with E2 (387, 388). CD81 is one of the first receptors that was shown to interact with E2 and has been extensively studied. It has been shown that monoclonal antibodies directed against CD81 (341, 342, 389), down-regulation of CD81 by siRNA (390) and soluble forms of CD81 (binds to viral E2 reducing its interaction with cell membrane CD81) (391) inhibit infectivity of HCVcc and HCV pseudo-particles (HCVpp). On the other hand, ectopic expression of CD81 in cells lacking CD81 (HepG2 and HH29) makes such cells permissive to HCVcc and HCVpp (341, 342, 390). LEL is the site of interaction with E2 protein and several specific amino acid residues have been shown to be important for this interaction (Leucine- 162, Isoleucine-182, Aspargine-184 and Phenyl Alanine-186)(392). Attachment of E2 to CD81 does not directly internalize HCV, but activates the Rho GTPase activity. The Rho GTPase activity mediates the relocalization of the E2/CD81 complex to the basolateral wall of cells (cell-cell contact area) where tight junction proteins such as CLDN-1 and Occludin reside (393). Epidermal Growth Factor Receptor (EGFR) and Ephrin Receptor-2A (EphA2), two receptor tyrosine kinases, have been identified as the host factor that mediates the interaction between E2/CD81 complex with CLDN-1 (394). The CD81 is considered as a post-binding receptor and the E2/CD81 binding takes place only after virus attachment to the cell (through other receptors). More interestingly, the presence of CD81 on T and B cells is related to viral persistence and polyclonal activation of B cells is believed to causes lymphoproliferative disorders and mediate cryoglobulinemia (395, 396).

C. 2. 2. Scavenger Receptor BI (SR-BI)

SR-BI is a glycoprotein formed by 509 amino acids and contains two TMDs, intracellular N- and C-terminals and a large extracellular loop. The primary lipoprotein interacting with this receptor is high-density lipoprotein (HDL), but it is a multi-ligand receptor for various classes of lipoproteins (LDL, VLDL and oxidized LDL) (397). SR-BI is also a putative HCV receptor. The HVR-1 of E2 is mapped as a region binding to SR-BI (341). The monoclonal antibodies against SR-BI efficiently block infection in-vitro (hepatoma cells) and in-vivo (Chimps) as well as down-regulation of SR-BI by siRNA(342-344). Like CD81,

SR-BI is also a post-binding receptor (398). Furthermore, HDL facilitates HCVcc and HCVpp cell entry while LDL, VLDL and oxidized LDL reduces serum HCV and HCVpp cell entry via SR-BI (337, 399, 400). This difference might be due to providing membrane cholesterol and boosting the permissiveness to HCV.

C. 2. 3. Glycosaminoglycans (GAGs)

GAGs are the polysaccharides expressed on cell membranes, attached to cell surface proteins or extracellular matrix proteins (401). Heparin Sulfate (HSPG) is a member of this family and contains variable number of sulfated repeating disaccharides particularly glucuronic acid and N-acetyl glucosamine (402). The structure of HSPG is closely related to heparin and has several ligands and regulates multiple biological events such as blood coagulation, angiogenesis, tumor metastasis, lipoprotein uptake and viral entry. Several findings have linked the HSPG to HCV entry. For instance, it has been shown that the soluble form of E2 (sE2) binds to heparin (as an analogue of HSPG) (345, 346). Treating cells with heparinase and glycosidase, both degrading HSPG, impairs HCV attachment to cells and reduces HCV infectivity respectively (347). In contrast, it has been shown that full E1-E2 heterodimer which occurs naturally, does not attach to HSPG. This finding raises questions as to whether GAGs (and HSPG) directly participate in HCV entry or whether the process is indirect and mediated by lipoprotein associated with LVP. Recently, it has been shown the interaction between HCV in the context of LVP and HSPG is mediated through apoE (403). ApoE is the natural ligand for HSPG and it has been shown that interaction between apoE and HSPG might be required for primary cell attachment of virus (403). With our current knowledge of HCV, GAGs might have a role in HCV entry, although this role is not direct and the attachment to GAGs is low. This effect seems to be prior to binding to high affinity receptors (such as SR-BI and CD81) and may be involved in the primary interaction between cell surface and the virus (403).

C. 2. 4. Lectins; DC-SIGN and L-SIGN

Dendritic **C**ell-**S**pecific **I**ntracellular Adhesion Molecule-3-**G**rabbing **N**on-Integrin (DC-SIGN) and its liver specific family member (L-SIGN) are protein members of the C-Lectin family. They bind to sugar (part of pathogen associated molecular pattern) using highly conserved carbohydrate recognition domains (404). This binding domain has a calcium-binding pocket that plays a major role for carbohydrate attachment. DC-SIGN is a type II membrane protein and participates in internalization of several viruses (405). In HIV, glycoprotein-120 (gp-120) attaches to DC-SIGN (which is abundant in dendritic cells of mucosa), but the virus is not internalized by macrophages (406, 407). Instead, it transfers the virus to CD4 lymphocytes, which are the permissive cells for HIV (406, 407). In HCV both DC-SIGN and L-SIGN are able to bind sE2 as well as HCVpp and HCV from patient

serum (408, 409). Interestingly L-SIGN is expressed in sinusoidal endothelial cells and it is believed that it may transfer the HCV to the underlying hepatocytes (HCV permissive cells) at space of Disse very similar to the role they have in HIV entry (410). Consequently L-SIGN may function as a capture receptor and may play a major role in tissue tropism.

C. 2. 5. Tight Junction Proteins; Claudin-1, -6 and -9

Claudin is a group of proteins composed of 24 different subclasses and a member of tetraspanin family. Among these subclasses, Claudin-1, -6 and -9 have been shown to mediate HCV cell entry (411, 412). Claudin-1 (CLDN-1) is a 22 kDa protein composed of 211 amino acids which is expressed on the basolateral wall of cells, predominantly in the liver (413) and is one of the tight junction proteins (414, 415). Claudin-6 and -9 (CLDN-6 and -9) have significant homology to CLDN-1 but they also can be expressed in peripheral blood monocular cells (lymphocytes) (416). Claudin has four TMDs a short intracellular N-terminal, a long cytoplasmic tail, two extracellular loops (EL1 and EL2) and a short 20 amino acids long intracellular loop (416). EL1 is formed by 60 amino acids several of them are charged and thought to influence paracellular charge selectivity (416) and two highly conserved cysteine residues which form a disulfide bond that stabilizes the structure of EL1 (414, 415, 417). This loop is mostly involved in maintaining cell polarity as well as preventing diffusion of some molecules across the junction (416). EL2 is composed of 24 amino acids and it was suggested that it forms a dimer with the claudin on opposing cell membrane by hydrophobic interaction with aromatic side chains (418). The C-terminal tail contains a PDZ-domain binding motif that interacts with cytoplasmic scaffolding proteins in zonula occludens, like ZO-1, ZO-2, ZO-3, PATJ and MAGUK (419, 420). The C-terminal also is the target of Serine/Threonine and Tyrosine phosphorylation (421) and palmitoylation (422), which signifies activity and localization of the protein. The role of claudin-1 as a receptor for HCV entry has been studied. It has been shown that CLDN-1 expression in 293T cells enhances the HCVpp and HCVcc infection (411, 423), but its overexpression to cell lines that are permissive to HCVpp did not enhance activity (411). Also, down-regulation of CLDN-1 by siRNA reduces the infection by HCVpp and HCVcc (411). The N-terminal 1/3 of ECL1 has been shown to be sufficient for HCVpp entry (411). CLDN-6 and -9 also mediate HCV entry as expression of these molecules in 293T cell resulted in permissiveness of these cells to HCVpp (412, 423). In hepatoma cells such as Huh7.5, in the absence of CLDN-1, CLDN-6 and -9, cells were not permissive to HCVpp (423). Although all this evidence supports the role for this protein in HCV entry, there is still no evidence showing direct interaction between virus and claudins. The interaction between virus and claudin is a post binding process which

occurs after the virus is attached to CD81 as pretreatment of cells with the anti-CD81 antibody completely abolishes the HCVpp and HCVcc interaction with CLDN-1 (411).

C. 2. 6. Tight Junction Proteins; Occludin

The resistance of some cell lines (HeLa and HepH) that are CD81 and SR-BI positive after overexpression of claudin-1 suggests there are additional factors mediating HCV entry. Recently another tight junction protein called occludin has been shown to play a major role in HCV entry. Occludin is a 60 kDa protein composed of 522 amino acids and structurally very similar to claudin, except for the presence of a very long C- and N-terminal in its structure. It contains four TMDs, intracellular N- and C-terminals, two extracellular loops (EL1 and EL2) and one intracellular loop. The N-terminal is composed of 149 amino acids, which is thought to play a major role in barrier properties of tight junction (424). The N-terminal truncated form of occludin was able to localize at tight junction area but it causes disruption of tight junctions and leakiness of basolateral space (425). The C-terminal contains 254 amino acids and is believe to be important for regulating the barrier function of tight junction as well as intracellular trafficking of occludin (424). It contains high contents of Tyrosine and Serine/Threonine residues, which are frequently phosphorylated by various protein kinases (424). The C-terminal region of occludin is capable of mediating endocytosis. It also contains a motif, which binds to Zonula occludens proteins such as ZO-1 and -2 and -3. The EL1 contains 45 amino acids and is exceptionally enriched in Tyrosine and Glycine and only a few non-polar amino acids are present in its structure (424). It is thought that EL1 is important for interaction and binding to its homologous regions on the adjacent cell membrane (424). The EL2 is composed of 44 amino acids and it is thought to be crucial for localization of occludin at tight junction (424). It has been shown that occludin interacts directly with E2. This was confirmed by co-immunoprecipitation of E2 and occludin (426). In addition targeting occludin with shRNA and siRNA inhibits both HCVpp and HCVcc cell entry (426). It has been shown that overexpression of occludin caused the murine hepatocytes to be permissive to HCVpp (427). All of these data support the role for occludin in HCV entry.

C. 2. 7. Low-Density Lipoprotein (LDL) Receptors

The mature LDL receptor (LDL-R) is a type 1 transmembrane protein with 839 amino acids. The physiological ligands of LDL-R are apoB100 in LDL structure and apoE in CM and VLDL structures or certain VLDL intermediates and high-density lipoproteins (HDL) (428-431). The extracellular region of LDL-R contains seven contiguous Cysteine-rich repeats referred as LDL-R type A repeats (LA). Each of these LA repeats contains 40 residues and can also be found in the structure of the terminal components of

complement cascade (428-433). Following these LA-repeats, there is a 400 residue region with homology to the epidermal growth factor precursor (EGFP). This EGFP homology domain contains two epidermal growth factor-like repeats (EGF repeats) (430, 431), a β-propeller YWTD-repeat domain followed by another EGF repeat. The β-propeller area is formed by six repeats containing YWTD consensus (named for conserved residues Tyrosine, Tryptophan, Threonine and Aspartate) (434, 435). Following this EGFP homology domain is a Serine/Threonine rich area composed of 58 residues, which is glycosylated heavily (429, 436). The cytoplasmic tail of LDL-R is involved in endocytosis through a NPxY motif (Aspargine-Proline-x-Tyrosine) which directs the receptors toward clathrin-coated pits (437, 438).

The LA repeats area is the lipoprotein-binding domain. It has been shown that LA3 through LA7 and first EGF repeats are essential for apoB100 attachment (439, 440), while LA4 and LA5 are required for apoE (and consequently VLDL) attachment (439, 440). In apoB100 structure, residues 3359-3367 are involved in attachment to LDL-R (372, 373). In structure of apoE, residues 141-153 are the receptor attachment motif(373). The receptor-ligand complex is taken up by clathrin-coated pits and is exposed to low-pH environment of endosome, which dissociates the lipoprotein from LDL-R. Majority of LDL-R is recycled back to the cell surface and the minority is degraded by lysosome. The EGFP homology domain plays a major role in dissociation of ligand from LDL-R (434, 441). Considering the structural features of YWTD propeller, a model has been proposed for dissociation of ligand from LDL-R. According to this model, at low pH LDL-R adopts a closed confirmation with LA4 and LA5 in direct contact with the top face of β-propeller domain. This alteration releases the ligands from LA4 and LA5 (434, 441).

The cytoplasmic tail of LDL-R mediates the clathrin-based endocytosis. Presence of NPxY (Aspargine-Proline-X-Tyrosine) sequence is required for this process. It has been shown that ADP-Ribosylarginine Hydrolase (ARH)-1 can directly interact with this sequence on LDL-R (442, 443) and also has a conserved consensus for attachment to β2-adaptin subunit of AP-2 clathrin adaptor (442, 443). Therefore ARH-1 is believed to act as an adaptor protein for attachment of LDL-R to endocytosis machinery.

Several findings support the hypothesis that LDL-R is involved in HCV entry. First, there is a correlation between HCV RNA accumulation in human hepatocytes and LDL-R mRNA and LDL entry (337). Second, absorption of HCV particles isolated from patient serum can be inhibited by antibody against apoB100 and apoE (338-340). Third, infectivity of HCVcc is reduced in cells treated with LDL-R siRNA (338). Fourth, the expression of LDL-R in COS-7 cells resulted in binding of HCV from patients sera to

these cells (340). It has been shown that there is no interaction between LDL-R and HCVpp (444) as HCVpp doesn't associate with lipoproteins. Considering all of these facts it is believe that LDL-R binds to lipoprotein compartment of LVPs (possibly apoB100) and mediates the HCV entry. As it was discussed earlier, attachment of LDL-R to its ligand (apoE or apoB100) induces the process, which results in activation of endocytosis and rapid internalization of LDL-R/ligand. Therefore initially the same process of LDL-R mediated internalization was assumed for LVPs. But it was shown that the LVPs are slowly internalized (half maximum rate of approximately 50 minutes) while all lipoprotein are internalized rapidly within 30 minutes (338). This suggests that LVPs and lipoproteins are internalized with distinct uptake pathway and attachment of LVPs to LDL-R does not result in endocytosis.

C. 2. 8. Lipoprotein Lipase and Its Role in HCV Cell Entry

Lipoprotein lipase (LPL) is a member of the lipase family and is located on the luminal surface of endothelial cells. This protein hydrolyzes the triacylglycerol (TG) of TG-rich lipoproteins such as VLDL and chylomicron to release fatty acids for tissues (445). Apart from this physiologic role, LPL has a second structural function as a bridge for lipoprotein (particularly VLDL and Chylomicron remnant) uptake by HSPG alone or in combination with LDL-R, LRP or SR-BI (446).

It has been shown that LPL may interfere with HCV entry. Exogenous LPL (bovine) inhibits the infectivity of HCVcc or HCVcc passaged through SCID/uPA mice (348). This inhibition could be partly due to LPL enzymatic activity, which alters lipid composition of LVP (as it has been shown that treating HCVcc media by LPL alters the buoyant density of LVPs to higher density). But tetrahydrolipstatin (a potent lipase inhibitor) in presence of LPL restored only a minor portion of HCV infectivity (348). In contrast, it has been shown that LPL mediates the cells attachment of HCV to HSPG. This mimics the attachment of lipoproteins to HSPG and internalization (which in this case should increase the HCV infectivity). To explain this discrepancy, it has been hypothesized that the attachment of virus to HSPG through LPL may either block the virus at the cell surface or direct it to internalization through pathways, which lead to abortive infection. When HCVcc is treated with both LPL and tetrahydrolipstatin (Orlistat, a portent inhibitor of LPL) the virus attachment to the cells is increased even more than HCVcc not treated with LPL. This suggests that in the absence of enzymatic activity, LPL increases the attachment of HCVcc to cells (by its structural function), but this attachment to the cells is not associated with internalization of virus even at presence of lipolytic activity. Therefore it seems that LPL enhances the attachment of virus to the cells but block the internalization (348). Furthermore as it was indicated earlier, apoE is required for attachment of virus to

HSPG. It has been shown that LPL reduces the association of HCV with apoE and by this way it should reduce the HCV attachment to HSPG (and consequently cells) (447) rather than increase in cell attachment as has been shown. In summary the exact mechanism by which LPL reduces HCV infectivity remains unclear.

C. 2. 9. Niemann-Pick-C1-Like-1 (NPC1L1) Cholesterol Uptake Receptor and Its Role in HCV Cell Entry

NPC1L1 is a membrane protein with 1332 amino acids (448) and is formed by a typical signal peptide, 13 TMDs and a conserved N-terminal similar to Niemann-Pick C1 protein (449). This protein has a well-known role in brush border of enterocytes and transfers the cholesterols across the apical membrane. This process is prevented by a clinically proven medication that inhibits NPC1L1 protein (Ezetimibe) (450). In the liver, NPC1L1 is localized to the bile canalicular membrane (451, 452) and is believed to reabsorb the cholesterol that is secreted in bile by ABCG5/ABCG8 (451). Recently it has shown that targeting NPC1L1 with blocking antibody or with Ezetimibe impairs the HCVcc entry. In addition silencing the NPC1L1 also diminishes the HCVcc entry. Furthermore when SCID/uPA mice were treated for two weeks with Ezetimibe before inoculation with HCV, the establishment of infection was hampered significantly. This effect was not seen when mice were treated two days after being infected. Therefore it was suggested that NPC1L1 are involved in HCV entry (453). As we indicated NPC1L1 is localized on canalicular side rather than in vascular side of hepatocytes where direct interaction between HCV and cells occurs. Therefore the direct role of NPC1L1 in HCV cell entry is questioned and it seems that NPC1L1 might be indirectly involved in HCV entry. This remains to be elucidated.

C. 2. 10. Suggested Model for HCV Entry

The requirement of these many receptors for HCV cell entry suggests that this is a multi-step process. It seems that L-SIGN and DC-SIGN located on the surface of sinusoidal cells, capture the circulating virus from blood and transfer it to the underlying space of Disse where hepatocytes (permissive cells for HCV) are located. The primary low affinity attachment of the virus requires Glycosaminoglycans (in particular HSPG) alone or in conjunction with LDL-R. LPL may acts as a bridge for attachment of the virus to HSPG. Association of HCV with lipoprotein particles (LVP) explains the importance of these two receptors and this primary attachment step is mediated mostly by lipoprotein components of LVP. In the second step HCV is transferred to higher affinity receptors such as SR-BI and in particular CD81. The association of virus with these receptors is taking place after attachment of virus to the cells by previous receptors. After attachment of virus to CD81

the complex is transferred to the basolateral wall where the tight junction proteins CLDN-1 and Occludin are residing. Interaction of virus with these receptors finally internalized the virus by clathrin-coated pit endocytosis.

C. 3. HCV Assembly: Lipid Droplets and Their Role

Lipid droplets (LDs) have a major role in HCV assembly. In addition majority of the lipid cargo that are assembled as VLDL for secretion originates from LDs(454). Furthermore VLDL has been implicated as the pathway by which HCV is exported from cells to plasma. The core of LDs is formed from neutral lipid and in particular TG and their size depends on the content of TG. Interestingly, hepatic intracellular accumulation of TG (steatosis) is highly associated with chronic HCV infection and as it may result in steatohepatitis that can intensify the fibrosis and results in premature cirrhosis. The prevalence of steatosis in chronic HCV infection is around 40-80% depending on concomitant alcohol consumption, obesity, type-2 diabetes [table 1 in (351)]. But if all of the risk factors for the steatosis are excluded, still 40% of the chronic HCV infected patients experience steatosis. This rate is about twice the frequency of steatosis in chronic hepatitis B (351). Therefore it has been hypothesized that the virion itself can directly induce steatosis. Several other observations support this hypothesis; 1) in patients infected with HCV genotype-3, steatosis is more prevalent and more severe than other genotypes (455, 456), 2) the severity of steatosis correlates with the level of HCV replication (455, 457, 458) and 3) steatosis is significantly reduced or disappeared in sustained responders to antiviral treatment (458, 459).

Obesity (high body mass index), diabetes and alcohol consumption are very common comorbidities among the HCV infected patients and are known steatogenic factors (351). It has been reported that in chronic HCV patients overall, BMI and steatosis are not correlated, but when patients with genotype-1 infection were specifically analyzed, there was a significant association between high visceral fat distribution and the grade of steatosis (455). This association was not observed in genotype-3 patients (455). In contrast in genotype-3 the steatosis is correlated with HCV replication (455). Therefore it is thought that in genotype other than 3 the steatosis is mainly related to metabolic factors (Metabolic Fat) although cytopathic effect of virus cannot be excluded while in genotype-3, steatosis is related to the cytopathic effect of virus (Viral Fat).

The mechanism(s) by which HCV induces steatosis (HCV-induced steatosis) have been extensively studied. In general steatosis occurs whenever there is more production/absorption than degradation/export of TG. Therefore four possibilities have been indicated as the mechanism by which virus induces steatosis:

1) Increased de novo lipogenesis, i.e. fatty acid synthesis and TG biogenesis,

2) Increased fatty acid influx from plasma,

3) Impaired VLDL secretion as the only major pathway for TG export out of hepatocytes,

4) Impaired fatty acid oxidation and therefore TG degradation.

From these four possibilities, impaired VLDL secretion and enhanced lipogenesis have been studied more and will be discussed in details in the next several sections.

C. 3. 1. De novo Fatty Acid Synthesis and Regulation

C. 3. 1. 1. De Novo Fatty Acid Synthesis a Pathway With Two Steps: Fatty acids serve several important roles in human body. They are 1) the structural blocks of lipid esters such as TG, PL and CE and 2) contain huge amount of energy in their carbon backbone therefore represent one of the major form of energy storage. Indeed some cells like cardiomyocytes specifically utilize fatty acid as their main source of energy. Fatty acid can be obtained from several sources including external source (food intake), breakdown of endogenous lipid esters and also production of fatty acid from acetyl-coA during anabolism (De novo synthesis) (460).

In the human body several tissues have the ability to produce fatty acids. In females, mammary glands are able to synthesis fatty acid to produce milk but the major sites of fatty acid synthesis are the liver and adipose tissue. The production of fatty acid in these tissues is extremely important during positive energy balance, as they are capable of transforming carbohydrates and proteins to fatty acids. The main proportion of these endogenously synthesized fatty acids are incorporated to the structure of TG which has much higher energy content per mass in comparison to carbohydrates and proteins. Although both liver and adipose tissue have an ability to produce TG but the fate of the TG in these tissue are different. In adipose tissue the majority of the TG is stored while in the liver is secreted by VLDL pathway to support endogenous lipid pathway. In some pathologic conditions, over production of fatty acids can increase the TG contents of hepatocytes and results in hepatic steatosis. As enhancement of de novo fatty acid synthesis is one of the mechanisms for steatosis, this part will be discussed in more detail (460).

In general the process of fatty acid synthesis is the production of palmitic acid (a 16 carbons saturated fatty acid) from a substrate, Acetyl-CoA. Although acetyl-CoA conveys the carbon atoms (two carbons) for fatty acid production, it is not directly incorporated into

the palmitic acid carbon structure. It is first transformed to a three-carbon intermediate, Malonyl-CoA, and consequently two carbon of the malonyl-CoA is utilized to the backbone structure of palmitic acid. Therefore de-novo synthesis of fatty acids is a two steps reaction.

In the first step, acetyl-CoA is carboxylated by an enzyme, Acetyl-CoA Carboxylase (ACC) to form malonyl-CoA. This reaction is endothermic and needs a molecule of ATP:

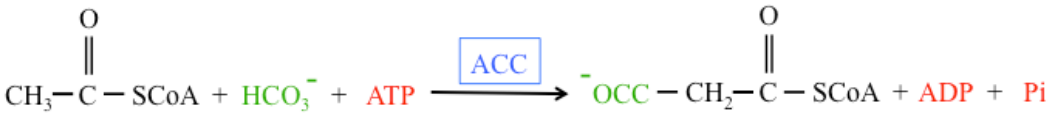

The second step is a cyclic process in which the acetyl-CoA primer attaches to seven molecules of malonyl-CoA (produced in the first step) to form palmitic acid. In each cycle of this reaction, one malonyl-CoA donates two carbons for chain elongation and releases a third carbon atom as a molecule of bicarbonate. This reaction is mediated by fatty acid synthase (FAS), which is formed by a complex of several enzymes and uses NADPH as a reducing agent (460):

C. 3. 1. 2. Carboxylation of Acetyl-CoA and Acetyl-CoA Carboxylase: ACC the rate-limiting enzyme for the fatty acid synthesis is a multifunctional protein containing two domains with enzymatic activities (biotin carboxylase and carboxyltransferase) and one carrier protein (biotin carboxyl carrier protein, BCCP). BCCP subunit covalently binds to biotin through its amino group lysine residue and acts as a carrier for transferring carboxyl group to acetyl-CoA. Carboxylation of acetyl-CoA and formation of malonyl-CoA is a two step reaction. In the first step N1 atom of biotin (in BCCP) is caroboxylated. This reaction is mediated by biotin carboxylase moiety of ACC and requires ATP and a divalent cation (Mg^{2+}). Then carboxyl biotin is translocated from biotin carboxylase domain to carboxyltransferase domain. BCCP acts as a carrier in this process. In the second step, carboxyl group on the biotin is transferred to acetyl-CoA to form malonyl-CoA in a process that is mediated by carboxyltransferase domain (461). Both biotin carboxylase and carboxyltransferase are inactive as a monomer and are activated as a dimer (462).

Acetyl-CoA is an energy producer intermediate, which is formed from pyruvate in mitochondria. The process of fatty acid synthesis is a cytosolic event; therefore acetyl-CoA should be transferred to the cytosol form mitochondria. As the inner membrane of mitochondria is impermeable, this translocation of acetyl-CoA to the cytosol is mediated through an accessory process, citrate shuttle pathway(463). In summary, during positive energy balance, a very high level of acetyl CoA that is produced from glycolysis enters the citric acid cycle and elevates the formation of the downstream product, citrate. On the other hand, due to the over use of NAD^+ during positive energy balance, the metabolism of citrate to the downstream products is also reduced, causing more accumulation of citrate. The extra citrate is then transferred to the cytosol by a tricarboxylate anion transporter and is catabolized to acetyl-CoA by ATP-Citrate-Lyase (460).

ACC is the rate-limiting enzyme for fatty acid synthesis and it is tightly regulated. During active de novo fatty acid synthesis, the rate of fatty acid β-oxidation (degradation of FA back to acetyl-CoA by mitochondria) is reciprocally regulated to prevent the vicious cycle of FA production/degradation. In this process product of ACC, malonyl-CoA is a potent inhibitor of Carnitine Palmitoyltransferase-1, an enzyme that mediates the transport of fatty acid from cytosol to mitochondria for oxidation. Therefore malonyl-CoA not only is a substrate for fatty acid synthesis but is able to shut down the fatty acid oxidation(460). Interestingly two major isoforms of ACC exist in cells. ACC1 is an isoform expressed in cytosol and its main function is to provide malonyl-CoA for FAS and channeling malonyl-CoA for fatty acid synthesis(464). The ACC2 isoform is structurally very similar to ACC1 but it is attached to the outer mitochondrial membrane through its unique hydrophobic N-terminal. Its function is more regulatory for preventing the fatty acid oxidation during fatty acid synthesis(465). ACC2 produces malonyl-CoA which allosterically inhibits CPT-1. Therefore malonyl-CoA functions as an on-off switch between fatty acid oxidation and fatty acid synthesis (460).

C. 3. 1. 3. Short-term Regulation of ACC and De Novo Fatty Acid Synthesis: ACC is regulated in several different levels. The activity of ACC is stimulated by citrate and inhibited by long-chain acyl-CoA such as palmitoyl-CoA (the product of fatty acid synthesis). This represents allosteric feed-forward and feedback control over ACC activity (466). Apart from allosteric regulation by substrate and products of fatty acid synthesis, hormones also regulate ACC. During catabolic states, high levels of glucagon and epinephrine induce phosphorylation of ACC through their downstream cAMP-dependent protein kinase (Protein Kinase A, PKA). The phosphorylation of ACC inactivates the enzymatic activity possibly through inhibition of dimer formation (460). In addition high levels of AMP/ATP ratio during catabolic states (such as fasting) activates the AMP-

activated protein kinase (AMPK) as a sensor of low energy state to phosphorylate ACC. The sites of the phosphorylation on ACC and PKA are different but similar to PKA, phosphorylation inactivates the ACC (460). In anabolic states (positive energy balance such as feeding state) the opposite process occurs. The levels of glucagon and epinephrine are low and consequently PKA signaling, and hence phosphorylation of ACC, also diminish. Also the decreased ratio of AMP/ATP inhibits the AMPK activity. These remove the inhibition on ACC. In addition, high level of insulin during anabolism activates the phosphatase A_2, which dephosphorylates and activates ACC (460). The ACC is also regulated at transcription level. As transcriptional regulation of ACC may also contain FAS transcription, it will be discussed later along with FAS.

C. 3. 1. 4. Synthesis of Fatty Acids from Malonyl-CoA and Role of Fatty Acid Synthase (FAS): Fatty acid synthase is not a single enzyme but a multi-enzyme protein complex composed of six enzymes and an acyl carrier protein (ACP) with a phosphopantethein prosthetic group (467). The pathway of fatty acid (palmitate) synthesis is a cycle of decarboxilic condensation reaction. In the first cycle, Acetyl-CoA functions as the primer and undergoes a condensation reaction with malonyl-CoA to form a C4 -saturated acyl chain product. The saturated acyl chain product of one cycle becomes the primer substrate for the following cycle and undergoes the condensation reaction with a malonyl-CoA. Each one of these six enzymes mediates a reaction in this cycle. The ACP translocates the various intermediate products of each reaction to the catalytic site of the next reaction [Reviewed in (460)].

The first reaction is mediated by β-ketoacyl synthase (KS), the condensation enzyme:

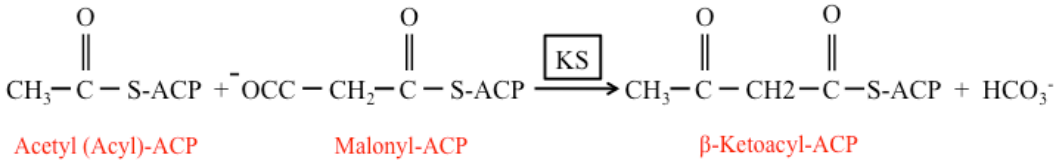

In the next three reactions, the β-ketocyl moiety is reduced by ketoreduction, dehydration and enoylreduction processes mediated by Ketoacyl Reductase (KR), Dehydrase (DH) and Enoyl Reductase (ER) respectively. Two NADPH molecules are used during these reactions for reduction.

1. Ketoacyl reduction:

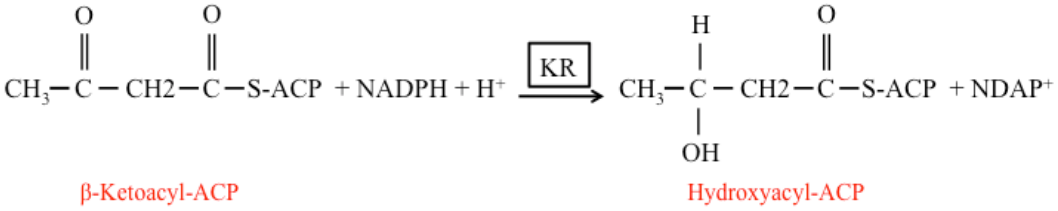

β-Ketoacyl-ACP Hydroxyacyl-ACP

2. Dehydration:

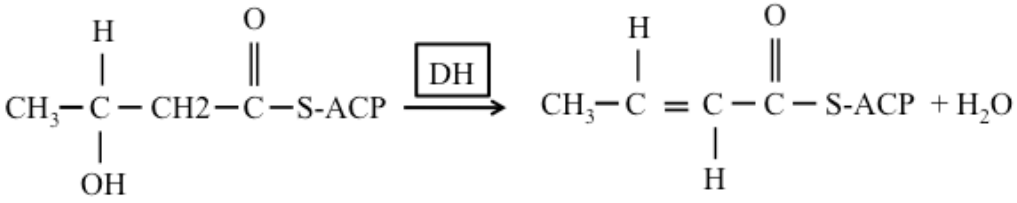

Hydroxyacyl-ACP Enoyl-ACP

3. Enoyl reduction:

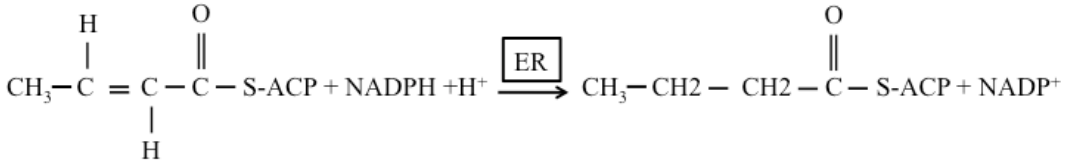

Enoyl-ACP Acyl-ACP

As it was explained above the acyl carrier protein (ACP) functions as a hanging arm that translocates the intermediates between active sites of enzymes. For this purpose the primer acetyl-CoA and Malonyl-CoA should be transformed first to an ACP intermediate. Malonyl/Acetyl-Transferase (MAT) mediates this process:

Acetyl-CoA Acetyl-ACP

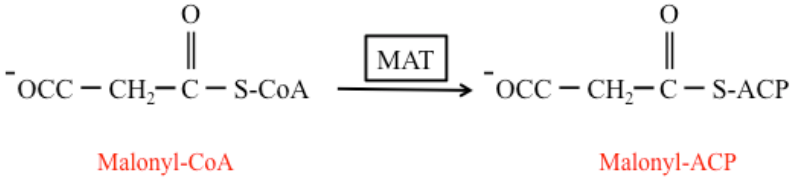

Malonyl-CoA Malonyl-ACP

The termination of the elongation process is very selective and as it was explained the major products of FAS is a saturated fatty acid, palmitate (C16:0). This selectivity is partly due to the unique structure of FAS. The condensation enzyme (KS) has a broad chain-length specificity (C2-C14). The KS Catalytic activity is reduced more than 200 times for chains longer than 14 carbons. On the other hand the sixth enzyme of the FAS complex, Thioesterase (TE), which removes the acyl moieties from the phosphopantethein thiol of ACP, release the FA and terminates the chain elongation and has an extremely low catalytic activity for Acyl-molecule with less than 16 carbons. Therefore the specific catalytic activities of chain-elongating (KS) and chain-terminating (TE) enzymes ensure that the 16 carbons fatty acid is the major product (468). In addition, KS is able to act only on completely reduced intermediates, therefore only the saturated intermediates are elongated. This also ensures the formation of saturated products by FAS (469).

Two types of FAS have been found in mammalian tissue, FAS1 and FAS2. FAS1 is located in cytosol and is the one responsible for formation of palmitate. FAS2 is located in mitochondria and one of its functions is to supply octanoyl moieties as a lipoyl moieties which is essential for mitochondrial function (460). Although FAS is not a rate-limiting enzyme for fatty acid synthesis its function is regulated tightly at transcriptional level. Due to the similarity of transcriptional regulation of ACC and FAS, this regulation will be discussed here.

C. 3. 1. 5. Long-term Regulation of FAS and ACC: In contrast to ACC that is under a short-term regulation, FAS is not regulated allosterically or post-transcriptionally. Regulation of FAS and other accessory enzymes of fatty acid synthesis such as ATP-citrate lyase, malic enzyme (both from Citrate shuttle pathway), Glucose-6-phosphate dehydrogenase (involved in NADPH formation) is at the transcriptional level. ACC expression can also be regulated at the transcriptional level. In the well-fed state (in particular high carbohydrate meal), the levels of these enzymes are high; in contrast their levels are low in the starving state. The high levels of insulin and glucose are partly responsible for these changes and induce the processes, which lead to the activation of the lipogenic genes, but presence of high levels of lipids (sterols) also can control the activation of genes through transcription factors. A role for polyunsaturated fatty acids has been declared in regulating lipogenic genes as high fat diet suppresses de novo lipogenesis.

Two separate genes encode the ACC1 and ACC2. Multiple promoters are involved in the transcription of ACC1 and ACC2. FAS is encoded by a single copy gene with two promoters. Apart from general transcription factors such as Sp1 and NF-Y, several

specific transcription factors have nuclear elements on promoters of FAS and ACC for binding. Upstream Stimulatory Factor (USF) is one of these transcription factors, which its role has been shown in FAS expression. USF binds to -65 and -332 E-Box and these attachments are essential for the activation of FAS transcription (470-474). Although the presence of this transcription factor and its attachment to -65 box is critical for induction of the lipogenic enzymes and USF knocked out mice exhibit severe impaired induction of lipogenic enzymes (474), the complete induction of these genes requires another specific transcription factor. Attachment of Sterol Regulatory Element Binding Protein (SREBP) to Sterol Regulatory Element (SRE) at promoter of these genes is required for maximum induction and in the absence of SREBP this response is not complete (470-473). SREBPs belong to the basic helix-loop-helix leucine zipper family of transcription factors and are synthesized as a transmembrane protein in ER and nuclear membrane. In the ER membrane they are attached to another protein SREBP Cleavage Activation Protein (SCAP). When sterols are abundant in ER, another ER resident protein, Insulin Induced Gene Protein (INSIG), traps the SCAP (and consequently SREBP) and prevents its translocation to the Golgi. Translocation of the SCAP-SREBP complex to the Golgi apparatus during low sterol levels exposes this complex to site-1 and site-2 proteases that release the N-terminal domain of SREBP (mature or nuclear form). The N-terminal of SREBPs constitutes a transcription factor, which binds to sterol regulatory elements at the promoters of target genes (460, 475). Three isoforms of SREBP exist in mammalian tissues; SREBP-1a, -1c and -2. SREBP-1a and -2 are expressed in all cell types. SREBP-1c is the predominant isoform in most adult non-dividing metabolic tissue such as liver and adipose tissue. SREBP-2 is responsible for activation of genes that are involved in cholesterol metabolism (such as HMG-CoA Reductase, LDLR), whereas SREBP-1c is primarily involved in genes responsible for fatty acid synthesis. SREBP-1a targets both sets of genes (476). Binding of USF to -65 and -332 E-Box is necessary for the SREBP maximum effect as in the absence of USF, the SREBP response is not complete. Therefore it seems that USF and SREBP act synergistically for activation of lipogenic genes) (470-473).

It was originally thought that SREBPs are exclusively controlled by sterols, but SREBPs can be tightly regulated by several other factors. As we discussed previously, insulin controls the lipogenesis at the enzyme level. Recently it has been shown that insulin signaling pathway might indeed regulate the SREBPs as well. This regulation is mediated through Phosphatidylinositol 3-Kinase (PI3K)/protein kinase B (Akt) signal transduction. The attachment of insulin (and insulin-like growth factor) to their receptors activates the PI3K in the cytosolic side. PI3K in turn catalyzes the conversion of a membrane phospholipid, Phosphatidylinositol 4,5-bisphosphate (PIP2) to phosphatidylinositol 3,4,5-

triphosphate (PIP-3). PIP-3 interacts and recruits Akt to the membrane where Phosphoinositide-dependent kinases (PDK) reside. From different members of PDK family, mammalian target of rapamycin (mTOR) complex has been the prime candidate for phosphorylation of Akt in PI3K/Akt pathway. MTORC phosphorylates and activates the Akt, which later targets several metabolic pathways and enhances the SREBPs-mediated lipogenesis (460). Interestingly SREBP-1c transcription is controlled by another transcription factor; Liver X receptors (LXR)(477). LXR is a nuclear hormone receptor that forms a heterodimer with a nuclear factor; Retinoid X Receptor (RXR) and can activate several lipogenic genes(477). Two isoforms of LXR exist; LXRα and β. There are two binding sites for LXR on SREBP-1c promoter and disruption of these sites abolishes the response to LXR agonist(478). In addition to activation of SREBP-1c, cell culture experiment has shown that LXR can directly activate the FAS expression and a binding site for LXR has been suggested at direct repeat-4 (DR-4) on -669 to -655 of FAS promoter(479). Therefore LXR may activate lipogenic enzymes such as ACC and FAS directly or indirectly through SREBP-1c.

In addition to insulin, glucose itself can induce the lipogenesis during feeding. Some of these effects are mediated through activation of glycolytic pathway and production of more citrate but it could also be mediated through FAS expression at the presence of constant level of insulin(480). Carbohydrate Responsive Element Binding Protein (ChREBP) has been shown to play a key role in this process. A carbohydrate response element has been found on both ACC1 and FAS promoters and has shown strong glucose mediated activation(481-483). ChREBP is a labile protein, which is undergo a phosphorylation or is stabilized by Max-like Protein X (Mlx). When the glucose level is low (during catabolic state) high cellular AMP concentration activates AMPK, which phosphorylates the ChREBP and enhances its cytosolic localization by attachment to protein 14-3-3(484). In contrast when the glucose level is high (thus AMP level is low) this deactivation is reduced(484). In addition exposure to high glucose enhances the pentose phosphate pathway and increases xylulose-5-phosphate(485). This intermediate activates protein phosphatase 2A that dephosphorylates ChREBP, therefore reduces the interaction of ChREBP with protein 14-3-3 and cytosolic localizatio(485)n. The ChREBP undergoes nuclear translocation and after interaction with Mlx binds to the lipogenic promoters and activates them(484). High fat diet is also able to inhibit the de novo lipogenesis. Polyunsaturated fatty acids (PUFA) suppress the SREBP mediated activation of lipogenic gens through enhanced SREBP mRNA decay(486) and increased SREBP degradation by proteasome(487).

C. 3. 2. Role of De novo fatty Acid Synthesis in HCV-related Steatosis

Enhanced de novo fatty acid synthesis has been assumed as one of the possible direct mechanisms by which HCV induces steatosis (see below). Using various models of HCV infection such as HCV protein expression models, subgenomic replicons, Huh7/JFH-1 cell culture, transgenic mice expressing HCV proteins and even human liver samples, impact of HCV infection on de novo fatty acid synthesis has been investigated. Numerous articles have been published during the last decade, evaluating this effect but unfortunately the majority of these articles are contradicting each other and the possible effect of HCV proteins on de novo fatty acid synthesis remains unclear. Some of these discrepancies are related to the different methods or various models that have been utilized by these experiments. For example, although very valuable, evaluating human liver samples are extremely difficult and the results can be skewed by patients' life styles, weight, age and possible undiagnosed metabolic conditions (such as hyperlipidemia, DM, etc.). In addition only a small population of hepatocytes are infected during CHC. Therefore inability to find a significant relationship between HCV infection and lipogenesis does not always indicate the absence of relationship. On the other hand, Chimpanzees, the most valuable animal model in HCV research field, are an endangered species and are not accessible to all investigators. Most of the data that has been achieved from this model are from only a limited number of animals making this data very difficult to be interpreted. Cell culture models are a useful method for studying the direct effect of HCV on lipogenesis as other factors affecting lipogenesis can be controlled, but the negative side is that they are not able to show the whole picture of the lipid metabolism as hormonal factors (insulin, epinephrine, glucagon, etc.) or the concomitant effect of other tissues (Sinusoidal endothelium, adipocytes, etc.) are not involved. In addition the only cell culture model, which supports the HCV infection (Huh7/JFH-1) is based on a very specific subtype of HCV infection (JFH-1) and the host cells (Huh7 cells) have a very different lipid metabolic condition compare to primary human hepatocytes. In animal or cell culture models that HCV proteins are expressed, the outcome is highly dependent on the level of expression of the target protein as different levels of expression may result in completely opposite outcomes. Therefore even though this is very useful, evaluation of these results should be performed cautiously and with consideration of the limitations of each one of these models.

Using Huh7 cells expressing core, Fukazawa et. al perform the most direct study investigating the impact of HCV on de novo fatty acid synthesis (488). They showed when cells were incubated with ^{3}H-radiolabelled acetate; almost the entire radioactivity was incorporated into lipid esters. In addition the level of radioactive lipid esters was higher in Huh7 cells expressing core protein (compare to naïve Huh7 cells) and this was

associated with higher levels of FAS and ACC activity as well as expression (both mRNA and protein). Although they were the only group that measured the fatty acid synthesis directly, they never demonstrated the incorporation of radiolabelled fatty acids in each lipid esters family separately. In addition accumulation of radiolabelled lipid esters in cells expressing core protein was attributed to enhanced de novo fatty acid synthesis while they didn't measure the amount of secreted radiolabelled lipid esters, therefore the role of reduced secretion of lipid esters cannot be excluded.

Several groups measure the expression levels of lipogenic genes in the liver biopsies taken from patients infected with HCV. In agreement with the hypothesis that HCV infection enhances the expression of the lipogenic genes, it was shown in genotype-1 infected patients, the LXRα, SREBP-1c and FAS expression levels (both mRNA and protein) were significantly higher in comparison to healthy individuals, but these enhancements were observed only in those patients whose biopsies showed steatosis. In patients without steatosis only LXRα and SREBP 1c protein levels were significantly higher and FAS level remained unchanged (489). In another study using liver biopsies taken from 100 patients infected with various genotypes of HCV, the levels of LXRα, SREBP 1c and FAS mRNA were enhanced significantly in comparison to normal healthy liver (490). In contrast several other studies have shown contradictory and sometimes opposite results. Recently, Ryan et al. have compared the lipogenic gens in HCV genotype 1, genotype 3 and HBV infected liver biopsies (491). They have shown that there was no significant difference in SREBP-1 and FAS mRNA between HCV and HBV infected patients and also between genotype 1 and 3. They concluded that de novo lipogenesis might not be responsible for HCV-induced steatosis. Another group has shown very similar results. Using liver biopsy samples from 124 HCV infected patients and 12 healthy individuals, McPherson et al. investigated the transcriptional levels of SREBP-1c, FAS, and Microsomal Triglyceride Transfer Protein (MTP)(492). They showed that there was no significant increase in FAS and SREBP 1c mRNA in HCV infected liver specimens but they found significant decrease in MTP mRNA level, a protein involved in VLDL secretion (see C. 4. 1. 3. Primary lipidation and role of Microsomal Triglyceride Transfer Protein). In order to determine if steatosis associated with HCV was mediated by altered lipogenic gens, they compared the transcriptional levels of SREBP 1c, FAS between patients with different stages of steatosis. Unexpectedly the results showed that there was a negative correlation between stage of steatosis and SREBP 1c or FAS mRNA. The same pattern was observed when stage of fibrosis was correlated to SREBP 1c and FAS mRNA. They also showed similar results in patients with genotype 3 and concluded that up regulation of lipogenesis might not be the mechanism by which HCV induces steatosis. Considering higher levels of AMPK activity

during fibrosis, they suggested that the observed decrease in SREBP-1c and FAS mRNA in regards to stages of steatosis and fibrosis might be mediated with increased level of AMPK (a negative regulator of lipogenesis). In another study liver biopsies obtained from 44 patients with genotype 1 were compared to normal liver biopsy (493). The mRNA levels of LXR, RXR and SREBP 1c were significantly lower in biopsies obtained from HCV infected patients. The FAS and ACC mRNA levels were also lower in HCV infected patients but it didn't reach to statistical significance. Although the level of FAS mRNA was lower in HCV infected liver biopsy, there was a positive correlation between FAS mRNA and HCV RNA load.

To overcome the difficulties of working with human samples and in order to better understand the possible mechanism by which HCV interacts with de novo fatty acid synthesis pathway, several other models have been used. Using FAS promoter-luciferase reporter in Huh7 cells expressing HCV genotype 1b and 3a core, the up-regulation of FAS promoter was observed and this enhancement was higher in cells expressing 3a core (494). The upregulation of FAS promoter was inhibited when FAS promoter-luciferase reporter with -63 to -46 deletion. Therefore the author concluded that this upregulation of FAS promoter is SREBP dependent (494). Although this upstream area is important for SREBP-1c-related upregulation of FAS promoter, as it was discussed earlier it is an E-box for USF binding not SRE and the effect of USF cannot be excluded. Interestingly they reported that the more profound increase in FAS promoter activity seen by HCV 3a core was related to the presence of Phenylalanine at position 164 in 3a core instead of Tyrosine in genotype 1b. This position is one of the sites for HCV core attachment to the lipid droplets. Although they have shown that substitution of Phe-164 with Tyr in 3a core dramatically reduced the FAS promoter up-regulation, they never tested if the substitution of Tyr-164 with Phe in 1b core could enhance the FAS promoter activity (494). The same author has further investigated the mechanism of this FAS upregulation by studying the SREBPs expression/activation in cell culture models expressing 1b or 3a core and in 1b subgenomic replicon or 3a core/1b chimeric subgenomic replicon (495). It was shown that the level of mature SREBP 1 (sliced SREBP 1 from SCAP) was increased in cells expressing 3a and 1b core and also in 1b and 3a core/1b subgenomic replicons. This effect was more profound with the 3a core constructs. In addition in HCV 3a core/1b replicon the phosphorylated form of SREBP-1a was enhanced significantly and it was correlated with SRE-driven transcription activation. These effects were abolished when PI3K inhibitor (LY294002) was added or when Akt-2 was knocked down in these cells. Therefore these results clearly support a mechanism for activation of SREBPs by HCV core protein through phosphorylation by PI3K/Akt pathway. But unfortunately this effect was only shown in SREBP-1a, which is not as

important as SREBP-1c in fatty acid de novo synthesis. In addition, they have never shown that these changes were associated with increased expression of downstream genes (FAS or ACC). In line with these experiments, the role of HCV core on lipogenesis was investigated in vivo, using HCV core transgenic mice (496). It was shown that the expression levels of SREBP-1c and its downstream genes (ACC, FAS and SCD) but not SREBP 1a and 2 were enhanced in the liver of HCV core transgenic mice. It was also shown that these changes were associated with increased area of cell covered by lipid droplets. This SREBP -1c activation was in a LXRα-RXRα dependent manner.

In addition to core other HCV proteins have shown to up regulate the lipogenic genes. Using SREBP-1c promoter-luciferase reporter it was shown that cells expressing NS2 had more SREBP-1c promoter activity (497). This upregulation of SREBP-1c promoter activity was LXR dependent as the deletion of LXR element on the promoter of SREBP-1c abolished this up regulation. In addition it was shown that enhanced SREBP-1c promoter activity in cells expressing NS2 protein lead to enhancement of SREBP-1c expression (both precursor and mature type) and resulted in higher FAS promoter activity and FAS mRNA level. Apart from NS2 and core, NS5a has also been shown to up regulate lipogenesis. In HCV 1b subgenomic replicon in which NS5A protein from genotype 3a was substituted, the levels of mature SREBP-1c both in cytosol and nucleus increased significantly (498). This was associated with enhanced SREBP-1c promoter activity and was mediated through Sp1 nuclear factor. The role of NS4B was also investigated by Hwang et. al. using Huh7 cells expressing HCV proteins or subgenomic replicon and in Huh7/JFH-1 culture system (499). They have shown that among HCV proteins, NS4B was able to enhance the SREBP-1 promoter activity, mRNA and protein (both mature and phosphorylated form) and its downstream gene, FAS. In addition they were able to show the same results with SREBP-2 and its downstream gene, HMG-CoA Synthase. Very similar results were observed in Huh7/JFH-1 cells culture and in subgenomic replicon. All of these upregulation in lipogenic genes were associated with intracellular lipid accumulation. They also confirmed the role of Akt signaling in this process as treating cells with Akt inhibitor (LY294002), prevented the up regulation of lipogenic genes. Interestingly none of the other non-structural protein was able to induce this up regulation except to core protein. Very similar results were observed by Waris G. et. al. for NS4B as they were able to show the upregulation of SREP-1c and 2 mediated genes such as FAS, ACC, HMG-CoA Reductase and Squalene Synthase in Huh7/JFH-1 culture system and cells expressing NS4B from genotype 1 and 3 (500). In addition they also were able to show the upregulation of LXRα mRNA and consequently higher SRE activity, SREBP 1 and 2 mRNA and mature forms of SREBPs. Furthermore all these effects were inhibited when cells were treated with PI3K inhibitor, calcium chelator and

antioxidants. It was shown that HCV infection induces the reactive oxygen synthase and calcium signaling. Therefore as SREBP activation is inhibited by antioxidant and calcium chelators, it seems that ROS or calcium signaling may activate SREBP-mediated lipogenesis through PI3K/Akt pathway (500).

The possible role of LXRα as the transcriptional factor for SREBPs in pathogenesis of steatosis during HCV infection was also investigated (501). Using Chang Liver cells (CCL13) expressing Core and NS5a and also Huh7 expressing full-length genotype 1b replicon, it was shown that the LXRα expression (mRNA and protein) was enhanced. This enhancement was PI3/AKT pathway dependent as LY294002 (the inhibitor of AKT) inhibited the up regulation of LXRα. This activation of LXRα was also associated with activation of downstream genes such as SREBP 1c, FAS, and PPARγ. In addition the enhanced interaction of LXRα with LXR element on FAS and SREBP-1c was observed. This enhancement of lipogenic genes in cells expressing HCV protein was reversed by SiRNA mediated knock down of LXRα. In contrast LXRα agonist enhanced this effect. Interestingly it was also shown that SiRNA mediated knock down of LXRα was associated with lower HCV RNA replication and reduced number of cells expressing HCV core and NS5a. The opposite occurred when cells were treated with LXRα agonist. The author concluded that probably this activation of LXRα is necessary for HCV production. Another role for LXR, not related to lipogenesis, has been indicated in HCV life cycle. LXR activates the E3 Ubiquitin Ligase Idol (inducible degrader of LDL receptors). As LDLR is one of the many receptors that mediate the HCV entry, activation of LXRα may induce the degradation of LDLR and therefore reduced the HCV entry. Indeed activation of LXR with GW3965 and T0901317 (LXR agonists) resulted in activation of Idol in Huh7.5 cells and reduced the LDLR levels (but not other HCV entry receptors) and HCV entry in HCVcc. In addition the HCV replication and/or secretion were not affected(502). This shows that LXRα may play a regulatory role by 1) increasing the replication of HCV in cells and 2) assuring that cells are not overloaded and overwhelmed by the virus by preventing HCV entry.

Other possible mechanisms by which HCV may induce lipogenesis were also investigated. Cannabinoid receptors (CB) have been shown to interact with lipid metabolism cycle in liver. Two receptors have been found in the human body, CB1 and CB2. CB1 have an important role in appetite stimulation and when it is inhibited reduces the serum TG and causes weight loss independent of food intake. In contrast CB1 activation is associated with obesity, insulin resistant and dyslipidemia. Although weakly expressed in human liver, CB1 is strongly upregulated in Liver fibrosis due to alcohol

overuse, HBV and PBC. In addition it has been shown that CB1 mediate the hepatic steatosis in alcoholic hepatitis and NASH by increasing the SREBPs expression and enhancement of de novo fatty acid synthesis. Therefore possible effect of HCV on CB1 was investigated in liver biopsy from 88 chronic hepatitis C patients and 12 healthy controls and 10 chronic hepatitis B patients. The results showed significant upregulation of CB1 in chronic hepatitis C patients compare to control and HBV patients. In HBV patients CB1 was upregulated but it was three times less than HCV patients. The upregulation of CB1 in chronic HCV patients was correlated with the levels of fibrosis and steatosis and HCV RNA titer but it could still be seen in patients with no fibrosis. Also SREBPs, FAS and ACC1 expressions were also upregulated but it was just seen in HCV genotype 3 patients. The same results were observed in Huh7.5/JFH cells as well (503).

The impact of HCV infection on accessory enzyme was also studied. Using Huh7 cells that replicate the full-length HCV genotype 1b replicons, it was shown that several lipogenic genes including ATP citrate lyase, Acetyl-CoA Synthase, were upregulated. In this study opposite to previous studies that were discussed above, the FAS, HMG-CoA reductase and synthase were not affected (504).

All of these experiments support that enhanced lipogenesis might be one of the mechanism by which HCV induces steatosis. But how does HCV benefit from enhanced lipogenesis? As it will be discussed later LDs have been considered as important organelles for HCV life cycle and therefore enlargement of LDs by enhanced lipogenesis may be beneficial for HCV replication/assembly. Apparently reducing lipogenesis decreases the LD size/number and may prevent production of HCV and might be a good candidate for antiviral therapy. Recently a group of scientists have used an interesting approach to investigate this hypothesis (505). They utilized Serine Protease Inhibitor (Serpins) scaffold that contains the reactive center loop conformation and specifically inhibits Subtilisin/kexin-isozyme-1/ site-1 protease (SKI-1/S1P). The S1P (site 1 protease) is necessary for the release of mature (active form) SREBPs in the Golgi apparatus. They have shown that Huh7.5 cells that were transfected with this construct had reduced expression of SREBP-2 and its downstream genes and also the CE amount in cells. These changes reduced the LD size and consequently the HCV RNA replication, and cellular core levels. In another approach polyunsaturated fatty acid (PUFA) was used. PUFA has been shown to inhibit the de novo fatty acid synthesis by antagonistic effect on LXRα. It was shown that PUFA could reduce the SREBP-1c and FAS genes and indeed the HCV replication. But interestingly it was shown that this effect was not due to inhibitory effect of PUFA on LXRα as LXRα agonist was not able to rescue the HCV replication while it rescued the SREBP-1c and FAS expression (504). Although these

results may support the hypothesis that productive HCV infection requires an intact lipogenesis pathway, it does not confirm if enhancement of lipogenesis is beneficial for HCV replication.

It was hypothesized that apart from increase LDs size, enhanced cholesterol biosynthesis pathway might be required for HCV by prenylation of the HCV proteins. Prenylation of protein by geranylgeranyl isoprenoids facilitates the interaction of certain proteins with lipid membrane and it is possible that this process is required for some of the HCV proteins, which closely interact with lipid bilayer. Indeed it was shown that prevention of cholesterol synthesis by lovastatin (HMG-CoA Reductase inhibitor) significantly reduced the HCV replication. More specifically L659, L699 and ZA the specific inhibitors of HMG-CoA Reductase and squalene synthase (two enzymes that are required for formation of isoprenoids) reduced the HCV replication (504).

Yang et al. has investigated if FAS level is altered by HCV infection in Huh7.5/JFH-1 cell culture model and subgenomic replicon (506). They also have studied if FAS down regulation has any impact on HCV production and infectivity. They have shown that FAS protein level was enhanced in infected cell culture and subgenomic replicons. To investigate if altered FAS level has any role in HCV life cycle, they knock down the FAS or utilized C75 (an inhibitor of FAS). They have shown reduced core expression, HCV RNA secretion into media and infectivity when FAS was inhibited by C75 or abolished by shRNAi targeting FAS. They also found a very interesting phenomenon in which HCVpp absorption was significantly reduced in cells treated with C75. They found in the same cells that CLDN-1 expression was also diminished and they concluded that down regulation of CLDN-1 was the reason for less HCVpp cell entry in these cells but the mechanism of this decrease remains to be evaluated.

C. 3. 3. Triacylglycerol Biosynthesis

C. 3. 3. 1. General Description of TG Biosynthesis: Triacylglycerol is the ester of three fatty acids with a molecule of glycerol. Apart from being the primary source of energy stored in virtually all eukaryotic cells, it has several other roles in the body. It prevents penetration of water and dissipation of heat, therefore forms a water barrier and heat insulation in skin. In addition it serves as a cushion within joints and around internal organs and prevent mechanical trauma. In every eukaryotic type of cell, stored TG sequesters FA and protects the cells from the detergent properties of FA.

In human, two major pathways for TG biosynthesis exist; 1) the glycerol phosphate also known as the Kennedy pathway (507) and 2) monoacylglycerol (MG) pathway (508, 509).

Monoacylglycerol pathway is the dominant mode of TG biosynthesis in enterocytes from components of partially hydrolyzed dietary lipids (508). Kennedy pathway is the dominant one in the majority of the tissue including hepatocytes (507).

In Kennedy pathway, the process of TG biosynthesis begins with sequential acylation of glycerol-3-phosphate (G3P, an intermediate molecule produced in glycolysis pathway) by acyl-CoA. In the initial step, G3P is esterified at its first carbon (sn-1 position) to form Lysophosphatidic acid (LPA) (507, 510). This step is mediated by sn-1-glycerol-3-phosphate acyltransferase (GPAT):

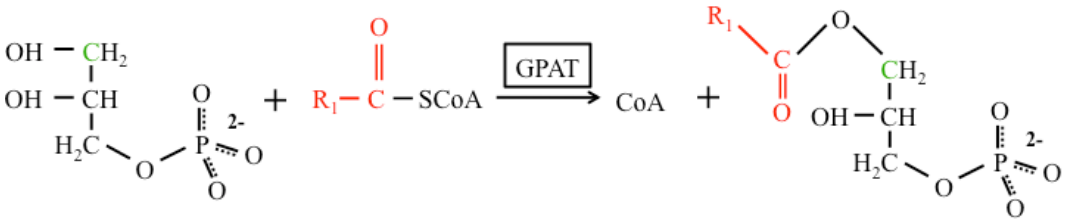

The second acylation takes place at sn-2 position of LPA to form Phosphatidic acid (PA). This step is mediated by acylglycerol-3-phosphate acyltransferase (AGPAT) also called Lysophosphatidic acyltransferase (LPAAT) (510).

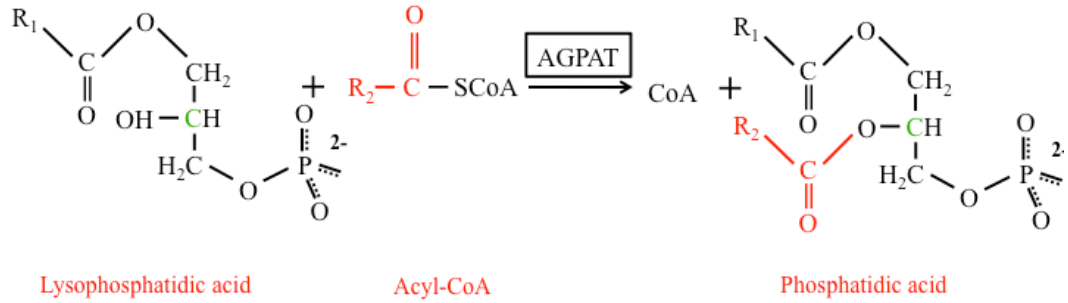

In the third step PA hydrolyzed by phosphatidic acid phosphatase-1 (PAP-1, also called lipin), to form diacylglycerol (DG) (507, 510).

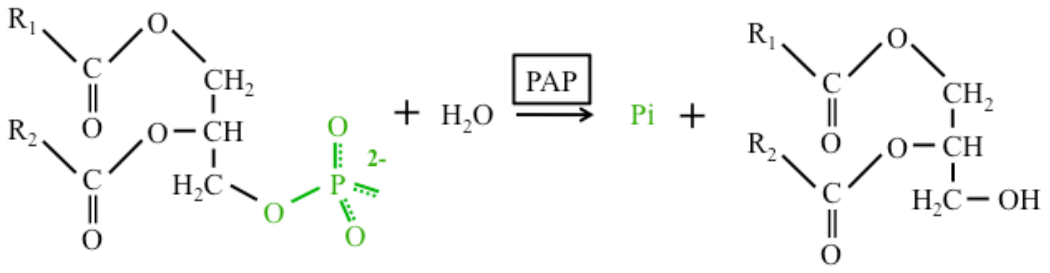

The final acylation step is mediated by diacylglycerol acyltransferase (DGAT) and forms TG (507, 510).

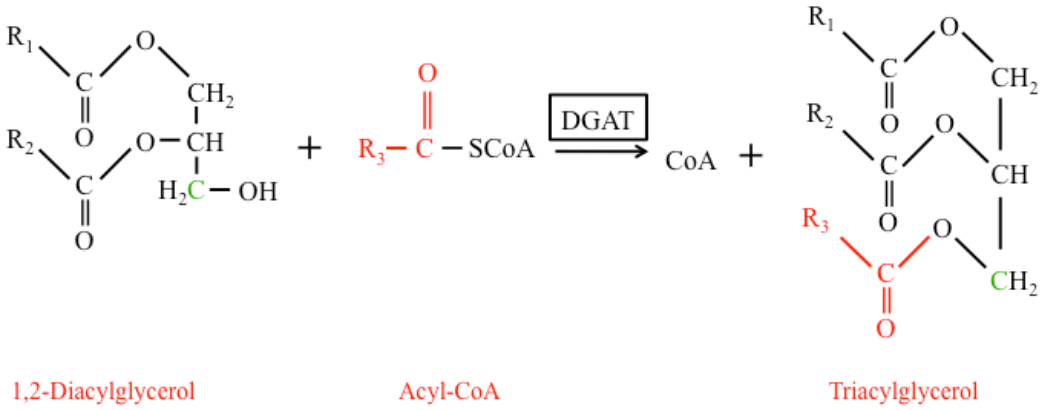

C.3. 3. 2. Sn-Glycerol-3-Phosphate Acyltransferases (GPATs): Four GPAT (GPAT 1-4) enzymes have already been discovered (510) and synthesis of TG via dihydroxyacetone phosphate suggests a possibility of an additional GPAT (511). GPAT-1 is a 94 kDa protein. It is enriched on the outer mitochondrial membrane and also ER-mitochondrial membrane contact sites. From these two locations, the GPAT-1 located on outer mitochondrial membrane has much higher activity (510, 512). GPAT-1 is highly expressed in liver and adipose tissue(513) and contributes to 30-50% of total GPAT liver activity(512). In other tissues the GPAT-1 activity contributes to approximately 10% of GPAT activity(512). Substrate specificity of GPAT-1 is unique among GPATs with a preference for saturated FA in particular C16 (palmitic acid) (514). Overexpression of GPAT-1 in CHO cells (515) results in enhanced incorporation of labeled FA into TG. Similarly adenovirus mediated overexpression of GPAT-1 into rat liver causes marked hepatic steatosis within 5-7 days (516). In contrast GPAT-1 knockout mice (Gpat-1-/-) have less body weight, and significantly less content of hepatic TG than control, under both high and low fat diets (514). Even in obese model of mice (ob/ob; leptin deficient mice) with high content of hepatic TG, knocking down of GPAT-1 normalized the hepatic

TG level (517). All these evidences confirm the role of GPAT-1 in biosynthesis of TG. In addition as both GPAT-1 and CPT-1 consume acyl-CoA as a substrate and both are located on mitochondrial outer membrane, it was assumed that they might compete for acyl-CoA. Indeed it has been shown that in GPAT-1 knockout mice the FA oxidation rate increased significantly with enhanced plasma β-hydroxybutyrate (product of FA β-oxidation) level (518). In contrast overexpression of GPAT-1 in rat hepatocytes reduces the FA oxidation (519).

GPAT-2 is a 88 kDa protein located on mitochondrial outer membrane (520). GPAT-2 accounts for about 60% of GPAT activity in mitochondria purified from liver (521). It is expressed in most of the tissue, but GPAT-2 mRNA is 50 times more abundant in testis (522). In contrast to GPAT-1 it does not have any preference for substrate (521)and the abundance of GPAT-2 mRNA in liver is not regulated in relation to fasting or feeding (522). Over expression of GPAT-2 into Cos-7 cells enhanced the incorporation of labeled oleate into TG but not phospholipids (515). As it is highly expressed in the testis in comparison to other tissue, it is believed that GPAT-2 likely has a specific function in the testis that has not been discovered yet. GPAT-3 is an ER resident protein with a predicted mass of 50 kDa (520). Recently it has been shown that GPAT-3 has both GPAT and AGPAT activity (523). In humans it is expressed mostly in kidney, heart and skeletal muscles and with lower amounts in adipose tissue and lungs (523). GPAT-3 is also expressed in liver but in a very low level in comparison to other tissues. The levels of GPAT-3 mRNA increases approximately 60 fold during differentiation of preadipocytes to adipocytes and is thought to have an important role for maturation of adipocytes (524). In contrast to GPAT-1, GPAT-3 does not possess substrate preference. In addition, GPAT-3 incorporates oleic acids into TG but not PL (523). GPAT-4 is also an ER-resident protein and has a predicted mass of 52 kDa (520). It is mostly expressed in adipose tissue with some moderate levels at liver, kidney, brain, intestine and testis (525-527). GPAT-4 does not have substrate preference. Surprisingly in most of the cells like HEK-293 and COS-7, over expression of GPAT-4 does not enhance the incorporation of exogenous fatty acid into TG, suggesting that the pool of substrate for GPAT-4 might be different than other GPATs (526, 528). But in HepG2 cells the overexpression of GPAT-4 enhances the incorporation of exogenous FA into TG by 20%, indicating the differences between cell types (526). GPAT-4 seems to have an important role in liver and adipose tissue. GPAT-4 knockout mice have 60% reduction in their hepatic and adipose GPAT activity, 25% lower weight, absence of subdermal fat and 45-50% hepatic and plasma TG level when they are fed with chow diet. These changes are associated with higher level of energy expenditure, possibly due to the compensation for the absence of subdermal fat tissue,

which the later acts as heat insulation. In addition ob/ob, GPAT-4 -/- mice are more resistant to weight gain than ob/ob mice (526, 527).

C. 3. 3. 3. Sn-1 Acyl-Glycerol-3-Phosphate-Acyltransferases (AGPATs): As it was discussed above AGPAT mediates the second acylation step and transfers the acyl group from acyl-CoA to lysophosphatidic acid at sn-2 position, therefore also called Lysophosphatidic acid acyl transferase (LPAAT). AGPAT-1 and AGPAT-2 are well established AGPATs that their LPAAT activities have been already confirmed. AGPAT-1 is located on ER membrane and has a calculated mass of 32 kDa (529). It is expressed in majority of tissues including liver, adipose, skeletal muscle, heart and lung tissue (530, 531). As it was indicated it has LPAAT activity with preference for fatty acid species C12-16:0, C16:1, C18:2 and C18:3 followed by C18:0 and C18:1 with poor activity for C20:0 (532). Overexpression of AGPAT-1 promotes the oleate incorporation into TG and suppresses the release of fatty acids in both adipose tissue (3T3-L1 cells) and muscles (C2C12 Myotubes). In addition in these cells AGPAT-1 overexpression reduces the conversion of glucose to glycogen and therefore alters the fate of up taken glucose toward fatty acid synthesis (533). AGPAT-2 is the second protein in AGPAT family and is the most potent one. It has a molecular mass of 31 kDa and is located on the ER membrane (534). It has the strongest LPAAT activity among the AGPATs [90% of liver LPAAT activity (535)] and is very specific for LPA with the lack of GPAT, LPEAT, LPCAT and LPSAT activities (530, 532, 534, 536). Its preferred acyl donors are C14:0, C16:0, C18:1 and C18:2 with lower incorporation of C18:0 and C20:4 CoAs (532). It has also a preferred acyl acceptor, 1-oleoyl-LPA (532). It is expressed in almost all tissue and particularly in adipose, liver, heart and pancreas (531, 534). Its absence is associated with a human disease, Berardinelli-Seip congenital generalized lipodystrophy (CGL) (537, 538). CGL is characterized by lack of visceral and subcutaneous fat with the exception of adipose tissue that maintain the mechanical barrier around palm, soles and scalps (indicating a role for another type of AGPAT in these area), hypothermia, insulin resistance and early onset of diabetes, hypertriglyceridemia, hepatic steatosis (539).

Based on structural and amino acid similarity, AGPAT-3 to 11 have been recognized. AGPAT-3 has also been shown to contain LPAAT activity. The activities of AGPAT-4 and 5 have not been recognized yet. AGPAT-6 was shown to have GPAT activity and later was reclassified as GPAT-4 (see above). AGPAT-7 shows to be important mostly for PL formation. This enzyme transfer acyl group from acyl-CoA to Lysophosphatidylcholine (LPC), Lysophophatidyl ethanolamine (LPE) and Lysophosphatidyl serine (LPS), which have choline, ethanolamine or serine attached to sn-3 phosphate group of Lysophosphatidic acid respectively, and therefore contains acyltransferase activity for

these substrates (LPCAT, LPEAT and LPSAT activity respectively). It shows no or a slight LPAAT activity. AGPAT-8 has lysocardiolipin acyltransferase activity. AGPAT-9 has LPCAT activity with a slight LPAAT activity. AGPAT-10 has both LPAAT and GPAT activity and later was reclassified as GPAT-3. AGPAT-11 has a slight LPAAT activity but predominantly is a LPCAT [table 2 in (510)].

C. 3. 3. 4. Phosphatidic Acid Phosphatase (PAP, Lipin): Phosphatidic acid phosphatase is a big family of hydrolase enzymes. It is classified to two major types. Type I (formerly known as PAP-1) is a soluble protein in cytosol that can transiently translocate to ER membrane and specifically consume phosphatidic acid as a substrate. They are codified by LIPIN genes and are involved in TG biosynthesis, and are more classified into lipin-1, -2 and -3 (540). Type II (formerly known as PAP-2 and currently known as lipid phosphate phosphatase) are located on plasma membrane and are involved in signal transduction and do not have any role in TG synthesis through Kennedy pathway (541).

Lipin-1 is a 91 kDa cytosolic protein with transient translocation to ER membrane or nucleus (542). The C-terminal portion of protein (called C-LIP) contains the PAP catalytic motif (DxDxT) (543) and N-terminal portion of the lipin-1 (also called N-LIP) contains a motif with glycine residue that is mandatory for PAP activity as well (519, 544). In addition to PAP activity, lipin-1 also exhibits transcriptional co-activator activity with PPARα, PPARγ, PPARδ, and nuclear factor 4α and is necessary for their actions (545). A motif at C-LIP (different than PAP catalytic motif) is responsible for this interaction (545). Lipin-1 is highly expressed in adipose tissue, liver and muscles (546). Lipin-1 deficient mice have failure in TG storage and low fat content compare to wild type mice and this is associated with reduced PAP activity (547, 548). In addition, lipin-1 deficient mice have enhanced fatty acid utilization for energy expenditure (549). During feeding state wild-type animal utilize mostly carbohydrate as their energy source while in Lipin-1 deficient mice, the hepatic fatty acid de novo synthesis enhanced 27 times and the resulting fatty acid is utilized in peripheral tissue as an energy source (550). During the fasting state, the wild type animals mostly utilize fatty acids in their liver for energy production for gluconeogenesis while the Lipin-1 deficient mice utilize glucose released from glycogen (as they do not have TG as energy stores) (550). In contrast overexpression of Lipin-1 is associated with 60% more TG storage when the mice are fed with high fat or carbohydrate diet (549). In addition Lipin-1 is also necessary for expression of key lipogenic genes, which this effect is related to its role as a co-activator of PPARs and specifically PPARγ (547).

Lipin-2 and 3 also contain the same motif DxDxT at its C-LIP and also conserve the motif that is responsible for interaction with nuclear receptors (551). Lipin-2 and 3 are also cytosolic and are not highly expressed in adipose and muscular tissue but are expressed in medium levels in liver (551). Their level in hepatocytes increases in the absence of lipin-1 that indicates they might act as an alternative pathway for TG synthesis in the liver in the absence of lipin-1 (552).

C. 3. 3. 5. Sn-1,2 Diacylglycerol Acyltransferases (DGATs): DGAT activity was discovered several decades ago but it was not until last decade that DGAT genes have been cloned. Two DGAT enzymes exist that are unrelated in their protein and DNA sequence. Human DGAT-1 protein is a 55 kDa protein that contains 488 amino acids (553, 554). The gene is located on chromosome 8 and composed of 17 exons and spans 10.62 kb (555). It is highly expressed in small intestine, testis, adipose tissue, mammary gland and skeletal muscles and low level at liver (555). DGAT-1 is located on the ER where it forms a homotetramer possibly by attachment of the N-terminal of each monomer (555). Its membrane topology has not been confirmed yet but it is thought to have several TMDs. It is thought that the N-terminal contains a motif that binds to fatty acyl-CoA, while the C-terminal is necessary for DG attachment (556, 557). DGAT-2 is a 40 kDa protein with 388 amino acids. The gene is located on chromosome 11 and composed of 8 exons and spans over 42 kb (555). It is highly expressed in liver, adipose tissue, mammary gland and testis (555). DGAT-2 is also located on the ER and on LDs and its topology has been more widely studied than DGAT-1 (555). Mice DGAT-2 is an integral membrane protein with two TMDs and N and C-termini facing toward cytosol. Majority of this protein is located on cytosolic site suggesting that the active site of the protein is located close to the cytosolic leaflet of the ER membrane (558-560). Human and mouse DGAT-2 have 95% identity in their C-terminal suggesting that the active site of the enzyme might be at this area (559, 560). In addition all DGAT-2 families, from yeast to humans, have a HPHG conserved area and mutation in this area significantly reduces the DGAT activity (559, 560). Close to N-terminal of DGAT-2 there is a consensus sequence composed of nonpolar amino acids, which attaches to neutral lipids (561).

Both DGAT-1 and DGAT-2 have DGAT activity but have a different role and characteristics in vivo (553, 560). DGAT-2 is the more portent DGAT with higher fatty acid affinity (K_m) than DGAT-1. Only in higher concentration of oleic acid (>100μM) the affinity of DGAT-1 and -2 are comparable (559, 562, 563). It is unclear if DGAT-1 and -2 have any preference for a specific fatty acid, although some evidence has shown that DGAT-1 prefers monounsaturated substrate such as C18:1 to saturated fatty acids

(C16:0) (559) and DGAT-2 prefers medium chain fatty acids (C12:0) to long chain fatty acids (C18:1) (558). Also the source of DG used by DGAT-1 and -2 for generation of TG might be different. DGAT-2 utilizes DG from endogenous source, while DGAT-1 is more dependent on added DG (558, 559). In addition, DGAT-1 has MGAT activity (esterifying TG from MG by sequential addition of two fatty acids) and is also able to add acyl-CoA to retinol and wax (554). DGAT-2 exhibits only DGAT activity (553, 560). In addition DGAT-1 and -2 participate in different pathways of TG synthesis. Two separate DGAT activities have been reported on hepatic microsomes, “overt” and latent “activity” which the second one appears only after microsomes became permeable. The “overt” and “latent” fractions reflects cytosolic and luminal activities respectively (564-566). One possibility is that the overt fraction represents the cytosolic DGAT which synthesizes TG for deposition into cytosolic LDs while the latent fraction is DGAT activity within ER lumen which synthesize TG destined for secretion by VLDL (see the VLDL secretion). Both overt and latent activities are diminished in the liver of DGAT-1 knockout mice suggesting that DGAT-1 participates in both fractions (555). In contrast, Niacin that selectively inhibits DGAT-2 is more active against overt activity (567). This is consistent with DGAT-2 membrane topology (locating DGAT-2 active site close to cytosolic leaflet of the ER membrane and close to cytosolic LDs). In addition it is believed that DGAT-2 is mostly responsible for incorporation of endogenously synthesized (by de novo fatty acid synthesis) monounsaturated de-novo fatty acid into TG (568). In contrast the DGAT-1 might be involved in formation of TG from FA, which is taken up from cells, or in a recycling pathway that involves the re-esterification of hydrolyzed TG (568), very consistent with VLDL secretory pathway. In addition over expression of DGAT-1, but not DGAT-2, enhances the luminal (latent) DGAT activity and was associated with less ApoB degradation and improved secretion of ApoB containing lipoproteins and TG in McArdle cells and in mice, indicating the possible role of DGAT-1 for VLDL-TG secretion (569). But some other studies both in vivo and in vitro have shown that overexpression of DGAT-1 had no effect on luminal or secreted VLDL-TG (570). With all of these discrepancies, considering the topology and substrate preferences, it is believed that in the liver DGAT-1 is responsible for cytosolic lipid droplets formation but can play a major role in luminal TG synthesis from exogenous fatty acid or re-esterification of hydrolyzed TG for secretion through VLDL pathway, while DGAT-2 specifically has a role in formation of cytosolic lipid droplets from de novo lipogenesis.

Using DGAT1 and DGAT-2 knockout mice, has shed light to the physiologic functions of these enzymes. DGAT-2 knockout mice survive only few hours after birth. The DGAT activity and TG content diminish about 90% in the carcass of these mice and TG was nearly absent in their liver. In addition, the plasma levels of TG, Fatty acids and glucose

were reduced by 64%, 80% and 60% respectively, indicating the dominant role of DGAT-2 in regulation of molecules that are important for the energy balance. One of the other important phenotypes of these mice was reduction in the barrier function of the skin that requires lipid. This results in rapid evaporation of water and dehydration (562). The DGAT-2 heterozoygocity shows that DGAT-2 is a highly potent enzyme as in these mice, fat pad, plasma and tissue TG content are similar to wild-type animals indicating that DGAT-2 expression by 50% is sufficient for normal life. In addition results of DGAT-2 knockout mice shows that DGAT-1 cannot compensate for DGAT-2 deficiency in vivo possibly due to its lower catalytic activity or its different substrate pool (562). In fact in DGAT-2 deficient hepatocytes, DGAT-1 is expressed but is only able to synthesized TG when exogenous FA are provided with higher concentrations than what can be achieved in vivo (see the affinity of DGAT-1 in paragraph above) (562). In comparison to DGAT-2, mild abnormalities are observed with DGAT-1 deficiency. DGAT-1 knockout mice are viable, but have 50% reduction in adiposity and are resistant to diet induced obesity (563). In addition, the TG content in non adipose tissue such as liver also diminishes (571). These mice exhibit no decreased food intake or fat malabsorption but slower gastric emptying and slower transit of fat from enterocyte to the circulation (572, 573). In addition the energy expenditure was higher in these mice partly due to lower levels of TG contents in their brown adipose tissue (thermogenic tissue) (563, 571, 573). Further, DGAT-1 knock out improves the insulin sensitivity and glucose tolerance, possibly due to enhanced needs of energy production (571).

The DGAT activity in tissue is regulated at several levels. DGAT-1 expression is upregulated by PPARγ. PPAR binding site has been found on DGAT-1 promoter and thiazolidandiones (PPARγ agonists) increase the DGAT-1 mRNA (574). C/EBPα and C/EBPβ enhance the expression of DGAT-2 during adipogenesis (575). In addition X-box binding protein 1 (XBP1) induces expression of DGAT-2 in the liver (576). In adipocytes, glucose enhances the DGAT-1 and DGAT-2 expression (577) DGAT activities can be modulated post transcriptionally by phosphorylation. Tyrosine kinases have been considered as the candidate for this phosphorylation and tyrosine phosphorylation sites have been found on DGAT-1 but not DGAT-2 structure (578). In addition hormones or nutritional factors may also regulate DGAT activity. Glucagon and epinephrine can reduce the DGAT activities in rat tissues (579-581), but it is not known if they act on the enzyme directly or by modulating the expression levels.

C. 3. 3. 6. GPAT, AGPAT, Lipin and DGAT in Hepatitis C infection: Impact of HCV on AGPATs and Lipins has not been investigated. GPAT-2 expression has been tested in one study and it was shown that in comparison to healthy liver, in the HCV infected liver,

the GPAT-2 expression was not significantly enhanced. When the GPAT-2 levels were compared in HCV infected patients with hepatic steatosis with those infected patients who had no steatosis in the liver, there was significant decrease in GPAT-2 mRNA. These results remain to be confirmed by other studies.

In contrast the role of DGATs in HCV life cycle has been investigated. It has been shown that DGAT-1 (but not DGAT-2) has a key role for HCV virion assembly. In the cells that were treated by shRNA targeting DGAT-1 or with DGAT-1 inhibitor, the HCV propagation (number of HCV infected cells) was reduced significantly. This reduction was mostly related to inhibition of virion assembly and/or viral egress and both HCV RNA replication and viral protein expression were not affected. These results indicate that active DGAT-1 (not inactive DGAT-1) is required for assembly or egress of HCV virion. As we have discussed before DGAT-1 and -2 are required for formation of LDs, the organelle that is crucial for virion assembly (see the role of lipid droplets in HCV assembly). Therefore it was initially thought that the impact of DGAT-1 on HCV assembly might be related to impaired formation of LD. But this possibility was ruled out as no significant change was observed in LD size or number and lipid contents when cells were treated with DGAT-1 inhibitor or shRNA targeting DGAT-1 or DGAT-2 (582). Translocation of HCV core protein from the ER onto LD is obligatory for virion assembly (see C. 3. 4. 3 Role of Lipid Droplets in HCV Assembly) and after translocation of core into LDs, the LDs that are decorated with core proteins are transferred into close proximity of replication complex where the RNA replication and initial step of nucleocapsid assembly is coupled. Therefore it was hypothesized that transport of core protein to LDs was affected when DGAT-1 was inhibited. Interestingly, it was shown that in cells that were treated with DGAT-1 inhibitor core proteins were retained in the ER membrane and were not translocated onto LDs. Considering the role of DGAT-1 (and also DGAT-2) for formation of lipid lens between two layers of the ER membrane (see C. 3. 4. 1. Lipid Droplets Structure and Formation), this data suggested a model in which core protein gains access to LDs during formation of new LD by DGAT-1. Why this effect is DGAT-1 specific (and DGAT-2 independent), might be related to the ability of DGAT-1 to interact directly with core protein (whereas DGAT-2 has not this capability). Interestingly in the presence of DGAT-1 inhibitor, core is still able to interact with DGAT-1, indicating that DGAT-1 activity is not required for this interaction, but still core is not able to move to LDs in the absence of DGAT-1 activity. Therefore it is possible that DGAT-1 role in initiating the process of virion assembly is multiple; i.e. physical interaction with core in order to translocate it to LD (activity independent) and formation of the LDs for which core is destined to (activity dependent). Both of these process is mandatory for core translocation onto LDs (582).

C. 3. 4. Lipid Droplets and Their Role in HCV Assembly

C. 3. 4. 1. Lipid Droplets Structure and Formation: LDs are aggregates of neutral hydrophobic lipids (Mostly TG and CE) that are surrounded by a layer of amphipathic lipids such as PL and Cholesterol with some proteins coating the surface of lipid droplets (583, 584). LDs are believed to be formed as a primordial structure at the ER membrane. Presence of enzymes that mediates synthesis of TG from G3P and fatty acids, such as GPAT, AGPAT, Lipin and DGAT on or in association with the ER membrane support this hypothesis that the origin of LDs is from the ER membrane. In a current model of LD formation it is believed that GPAT, and AGPAT mediates the acylation of G3P at sn-1 and sn-2 positions to form Lysophosphatidic acid and phosphatidic acid. As these intermediates and also DG that is formed by dephosphorylation of sn-3 position by lipin are amphipathic molecules, they reside within the monolayer of the ER membrane. The last acylation process that is mediated by DGAT forms TG that is completely a hydrophobic molecule and has a very limited solubility in hydrophilic area such as cytosol or the ER lumen and within the ER membrane. Therefore a newly synthesized TG released between two monolayer of ER membrane and forms a lentil shape (lens) at the ER, until this part buds off from ER membrane and forms small LDs. Considering this model, the membrane that surrounds the LDs originates from the ER membrane, and consequently may contain some proteins that are attached to ER membrane (584, 585). There is still no direct evidence for this model. The newly formed LDs have a diameter of about 0.1-0.4 μm that is significantly smaller than LDs in cytosol(585). Two mechanisms have been postulated for enlargement of LDs; 1) addition of newly synthesized TG into LDs and 2) fusion of LDs (586).

LDs are not only a globule of fat as it was thought before. These organelles are transported across the cytosol on microtubules and therefore can transport the molecules that are attached on their surface (586). In addition mobility of LDs are required for the availability of the TGs to mitochondria for β-oxidation of fatty acids that are incorporated into TG structure. The release of fatty acid from TG in LDs is mediated by lipases and will be discussed later. The mobility of the LDs on microtubules requires motor protein such as dynein and also kinases such as ERK2 that phosphorylate the dynein (586, 587). In organs that secrete TG such as the liver, intestine and mammary glands, LDs are the major source for TG that is secreted out of cells. In hepatocytes, two types of LDs are present, cytosolic and luminal. It has been shown that the majority of TG that is secreted by VLDL pathway originates from cytosolic LDs (454, 588, 589). The role of LDs in VLDL assembly and secretion will be discussed later.

C. 3. 4. 2 Lipid Droplets Resident Proteins: As it was indicated above several proteins are present on the surface of cytosolic LDs. The PAT proteins that were either named after **P**erilipin, **A**dipocyte differentiation related protein (ADRP) and **T**ail interacting protein 47 (TIP47) or **P**erilipin **A**mino-**T**erminal, are the most well known proteins which are associated with LDs (590, 591).

Perilipin is a 56 kDa protein that is encoded by a single copy of gene on chromosome 15 (590), [reviewed in (592)]. It is only expressed in adipocyte and steroidogenic tissue but not in the liver (593). Three different types of perilipin (A, B and C) are formed as a result of alternative splicing (594). Perilipin A is the most abundant form that covers and protects the LDs from lipolytic activities of lipases such as Hormone Sensitive Lipase (HSL) and Adipocyte Triglyceride Lipase (ATGL). Therefore perilipin knock down resulted in enhanced lipolysis of LD-TG (595, 596). Interestingly it has been shown that in the absence of perilipin, the β-adrenergic stimulation of HSL cannot affect the TG in LDs, indicating that perilipin is required for HSL mediated lipolysis (595, 596). It is thought that activation of PKA may concomitantly phosphorylate the perilipin and HSL and transfer the HSL on the surface of perilipin where it can access to LDs (595-597), whereas the non-phosphorylated form of perilipin protects the LDs from lipolysis (598). Furthermore ATGL and its coactivator protein CGI-58, that interacts with perilipin, also may be processed the same way. Phosphorylation of perilipin by PKA dissociates the perilipin from CGI-58 that then associates with ATGL on LDs for lipolysis (599, 600).

ADRP is a 48 kDa protein that ubiquitously expressed in tissue. Their expression level is controlled at two levels; by PPARα (601-603) or post-transcriptional degradation through proteasomes (604-606). In the absence of lipids ADRP is degraded by the proteasome. The lack of ADRP results in lower levels of TG in tissue and smaller LDs (607). In the absence of ADRP, TIP47 can be translocated onto LDs and compensate the absence of ADRP. TIP47 is a 47 kDa protein that is ubiquitously expressed (608, 609). In contrast to ADRP that is always associated with LDs and is degraded in the absence of LDs, TIP47 is a cytosolic protein that is translocated to the LDs surface (610). It was originally known as an effector for the Rab9 protein in the process causing budding of vesicles directed to lysosomes (611). Very interesting feature of TIP47 is its C-terminal homology to LDL receptor binding domain for apoE (612). This structure suggests that this analogy might be involved in protein-protein interaction between plasma apolipoprotein and TIP47 on the surface of LDs. LDSP5 is expressed in tissue with very high level of β-oxidation such as liver, muscles and heart (613). Its functions is very similar to perilipin and protects the core of LDs from lipolysis by lipases (591). Some of the other proteins that are present on LDs surface are S3-12, ATGL, CGI-58, Rab, caveolin.

C. 3. 4. 3. Role of Lipid Droplets in HCV assembly: Association of steatosis with HCV infection suggested that LDs might have a role in HCV life cycle. In fact in 1997, for the first time, HCV core protein was found attached to the surface of LDs. It was shown that In HCV core-expressing HepG2 and CHO cells, two patterns of core staining were observed; 1) reticular pattern corresponding to the ER localization and 2) globular pattern. Using electron microscopy and specific staining for lipids, the globular pattern of core staining was linked to the attachment of core to LDs. The sequential ultracentrifugation confirmed the composition of these globules, which were mostly formed by TG (349). The same results were observed in liver tissue obtained from chimpanzees infected with HCV (349) and HCVcc, confirming the attachment of core protein to the surface of LDs (350).

Following these findings, efforts were directed to find a motif or motifs in core protein structure that mediate the attachment to LDs. Analysis of amino acid sequence of core from various genotypes of HCV showed that the majority of amino acids from residues 1-118 (called domain I) are hydrophilic and basic. Beyond residue 118, very few basic residues were found and majority of amino acids were hydrophobic particularly between amino acids 119-145 and 170-190. More detailed investigation showed that residues 170-190 are indeed a signal peptide located between core and E1 protein that keep the HCV polyprotein on ER until later processing. When truncated mutant of core was expressed in cells, it was shown that the first 118 (called domain I) residues and residues after 160 were dispensable for core attachment to LDs, whereas in all truncated mutants of 125-160 residues (within domain II), the LD attachment was impaired or completely abolished. This data suggests that the domain I and signal peptide indeed do not participate in LDs attachment, whereas there are motifs within domain II which mediate this attachment. More interestingly it was shown that in the absence of domain II, the mature protein is degraded by proteasome, indicating that this domain might be required for proper folding of the core (614).

To further investigate which amino acids in domain II are required for the attachment of core protein to LDs, the HCV core amino acid sequence was compared with other LD-resident proteins (ADRP, Perilipin, TIP47). No similarity was found between these proteins and HCV core protein. But a plant protein, Oleosins, which is attached to plant LDs shares a similar feature to domain II of HCV core protein. The Oleosins are characterized by a central hydrophobic region that is believed to be essential for the attachment to LDs. At the middle of this hydrophobic region there is a motif with three proline residues (named proline knot) that plays a critical role for targeting oleosins to LDs. HCV core protein shares the same features with a proline residues at positions 138 and 143 and the presence of hydrophobic amino acids surrounding these proline

residues. When these proline residues were substituted with Alanine, the mature core was formed but remained at ER and was not able to attach to LDs (615). Later the structure of domain II and the residues that are critical for LD attachment were more extensively investigated. A model of domain II was introduced with two amphipathic α-helices, helix-1 (amino acids 119-136) and helix-2 (amino acids 148-163) separated by a short hydrophobic loop (HL) which contained the proline knot (figure 1-5). Helix-1 and -2 are lying in plane with the membranous surface. Based on this model, the hydrophilic residues on helix-1 and helix-2 face toward the cytosol, whereas the hydrophobic residues face the opposite site (ER membrane surface). The hydrophobic loop (137-147) has no secondary structure (189, 190). Apart from proline 138 and 143 that are critical for LD attachment, several hydrophobic residues at helix-1 and helix-2 are also important. Mutation in the majority of these residues, results in lower association of core with LDs and proteasomal degradation of mutant, but only one residue, phenylalanine-130, was critical and its mutation resulted in complete abolishment of core from LDs. In summary this data shows that phenyalanine-130, proline-138 and proline-143 are three essential residues for core attachment to LDs (189, 190).

Maturation of core by signal peptidase (SP) and signal peptide peptidase (SPP) is required for trafficking of core to LDs. It has been shown that signal peptide between HCV core and E1 is first cleaved by signal peptidase (SP) at ER. This results in the release of core-signal peptide from polyprotein and remains attached to the ER membrane. Signal peptide is a substrate for subsequent intramembranous proteolysis and cleavage by signal peptide peptidase (SPP). The inhibition of SP prevents further maturation of core by SPP and therefore core remains attached to ER. Interestingly mutations at signal peptide which disrupt the processing of core-signal peptide by SPP blocks the trafficking of core protein to LDs, indicating that cleavage of signal peptide from core-signal peptide, is required for release of core and trafficking to LDs (176). This is completely in line with a time dependent manner of the trafficking of HCV core protein into LDs that was reported in Huh7.5/JFH-1 cell culture system. It was shown 12-24h after electroporation of JFH-1 RNA into Huh7.5 cells, the majority of core protein are adjacent but not co-localized to ADRP (LDs), but later at 38h, 40% of core proteins are co-localized with ADRP on the surface of LDs. Beyond this time 80-95% of the core are co-localized with ADRP on LDs (184). Interestingly when mutant JFH-1 that disrupts the signal peptide processing by SPP was analyzed, majority of core were adjacent to ADRP, very similar to initial phase of infection (12-24h) (616).

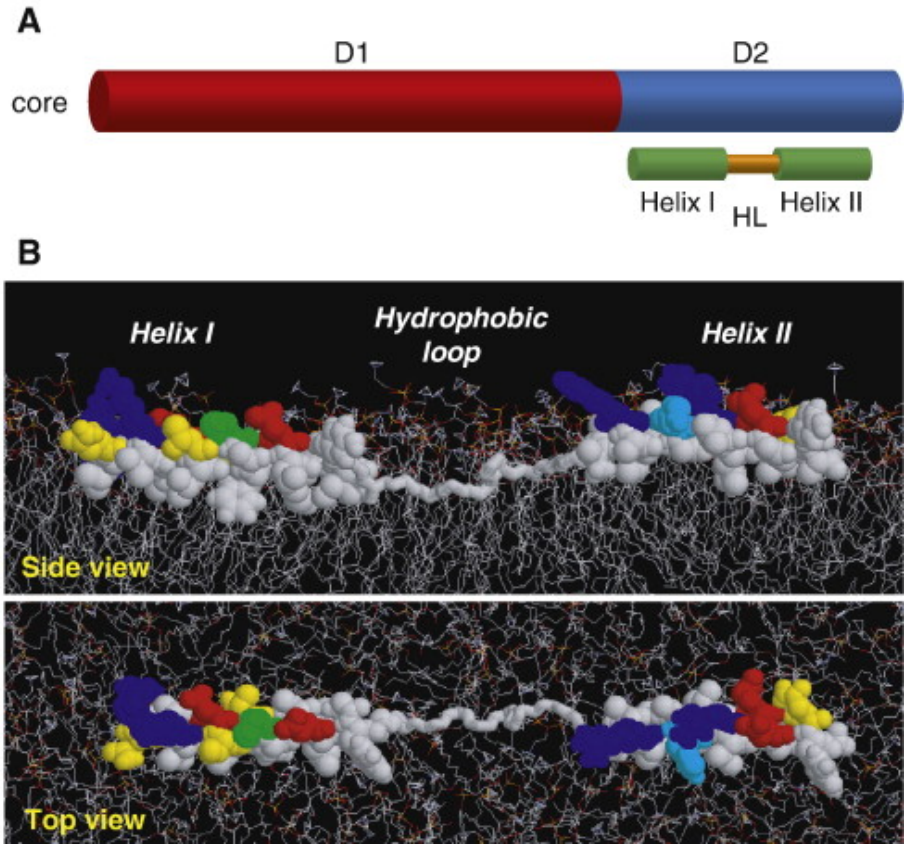

Figure 1-5. The lipid droplet-association domain of HCV core. **A.** Location of the D1 and D2 domains in core protein. The position of the amphipathic helices (Helix I and Helix II) and the hydrophobic loop (HL) within D2 are shown. **B.** Model of the interaction between the helices in D2 and membrane surfaces. Hydrophobic amino acids directed towards the lipid interior are shown in grey; colored residues represent hydrophilic amino acids. Taken from (617) with permission.

But is the association of core protein on LDs important for HCV assembly/production? It is believed that LDs are the place that replication and assembly are coupled. The core mutants that are not able to attach to LDs (phenylalanine-130, Proline 138 and 143 Alanine mutations) are deficient in producing infectious HCV progeny. This occurs while the RNA replication remains intact and the cellular core contents are comparable to wild-type virus. This suggests that attachment of core is necessary for assembly of newly synthesized RNA into a virion structure (184). In line with this data it has also shown that in wild-type infection, core attached on LDs is in close proximity of NS3-NS5A and minus strand HCV RNA (template for formation of HCV genome). More importantly the minus

strand RNA was resistant to nucleases, indicating that two layers of membrane covered it. All this evidence indicates that core covered LDs are in close proximity of the replication complex (618). In addition NS5A is not only found in close proximity of LDs in replication complex, it can be found on LDs surface facing toward ER (618). The localization of NS5A on LDs was completely absent and infectious progeny were not produced, when core was not able to attach to LDs due to proline and phenylalanine mutations or due to disruption of signal peptide processing by SPP (616). Trans-complementation of wild-type core reverses this phenotype. This data suggests that core protein may interact with NS5A and this process may be required for stabilizing the LDs to close proximity of replication complex to couple the RNA replication to initial steps of virion assembly (618). Furthermore it was shown that domain III of NS5A is critical for the interaction with core and deletion or mutation in this region results in disruption of co-localization with core and the absence of infectious virion in the media (619). Therefore it is believed that NS5A interacts with core on LDs through its domain III and this interaction is mandatory for virion assembly.

To investigate why the interaction of core and NS5A is critical for virion assembly, it was shown that NS5A appears on LDs at the early stage of LDs formation and it was proposed that NS5A might use the DGAT dependent pathway for transferring to LDs(620). As the replication complex is extremely immotile, it was hypothesized that LDs covered with core move to the proximity of the replication complex (621). It has been shown that NS5A forms a dimer at its N-terminal and it is possible that the dimerization between NS5A on LDs and the ER keeps the LDs and replication complex in close proximity (621). This hypothesis has not yet been confirmed.

How do LDs move into close proximity of the replication complex? It has been shown that the presence of core on LDs reduces the ADRP attachment to LDs. In addition when core is located on LDs, it causes redistribution of LDs around the nucleus where the replication complex is localized. As the same pattern of redistribution occurs when ADRP is abolished with siRNA knock down, therefore it has been suggested that this redistribution of LDs by core is related to low level of ADRP on the surface of these lipid droplets (622). This redistribution is dependent on microtubule and is directed toward the microtubule-organizing center (MTOC) which are located in the peri-nuclear region (622, 623). This movement of core containing LDs might be the results of an imbalance of dynein and kinesin and as the movement is retrograde toward the MTOC it suggests that dynein is overcoming kinesin. It is possible that kinesin is removed or inhibited on LDs resulting in backward motion of LDs (623).

Therefore core located on LDs is translocated to a close proximity of replication complex and is stabilized by dimerization of NS5A resides on LDs with another NS5A that is located on the ER in close proximity of the replication complex. This process couples the RNA replication to the early stage of virion assembly, i.e. encapsidation of newly synthesize RNA and formation of nucleocapsid. As we already know the HCV structure is formed from nucleocapsid and a lipid membrane (possibly from the ER) in which E1 and E2 reside. E1 and E2 are ER membrane proteins and are distributed all over the ER. How the nucleocapsid gains access to these proteins is not still clear. Recently a bridging role for NS2 protein has been proposed. Using confocal microscopy and co-imunoprecipitation techniques, it has been shown that NS2 protein interacts with NS5A, E1, E2, NS3 and P7 protein and possibly brings the E1 and E2 into close proximity of LDs and the replication complex. This interaction depends on P7 activity as an ion channel. P7 deletion or P7 mutant with defective ion channel activity disrupts the interactions between NS2 and E1, E2 and NS5A and consequently abolish the presence of infectious HCV particles in media. It was initially thought that P7 might act as an adaptor molecule between NS2 and the above HCV proteins but it was shown that P7 is not able to directly interact with these structural and non-structural proteins. Therefore it was suggested that P7 stabilize the proper topology of NS2 for interaction with other proteins (see B. 2 Non-Structural Protein-2) (624).

In a very interesting microscopic approach the initial steps of HCV assembly was investigated. When cells are actively producing HCV, NS2 was seen in a dotted pattern on ER associated with NS5A, NS3 (replication complex) in the vicinity of LDs (associated with core). E1 and E2 were also observed at this area. The abundance of the dotted area in cells correlated strongly with the level of infectious virion in media suggesting that this area might be the primary assembly area. It was shown that disruption of interaction between NS2 with NS5A reduced the dotted area. In addition presence of infectious particles in media was completely abolished (625) Interestingly in the absence of P7 (or functional P7), the dotted area completely disappeared and the NS2 localization was more aberrant on ER and there was no co-localization between NS2 with NS5A, E1, E2, and LDs. Again no HCV progeny was found in the media. These observations confirm that P7 activity is required for NS2 interaction with NS5A, E1 and E2 and these interactions are mandatory for the primary process of virion assembly. Furthermore when E1 and E2 were deleted, the number of dotted areas increased significantly without producing HCV particles. This indicates that the interaction between NS2 with NS5A (and therefore replication complex and LDs) was not disrupted and possibly primary nucleocapsid formation was not affected, but it was not able to gain access to E1 and E2 to be assembled as a virion and get secreted, therefore it accumulated in the cells. Finally

in the presence of proline mutant core (that are not able to coat LDs), the number of the dotted area (and interaction between NS2-NS5A) increased whereas LD was not at close proximity of this dotted area linking the initial steps of nucleocapsid assembly to primary process of virion assembly (625). In conclusion it is thought that interaction of NS2 with NS5A, NS3 and E1 and E2 functions as a bridge that links the nucleocapsid assembly process to E1 and E2 and formation of primary virion.

In agreement with the role of P7 and NS2 in virion assembly, it has been shown that more proper interaction between NS2 and P7 causes better structural integrity in NS2 for interaction with E1 and E2 and may enhance the HCV production. In highly infectious HCV variant such as Jc1 or cell culture adapted JFH-1, although some core proteins can be found on LDs, the majority of the core are rapidly translocated into the ER as nucleocapsid structure, where they are assembled with E1 and E2. The more proper interaction between P7 and NS2 protein seen in culture adapted JFH-1 or Jc1 are shown to be the reason for this higher rate of core translocation from LDs to ER and higher HCV secreted into media. Substitution of P7 and NS2 in these viruses with one in wild type JFH-1 abolishes this phenomenon (626).

But which part of NS2 is required for this role? Using NS2 TMD1/TMD2 deletion or alanine mutation at TMD1/TMD2, it was shown in all cases the replication of virus remains intact, whereas released virus in media was abolished or diminished. As core protein was not accumulated in these mutants, it was suggested that secretion remains intact while assembly was affected. TMD1/TMD2 deletion, and mutation in TMDs, reduced the interaction of NS2 with E2 therefore it seems that these transmembrane domains might be involved in the interaction of NS2 with E1 and E2 (249).

NS3 helicase (domain I) also has been linked to the very early stage of HCV assembly. Substitution of Leucine-221 to Glutamine prevented the formation of intracellular and extracellular infectious particles. In this mutant, core and NS5A are still located on LDs and RNA replication remains intact indicating that initial stage of HCV production (RNA replication and encapsidation) was not affected. When Leucine was substituted back, robust infectious particles were found both intracellularly and extracellularly indicating that NS3 helicase is essential for early stages of viral assembly (627). In addition it has been shown that NS3 helicase may interact with domain I of core protein. In core protein, residues 64-66 are essential for this interaction and mutation in these residues, disrupts the NS3-core interaction and prevents the formation of HCV particles (628).

After nucleocapsid gains access to E1 and E2 on ER membrane the primary virion is formed. The sequence of events and the mechanism by which the virion gain lipid coat

and buds into ER lumen is not known, In addition the mechanism of HCV egress is also under investigation. As HCV is not a cytolytic virus, it is believed that one of the major secretory pathways in cells might be responsible for HCV egress. The mechanism is still unclear but the association of HCV with LDs in cells and with lipoprotein in plasma supports the possibility that VLDL secretory pathway might be the mechanism by which HCV is secreted. The VLDL secretory pathway and its role in HCV secretion will be discussed in the next section.

C. 4. VLDL Assembly and Secretion and Its Importance for HCV Egress

C. 4. 1. VLDL Assembly and Secretion

The structure of VLDL was discussed in C. 1. 1. 1 Lipoprotein Components and Structure and table 1-3. This TG-rich lipoprotein that is secreted by the liver during both starvation and feeding, is responsible for transferring of endogenous lipids from liver to peripheral tissue (Endogenous Lipid Pathway). The major apolipoprotein of VLDL, apoB100, is not a transferable apolipoprotein and is obligatory for VLDL production and secretion. ApoB100 is one of the largest proteins in our body (MW= 513 kDa) and contains 4,536 amino acids (629). It is encoded by ApoB gene on P arm of the second chromosome (630). Similar to the majority of typical secretory proteins, it is synthesized by ribosomes on the ER and is secreted out by the ER-Golgi pathway (631). But unlike the majority of secretory proteins apoB is not secreted as a free protein and without lipidation. In fact, if an inappropriate amount of lipidation occurs, apoB is destined for degradation by cellular machinery (see apoB degradation). The lipidation process of apoB demonstrates the amount of apoB (and therefore VLDL) that is being secreted (632).

C. 4. 1. 1. ApoB100 Structure: Based on current knowledge a structural model of apoB100 has been proposed. According to this model, apoB100 has a unique pentapartite domain structure, consisting of a N-terminal globular domain followed by alternating three β-sheets and three α-helices designated in $\beta\alpha_1$-β_1-α_2-β_2-α_3 pattern (633). This structure is very similar to an egg yolk protein lipovitellin, with a lipid pocket in the middle surrounded by three antiparallel β-strands (634, 635). The $\beta\alpha_1$ domain contains the first β-sheet (the first 264 residue) and a α-helical bundle (residue 292-593), followed by two amphipathic β-sheets termed C-sheet (residues 611-782) and A sheet (residues 783-930)(636). When the first β-strand is formed, it is cotranslationally folded, by the addition of TG, in a way that hydrophobic residues face toward the TG whereas hydrophilic residues face to the outside. By translation of more of apoB more TG is added.

The sequence that lies between apoB32.5 (32.5% of structure) and apoB41 (41% of structure) has the highest affinity for TG and is responsible for binding most of the TG (637). In addition, the N-terminal region of ApoB100, in particular $\beta\alpha_1$ domain, contains several binding sites for Microsomal MTP and also for apoB-specific chaperone molecules that are required for proper apoB folding (638-640). In addition this domain also contains binding sites for scavenger receptors in human macrophages and LPL. The β_1 domain is mostly involved in high capacity binding of lipids (641, 642). The β_2 domain contains a LDL receptor binding site which is absent in apoB48 (643, 644). The α strands are believed to be important for flexibility of the molecule for accepting more lipids (645).

Like many other secretory proteins, apoB is translated on ribosomes on the cytosolic surface of the ER and is targeted to the ER lumen by signal peptide located at residue 1-27 (646). The translocation of apoB into the ER lumen is mediated by protein channels (translocons) in the ER membrane that are formed by the Sec61 protein that is tightly attached to ribosomes (647, 648). The transfer of apoB occurs cotranslationally in a pause-transfer manner (649, 650). This pause-transfer manner permits time for the lumental segment of nascent apoB to obtain lipids and undergo proper folding (649, 650). In addition it is possible that the Sec61 and ribosomes seals, induce a gap in the ER membrane and expose the nascent apoB to cytosol. This may induce the apoB degradation in the case of incorrect folding (647, 648). In the N-terminal of apoB there are sites for attachment of chaperones such as Protein Disulfide Isomerase (PDI), Binding immunoglobulin Protein, cyclophilin, Heat shock protein 90 (Hsp90), calnexin and calreticulin, that help the apoB folding or direct it for degradation (651-656).

As it was noted above, apoB100 is mandatory for secretion of VLDL, and any mutation resulting in truncation or underproduction of apoB100 leads to low plasma levels of apoB-containing lipoproteins (VLDL, LDL), cholesterol and TG, a disorder called Familial Hypobetalipoproteinemia. In addition as VLDL secretion is the main pathway for the TG secretion, all these mutations also cause hepatic steatosis (657).

C. 4. 1. 2. Regulation of ApoB synthesis: Unlike the majority of proteins, the amount of apoB that is secreted in the context of VLDL is not tightly regulated at transcriptional level. The apoB secretion can be altered seven times without any significant change in its mRNA level. In contrast apoB secretion is mostly regulated post-transcriptionally and in particular depends on the availability of lipid. But still some nuclear factors and DNA elements positively or negatively regulate apoB transcription. The post-transcriptional regulation of apoB secretion has been shown to occur at different levels with various mechanisms.

Hormones and in particular insulin regulate the apoB100 contents at translational levels. At 5'-UTR of apoB mRNA, there is a GC rich region which is able to form a secondary structure and has been shown to be important for optimal translation of apoB mRNA. A 110 kDa insulin-sensitive factor has been recently identified that binds to 5'-UTR and increase the apoB translation (658). In contrast in 3'-UTR side there is an AUUUA and AUUUUUA rich areas that are also able to form a secondary structure and possibly attenuate the apoB mRNA translation (658).

The initial lipidation of apoB also regulates the apoB levels by assisting apoB to obtain proper structure during translation and preventing it from degradation. The initial addition of neutral lipid to apoB during translation is required for this proper folding and is mediated by MTP. Due to the importance of this initial lipidation in apoB100 and VLDL secretion it will be discussed separately later (659, 660).

Several post-translational modifications occur in apoB structures such as glycosylation, phosphorylation and palmitoylation. About 10% of apoB weight is formed by carbohydrate and the glycosylation may alter the apoB lipidation and/or secretion (661). Preventing N-glycosylation at Aspargine residues specifically Aspargine-1496 results in reduced apoB stability and impairs the secretion of VLDL (662). Phosphorylation mostly occurs in Golgi apparatus and there is no direct evidence that these phosphorylations may change the VLDL secretion or density (663). Palmitoylation of cysteine residues of human apoB has been observed in plasma LDL and cultured hepatic cell lines. Preventing the palmitoylation had no effect on ability of apoB lipidation (664).

C. 4. 1. 3. Primary lipidation and role of Microsomal Triglyceride Transfer Protein (MTP): MTP is a 97 kDa ER-resident protein that plays a major role in VLDL secretion (665). Its localization to ER membrane depends on heterodimerization with Protein Disulfide Isomerase (PDI) as it does not contain an ER retention motif (such as KDEL)(666). Therefore the MTP complex is divided to two parts, M subunit (MTP protein) and P subunit (PDI protein) (666). The structure of MTP is very similar to other proteins that have the ability to attach to lipids. Based on homology with lipovitellin, it is proposed that M subunit of MTP is formed by 894 amino acids (650). This M subunit is attached to apoB and contains the residues that are required for lipid transfer activity of MTP. The M subunit is shaped like a lobster claw and is formed by N-terminal barrel shaped domain that is believed to take part in membrane attachment, a central α-helical domain and a C-terminal lipid-binding cavity (650, 667).

The importance of MTP for VLDL secretion was first observed in a genetic disorder called abetalipoproteinemia. In this disorder, mutation in MTP gene results in complete absence

of MTP. Abetalipoproteinemia is presented with complete disappearance of apoB (and apoB containing lipoproteins) in plasma and hepatic steatosis (668, 669). In addition, the inhibition of MTP both in vitro and in vivo, results in reduced secretion of VLDL and TG (670-672). In contrast overexpression of MTP in mouse liver leads to increase secretion of VLDL and TG. All this evidence confirms that MTP has a critical role in VLDL secretion (673). The exact mechanism by which MTP affects apoB secretion is not completely known.

It has been shown that MTP is able to transfer lipids between two membranes in vitro (674). This transfer activity is most robust for TG and with lower amounts for CE, DG and PC. Therefore, it has been suggested that MTP might be able to transfer TG from cytosolic LDs to luminal LDs (675). Indeed in the liver of Mtp -/- mice or when MTP inhibitor was applied, both luminal TG levels and apoB free luminal LDs diminished significantly (676). Another role that is mostly accepted among the experts in this field is that MTP may be involved in the initial co-translational lipidation of nascent apoB and assists the apoB molecule to fold correctly. This may rescue the apoB from degradation (659, 660). Studies in McArdle cells have supported the MTP-dependent early stages of apoB lipidation and it has been shown that MTP is required for proper folding of apoB and without this lipidation the majority of apoB is destined for degradation. The later stage of lipidation during which the bulk of lipid is added to VLDL (see VLDL assembly) has been shown to be MTP-independent (672). Another possible role has been suggested for MTP. Interaction of MTP with N-terminal of apoB suggests that MTP may act as a chaperone for apoB, although this remains to be confirmed. In summary although the exact role of MTP in VLDL assembly is still not completely clear, but its presence is mandatory for VLDL secretion and its inhibition or absence hampers the secretion of VLDL (and TG) and results in steatosis.

C. 4. 1. 5. Assembly and Secretion of VLDL: The exact mechanism and the factors that play a role in VLDL assembly/secretion are not clearly understood. Based on our current knowledge a two-step model of VLDL secretion has been suggested and is the model that is widely accepted (figure 1-6). According to this model, in the first step, apoB100 is lipidated during translation to form a very dense poorly lipidated pre-VLDL (primordial VLDL). As it was indicated before, this initial lipidation is required for proper folding of apoB. If not sufficiently lipidated the apoB is targeted for degradation. In the second step the dense partially lipidated pre-VLDL acquires more lipid (in particular TG) to form a mature highly lipidated VLDL. It is not clearly known how the lipids are added to pre-VLDL to form mature VLDL. First it was thought that luminal apoB-free LDs fuse with pre-VLDL to form mature VLDL, although nowadays we know that this process in not an en-

bloc addition of TG [Reviewed in (677)].

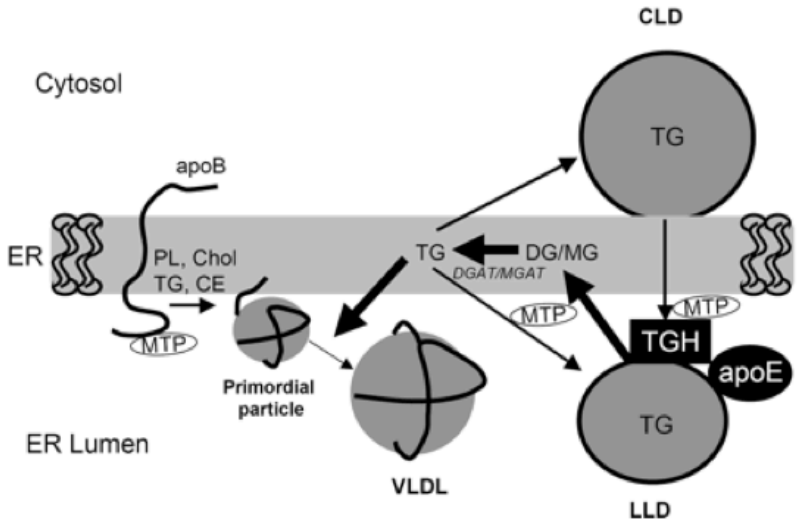

Figure 1-6. Model for the role of LLD in VLDL assembly. TGH localizes to the lumen of the ER, associates with LLD, and mobilizes this pool of TG for VLDL assembly. The hydrolysis of TG by TGH may be modulated through interactions with apoE. LLD serve as a direct source for VLDL-TG. TG from the CLD replenishes LLD. The transfer of TG from CLD to LLD may involve MTP and TGH. Excessive TG can be returned to either LLD or to CLD (futile cycle). Taken from (678) with permission.

TG that is utilized in VLDL structure potentially originates from several sources. The fatty acid incorporated to TG structure can be derived from de novo biosynthesis (see de novo fatty acid synthesis) (679), from fatty acid absorbed from plasma (680) or from hydrolysis of existing TG or TG associated with take up of lipoprotein remnants (588). The exogenous fatty acids that are taken up by cells are first incorporated in the TG structure but this TG is not directly utilized into VLDL structure for secretion. In contrast, it is first stored in cytosolic lipid droplets and then is mobilized for loading into VLDL. It has been shown that 70% of VLDL-TG is from cytosolic stores confirming that the majority of

exogenous fatty acids are first stored as TG in cytosolic LDs before being utilized for secretion with VLDL (454, 588).

As it was indicated above the addition of TG during VLDL maturation is not en-bloc fusion but requires a process of lipolysis and re-esterification. The model of lipidation has been proposed. Based on this model, lipolysis of TG produces fatty acids, DG and MG which are all amphipathic molecules and are translocated to the amphipathic structure of the ER from LDs (681). In the ER presence of lipogenic enzymes that synthesize TG (MGAT and DGAT) re-esterify the MG, DG and fatty acids back to TG. This TG can be loaded to pre-VLDL that is located in close proximity of the ER membrane (681). In agreement with this model, HepG2 and McArdle cells that are deficient in lipases, which mediate the lipolysis of this process, secrets VLDL that is poorly lipidated and has a density close to LDL and pre-VLDL (682-684). Therefore, the process of formation of mature VLDL is more complex than direct fusion of non-apoB luminal LDs with pre-VLDL. As VLDL maturation occurs in the ER lumen, lipases that mediate the lipolysis of TG for secretion with VLDL, are believed to be also luminal. Two candidate luminal lipases are Triacylglycerol Hydrolase (TGH) and Arylacetamide Deacetylase (AADAC). The structure of these proteins will be discussed in detail separately.

Although there are some evidences that maturation of pre-VLDL to VLDL occurs in ER, several other data sources have proposed that it may occur in the Golgi system. Trafficking of VLDL from the ER to the Golgi (like most of the secretory proteins) requires anterograde transport of vesicles coated with coat protein complex II (COPII) (685). This anterograde transport from ER to Golgi is driven by a small GTPase ADP ribosylation factor 1 (ARF1) very similar to HCV secretory pathway (686). Deletion of ARF1 (686) or inhibition with Brefeldin A diminishes the secretion of TG-rich VLDL with minimum effect on pre-VLDL, indicating that lipidation of VLDL possibly occur in Golgi system (687). In addition two phospholipases (Phospholipase D1 and Calcium independent Phospholipase A2) that are important for ER-Golgi transport are also required for VLDL maturation (687-689).

VLDL contains other apolipoproteins such as apoE and apoC. Majority of these apolipoproteins reside on non-apoB lipid droplets in the Golgi apparatus. ApoE is an important part of CM which is also present on the surface of VLDL. It was first thought that apoE is obligatory for VLDL secretion but studies on apoE deficient mice showed that fully lipidated VLDL could be secreted in the absence of apoE (690). Three sites have been considered for apoE addition to VLDL; intracellular, on the unstirred layer of cells or in the plasma from HDL or other lipoprotein.

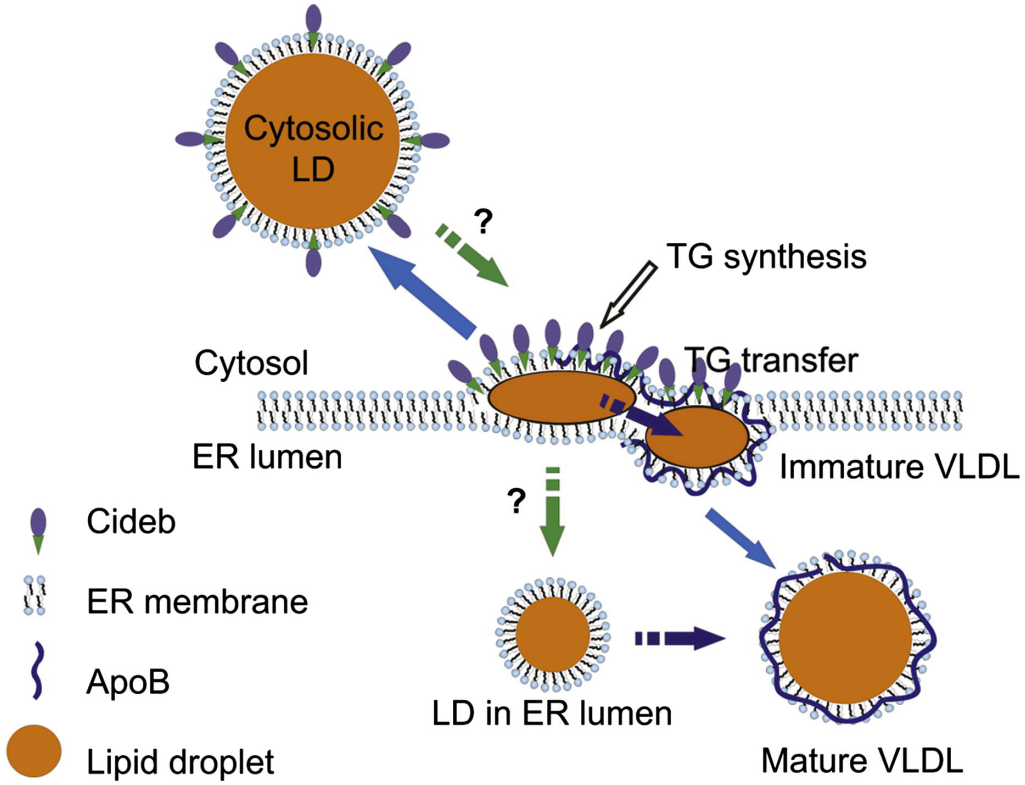

Figure 1-7. Schematic illustration of the role of Cideb in VLDL lipidation and maturation. Cideb, by localizing to cytosolic side of ER and the surface of LDs, could interact with the both apoB-100 and facilitate the transfer of TG synthesized on ER and in cytosolic LD to immature VLDL particles, leading to the sufficient lipidation and maturation of VLDL precursors. In the absence of Cideb, TG could not be effectively transported to VLDL precursors, resulting in inefficient VLDL lipidation and accumulation of neutral lipid in the cytosolic fraction of hepatocytes. Taken from (691) with permission.

C. 4. 1. 6. ApoB Degradation: As it was discussed before, poorly-lipidated apoB are not folded correctly and are destined for degradation. On the other hand, sometimes apoB can be degraded even when they are fully lipidated. For example addition of polyunsaturated fatty acids (PUFA) specifically (n-3) PUFA, reduces the VLDL secretion and enhances the apoB degradation (692). In addition acute increase in insulin level also results in lower VLDL secretion and enhanced apoB degradation (663, 693).

ER-associated degradation (ERAD) is a well-known pathway for degradation of misfolded

or faulty proteins and prevents the damages that may occur in the presence of misfolded proteins (694). During ERAD, chaperons detect and select the misfolded proteins and facilitate the addition of an ubiquitin tag on the protein (695). The poly-ubiquitin tag added to the misfolded protein, targets the protein to proteasome a 2.5 mega Dalton machinery that destroys the aberrant protein (695). The ERAD response per se is regulated by the presence of misfolded protein. Accumulation of misfolded proteins in ER induces the unfolded protein response (UPR) in the ER and augments the ERAD (696, 697). The poorly-lipidated misfolded apoB is generally tagged for proteasomal degradation. As it was discussed before, MTP-mediated primary addition of lipids to nascent apoB is required for proper folding of apoB. When aberrant apoB is formed, the cytosolic chaperon proteins Hsp70 and Hsp90 and ER lumental chaperons, BiP and p58 facilitate the apoB degradation (654-656).

ERAD is not the only mechanism for apoB degradation. Post-ER Presecretory Proteolysis (PERPP) is another pathway by which apoB is degraded (692). In this pathway aggregated apoB is targeted to autophagosomes for autophagy. As it was indicated above addition of PUFA mediates the post ER degradation of apoB (692). Incubation of hepatic cells with PUFA leads to oxidative modification of apoB and aggregation which activates PERPP response and autophagy (692, 698). The insulin mediated apoB degradation is also believed to be mediated by PERPP-related autophagy (663, 693).

C. 4. 1. 7. Cellular TG Lipases: As it was discussed above, in the second step of VLDL secretion pathway more lipids (in particular TG) are added into pre-VLDL in a process that involved lipolysis and re-esterification of TG. Cellular lipases that mediate the lipolytic process are discussed here.

In the human body several lipases are found that are capable to mediate hydrolysis of TG and DG. The first TG lipase that was discovered was Hormone Sensitive Lipase (525), which is mostly expressed in adipose tissue (699). This 84 kDa enzyme contains 775 amino acids (700) and its size is variable in the testis (701) and β-cells of islets (702). It is more active for hydrolysis of DG and its active site contains the famous motif of Glycine-x-Serine-x-Glycine (700). It is inactivated during feeding by the high ratio of insulin to counter regulatory hormones such as glucagon and epinephrine. During fasting, this enzyme is activated by a low level of insulin and high levels of glucagon and epinephrine, and hydrolyses the TG in adipose tissue to provide fatty acid for peripheral tissue and the liver (525). This process is mediated through Protein kinase A (PKA) that phosphorylates and translocates HSL from cytosol into LDs where it reacts with perilipin (see C. 3. 4. 2 Lipid Droplets Resident Proteins) (595-597). HSL is absent in the liver (699). For several

years it was thought that HSL mediates TG hydrolysis, but in 2004 Adipose Triglyceride Lipase (ATGL), another lipase, was discovered (703). ATGL mediates the hydrolysis of TG to DG and fatty acids. ATGL is expressed in high levels in adipose tissue and is also expressed in lower level in hepatocytes (703). Soon after discovery of ATGL it was thought that it might be involved in the process of VLDL lipidation but it was shown that ablation of hepatic ATGL (704) or overexpression of ATGL and/or HSL have no effect on VLDL lipidation(705). Therefore other enzymes were considered for this process. The lipidation of VLDL occurs in ER lumen, therefore the lipases that are involved in this process are believed to be luminal as well. At least two candidate enzymes have been suggested to mediate this process named, Triacylglycerol Hydrolase (TGH) and Arylacetamide Deacetylase (AADAC).

C. 4. 1. 8. Triacylglycerol Hydrolase (TGH) and its Role in HCV Life Cycle: Human TGH is a 60 kDa luminal protein which contains 568 amino acids (706). It belongs to carboxyl esterase (CES) family and phylogenetically is classified in subclass CES1A (707). It is inhibited with serine modifying chemicals such as diethyl-*p*-nitrophenylphosphate (E600) and tetrahydrolipstatin (orlistat) therefore is a serine esterase (684, 708). The N-terminal part of TGH contains 18 amino acids and acts as signal peptide directing the protein into ER and is cleaved by signal peptidase (684, 708). The C-terminal of TGH contains Histidine, Isoleucine, Glutamic acid and Leucine (HIEL) sequence that are responsible for retention of enzyme within the ER lumen (709). The active site of the enzyme is formed by a triad of amino acids Serine-221, Glutamic acid-354 and Histidine-468 (707, 710, 711). Hydrolysis of TG by TGH is a two-step process (712). In the first step, the weak hydrogen bond between Glutamate-354 and Histidine 468 of catalytic triad, facilitate the transfer of proton to Serine-221 and nucleophilic attack by Serine-221 which forms the Enzyme-acyl compound at Serine-221 and releases the DG. In the second step, fatty acid is released in the process that requires water (712). The protein structure is believed to have 17 α-helices and 17 β strands (712-715). The α-helix 1 acts as a lid for access to active site and plays a vital role in lipolysis at the lipid-water interface. In the presence of hydrophobic substance (lipids) the lid is open whereas in the absence of lipid-water interface it is closed (716). Another important structural feature of TGH is the presence of five cysteine residues in human TGH that form disulfide bounds and stabilize the secondary structure of the protein (714). In addition the presence of at least one glycosylation site has been shown (Aspargine-79) in human TGH (711).

TGH is highly expressed in the liver and, with lower levels, in the small intestine and adipose tissue (684). TGH gene is located on the q arm of chromosome 16 and spans

about 30 kb (717). The promoter region of this gene contains several binding sites for various transcriptional factors. Human TGH promoter has three sites for binding of Sp1, a CCAAT box and binding sites for NF-Y, glucocorticoid response elements and CCAAT enhancer-biding protein (718). Rat and mouse promoter also contains sterol regulatory elements and peroxisomal proliferator-activated receptor response element (PPRE) [reviewed in(716)]. TGH expression is regulated at different levels. Apart from general transcription factors that can bind to the promoter of TGH and activates its expression, TGH can also be regulated by diet, hormones and possibly by modification of enzyme through phosphorylation. In regards to diet, hepatic TGH expression is enhanced twice when high cholesterol is supplemented with fatty acid but is not affected by the diet with only high content of fatty acids, indicating that cholesterol may increase the hepatic TGH expression (719). As murine TGH promoter contains SRE, it was believed that this enhancement of TGH expression might be SREBP dependent. But expression of the nuclear form of SREBP-1a in transgenic mice did not affect hepatic TGH mRNA expression (716). Therefore it is still not clear if the enhancement of TGH expression by cholesterol is due to SREBPs, oxysterol receptors or is an indirect mechanism. In addition to diet, hormones, in particular glucocorticoids, regulate the expression levels of TGH. It has been shown that Dexamethasone, reduces the expression of hepatic TGH (720), whereas it enhances the expression of lipogenic genes such as DGATs, PAP-1 (721). This enhances the storage of TG and reduces the TG secretion (722, 723). Finally TGH can be regulated by post-transcriptional modification. A glycosylation site at Aspargine-79 has no effect on TGH activity (711). A potential Tyrosine phosphorylation site at Tyrosine-118 has been found. This site is close to the lid domain and its phosphorylation may enhance the TGH activity. Several Serine/Threonine phosphorylation sites are also suggested on TGH structure but their roles in TGH activity remains to be elucidated (724).

TGH has TG lipase activity and its participation in VLDL assembly and secretion has been confirmed both in vitro and in vivo. In vitro, McArdle rat hepatoma and human hepatoma cell lines (HepG2 and Huh7), that do not express TGH, secrete very low amounts of TG in comparison to human hepatocytes (682-684). In addition the majority of VLDL that is secreted from these cells have density at the range of LDL (682-684). This suggests that in the absence of TGH the lipidation process of pre-VLDL is not complete and VLDL is secreted with lower TG content (poorly lipidated). When McArdle cells were transfected with rat TGH cDNA, they exhibit about a four time increase in lipase activity and this was associated with two fold increase in depletion of preformed cellular TG stores, 30% higher utilization of intracellular TG stores for secretion with VLDL and 25% increase in apoB secretion. In addition, the secreted apoB containing lipoproteins were at

the density of VLDL. This indicates that TGH is important for mobilization of TG into pre-VLDL and lipidation of VLDL (725). Incubation of TGH cDNA transfected McArdle cells with E600 (esterase inhibitor) resulted in reduced mobilization of preformed TG stores and hence reduced TG secretion from these stores. The same results were obtained when primary rat hepatocytes were incubated with E600. In addition, apoB synthesis and secretion were also reduced when hepatocytes were treated with E600 and a specific inhibitor of TGH. This clearly shows that enhanced mobilization of TG from preformed stores for secretion with VLDL was TGH dependent (681). Furthermore, luminal lipid droplets (LLDs), corresponding to non-apoB LLDs were extracted from mouse livers and it was found that apoE, MTP and TGH reside on these LLDs (figure 1-6). As it was discussed before these LLDs are responsible for lipidation of pre-VLDL in the second step of assembly and presence of TGH on their surface supports the role of TGH in lipidation of VLDL (678). The lipid composition of CLDs and LLDs of wild type McArdle cells were compared to TGH cDNA transfected McArdle cells and it was shown, although TG contents of CLDs reduced significantly in TGH-McArdle cells, TG contents of LLD remained similar in both cells (678). Considering that 70% of TG secreted in VLDL originates from CLDs, it was suggested that LLDs acts only as an intermediate and their size and contents remain constant as far as enough lipids are available in CLDs to transfer to these droplets. The role of TGH was also investigated in vivo. In human TGH transgenic mice, the levels of plasma apoB and lipids were enhanced. The plasma level of TG enhanced both in female and male mice but it reached to statistical significant level only in male mice. The secretion rate of apoB and TG were also enhanced but only apoB reached to statistical significant levels (726). In contrast in TGH knock out mice, the plasma apoB100, TG, CE and Cholesterol levels reduced significantly in respect to wild type mice. In addition, hepatocytes isolated from TGH knock out mice secreted less TG and apoB100 into media compare to wild type. Furthermore, the reduced secretion of TG from hepatocytes isolated from TGH knock out mice was associated with intracellular accumulation of TG (steatosis). But interestingly in TGH knock out mice steatosis was not present; instead, these mice had enhanced energy expenditure, indicating that the accumulated cellular TG was channeled for β-oxidation (727). The TGH knock out also improves the lipid profile in hyperlipoproteinemia LDLR -/- mice model. LDLR knockout mice are presented with high level of plasma lipid due to the absence of LDLR for clearing the lipoproteins from plasma. In TGH, LDLR double knock out mice, the plasma TG, apoB levels were reduced dramatically. This demonstrates that deficiency of TGH results in decrease secretion of VLDL which is protective in hyperlipidemic mice (728). All these results confirm that TGH has a critical role in lipidation of pre-VLDL and its absence or inhibition results in reduced VLDL-TG secretion.

Recently, the role of TGH in HCV life cycle has been investigated (729). Using Activity Based Protein Profiling (ABPP) and Mass Spectrometry, the author had identified CES1 (TGH) in a specific colony of Huh7.5 cells that was harboring NS3-NS5B HCV replicon. Although it is well known that wild type Huh7.5 cells are deficient in CES1, the authors have indicated that the presence of CES1 was only found in this unique colony of Huh7.5 cells and both typical Huh7.5 cells and other Huh7.5 cells that were stably transfected with the NS3-NS5B replicon (other than this unique colony) were deficient in CES1. They called this colony Huh7/CES-1 and utilized it for investigating the impact of CES-1 on HCV life cycle.

Interestingly when Huh7/CES-1 cells (that were harboring replicons) were cured with IFNγ and NS5B-6367 siRNA, the CES1 mRNA and protein were both reduced dramatically. This shows that expression of CES-1 in these cells was dependent on HCV (replicon) replication. In order to test the role of CES-1 (TGH) in HCV life cycle, CES-1 was abolished by siRNA knockdown in Huh7/CES-1 (that harboring NS3-NS5B replicon) and it was shown that CES-1 knock down was associated with a lower intracellular HCV RNA and viral proteins. In contrast transient overexpression of CES-1 in these cells was associated with enhanced intracellular HCV RNA and viral proteins. This indicates that CES-1 is required for HCV RNA replication and possibly viral production. Interestingly, opposite to these findings, when Huh7/CES-1 cells were inoculated with JFH-1 virus, 96 hours after inoculation, the core staining was much lower in Huh7/CES-1 in comparison to wild type Huh7.5 cells. In addition, HCV RNA in media was also diminished but did not reach to statistical significance (729).

To test if the presence of CES-1 (TGH) in these cells is associated with any alteration in cellular lipid contents, the levels of cellular TG, Chol, CE and secreted apoB were measured in wild type Huh7 and Huh7.5 cells and also Huh7/CES-1. It was found that in Huh7/CES1 cells the levels of cellular TG, Chol, CE and secreted apoB were enhanced 3, 11, 3 and 2 folds respectively in comparison to wild type cells. In addition when Huh7, Huh7.5 cells and Huh7/CES-1 cells were transiently transfected with CES-1, cellular TG, Chol, CE and secreted apoB were enhanced compare to mock-transfected cells. These enhancements were 2, 10, 3 and 2 folds in Huh/CES-1 cells. In addition, immunofluorescent microscopy showed enhanced number and size of LDs in cells transfected with CES-1. Using SCID/uPA mice, the authors have confirmed that the liver of mice that were infected with HCV had higher levels of CES-1 expression. In addition the levels of hepatic CES-1 was higher in mice with higher levels of hepatic steatosis. Therefore the authors have concluded that the overexpression of CES-1 during infection

enhanced the LD size that is consistent with HCV related steatosis and this provides better microenvironment for HCV replication and assembly (729).

Despite of novelty of this experiment several serious discrepancies were observed. The authors showed that CES-1 expression was associated with accumulation of TG, Chol and CE and therefore steatosis. This is completely opposite to the majority of recent studies that have shown CES-1 (TGH) expression is associated with enhanced TG secretion and reduced cellular TG (681, 725-727). In addition Chol and CE levels remain intact when TGH is expressed, consistent with TG lipase activity of TGH (681, 725-727). It is not clear if the enhancement of cellular TG in this experiment was a secondary effect of other unknown compensatory cellular mechanisms or enhanced CES-1 expression was the compensatory mechanism due to accumulation of TG due to other unknown mechanism. In addition in their experiment, when Huh7/CES-1 cells were inoculated with JFH-1, 96 h after inoculation there was much less core staining and lower (but not statistically significant) secreted HCV RNA in Huh7/CES-1 in comparison to wild type Huh7.5 cells. This was opposite to their other findings indicating that presence of CES-1 enhances the cellular HCV RNA and proteins. Although the author explained that the reduced core staining shows that CES-1 might play a role in the export of HCV virions rather than replication and therefore the presence of CES-1 enhances the HCV export and results in reduced core content in cells, this explanation is also debatable. First, secreted HCV RNA was also reduced in Huh7/CES-1 cells (although not significantly) and the authors did not show if the secreted level of core protein was enhanced. Second, their previous results clearly showed significant enhancement of HCV RNA when cells were overexpressed with CES-1 that indicates in their model CES-1 might be also involved in RNA replication (729). In summary the impact of CES-1 (TGH) on HCV life cycle is not known and this impact (if any) remains to be elucidated.

C. 4. 1. 9. Arylacetamide Deacetylase (AADAC) a Putative Cellular Lipase: Another ER resident protein that is believed to have lipase activity is Arylacetamide Deacetylase (AADAC). This protein was initially introduced as an enzyme involved in metabolism of Arylamine carcinogen. Arylamines are well-known carcinogens that enhance the risk of transitional cell carcinoma of the bladder. Apart from industrial exposure, the two other recognized sources of arylamines are cigarette smoking and hair dyes (730). This compound is metabolized by the liver to arylnitrenium ions, highly unstable electrophiles that attach to C_8 position of guanine as the ultimate carcinogen. N-acyltransferase acetylates the arylamines to arylacetamides to reduce the toxicity of these compounds. AADAC reverts this reaction (731). Following this discovery, human hepatic AADAC cDNA was isolated and it was shown that it encodes a protein with a 399 amino acids

and molecular mass of 45.7 kDa (731). Later AADAC with CYP2A1 were shown to have a role in metabolizing several drugs in the liver such as Flutamide and Phenacetin and produces toxic metabolites that are either hepatotoxic (in the case of flutamide) or causes methemoglobinemia (Phenacetin) (732, 733).

The AADAC genes is located on the q arm of chromosome 3 (734). The promoter region of Human AADAC genome shows a Glucocorticoid Response Element at -926 (735). Structurally human AADAC is a single-pass type II transmembrane protein located on the ER membrane, with an active site in the luminal side of the ER(733). The 17 N-terminal hydrophobic amino acids are believed to anchor the protein to ER membrane but they do not act as a signal peptide and are not cleaved by SP (733). A significant homology was found between AADAC and HSL in particular Glycine-x-Serine-x-Glycine active site. AADAC also has a very similar catalytic site to CES (731). In addition AADAC, reacts with Fluorophosphonate (a specific substrate for serine hydrolases). Therefore it is classified as a serine hydrolase (736). Two potential glycosylation sites at amino acid 78 and 282 were identified (731). AADAC is highly expressed in liver, adrenal glands and less in other tissues such as small intestine, kidney and pancreas (735). Among the cell lines, AADAC is not expressed in HepG2 (735). Following isolation of human AADAC, rat and mouse hepatic AADAC cDNA were also isolated. Similar to humans, in both rat and mice, a significant homology was found between HSL and AADAC and in particular in active site regions of the two enzymes. The same N-terminal hydrophobic structure was found and believed to be responsible for anchoring AADAC to the ER membrane (735).

Due to its homology to HSL and CES, it has been suggested that AADAC, has lipase activity and might be involved in maturation and lipidation of primordial VLDL. Although not directly observed, some evidence has supported this hypothesis. The expression levels (mRNA) of AADAC in mice show a diurnal change and steadily increases during light phase and reaches to the maximum at the end of light time. Hepatic VLDL secretion shows an identical pattern in vivo (737). This diurnal change is believed to be PPARα-dependent, as this diurnal pattern was ablated in PPARα knockout mice. However treating mice with PPARα agonists did not enhance the hepatic AADAC (738). In addition, in acutely diabetic and orotic acid-treated rat (both conditions are known to markedly reduce VLDL-TG Secretion), the steady state of AADAC mRNA was reduced significantly. When the diabetic mice were treated with insulin the AADAC mRNA levels were reversed. This was one of the first times that a possible role for AADAC as a lipase in VLDL-TG secretion was introduced (735).

In chickens a role for AADAC in VLDL-TG secretion has been suggested (739). It has been shown that in chickens, the protein and mRNA levels of AADAC increase by fasting and are reduced by feeding. This is in line with VLDL changes during feeding and fasting phase. In addition, it was shown that administration of estrogen resulted in higher AADAC mRNA and protein levels. High levels of estrogen in laying hens enhance the VLDL-TG secretion to provide the lipids that are required for eggs. Therefore it was suggested that in chickens, AADAC might be involved in enhanced VLDL assembly and secretion during the rise of estrogen level. However, it is not clear why the authors did not simultaneously measure the plasma VLDL levels during administration of estrogen and only referenced that the administration of estrogen enhances the secretion of VLDL from the liver (739).

In contrast to the above results, Lo. et al have shown that AADAC does not play a role in VLDL-TG secretion in McArdle cells. Similar to HepG2, McArdle cells are AADAC deficient. Expression of AADAC into McArdle cells showed enhanced esterase activity for both water soluble and insoluble substrates. Also it shows lipase activity specifically for DG rather than TG. When TG synthesis was induced by addition of oleic acid into culture, cells expressing AADAC, accumulate less TG than wild type cells. This effect was not related to less TG synthesis or OA uptake and was related to higher lipolysis due to lipase activity of AADAC. Four hours after removal of oleic acid, both wild type and AADAC-expressing cells had reduced cellular TG showing secretion of TG from preformed stores but the level of cellular TG reduction remained similar in both cells line, indicating that AADAC possibly have lipolytic activity towards the newly synthesized TG not preformed stores. This is consistent with the membrane topology of AADAC that has access to newly formed TG in ER membrane but not have access to cytosolic lipid droplets (due to its luminal active site). Interestingly the authors showed that reduced cellular TG in AADAC-expressing cells during oleic acid loading period, was not due to enhanced VLDL-TG secretion. In contrast TG levels in media were even reduced. This was associated with enhanced acid soluble metabolites in media during oleic acid loading that indicates increase in β-oxidation of fatty acids. The TG secretion and acid soluble metabolites in media was similar in both wild type and AADAC-expressing cells after removal of OA. Therefore it seems that AADAC lipolytic activity channeled the fatty acids released from newly synthesized (but not preformed) TG for β-oxidation by mitochondria and it did not show any effect in VLDL secretion or any effect on preformed TG stores (740).

The role of AADAC in HCV infection is unknown. AADAC is one of the proteins that is present on the ER-derived membranous web and HCV replication complex, but if its

presence is related to association between the ER-membrane (where AADAC reside) and replication complex, or it plays any role in virus life cycle remains to be studied (741).

C. 4. 2. Participation of VLDL Assembly in HCV Life Cycle

Hepatitis C virus and VLDL are both secreted exclusively by hepatocytes. The restriction of HCV production to the liver and association of HCV with VLDL (or VLDL derived) lipoproteins provide this possibility that HCV adopts VLDL secretion pathway and is secreted in conjunction with VLDL. Several evidences have confirmed this possibility and it is believed that HCV uses the VLDL secretion pathway for egress.

The cellular vesicles containing replication complex has been extracted from Huh7 cells harboring a genotype 1b replicon. The proteins associated with these vesicles were identified using mass spectrometry (MS). Approximately, 60 cellular proteins were identified. ApoE, MTP, and AADAC were among the proteins that were found on these vesicles and have a role in VLDL assembly and secretion. ApoB was not found by MS but it was detected by immunoblot analysis of these extracted vesicles. ApoB was also co-localized with viral NS5A protein. Presence of these VLDL-related proteins on these particles (containing replication complex) suggested that they might have a role in HCV life cycle. Furthermore, inhibition of MTP by an inhibitor significantly reduced the apoB secretion, HCV RNA secretion and HCV infectivity titer in the media. Identical results were obtained when cells were treated with siRNA targeting apoB. This reduction in HCV secretion was not associated with impaired RNA replication, as cellular HCV RNA remained unchanged. Therefore apoB, and MTP that have a cortical role in VLDL secretion are also required for HCV secretion and inhibition of these key regulators not only reduces the VLDL (apoB) secretion but also impairs the HCV egress. Thus these results postulate the importance of VLDL secretory pathway in HCV export (741).

ApoE role in HCV assembly and secretion was also investigated (742). It was shown that apoE knock down has no effect on HCV RNA replication but the intracellular and media HCV infectivity titers were reduced significantly. As infectivity titer of cells and media reduced at the same ratio, it was suggested that apoE is required for HCV particle formation, rather than secretion. Ectopic expression of apoE in these cells reversed the impaired HCV infectivity titers. Interestingly, in contrast to the previous studies, siRNA knock down of apoB, and inhibition of MTP by an inhibitor had no effect on cellular and media infectivity titer. Although when high level of MTP inhibitor was used it reduced the HCV infectivity titers, but this was associated with reduced apoE formation as well, indicating that the observed reduced HCV infectivity titer was the result of apoE reduction rather than MTP inhibition alone. The role of apoE and apoB was further investigated and

it was shown that incubating the secreted HCV with apoE antibody but not apoB antibody reduced the infectivity of HCV particles. The presence of apoE was shown on HCV particles but the author was not able to find apoB in HCV particles secreted in this cell culture. In addition in HCV particles extracted from cellular lysate, apoE and NS5A were co-immunopreciptated, suggesting that these two proteins might interact during HCV assembly (742). Results of this study debated the importance of VLDL secretory pathway for HCV production and egression. In this study it was shown that only apoE is required for HCV life cycle and it is mostly important for HCV assembly rather than secretion. In this study when MTP inhibitor was used with low concentration no change was observed in HCV secretion but when MTP inhibitor was applied by high concentration (similar to the concentration used in the previous study), the apoE production and secretion were reduced in addition to apoB. This was associated with simultaneous reduction on HCV secretion, therefore the author concluded that the reduction of HCV secretion that was observed by MTP inhibitor in the previous study was the results of apoE reduction rather than reduction of apoB secretion. Therefore it is possible that effect of MTP inhibitor for impairing HCV secretion was confounded by this fact that the concentration of inhibitor that was used in the previous experiment was highly beyond the level that is required for specific inhibition of VLDL assembly. But this study had no comments about the reduction of HCV secretion by siRNA knock down of apoB that was observed in the previous study. Although the presence of apoB on virus particles have been confirmed in HCV derived from patient's serum, it has not been found yet on HCVcc derived particles.

In another study the role of apoE on HCV life cycle was investigated. It was shown that apoE knock down reduces both HCV particle assembly and egress. When apoE knock down was complete, both cellular and media HCV infectivity titers were reduced. But when apoE knock down was not complete only media infectivity titer reduced significantly and cellular infectivity titer remained unchanged. These results indicate that apoE might have dual action and is required for both HCV virion assembly and secretion. The HCV replication remained unchanged in both conditions indicating that apoE does not have any role in this process. The role of apoE for HCV assembly depends on its interaction with NS5A and when this interaction was lost (by mutant of NS5A which doesn't interact with HCV), the HCV assembly reduced significantly. The results of this experiment coupled the role of apoE in HCV assembly to HCV secretion by VLDL pathway. Although what is still not clear as to how NS5A protein interacts with a luminal protein like apoE (743). The domains that are responsible for interaction between apoE and NS5A were found and it was shown that on apoE structure, the C-terminal α-helix of apoE is important for interaction with NS5A. In NS5A structure, the ApoE binding domain was

mapped to the residues 205-280, in the middle of C-terminal α-helix. Interestingly all isoforms of apoE are able to equally interact with NS5A (744).

Using Caco-2 cells in two various conditions Icard et al. (745) have studied the role of VLDL secretory pathway for HCV egression. Caco-2 cells do not produce MTP and are not able to secrete apoB-containing lipoproteins under standard culture condition. But when they are cultured under asymmetrical condition on a porous filter with serum free media on upper chamber and complete media at lower chamber, they are able to differentiate and secrete apoB-containing lipoproteins. When these cells were infected with E1-E2 HIV-SIN lentiviral vectors, while all cells were able to produce E1 and E2 only differentiated cells were able to secrete E1 and E2 into media, the secreted E2 was associated with apoB in media. When this media was applied to iodixanol gradient, E1 and E2 were exclusively observed in fractions where apoB was present. In addition, it was shown that although the majority of apoB was in lower density, the E1 and E2 were co-sedimented with apoB in a fraction with higher density. This suggests that two forms of apoB were secreted, an E1, E2 free apoB with lower density (more lipidated) and E1-E2 associated apoB with higher density (less lipidated). Very similar results were observed in HepG2 cells. In contrast in Huh7.5 cells, no association was observed between apoB and E1-E2 protein and the author was not able to co-immunoprecipitate E1 and E2 with apoB. When MTP inhibitor was used in low concentration, apoB secretion from differentiated Caco-2 cells into media was reduced significantly and correlated to decrease secretion of E1 and E2. Very similar results were observed in both HepG2 and Huh7.5 cells. This experiment clearly stated the importance of VLDL secretory pathway for HCV egress. It also shows the variability between various cell culture models that can explain the discrepancies between results obtained from these cell cultures.

Cellular determinant of HCV assembly, maturation, degradation and secretion have been recently studied and a similarity has been found between the factors that are involved in VLDL maturation and secretion and HCV assembly and secretion. It has been shown similar to VLDL, HCV also adopts the ER-Golgi pathway for secretion. Incubating cells with Brefeldin-A (BFA, an inhibitor of ARF1) reduces HCV infectivity titer in media and enhanced intracellular infectivity. The intracellular viral particles had a very high buoyant density (1.15 g/ml) compared to regular mature HCV particles secreted into media. This indicates that possibly virion particle gains more lipid in post ER to form a lower density mature particle. As it was discussed before, treating cells with BFA also impairs VLDL maturation and lipidation (possibly in post ER compartment). As poorly lipidated apoB are destined for degradation by proteasome, the possibility of degradation of the immature intracellular HCV particles was also investigated. Using MG132 and ALLN (two well-

known inhibitors of proteasomes) it was shown that ALLN (but not MG132) provoked accumulation of intracellular infectious particles. In addition to its ability to inhibit proteasome (similar to MG132), ALLN has an extra inhibitory function against cysteine proteases (746). When cells were treated with a combination of ALLN and BFA, no additive effect to treatment with only BFA was seen, indicating that degradation of cellular infectious particles occurs post-ER. Interestingly treating cells with E64 a cysteine protease inhibitor known to inhibit post-ER degradation of apoB (692), resulted in accumulation of intracellular infectious particles, very similar to ALLN treatment. These results confirm that HCV cellular particles can be degraded by post-ER process and not by the proteasomal degradation. When MTP inhibitor was used, a dose-dependent inhibition of both apoB secretion and HCV infectivity titer (intracellular and extracellular) was observed. Importantly cellular HCV RNA was not affected, indicating that MTP is required for HCV secretion and assembly rather than replication. As we discussed before, MTP is required for the primary lipidation of apoB and its absence results in improper folding of apoB and degradation with proteasomes. Therefore it is tempting to speculate that MTP inhibition resulted in enhanced apoB degradation (and reduced apoB secretion) and this may affect HCV secretion and clearly shows that HCV egress required VLDL secretory pathway (747).

As it was discussed before, similar to the majority of secretory proteins, apoB (therefore VLDL) recruits the ER-Golgi pathway for secretion. Therefore secretory pathway of HCV was also investigated and it was shown that HCV also recruits the ER-Golgi pathway. It has been shown that HCV core protein is co-localized with markers of the ER-Golgi pathway such as early endosomal markers Rab5a and EEA1 and the late endosomal marker, CD63. When cells were treated with U18666A, an inhibitor that causes arrest of late endosomes, the colocalization of core with CD63 was increased twice, whereas HCV RNA and core and infectivity diminished in media, suggesting that release of HCV particles was prevented. Interestingly the infectivity of cell lysate enhanced indicating that by arresting late endosomes HCV particles remained and were accumulated inside the cells. In addition when cells were treated with Baf-A1 (which blocks the fusion of early endosome with late endosomes), colocalization of core with CD63 was reduced dramatically in addition to HCV parameters in media, whereas colocalization of core with EEA1 (early endosomal marker) was enhanced. Finally when cells were treated with wortmannin (which inhibits the formation of early endosomes, the core localization with EEA1 also reduced. These results showed the step by step anterograde movement of HCV particles and confirm that HCV secretion is paralleled to the ER-Golgi pathway, similar to VLDL (748).

Using siRNA the proteins that are involved in ER to Golgi and Golgi to membrane trafficking were knocked down and the role of these proteins was investigated in HCV secretion. Knocking down of 14 genes were found to reduce the HCV secretion by more than 60%, while they had no effect on HCV replication. Four of these proteins are involved in Golgi sorting (CLINT1, PIK4B, PRKD1, AP1M1), one protein is involved in ER to Golgi trafficking (SAR1A), two in Golgi function and trafficking (CYTH3 and ARF3), one in vesicle trafficking (PACSIN3), three in exocytosis (RAB11A, RAB3d and VAMP1) and three in actin remodeling (RHOA, GIT1 and WAS)(749). Several of these proteins were investigated more. Inhibition of ARF3 and PI4KB involved in ER-Golgi and Golgi to plasma transports respectively resulted in reduction of HCV secretion without any effect on HCV replication (749). The siRNA knock down cells of RAB11A [which is involved in transferring cargo from Golgi to plasma membrane (750)] was associated with the accumulation of HCV core in Golgi apparatus of these cells. Silencing VAMP1, a protein which forms a complex with syntaxins, and SNAP25, that forms SNARE complex involved in docking or fusion of vesicles at the plasma membrane (751), resulted in accumulation of core in Golgi as well (749). Golgi localized phosphatidylinositol-4-phosphate (PI4P) has been shown to be essential for HCV secretion as depletion of Golgi specific PI4P pool resulted in significant reduction in HCV secretion without any effect on HCV replication. PI4P facilitate the anterograde movement of Golgi vesicle for secretion by recruiting proteins involved in Golgi trafficking. In addition silencing the GOLPH3, an anchoring protein for PI4P has shown to reduce the HCV secretion and cause accumulation of HCV in Golgi system (752). Finally it has been shown that a motif on core protein (YXXΦ, Φ as a bulky hydrophobic residue) mediate binding of AP2M1 the μ subunit of clathrin adaptor protein complex 2 (AP-2) into LDs. AP2M1 plays an important role in cellular trafficking. YXXΦ mutations, silencing AP2M1 expression has no effect on HCV RNA replication, however, they dramatically inhibits intra- and extracellular infectivity, consistent with a defect in viral assembly. Quantitative confocal immunofluorescence analysis revealed that core's YXXΦ motif mediates recruitment of AP2M1 to lipid droplets and that the observed defect in HCV assembly following disruption of core-AP2M1 binding reduced core localization to trans-Golgi network (TGN), the presumed site of viral particles maturation (753). These results confirmed more strongly that the ER-Golgi secretory pathway is required for HCV secretion.

All of this evidence supports the hypothesis that HCV hijacks the VLDL secretory pathway for egress. Interestingly, clinical data indicate that HCV may impair the VLDL secretion pathway and this may result in HCV-induced hepatitis. It has been shown that patients with chronic HCV infection exhibit significantly lower plasma TG, LDL and apoB containing lipoprotein (hypobetalipoproteinemia, HBL) compared to healthy controls (459,

754-756). The severity of these lipid abnormalities was also correlated with the severity of steatosis. The patients with genotype-3 had more severe HBL compared to genotype non-3 (755, 757). In addition the HBL was resolved in patients treated with anti HCV therapy (459, 754-756). These results suggest that VLDL secretion is impaired in chronically HCV infected patients and this reduction is HCV-dependent. The role of MTP as one of the key regulators of VLDL has been explained before. The MTP expression was measured in liver biopsies taken from 124 HCV infected patients and it was shown that MTP mRNA was significantly decreased in these patients relative to healthy individuals (492). In addition, an inverse correlation was found between the severity of steatosis and MTP mRNA in chronic HCV infected patients (758). It has been shown that from various HCV proteins, core might be responsible for reduction in VLDL secretion. Using HCV core transgenic mice, it was shown that hepatic MTP expression was reduced significantly and this was associated with enhanced hepatic TG accumulation (759, 760). In addition, in another study HCV core transgenic mice secrete a lesser amount of TG and apoB into plasma. This was associated with reduced MTP activity (but not expression) and reduced VLDL particles size (760). All this evidence suggests that HCV infection, in particular core protein, interferes with the VLDL assembly/secretion process (or key factors of this process such as MTP) and limits the secretion of VLDL which results in hepatic steatosis. The exact mechanism of how HCV impairs the VLDL assembly/secretion remains to be elucidated.

References

1. Simmonds P, Alberti A, Alter HJ, Bonino F, Bradley DW, Brechot C, et al. A proposed system for the nomenclature of hepatitis C viral genotypes. Hepatology. 1994;19(5):1321-4. Epub 1994/05/01.

2. Simmonds P, Bukh J, Combet C, Deleage G, Enomoto N, Feinstone S, et al. Consensus proposals for a unified system of nomenclature of hepatitis C virus genotypes. Hepatology. 2005;42(4):962-73. Epub 2005/09/09.

3. http://hcv.lanl.gov/content/index.

4. El-Zanaty F WA. Egypt Demographic and Health Survey 2008. Cairo, Egypt: Ministry of Health, El-Zanaty and Associates, and Macro International. 2009. p. 252.

5. Daniels D, Grytdal, S, Wasley, A,. Surveillance for Acute Viral Hepatitis — United States, 2007. In: Prevention CfDCa, editor.: Centers For Disease Control and Prevention; 2009.

6. Armstrong GL, Wasley A, Simard EP, McQuillan GM, Kuhnert WL, Alter MJ. The prevalence of hepatitis C virus infection in the United States, 1999 through 2002. Ann Intern Med. 2006;144(10):705-14. Epub 2006/05/17.

7. Remis R. Modeling of the Incidence and Prevalence of Hepatitis C Infection and its Sequelae in Canada, 2007. 2009.

8. Epidemiology of Acute Hepatitis C Infection in Canada, Results from the Enhanced Hepatitis Strain Surveillance System (EHSSS). In: Canada PHAo, editor.

9. Nelson PK, Mathers BM, Cowie B, Hagan H, Des Jarlais D, Horyniak D, et al. Global epidemiology of hepatitis B and hepatitis C in people who inject drugs: results of systematic reviews. Lancet. 2011;378(9791):571-83. Epub 2011/08/02.

10. Crofts N, Aitken CK. Incidence of bloodborne virus infection and risk behaviours in a cohort of injecting drug users in Victoria, 1990-1995. Med J Aust. 1997;167(1):17-20. Epub 1997/07/07.

11. Garfein RS, Doherty MC, Monterroso ER, Thomas DL, Nelson KE, Vlahov D. Prevalence and incidence of hepatitis C virus infection among young adult injection drug users. J Acquir Immune Defic Syndr Hum Retrovirol. 1998;18 Suppl 1:S11-9. Epub 1998/07/15.

12. Hagan H, McGough JP, Thiede H, Weiss NS, Hopkins S, Alexander ER. Syringe exchange and risk of infection with hepatitis B and C viruses. Am J Epidemiol. 1999;149(3):203-13. Epub 1999/02/02.

13. Thorpe LE, Ouellet LJ, Hershow R, Bailey SL, Williams IT, Williamson J, et al. Risk of hepatitis C virus infection among young adult injection drug users who share injection equipment. Am J Epidemiol. 2002;155(7):645-53. Epub 2002/03/27.

14. Villano SA, Vlahov D, Nelson KE, Lyles CM, Cohn S, Thomas DL. Incidence and risk factors for hepatitis C among injection drug users in Baltimore, Maryland. J Clin Microbiol. 1997;35(12):3274-7. Epub 1997/12/17.

15. Garten RJ, Lai S, Zhang J, Liu W, Chen J, Vlahov D, et al. Rapid transmission of hepatitis C virus among young injecting heroin users in Southern China. Int J Epidemiol. 2004;33(1):182-8. Epub 2004/04/13.

16. Garfein RS, Vlahov D, Galai N, Doherty MC, Nelson KE. Viral infections in short-term injection drug users: the prevalence of the hepatitis C, hepatitis B, human immunodeficiency, and human T-lymphotropic viruses. Am J Public Health. 1996;86(5):655-61. Epub 1996/05/01.

17. Thorpe LE, Ouellet LJ, Levy JR, Williams IT, Monterroso ER. Hepatitis C virus infection: prevalence, risk factors, and prevention opportunities among young injection drug users in Chicago, 1997-1999. J Infect Dis. 2000;182(6):1588-94. Epub 2000/11/09.

18. Hahn JA, Page-Shafer K, Lum PJ, Ochoa K, Moss AR. Hepatitis C virus infection and needle exchange use among young injection drug users in San Francisco. Hepatology. 2001;34(1):180-7. Epub 2001/06/30.

19. Trim JC, Elliott TS. A review of sharps injuries and preventative strategies. J Hosp Infect. 2003;53(4):237-42. Epub 2003/03/28.

20. Yazdanpanah Y, De Carli G, Migueres B, Lot F, Campins M, Colombo C, et al. Risk factors for hepatitis C virus transmission to health care workers after occupational exposure: a European case-control study. Clinical infectious diseases : an official publication of the Infectious Diseases Society of America. 2005;41(10):1423-30. Epub 2005/10/19.

21. Ross RS, Viazov S, Roggendorf M. Risk of hepatitis C transmission from infected medical staff to patients: model-based calculations for surgical settings. Arch Intern Med. 2000;160(15):2313-6. Epub 2000/08/06.

22. Yeung LT, King SM, Roberts EA. Mother-to-infant transmission of hepatitis C virus. Hepatology. 2001;34(2):223-9. Epub 2001/08/02.

23. Pappalardo BL. Influence of maternal human immunodeficiency virus (HIV) co-infection on vertical transmission of hepatitis C virus (HCV): a meta-analysis. Int J Epidemiol. 2003;32(5):727-34. Epub 2003/10/16.

24. Gibb DM, Goodall RL, Dunn DT, Healy M, Neave P, Cafferkey M, et al. Mother-to-child transmission of hepatitis C virus: evidence for preventable peripartum transmission. Lancet. 2000;356(9233):904-7. Epub 2000/10/19.

25. McIntyre PG, Tosh K, McGuire W. Caesarean section versus vaginal delivery for preventing mother to infant hepatitis C virus transmission. Cochrane Database Syst Rev. 2006(4):CD005546. Epub 2006/10/21.

26. Pembrey L, Newell ML, Tovo PA. The management of HCV infected pregnant women and their children European paediatric HCV network. J Hepatol. 2005;43(3):515-25. Epub 2005/09/07.

27. Kumar RM, Shahul S. Role of breast-feeding in transmission of hepatitis C virus to infants of HCV-infected mothers. J Hepatol. 1998;29(2):191-7. Epub 1998/08/29.

28. Lin HH, Kao JH, Hsu HY, Ni YH, Chang MH, Huang SC, et al. Absence of infection in breast-fed infants born to hepatitis C virus-infected mothers. J Pediatr. 1995;126(4):589-91. Epub 1995/04/01.

29. Resti M, Azzari C, Galli L, Zuin G, Giacchino R, Bortolotti F, et al. Maternal drug use is a preeminent risk factor for mother-to-child hepatitis C virus transmission: results from a multicenter study of 1372 mother-infant pairs. J Infect Dis. 2002;185(5):567-72. Epub 2002/02/28.

30. Chiavetta JA, Escobar M, Newman A, He Y, Driezen P, Deeks S, et al. Incidence and estimated rates of residual risk for HIV, hepatitis C, hepatitis B and human T-cell lymphotropic viruses in blood donors in Canada, 1990-2000. CMAJ. 2003;169(8):767-73. Epub 2003/10/15.

31. Thomas DL, Seeff LB. Natural history of hepatitis C. Clin Liver Dis. 2005;9(3):383-98, vi. Epub 2005/07/19.

32. Mondelli MU, Cerino A, Cividini A. Acute hepatitis C: diagnosis and management. J Hepatol. 2005;42 Suppl(1):S108-14. Epub 2005/03/22.

33. Gordon SC. New insights into acute hepatitis C. Gastroenterology. 2003;125(1):253-6. Epub 2003/07/10.

34. Chung RT. Acute hepatitis C virus infection. Clinical infectious diseases : an official publication of the Infectious Diseases Society of America. 2005;41 Suppl 1:S14-7. Epub 2005/11/03.

35. Trey C, Davidson CS. The management of fulminant hepatic failure. Prog Liver Dis. 1970;3:282-98. Epub 1970/01/01.

36. O'Grady JG, Schalm SW, Williams R. Acute liver failure: redefining the syndromes. Lancet. 1993;342(8866):273-5. Epub 1993/07/31.

37. Bernal W, Auzinger G, Dhawan A, Wendon J. Acute liver failure. Lancet. 2010;376(9736):190-201. Epub 2010/07/20.

38. Vento S, Garofano T, Renzini C, Cainelli F, Casali F, Ghironzi G, et al. Fulminant hepatitis associated with hepatitis A virus superinfection in patients with chronic hepatitis C. N Engl J Med. 1998;338(5):286-90. Epub 1998/01/29.

39. Bellentani S, Tiribelli C. The spectrum of liver disease in the general population: lesson from the Dionysos study. J Hepatol. 2001;35(4):531-7. Epub 2001/10/30.

40. Kenny-Walsh E. Clinical outcomes after hepatitis C infection from contaminated anti-D immune globulin. Irish Hepatology Research Group. N Engl J Med. 1999;340(16):1228-33. Epub 1999/04/22.

41. Alter MJ, Kruszon-Moran D, Nainan OV, McQuillan GM, Gao F, Moyer LA, et al. The prevalence of hepatitis C virus infection in the United States, 1988 through 1994. N Engl J Med. 1999;341(8):556-62. Epub 1999/08/19.

42. Luetkemeyer A, Hare CB, Stansell J, Tien PC, Charlesbois E, Lum P, et al. Clinical presentation and course of acute hepatitis C infection in HIV-infected patients. J Acquir Immune Defic Syndr. 2006;41(1):31-6. Epub 2005/12/13.

43. Graham CS, Baden LR, Yu E, Mrus JM, Carnie J, Heeren T, et al. Influence of human immunodeficiency virus infection on the course of hepatitis C virus infection: a meta-analysis. Clinical infectious diseases : an official publication of the Infectious Diseases Society of America. 2001;33(4):562-9. Epub 2001/07/20.

44. Onji M, Kikuchi T, Kumon I, Masumoto T, Nadano S, Kajino K, et al. Intrahepatic lymphocyte subpopulations and HLA class I antigen expression by hepatocytes in chronic hepatitis C. Hepatogastroenterology. 1992;39(4):340-3. Epub 1992/08/01.

45. Garcia-Monzon C, Sanchez-Madrid F, Garcia-Buey L, Garcia-Arroyo A, Garcia-Sanchez A, Moreno-Otero R. Vascular adhesion molecule expression in viral chronic

hepatitis: evidence of neoangiogenesis in portal tracts. Gastroenterology. 1995;108(1):231-41. Epub 1995/01/01.

46. Bertoletti A, D'Elios MM, Boni C, De Carli M, Zignego AL, Durazzo M, et al. Different cytokine profiles of intraphepatic T cells in chronic hepatitis B and hepatitis C virus infections. Gastroenterology. 1997;112(1):193-9. Epub 1997/01/01.

47. Napoli J, Bishop GA, McGuinness PH, Painter DM, McCaughan GW. Progressive liver injury in chronic hepatitis C infection correlates with increased intrahepatic expression of Th1-associated cytokines. Hepatology. 1996;24(4):759-65. Epub 1996/10/01.

48. Reiser M, Marousis CG, Nelson DR, Lauer G, Gonzalez-Peralta RP, Davis GL, et al. Serum interleukin 4 and interleukin 10 levels in patients with chronic hepatitis C virus infection. J Hepatol. 1997;26(3):471-8. Epub 1997/03/01.

49. Nelson DR, Lau JY. Pathogenesis of hepatocellular damage in chronic hepatitis C virus infection. Clin Liver Dis. 1997;1(3):515-28, v. Epub 2004/11/25.

50. Ando K, Hiroishi K, Kaneko T, Moriyama T, Muto Y, Kayagaki N, et al. Perforin, Fas/Fas ligand, and TNF-alpha pathways as specific and bystander killing mechanisms of hepatitis C virus-specific human CTL. J Immunol. 1997;158(11):5283-91. Epub 1997/06/01.

51. Gremion C, Grabscheid B, Wolk B, Moradpour D, Reichen J, Pichler W, et al. Cytotoxic T lymphocytes derived from patients with chronic hepatitis C virus infection kill bystander cells via Fas-FasL interaction. Journal of virology. 2004;78(4):2152-7. Epub 2004/01/30.

52. Koziel MJ, Dudley D, Afdhal N, Grakoui A, Rice CM, Choo QL, et al. HLA class I-restricted cytotoxic T lymphocytes specific for hepatitis C virus. Identification of multiple epitopes and characterization of patterns of cytokine release. J Clin Invest. 1995;96(5):2311-21. Epub 1995/11/01.

53. Guicciardi ME, Gores GJ. Apoptosis: a mechanism of acute and chronic liver injury. Gut. 2005;54(7):1024-33. Epub 2005/06/14.

54. Kafrouni MI, Brown GR, Thiele DL. Virally infected hepatocytes are resistant to perforin-dependent CTL effector mechanisms. J Immunol. 2001;167(3):1566-74. Epub 2001/07/24.

55. Fischer R, Schmitt M, Bode JG, Haussinger D. Expression of the peripheral-type benzodiazepine receptor and apoptosis induction in hepatic stellate cells. Gastroenterology. 2001;120(5):1212-26. Epub 2001/03/27.

56. Fischer R, Cariers A, Reinehr R, Haussinger D. Caspase 9-dependent killing of hepatic stellate cells by activated Kupffer cells. Gastroenterology. 2002;123(3):845-61. Epub 2002/08/29.

57. Kumar S. Caspase function in programmed cell death. Cell Death Differ. 2007;14(1):32-43. Epub 2006/11/04.

58. Machida K, Tsukiyama-Kohara K, Seike E, Tone S, Shibasaki F, Shimizu M, et al. Inhibition of cytochrome c release in Fas-mediated signaling pathway in transgenic mice induced to express hepatitis C viral proteins. J Biol Chem. 2001;276(15):12140-6. Epub 2001/03/30.

59. Dumoulin FL, vsn dem Bussche A, Sohne J, Sauerbruch T, Spengler U. Hepatitis C virus core protein does not inhibit apoptosis in human hepatoma cells. Eur J Clin Invest. 1999;29(11):940-6. Epub 1999/12/03.

60. Ray RB, Steele R, Meyer K, Ray R. Transcriptional repression of p53 promoter by hepatitis C virus core protein. The Journal of biological chemistry. 1997;272(17):10983-6. Epub 1997/04/25.

61. Kao CF, Chen SY, Chen JY, Wu Lee YH. Modulation of p53 transcription regulatory activity and post-translational modification by hepatitis C virus core protein. Oncogene. 2004;23(14):2472-83. Epub 2004/02/18.

62. Otsuka M, Kato N, Taniguchi H, Yoshida H, Goto T, Shiratori Y, et al. Hepatitis C virus core protein inhibits apoptosis via enhanced Bcl-xL expression. Virology. 2002;296(1):84-93. Epub 2002/05/31.

63. Zhu N, Khoshnan A, Schneider R, Matsumoto M, Dennert G, Ware C, et al. Hepatitis C virus core protein binds to the cytoplasmic domain of tumor necrosis factor (TNF) receptor 1 and enhances TNF-induced apoptosis. J Virol. 1998;72(5):3691-7. Epub 1998/04/29.

64. Otsuka M, Kato N, Lan K, Yoshida H, Kato J, Goto T, et al. Hepatitis C virus core protein enhances p53 function through augmentation of DNA binding affinity and transcriptional ability. The Journal of biological chemistry. 2000;275(44):34122-30. Epub 2000/08/05.

65. Chou AH, Tsai HF, Wu YY, Hu CY, Hwang LH, Hsu PI, et al. Hepatitis C virus core protein modulates TRAIL-mediated apoptosis by enhancing Bid cleavage and activation of mitochondria apoptosis signaling pathway. J Immunol. 2005;174(4):2160-6. Epub 2005/02/09.

66. Okuda M, Li K, Beard MR, Showalter LA, Scholle F, Lemon SM, et al. Mitochondrial injury, oxidative stress, and antioxidant gene expression are induced by hepatitis C virus core protein. Gastroenterology. 2002;122(2):366-75. Epub 2002/02/08.

67. Machida K, Cheng KT, Lai CK, Jeng KS, Sung VM, Lai MM. Hepatitis C virus triggers mitochondrial permeability transition with production of reactive oxygen species, leading to DNA damage and STAT3 activation. Journal of virology. 2006;80(14):7199-207. Epub 2006/07/01.

68. Kamegaya Y, Hiasa Y, Zukerberg L, Fowler N, Blackard JT, Lin W, et al. Hepatitis C virus acts as a tumor accelerator by blocking apoptosis in a mouse model of hepatocarcinogenesis. Hepatology. 2005;41(3):660-7. Epub 2005/02/22.

69. Chiou HL, Hsieh YS, Hsieh MR, Chen TY. HCV E2 may induce apoptosis of Huh-7 cells via a mitochondrial-related caspase pathway. Biochem Biophys Res Commun. 2006;345(1):453-8. Epub 2006/05/10.

70. Meylan E, Curran J, Hofmann K, Moradpour D, Binder M, Bartenschlager R, et al. Cardif is an adaptor protein in the RIG-I antiviral pathway and is targeted by hepatitis C virus. Nature. 2005;437(7062):1167-72. Epub 2005/09/24.

71. Prikhod'ko EA, Prikhod'ko GG, Siegel RM, Thompson P, Major ME, Cohen JI. The NS3 protein of hepatitis C virus induces caspase-8-mediated apoptosis independent of its protease or helicase activities. Virology. 2004;329(1):53-67. Epub 2004/10/13.

72. Nomura-Takigawa Y, Nagano-Fujii M, Deng L, Kitazawa S, Ishido S, Sada K, et al. Non-structural protein 4A of Hepatitis C virus accumulates on mitochondria and renders the cells prone to undergoing mitochondria-mediated apoptosis. J Gen Virol. 2006;87(Pt 7):1935-45. Epub 2006/06/09.

73. Wang J, Tong W, Zhang X, Chen L, Yi Z, Pan T, et al. Hepatitis C virus non-structural protein NS5A interacts with FKBP38 and inhibits apoptosis in Huh7 hepatoma cells. FEBS Lett. 2006;580(18):4392-400. Epub 2006/07/18.

74. Nanda SK, Herion D, Liang TJ. The SH3 binding motif of HCV [corrected] NS5A protein interacts with Bin1 and is important for apoptosis and infectivity. Gastroenterology. 2006;130(3):794-809. Epub 2006/03/15.

75. Der SD, Yang YL, Weissmann C, Williams BR. A double-stranded RNA-activated protein kinase-dependent pathway mediating stress-induced apoptosis. Proceedings of the National Academy of Sciences of the United States of America. 1997;94(7):3279-83. Epub 1997/04/01.

76. Gil J, Esteban M. Induction of apoptosis by the dsRNA-dependent protein kinase (PKR): mechanism of action. Apoptosis. 2000;5(2):107-14. Epub 2001/03/10.

77. Friedman SL. Liver fibrosis -- from bench to bedside. J Hepatol. 2003;38 Suppl 1:S38-53. Epub 2003/02/20.

78. Bataller R, Brenner DA. Liver fibrosis. J Clin Invest. 2005;115(2):209-18. Epub 2005/02/04.

79. Benyon RC, Iredale JP. Is liver fibrosis reversible? Gut. 2000;46(4):443-6. Epub 2000/03/15.

80. Arthur MJ. Fibrogenesis II. Metalloproteinases and their inhibitors in liver fibrosis. Am J Physiol Gastrointest Liver Physiol. 2000;279(2):G245-9. Epub 2000/08/01.

81. Gabele E, Brenner DA, Rippe RA. Liver fibrosis: signals leading to the amplification of the fibrogenic hepatic stellate cell. Front Biosci. 2003;8:d69-77. Epub 2002/11/29.

82. Marra F. Hepatic stellate cells and the regulation of liver inflammation. J Hepatol. 1999;31(6):1120-30. Epub 1999/12/22.

83. Kinnman N, Housset C. Peribiliary myofibroblasts in biliary type liver fibrosis. Front Biosci. 2002;7:d496-503. Epub 2002/01/30.

84. Canbay A, Friedman S, Gores GJ. Apoptosis: the nexus of liver injury and fibrosis. Hepatology. 2004;39(2):273-8. Epub 2004/02/10.

85. Casini A, Ceni E, Salzano R, Biondi P, Parola M, Galli A, et al. Neutrophil-derived superoxide anion induces lipid peroxidation and stimulates collagen synthesis in human hepatic stellate cells: role of nitric oxide. Hepatology. 1997;25(2):361-7. Epub 1997/02/01.

86. Gressner AM, Weiskirchen R, Breitkopf K, Dooley S. Roles of TGF-beta in hepatic fibrosis. Front Biosci. 2002;7:d793-807. Epub 2002/03/19.

87. Pinzani M, Gesualdo L, Sabbah GM, Abboud HE. Effects of platelet-derived growth factor and other polypeptide mitogens on DNA synthesis and growth of cultured rat liver fat-storing cells. J Clin Invest. 1989;84(6):1786-93. Epub 1989/12/01.

88. Naito M, Hasegawa G, Ebe Y, Yamamoto T. Differentiation and function of Kupffer cells. Med Electron Microsc. 2004;37(1):16-28. Epub 2004/04/02.

89. Wheeler MD, Kono H, Yin M, Nakagami M, Uesugi T, Arteel GE, et al. The role of Kupffer cell oxidant production in early ethanol-induced liver disease. Free Radic Biol Med. 2001;31(12):1544-9. Epub 2001/12/18.

90. Maher JJ, Zia S, Tzagarakis C. Acetaldehyde-induced stimulation of collagen synthesis and gene expression is dependent on conditions of cell culture: studies with rat lipocytes and fibroblasts. Alcohol Clin Exp Res. 1994;18(2):403-9. Epub 1994/04/01.

91. Wanless IR, Shiota K. The pathogenesis of nonalcoholic steatohepatitis and other fatty liver diseases: a four-step model including the role of lipid release and hepatic venular obstruction in the progression to cirrhosis. Semin Liver Dis. 2004;24(1):99-106. Epub 2004/04/16.

92. El-Serag HB. Hepatocellular carcinoma. N Engl J Med. 2011;365(12):1118-27. Epub 2011/10/14.

93. Tanaka Y, Hanada K, Mizokami M, Yeo AE, Shih JW, Gojobori T, et al. A comparison of the molecular clock of hepatitis C virus in the United States and Japan predicts that hepatocellular carcinoma incidence in the United States will increase over the next two decades. Proceedings of the National Academy of Sciences of the United States of America. 2002;99(24):15584-9. Epub 2002/11/20.

94. Perz JF, Alter MJ. The coming wave of HCV-related liver disease: dilemmas and challenges. J Hepatol. 2006;44(3):441-3. Epub 2006/01/24.

95. McGivern DR, Lemon SM. Virus-specific mechanisms of carcinogenesis in hepatitis C virus associated liver cancer. Oncogene. 2011;30(17):1969-83. Epub 2011/01/25.

96. Fattovich G, Stroffolini T, Zagni I, Donato F. Hepatocellular carcinoma in cirrhosis: incidence and risk factors. Gastroenterology. 2004;127(5 Suppl 1):S35-50. Epub 2004/10/28.

97. Daghestani L, Pomeroy C. Renal manifestations of hepatitis C infection. Am J Med. 1999;106(3):347-54. Epub 1999/04/06.

98. Iannuzzella F, Vaglio A, Garini G. Management of hepatitis C virus-related mixed cryoglobulinemia. Am J Med. 2010;123(5):400-8. Epub 2010/04/20.

99. Sansonno D, Cornacchiulo V, Iacobelli AR, Di Stefano R, Lospalluti M, Dammacco F. Localization of hepatitis C virus antigens in liver and skin tissues of chronic hepatitis C virus-infected patients with mixed cryoglobulinemia. Hepatology. 1995;21(2):305-12. Epub 1995/02/01.

100. Ferri C, La Civita L, Cirafisi C, Siciliano G, Longombardo G, Bombardieri S, et al. Peripheral neuropathy in mixed cryoglobulinemia: clinical and electrophysiologic investigations. J Rheumatol. 1992;19(6):889-95. Epub 1992/06/01.

101. Tembl JI, Ferrer JM, Sevilla MT, Lago A, Mayordomo F, Vilchez JJ. Neurologic complications associated with hepatitis C virus infection. Neurology. 1999;53(4):861-4. Epub 1999/09/17.

102. Agnello V, De Rosa FG. Extrahepatic disease manifestations of HCV infection: some current issues. J Hepatol. 2004;40(2):341-52. Epub 2004/01/24.

103. Sene D, Limal N, Cacoub P. Hepatitis C virus-associated extrahepatic manifestations: a review. Metab Brain Dis. 2004;19(3-4):357-81. Epub 2004/11/24.

104. Galossi A, Guarisco R, Bellis L, Puoti C. Extrahepatic manifestations of chronic HCV infection. J Gastrointestin Liver Dis. 2007;16(1):65-73. Epub 2007/04/06.

105. Rasul I, Shepherd FA, Kamel-Reid S, Krajden M, Pantalony D, Heathcote EJ. Detection of occult low-grade b-cell non-Hodgkin's lymphoma in patients with chronic hepatitis C infection and mixed cryoglobulinemia. Hepatology. 1999;29(2):543-7. Epub 1999/01/27.

106. Mele A, Pulsoni A, Bianco E, Musto P, Szklo A, Sanpaolo MG, et al. Hepatitis C virus and B-cell non-Hodgkin lymphomas: an Italian multicenter case-control study. Blood. 2003;102(3):996-9. Epub 2003/04/26.

107. Fargion S, Piperno A, Cappellini MD, Sampietro M, Fracanzani AL, Romano R, et al. Hepatitis C virus and porphyria cutanea tarda: evidence of a strong association. Hepatology. 1992;16(6):1322-6. Epub 1992/12/01.

108. Huang MJ, Tsai SL, Huang BY, Sheen IS, Yeh CT, Liaw YF. Prevalence and significance of thyroid autoantibodies in patients with chronic hepatitis C virus infection: a prospective controlled study. Clin Endocrinol (Oxf). 1999;50(4):503-9. Epub 1999/09/01.

109. Antonelli A, Ferri C, Pampana A, Fallahi P, Nesti C, Pasquini M, et al. Thyroid disorders in chronic hepatitis C. Am J Med. 2004;117(1):10-3. Epub 2004/06/24.

110. Prummel MF, Laurberg P. Interferon-alpha and autoimmune thyroid disease. Thyroid. 2003;13(6):547-51. Epub 2003/08/22.

111. Fernandez-Soto L, Gonzalez A, Escobar-Jimenez F, Vazquez R, Ocete E, Olea N, et al. Increased risk of autoimmune thyroid disease in hepatitis C vs hepatitis B before, during, and after discontinuing interferon therapy. Arch Intern Med. 1998;158(13):1445-8. Epub 1998/07/17.

112. Knobler H, Schihmanter R, Zifroni A, Fenakel G, Schattner A. Increased risk of type 2 diabetes in noncirrhotic patients with chronic hepatitis C virus infection. Mayo Clin Proc. 2000;75(4):355-9. Epub 2000/04/13.

113. Haddad J, Deny P, Munz-Gotheil C, Ambrosini JC, Trinchet JC, Pateron D, et al. Lymphocytic sialadenitis of Sjogren's syndrome associated with chronic hepatitis C virus liver disease. Lancet. 1992;339(8789):321-3. Epub 1992/02/08.

114. Rosner I, Rozenbaum M, Toubi E, Kessel A, Naschitz JE, Zuckerman E. The case for hepatitis C arthritis. Semin Arthritis Rheum. 2004;33(6):375-87. Epub 2004/06/11.

115. Matsumori A, Ohashi N, Hasegawa K, Sasayama S, Eto T, Imaizumi T, et al. Hepatitis C virus infection and heart diseases: a multicenter study in Japan. Jpn Circ J. 1998;62(5):389-91. Epub 1998/06/17.

116. Ohta K, Ueda T, Nagai S, Yamada K, Yamaguchi M, Nakano J, et al. [Pathogenesis of idiopathic pulmonary fibrosis--is hepatitis C virus involved?]. Nihon Kyobu Shikkan Gakkai Zasshi. 1993;31 Suppl:32-5. Epub 1993/12/01.

117. Moazami G, Auran JD, Florakis GJ, Wilson SE, Srinivasan DB. Interferon treatment of Mooren's ulcers associated with hepatitis C. American journal of ophthalmology. 1995;119(3):365-6. Epub 1995/03/01.

118. Khosla S, Hassoun AA, Baker BK, Liu F, Zein NN, Whyte MP, et al. Insulin-like growth factor system abnormalities in hepatitis C-associated osteosclerosis. Potential insights into increasing bone mass in adults. J Clin Invest. 1998;101(10):2165-73. Epub 1998/05/29.

119. Thomson BJ, Kwong G, Ratib S, Sweeting M, Ryder SD, De Angelis D, et al. Response rates to combination therapy for chronic HCV infection in a clinical setting and derivation of probability tables for individual patient management. J Viral Hepat. 2008;15(4):271-8. Epub 2007/12/19.

120. Hill L, Henry B, Schweikert S. Screening for chronic hepatitis C: American College of Preventive Medicine practice policy statement. Am J Prev Med. 2005;28(3):327-30. Epub 2005/03/16.

121. Lapane KL, Jakiche AF, Sugano D, Weng CS, Carey WD. Hepatitis C infection risk analysis: who should be screened? Comparison of multiple screening strategies based on the National Hepatitis Surveillance Program. Am J Gastroenterol. 1998;93(4):591-6. Epub 1998/05/12.

122. Ghany MG, Strader DB, Thomas DL, Seeff LB. Diagnosis, management, and treatment of hepatitis C: an update. Hepatology. 2009;49(4):1335-74. Epub 2009/03/31.

123. Albeldawi M, Ruiz-Rodriguez E, Carey WD. Hepatitis C virus: Prevention, screening, and interpretation of assays. Cleve Clin J Med. 2010;77(9):616-26. Epub 2010/09/03.

124. Colin C, Lanoir D, Touzet S, Meyaud-Kraemer L, Bailly F, Trepo C. Sensitivity and specificity of third-generation hepatitis C virus antibody detection assays: an analysis of the literature. J Viral Hepat. 2001;8(2):87-95. Epub 2001/03/27.

125. Pawlotsky JM, Lonjon I, Hezode C, Raynard B, Darthuy F, Remire J, et al. What strategy should be used for diagnosis of hepatitis C virus infection in clinical laboratories? Hepatology. 1998;27(6):1700-2. Epub 1998/06/10.

126. Thio CL, Nolt KR, Astemborski J, Vlahov D, Nelson KE, Thomas DL. Screening for hepatitis C virus in human immunodeficiency virus-infected individuals. J Clin Microbiol. 2000;38(2):575-7. Epub 2000/02/03.

127. Kalantar-Zadeh K, Miller LG, Daar ES. Diagnostic discordance for hepatitis C virus infection in hemodialysis patients. Am J Kidney Dis. 2005;46(2):290-300. Epub 2005/08/23.

128. Chamot E, Hirschel B, Wintsch J, Robert CF, Gabriel V, Deglon JJ, et al. Loss of antibodies against hepatitis C virus in HIV-seropositive intravenous drug users. AIDS. 1990;4(12):1275-7. Epub 1990/12/01.

129. Hadziyannis SJ, Sette H, Jr., Morgan TR, Balan V, Diago M, Marcellin P, et al. Peginterferon-alpha2a and ribavirin combination therapy in chronic hepatitis C: a randomized study of treatment duration and ribavirin dose. Ann Intern Med. 2004;140(5):346-55. Epub 2004/03/05.

130. Manns MP, McHutchison JG, Gordon SC, Rustgi VK, Shiffman M, Reindollar R, et al. Peginterferon alfa-2b plus ribavirin compared with interferon alfa-2b plus ribavirin for initial treatment of chronic hepatitis C: a randomised trial. Lancet. 2001;358(9286):958-65. Epub 2001/10/05.

131. Fried MW, Shiffman ML, Reddy KR, Smith C, Marinos G, Goncales FL, Jr., et al. Peginterferon alfa-2a plus ribavirin for chronic hepatitis C virus infection. N Engl J Med. 2002;347(13):975-82. Epub 2002/09/27.

132. Kobayashi S, Takeda T, Enomoto M, Tamori A, Kawada N, Habu D, et al. Development of hepatocellular carcinoma in patients with chronic hepatitis C who had a sustained virological response to interferon therapy: a multicenter, retrospective cohort study of 1124 patients. Liver international : official journal of the International Association for the Study of the Liver. 2007;27(2):186-91. Epub 2007/02/22.

133. Ferenci P, Fried MW, Shiffman ML, Smith CI, Marinos G, Goncales FL, Jr., et al. Predicting sustained virological responses in chronic hepatitis C patients treated with peginterferon alfa-2a (40 KD)/ribavirin. J Hepatol. 2005;43(3):425-33. Epub 2005/07/02.

134. Davis GL, Wong JB, McHutchison JG, Manns MP, Harvey J, Albrecht J. Early virologic response to treatment with peginterferon alfa-2b plus ribavirin in patients with chronic hepatitis C. Hepatology. 2003;38(3):645-52. Epub 2003/08/27.

135. Zeuzem S, Welsch C, Herrmann E. Pharmacokinetics of peginterferons. Semin Liver Dis. 2003;23 Suppl 1:23-8. Epub 2003/08/23.

136. Ferenci P. Safety and efficacy of treatment for chronic hepatitis C with a focus on pegylated interferons: the backbone of therapy today and in the future. Expert Opin Drug Saf. 2011;10(4):529-44. Epub 2011/02/25.

137. Kamal SM. Acute hepatitis C: a systematic review. Am J Gastroenterol. 2008;103(5):1283-97; quiz 98. Epub 2008/05/15.

138. Vermehren J, Sarrazin C. New HCV therapies on the horizon. Clin Microbiol Infect. 2011;17(2):122-34. Epub 2010/11/20.

139. Lamarre D, Anderson PC, Bailey M, Beaulieu P, Bolger G, Bonneau P, et al. An NS3 protease inhibitor with antiviral effects in humans infected with hepatitis C virus. Nature. 2003;426(6963):186-9. Epub 2003/10/28.

140. Jacobson IM, McHutchison JG, Dusheiko G, Di Bisceglie AM, Reddy KR, Bzowej NH, et al. Telaprevir for previously untreated chronic hepatitis C virus infection. N Engl J Med. 2011;364(25):2405-16. Epub 2011/06/24.

141. Zeuzem S, Andreone P, Pol S, Lawitz E, Diago M, Roberts S, et al. Telaprevir for retreatment of HCV infection. N Engl J Med. 2011;364(25):2417-28. Epub 2011/06/24.

142. Poordad F, McCone J, Jr., Bacon BR, Bruno S, Manns MP, Sulkowski MS, et al. Boceprevir for untreated chronic HCV genotype 1 infection. N Engl J Med. 2011;364(13):1195-206. Epub 2011/04/01.

143. Bacon BR, Gordon SC, Lawitz E, Marcellin P, Vierling JM, Zeuzem S, et al. Boceprevir for previously treated chronic HCV genotype 1 infection. N Engl J Med. 2011;364(13):1207-17. Epub 2011/04/01.

144. Poordad F, Dieterich D. Treating hepatitis C: current standard of care and emerging direct-acting antiviral agents. J Viral Hepat. 2012;19(7):449-64. Epub 2012/06/09.

145. Lok AS, Gardiner DF, Lawitz E, Martorell C, Everson GT, Ghalib R, et al. Preliminary study of two antiviral agents for hepatitis C genotype 1. N Engl J Med. 2012;366(3):216-24. Epub 2012/01/20.

146. Watashi K, Ishii N, Hijikata M, Inoue D, Murata T, Miyanari Y, et al. Cyclophilin B is a functional regulator of hepatitis C virus RNA polymerase. Mol Cell. 2005;19(1):111-22. Epub 2005/07/02.

147. Ahmed-Belkacem A, Ahnou N, Barbotte L, Wychowski C, Pallier C, Brillet R, et al. Silibinin and related compounds are direct inhibitors of hepatitis C virus RNA-dependent RNA polymerase. Gastroenterology. 2010;138(3):1112-22. Epub 2009/12/08.

148. Rossignol JF. Thiazolides: a new class of antiviral drugs. Expert Opin Drug Metab Toxicol. 2009;5(6):667-74. Epub 2009/05/16.

149. Andre P, Perlemuter G, Budkowska A, Brechot C, Lotteau V. Hepatitis C virus particles and lipoprotein metabolism. Semin Liver Dis. 2005;25(1):93-104. Epub 2005/02/26.

150. Lindenbach BD, Rice CM. Unravelling hepatitis C virus replication from genome to function. Nature. 2005;436(7053):933-8. Epub 2005/08/19.

151. Merrick WC. Cap-dependent and cap-independent translation in eukaryotic systems. Gene. 2004;332:1-11. Epub 2004/05/18.

152. Kapp LD, Lorsch JR. The molecular mechanics of eukaryotic translation. Annu Rev Biochem. 2004;73:657-704. Epub 2004/06/11.

153. Hellen CU, Sarnow P. Internal ribosome entry sites in eukaryotic mRNA molecules. Genes & development. 2001;15(13):1593-612. Epub 2001/07/11.

154. Kieft JS, Zhou K, Jubin R, Doudna JA. Mechanism of ribosome recruitment by hepatitis C IRES RNA. RNA. 2001;7(2):194-206. Epub 2001/03/10.

155. Otto GA, Puglisi JD. The pathway of HCV IRES-mediated translation initiation. Cell. 2004;119(3):369-80. Epub 2004/10/28.

156. Kieft JS, Zhou K, Jubin R, Murray MG, Lau JY, Doudna JA. The hepatitis C virus internal ribosome entry site adopts an ion-dependent tertiary fold. J Mol Biol. 1999;292(3):513-29. Epub 1999/09/25.

157. Pestova TV, Hellen CU. Internal initiation of translation of bovine viral diarrhea virus RNA. Virology. 1999;258(2):249-56. Epub 1999/06/15.

158. Pestova TV, de Breyne S, Pisarev AV, Abaeva IS, Hellen CU. eIF2-dependent and eIF2-independent modes of initiation on the CSFV IRES: a common role of domain II. EMBO J. 2008;27(7):1060-72. Epub 2008/03/14.

159. Fukushi S, Katayama K, Kurihara C, Ishiyama N, Hoshino FB, Ando T, et al. Complete 5' noncoding region is necessary for the efficient internal initiation of hepatitis C virus RNA. Biochem Biophys Res Commun. 1994;199(2):425-32. Epub 1994/03/15.

160. Reynolds JE, Kaminski A, Carroll AR, Clarke BE, Rowlands DJ, Jackson RJ. Internal initiation of translation of hepatitis C virus RNA: the ribosome entry site is at the authentic initiation codon. RNA. 1996;2(9):867-78. Epub 1996/09/01.

161. Rijnbrand R, Bredenbeek P, van der Straaten T, Whetter L, Inchauspe G, Lemon S, et al. Almost the entire 5' non-translated region of hepatitis C virus is required for cap-independent translation. FEBS Lett. 1995;365(2-3):115-9. Epub 1995/05/29.

162. Lukavsky PJ. Structure and function of HCV IRES domains. Virus Res. 2009;139(2):166-71. Epub 2008/07/22.

163. Brown EA, Zhang H, Ping LH, Lemon SM. Secondary structure of the 5' nontranslated regions of hepatitis C virus and pestivirus genomic RNAs. Nucleic Acids Res. 1992;20(19):5041-5. Epub 1992/10/11.

164. Lukavsky PJ, Otto GA, Lancaster AM, Sarnow P, Puglisi JD. Structures of two RNA domains essential for hepatitis C virus internal ribosome entry site function. Nat Struct Biol. 2000;7(12):1105-10. Epub 2000/12/02.

165. Pestova TV, Shatsky IN, Fletcher SP, Jackson RJ, Hellen CU. A prokaryotic-like mode of cytoplasmic eukaryotic ribosome binding to the initiation codon during internal translation initiation of hepatitis C and classical swine fever virus RNAs. Genes & development. 1998;12(1):67-83. Epub 1998/02/21.

166. Kieft JS, Zhou K, Grech A, Jubin R, Doudna JA. Crystal structure of an RNA tertiary domain essential to HCV IRES-mediated translation initiation. Nat Struct Biol. 2002;9(5):370-4. Epub 2002/04/03.

167. Spahn CM, Kieft JS, Grassucci RA, Penczek PA, Zhou K, Doudna JA, et al. Hepatitis C virus IRES RNA-induced changes in the conformation of the 40s ribosomal subunit. Science. 2001;291(5510):1959-62. Epub 2001/03/10.

168. Kolupaeva VG, Pestova TV, Hellen CU. An enzymatic footprinting analysis of the interaction of 40S ribosomal subunits with the internal ribosomal entry site of hepatitis C virus. Journal of virology. 2000;74(14):6242-50. Epub 2000/06/23.

169. Locker N, Easton LE, Lukavsky PJ. HCV and CSFV IRES domain II mediate eIF2 release during 80S ribosome assembly. EMBO J. 2007;26(3):795-805. Epub 2007/01/27.

170. Shimoike T, Koyama C, Murakami K, Suzuki R, Matsuura Y, Miyamura T, et al. Down-regulation of the internal ribosome entry site (IRES)-mediated translation of the hepatitis C virus: critical role of binding of the stem-loop IIId domain of IRES and the viral core protein. Virology. 2006;345(2):434-45. Epub 2005/11/22.

171. Zhang J, Yamada O, Yoshida H, Iwai T, Araki H. Autogenous translational inhibition of core protein: implication for switch from translation to RNA replication in hepatitis C virus. Virology. 2002;293(1):141-50. Epub 2002/02/21.

172. Wang TH, Rijnbrand RC, Lemon SM. Core protein-coding sequence, but not core protein, modulates the efficiency of cap-independent translation directed by the internal ribosome entry site of hepatitis C virus. Journal of virology. 2000;74(23):11347-58. Epub 2000/11/09.

173. Moradpour D, Penin F, Rice CM. Replication of hepatitis C virus. Nat Rev Microbiol. 2007;5(6):453-63. Epub 2007/05/10.

174. Yasui K, Wakita T, Tsukiyama-Kohara K, Funahashi SI, Ichikawa M, Kajita T, et al. The native form and maturation process of hepatitis C virus core protein. Journal of virology. 1998;72(7):6048-55. Epub 1998/06/17.

175. Kopp M, Murray CL, Jones CT, Rice CM. Genetic analysis of the carboxy-terminal region of the hepatitis C virus core protein. Journal of virology. 2010;84(4):1666-73. Epub 2009/12/17.

176. McLauchlan J, Lemberg MK, Hope G, Martoglio B. Intramembrane proteolysis promotes trafficking of hepatitis C virus core protein to lipid droplets. EMBO J. 2002;21(15):3980-8. Epub 2002/07/30.

177. Pene V, Hernandez C, Vauloup-Fellous C, Garaud-Aunis J, Rosenberg AR. Sequential processing of hepatitis C virus core protein by host cell signal peptidase and signal peptide peptidase: a reassessment. J Viral Hepat. 2009;16(10):705-15. Epub 2009/03/14.

178. Matsumoto M, Hwang SB, Jeng KS, Zhu N, Lai MM. Homotypic interaction and multimerization of hepatitis C virus core protein. Virology. 1996;218(1):43-51. Epub 1996/04/01.

179. Nolandt O, Kern V, Muller H, Pfaff E, Theilmann L, Welker R, et al. Analysis of hepatitis C virus core protein interaction domains. J Gen Virol. 1997;78 (Pt 6):1331-40. Epub 1997/06/01.

180. Klein KC, Dellos SR, Lingappa JR. Identification of residues in the hepatitis C virus core protein that are critical for capsid assembly in a cell-free system. J Virol. 2005;79(11):6814-26. Epub 2005/05/14.

181. Fan Z, Yang QR, Twu JS, Sherker AH. Specific in vitro association between the hepatitis C viral genome and core protein. Journal of medical virology. 1999;59(2):131-4. Epub 1999/08/25.

182. Klein KC, Polyak SJ, Lingappa JR. Unique features of hepatitis C virus capsid formation revealed by de novo cell-free assembly. J Virol. 2004;78(17):9257-69. Epub 2004/08/17.

183. Shavinskaya A, Boulant S, Penin F, McLauchlan J, Bartenschlager R. The lipid droplet binding domain of hepatitis C virus core protein is a major determinant for efficient virus assembly. J Biol Chem. 2007;282(51):37158-69. Epub 2007/10/19.

184. Boulant S, Targett-Adams P, McLauchlan J. Disrupting the association of hepatitis C virus core protein with lipid droplets correlates with a loss in production of infectious virus. J Gen Virol. 2007;88(Pt 8):2204-13. Epub 2007/07/12.

185. Kunkel M, Lorinczi M, Rijnbrand R, Lemon SM, Watowich SJ. Self-assembly of nucleocapsid-like particles from recombinant hepatitis C virus core protein. Journal of virology. 2001;75(5):2119-29. Epub 2001/02/13.

186. Bukh J, Purcell RH, Miller RH. Sequence analysis of the core gene of 14 hepatitis C virus genotypes. Proceedings of the National Academy of Sciences of the United States of America. 1994;91(17):8239-43. Epub 1994/08/16.

187. Santolini E, Migliaccio G, La Monica N. Biosynthesis and biochemical properties of the hepatitis C virus core protein. Journal of virology. 1994;68(6):3631-41. Epub 1994/06/01.

188. Shimoike T, Mimori S, Tani H, Matsuura Y, Miyamura T. Interaction of hepatitis C virus core protein with viral sense RNA and suppression of its translation. Journal of virology. 1999;73(12):9718-25. Epub 1999/11/13.

189. Boulant S, Montserret R, Hope RG, Ratinier M, Targett-Adams P, Lavergne JP, et al. Structural determinants that target the hepatitis C virus core protein to lipid droplets. J Biol Chem. 2006;281(31):22236-47. Epub 2006/05/18.

190. Boulant S, Vanbelle C, Ebel C, Penin F, Lavergne JP. Hepatitis C virus core protein is a dimeric alpha-helical protein exhibiting membrane protein features. J Virol. 2005;79(17):11353-65. Epub 2005/08/17.

191. Duvignaud JB, Savard C, Fromentin R, Majeau N, Leclerc D, Gagne SM. Structure and dynamics of the N-terminal half of hepatitis C virus core protein: an intrinsically unstructured protein. Biochem Biophys Res Commun. 2009;378(1):27-31. Epub 2008/11/11.

192. Duvignaud JB, Leclerc D, Gagne SM. Structure and dynamics changes induced by 2,2,2-trifluoro-ethanol (TFE) on the N-terminal half of hepatitis C virus core protein. Biochemistry and cell biology = Biochimie et biologie cellulaire. 2010;88(2):315-23. Epub 2010/05/11.

193. Kushima Y, Wakita T, Hijikata M. A disulfide-bonded dimer of the core protein of hepatitis C virus is important for virus-like particle production. Journal of virology. 2010;84(18):9118-27. Epub 2010/07/02.

194. Suzuki R, Sakamoto S, Tsutsumi T, Rikimaru A, Tanaka K, Shimoike T, et al. Molecular determinants for subcellular localization of hepatitis C virus core protein. Journal of virology. 2005;79(2):1271-81. Epub 2004/12/23.

195. Schwer B, Ren S, Pietschmann T, Kartenbeck J, Kaehlcke K, Bartenschlager R, et al. Targeting of hepatitis C virus core protein to mitochondria through a novel C-terminal localization motif. Journal of virology. 2004;78(15):7958-68. Epub 2004/07/16.

196. Falcon V, Acosta-Rivero N, Chinea G, de la Rosa MC, Menendez I, Duenas-Carrera S, et al. Nuclear localization of nucleocapsid-like particles and HCV core protein in hepatocytes of a chronically HCV-infected patient. Biochem Biophys Res Commun. 2003;310(1):54-8. Epub 2003/09/27.

197. Cerutti A, Maillard P, Minisini R, Vidalain PO, Roohvand F, Pecheur EI, et al. Identification of a functional, CRM-1-dependent nuclear export signal in hepatitis C virus core protein. PloS one. 2011;6(10):e25854. Epub 2011/11/01.

198. Suzuki R, Matsuura Y, Suzuki T, Ando A, Chiba J, Harada S, et al. Nuclear localization of the truncated hepatitis C virus core protein with its hydrophobic C terminus deleted. J Gen Virol. 1995;76 (Pt 1):53-61. Epub 1995/01/01.

199. Ravaggi A, Natoli G, Primi D, Albertini A, Levrero M, Cariani E. Intracellular localization of full-length and truncated hepatitis C virus core protein expressed in mammalian cells. J Hepatol. 1994;20(6):833-6. Epub 1994/06/01.

200. Realdon S, Gerotto M, Dal Pero F, Marin O, Granato A, Basso G, et al. Proapoptotic effect of hepatitis C virus CORE protein in transiently transfected cells is enhanced by nuclear localization and is dependent on PKR activation. J Hepatol. 2004;40(1):77-85. Epub 2003/12/16.

201. Piccoli C, Quarato G, Ripoli M, D'Aprile A, Scrima R, Cela O, et al. HCV infection induces mitochondrial bioenergetic unbalance: causes and effects. Biochimica et biophysica acta. 2009;1787(5):539-46. Epub 2008/12/20.

202. Piccoli C, Scrima R, Quarato G, D'Aprile A, Ripoli M, Lecce L, et al. Hepatitis C virus protein expression causes calcium-mediated mitochondrial bioenergetic dysfunction and nitro-oxidative stress. Hepatology. 2007;46(1):58-65. Epub 2007/06/15.

203. Fournillier Jacob A, Cahour A, Escriou N, Girard M, Wychowski C. Processing of the E1 glycoprotein of hepatitis C virus expressed in mammalian cells. J Gen Virol. 1996;77 (Pt 5):1055-64. Epub 1996/05/01.

204. Grakoui A, Wychowski C, Lin C, Feinstone SM, Rice CM. Expression and identification of hepatitis C virus polyprotein cleavage products. J Virol. 1993;67(3):1385-95. Epub 1993/03/01.

205. Cocquerel L, Wychowski C, Minner F, Penin F, Dubuisson J. Charged residues in the transmembrane domains of hepatitis C virus glycoproteins play a major role in the processing, subcellular localization, and assembly of these envelope proteins. J Virol. 2000;74(8):3623-33. Epub 2000/03/23.

206. Dubuisson J. Folding, assembly and subcellular localization of hepatitis C virus glycoproteins. Curr Top Microbiol Immunol. 2000;242:135-48. Epub 1999/12/11.

207. Op De Beeck A, Montserret R, Duvet S, Cocquerel L, Cacan R, Barberot B, et al. The transmembrane domains of hepatitis C virus envelope glycoproteins E1 and E2 play a major role in heterodimerization. J Biol Chem. 2000;275(40):31428-37. Epub 2000/05/16.

208. Monne M, Nilsson I, Elofsson A, von Heijne G. Turns in transmembrane helices: determination of the minimal length of a "helical hairpin" and derivation of a fine-grained turn propensity scale. J Mol Biol. 1999;293(4):807-14. Epub 1999/11/02.

209. Reed KE, Rice CM. Molecular characterization of hepatitis C virus. Curr Stud Hematol Blood Transfus. 1998(62):1-37. Epub 1998/03/21.

210. Cocquerel L, Op de Beeck A, Lambot M, Roussel J, Delgrange D, Pillez A, et al. Topological changes in the transmembrane domains of hepatitis C virus envelope glycoproteins. EMBO J. 2002;21(12):2893-902. Epub 2002/06/18.

211. Clayton RF, Owsianka A, Aitken J, Graham S, Bhella D, Patel AH. Analysis of antigenicity and topology of E2 glycoprotein present on recombinant hepatitis C virus-like particles. Journal of virology. 2002;76(15):7672-82. Epub 2002/07/05.

212. Flint M, Maidens C, Loomis-Price LD, Shotton C, Dubuisson J, Monk P, et al. Characterization of hepatitis C virus E2 glycoprotein interaction with a putative cellular receptor, CD81. Journal of virology. 1999;73(8):6235-44. Epub 1999/07/10.

213. Owsianka AM, Timms JM, Tarr AW, Brown RJ, Hickling TP, Szwejk A, et al. Identification of conserved residues in the E2 envelope glycoprotein of the hepatitis C virus that are critical for CD81 binding. Journal of virology. 2006;80(17):8695-704. Epub 2006/08/17.

214. Owsianka A, Clayton RF, Loomis-Price LD, McKeating JA, Patel AH. Functional analysis of hepatitis C virus E2 glycoproteins and virus-like particles reveals structural dissimilarities between different forms of E2. J Gen Virol. 2001;82(Pt 8):1877-83. Epub 2001/07/18.

215. von Hahn T, Yoon JC, Alter H, Rice CM, Rehermann B, Balfe P, et al. Hepatitis C virus continuously escapes from neutralizing antibody and T-cell responses during chronic infection in vivo. Gastroenterology. 2007;132(2):667-78. Epub 2007/01/30.

216. Scarselli E, Ansuini H, Cerino R, Roccasecca RM, Acali S, Filocamo G, et al. The human scavenger receptor class B type I is a novel candidate receptor for the hepatitis C virus. EMBO J. 2002;21(19):5017-25. Epub 2002/10/03.

217. Lavillette D, Bartosch B, Nourrisson D, Verney G, Cosset FL, Penin F, et al. Hepatitis C virus glycoproteins mediate low pH-dependent membrane fusion with liposomes. J Biol Chem. 2006;281(7):3909-17. Epub 2005/12/17.

218. Lavillette D, Pecheur EI, Donot P, Fresquet J, Molle J, Corbau R, et al. Characterization of fusion determinants points to the involvement of three discrete regions of both E1 and E2 glycoproteins in the membrane fusion process of hepatitis C virus. Journal of virology. 2007;81(16):8752-65. Epub 2007/06/01.

219. Pless DD, Lennarz WJ. Enzymatic conversion of proteins to glycoproteins. Proceedings of the National Academy of Sciences of the United States of America. 1977;74(1):134-8. Epub 1977/01/01.

220. Dubuisson J, Duvet S, Meunier JC, Op De Beeck A, Cacan R, Wychowski C, et al. Glycosylation of the hepatitis C virus envelope protein E1 is dependent on the presence of a downstream sequence on the viral polyprotein. The Journal of biological chemistry. 2000;275(39):30605-9. Epub 2000/07/07.

221. Goffard A, Callens N, Bartosch B, Wychowski C, Cosset FL, Montpellier C, et al. Role of N-linked glycans in the functions of hepatitis C virus envelope glycoproteins. Journal of virology. 2005;79(13):8400-9. Epub 2005/06/16.

222. Helle F, Dubuisson J. Hepatitis C virus entry into host cells. Cell Mol Life Sci. 2008;65(1):100-12. Epub 2007/10/05.

223. Pavlovic D, Neville DC, Argaud O, Blumberg B, Dwek RA, Fischer WB, et al. The hepatitis C virus p7 protein forms an ion channel that is inhibited by long-alkyl-chain

iminosugar derivatives. Proceedings of the National Academy of Sciences of the United States of America. 2003;100(10):6104-8. Epub 2003/04/30.

224. Premkumar A, Wilson L, Ewart GD, Gage PW. Cation-selective ion channels formed by p7 of hepatitis C virus are blocked by hexamethylene amiloride. FEBS Lett. 2004;557(1-3):99-103. Epub 2004/01/27.

225. Gonzalez ME, Carrasco L. Viroporins. FEBS Lett. 2003;552(1):28-34. Epub 2003/09/16.

226. Ewart GD, Sutherland T, Gage PW, Cox GB. The Vpu protein of human immunodeficiency virus type 1 forms cation-selective ion channels. Journal of virology. 1996;70(10):7108-15. Epub 1996/10/01.

227. Lin C, Lindenbach BD, Pragai BM, McCourt DW, Rice CM. Processing in the hepatitis C virus E2-NS2 region: identification of p7 and two distinct E2-specific products with different C termini. Journal of virology. 1994;68(8):5063-73. Epub 1994/08/01.

228. Mizushima H, Hijikata M, Tanji Y, Kimura K, Shimotohno K. Analysis of N-terminal processing of hepatitis C virus nonstructural protein 2. Journal of virology. 1994;68(4):2731-4. Epub 1994/04/01.

229. Dubuisson J, Hsu HH, Cheung RC, Greenberg HB, Russell DG, Rice CM. Formation and intracellular localization of hepatitis C virus envelope glycoprotein complexes expressed by recombinant vaccinia and Sindbis viruses. Journal of virology. 1994;68(10):6147-60. Epub 1994/10/01.

230. Carrere-Kremer S, Montpellier C, Lorenzo L, Brulin B, Cocquerel L, Belouzard S, et al. Regulation of hepatitis C virus polyprotein processing by signal peptidase involves structural determinants at the p7 sequence junctions. The Journal of biological chemistry. 2004;279(40):41384-92. Epub 2004/07/13.

231. Haqshenas G, Mackenzie JM, Dong X, Gowans EJ. Hepatitis C virus p7 protein is localized in the endoplasmic reticulum when it is encoded by a replication-competent genome. J Gen Virol. 2007;88(Pt 1):134-42. Epub 2006/12/16.

232. Griffin SD, Harvey R, Clarke DS, Barclay WS, Harris M, Rowlands DJ. A conserved basic loop in hepatitis C virus p7 protein is required for amantadine-sensitive ion channel activity in mammalian cells but is dispensable for localization to mitochondria. J Gen Virol. 2004;85(Pt 2):451-61. Epub 2004/02/11.

233. Griffin S, Clarke D, McCormick C, Rowlands D, Harris M. Signal peptide cleavage and internal targeting signals direct the hepatitis C virus p7 protein to distinct intracellular membranes. Journal of virology. 2005;79(24):15525-36. Epub 2005/11/25.

234. Carrere-Kremer S, Montpellier-Pala C, Cocquerel L, Wychowski C, Penin F, Dubuisson J. Subcellular localization and topology of the p7 polypeptide of hepatitis C virus. Journal of virology. 2002;76(8):3720-30. Epub 2002/03/22.

235. Meshkat Z, Audsley M, Beyer C, Gowans EJ, Haqshenas G. Reverse genetic analysis of a putative, influenza virus M2 HXXXW-like motif in the p7 protein of hepatitis C virus. J Viral Hepat. 2009;16(3):187-94. Epub 2009/01/30.

236. Griffin SD, Beales LP, Clarke DS, Worsfold O, Evans SD, Jaeger J, et al. The p7 protein of hepatitis C virus forms an ion channel that is blocked by the antiviral drug, Amantadine. FEBS Lett. 2003;535(1-3):34-8. Epub 2003/02/01.

237. Patargias G, Zitzmann N, Dwek R, Fischer WB. Protein-protein interactions: modeling the hepatitis C virus ion channel p7. J Med Chem. 2006;49(2):648-55. Epub 2006/01/20.

238. Sakai A, Claire MS, Faulk K, Govindarajan S, Emerson SU, Purcell RH, et al. The p7 polypeptide of hepatitis C virus is critical for infectivity and contains functionally important genotype-specific sequences. Proceedings of the National Academy of Sciences of the United States of America. 2003;100(20):11646-51. Epub 2003/09/25.

239. Jones CT, Murray CL, Eastman DK, Tassello J, Rice CM. Hepatitis C virus p7 and NS2 proteins are essential for production of infectious virus. Journal of virology. 2007;81(16):8374-83. Epub 2007/06/01.

240. Lohmann V, Korner F, Koch J, Herian U, Theilmann L, Bartenschlager R. Replication of subgenomic hepatitis C virus RNAs in a hepatoma cell line. Science. 1999;285(5424):110-3. Epub 1999/07/03.

241. Brohm C, Steinmann E, Friesland M, Lorenz IC, Patel A, Penin F, et al. Characterization of determinants important for hepatitis C virus p7 function in morphogenesis by using trans-complementation. Journal of virology. 2009;83(22):11682-93. Epub 2009/09/04.

242. Steinmann E, Penin F, Kallis S, Patel AH, Bartenschlager R, Pietschmann T. Hepatitis C virus p7 protein is crucial for assembly and release of infectious virions. PLoS Pathog. 2007;3(7):e103. Epub 2007/07/31.

243. Griffin S, Stgelais C, Owsianka AM, Patel AH, Rowlands D, Harris M. Genotype-dependent sensitivity of hepatitis C virus to inhibitors of the p7 ion channel. Hepatology. 2008;48(6):1779-90. Epub 2008/10/02.

244. Grakoui A, McCourt DW, Wychowski C, Feinstone SM, Rice CM. A second hepatitis C virus-encoded proteinase. Proc Natl Acad Sci U S A. 1993;90(22):10583-7. Epub 1993/11/15.

245. Pieroni L, Santolini E, Fipaldini C, Pacini L, Migliaccio G, La Monica N. In vitro study of the NS2-3 protease of hepatitis C virus. Journal of virology. 1997;71(9):6373-80. Epub 1997/09/01.

246. Welbourn S, Pause A. The hepatitis C virus NS2/3 protease. Curr Issues Mol Biol. 2007;9(1):63-9. Epub 2007/02/01.

247. Schregel V, Jacobi S, Penin F, Tautz N. Hepatitis C virus NS2 is a protease stimulated by cofactor domains in NS3. Proceedings of the National Academy of Sciences of the United States of America. 2009;106(13):5342-7. Epub 2009/03/14.

248. Reed KE, Grakoui A, Rice CM. Hepatitis C virus-encoded NS2-3 protease: cleavage-site mutagenesis and requirements for bimolecular cleavage. Journal of virology. 1995;69(7):4127-36. Epub 1995/07/01.

249. Jirasko V, Montserret R, Lee JY, Gouttenoire J, Moradpour D, Penin F, et al. Structural and functional studies of nonstructural protein 2 of the hepatitis C virus reveal its key role as organizer of virion assembly. PLoS pathogens. 2010;6(12):e1001233. Epub 2010/12/29.

250. Lorenz IC, Marcotrigiano J, Dentzer TG, Rice CM. Structure of the catalytic domain of the hepatitis C virus NS2-3 protease. Nature. 2006;442(7104):831-5. Epub 2006/07/25.

251. Thibeault D, Maurice R, Pilote L, Lamarre D, Pause A. In vitro characterization of a purified NS2/3 protease variant of hepatitis C virus. J Biol Chem. 2001;276(49):46678-84. Epub 2001/10/10.

252. Love RA, Parge HE, Wickersham JA, Hostomsky Z, Habuka N, Moomaw EW, et al. The crystal structure of hepatitis C virus NS3 proteinase reveals a trypsin-like fold and a structural zinc binding site. Cell. 1996;87(2):331-42. Epub 1996/10/18.

253. Hijikata M, Mizushima H, Akagi T, Mori S, Kakiuchi N, Kato N, et al. Two distinct proteinase activities required for the processing of a putative nonstructural precursor protein of hepatitis C virus. Journal of virology. 1993;67(8):4665-75. Epub 1993/08/01.

254. Welbourn S, Green R, Gamache I, Dandache S, Lohmann V, Bartenschlager R, et al. Hepatitis C virus NS2/3 processing is required for NS3 stability and viral RNA replication. J Biol Chem. 2005;280(33):29604-11. Epub 2005/06/28.

255. Liu Q, Bhat RA, Prince AM, Zhang P. The hepatitis C virus NS2 protein generated by NS2-3 autocleavage is required for NS5A phosphorylation. Biochem Biophys Res Commun. 1999;254(3):572-7. Epub 1999/01/28.

256. Kaukinen P, Sillanpaa M, Kotenko S, Lin R, Hiscott J, Melen K, et al. Hepatitis C virus NS2 and NS3/4A proteins are potent inhibitors of host cell cytokine/chemokine gene expression. Virol J. 2006;3:66. Epub 2006/09/02.

257. Erdtmann L, Franck N, Lerat H, Le Seyec J, Gilot D, Cannie I, et al. The hepatitis C virus NS2 protein is an inhibitor of CIDE-B-induced apoptosis. The Journal of biological chemistry. 2003;278(20):18256-64. Epub 2003/02/22.

258. Yang XJ, Liu J, Ye L, Liao QJ, Wu JG, Gao JR, et al. HCV NS2 protein inhibits cell proliferation and induces cell cycle arrest in the S-phase in mammalian cells through down-regulation of cyclin A expression. Virus Res. 2006;121(2):134-43. Epub 2006/06/27.

259. Bartenschlager R, Ahlborn-Laake L, Mous J, Jacobsen H. Nonstructural protein 3 of the hepatitis C virus encodes a serine-type proteinase required for cleavage at the NS3/4 and NS4/5 junctions. Journal of virology. 1993;67(7):3835-44. Epub 1993/07/01.

260. Kim JL, Morgenstern KA, Lin C, Fox T, Dwyer MD, Landro JA, et al. Crystal structure of the hepatitis C virus NS3 protease domain complexed with a synthetic NS4A cofactor peptide. Cell. 1996;87(2):343-55. Epub 1996/10/18.

261. Yan Y, Li Y, Munshi S, Sardana V, Cole JL, Sardana M, et al. Complex of NS3 protease and NS4A peptide of BK strain hepatitis C virus: a 2.2 A resolution structure in a hexagonal crystal form. Protein Sci. 1998;7(4):837-47. Epub 1998/05/06.

262. Brass V, Berke JM, Montserret R, Blum HE, Penin F, Moradpour D. Structural determinants for membrane association and dynamic organization of the hepatitis C virus NS3-4A complex. Proceedings of the National Academy of Sciences of the United States of America. 2008;105(38):14545-50. Epub 2008/09/19.

263. Yao N, Reichert P, Taremi SS, Prosise WW, Weber PC. Molecular views of viral polyprotein processing revealed by the crystal structure of the hepatitis C virus bifunctional protease-helicase. Structure. 1999;7(11):1353-63. Epub 1999/11/27.

264. Raney KD, Sharma SD, Moustafa IM, Cameron CE. Hepatitis C virus non-structural protein 3 (HCV NS3): a multifunctional antiviral target. J Biol Chem. 2010;285(30):22725-31. Epub 2010/05/12.

265. Morikawa K, Lange CM, Gouttenoire J, Meylan E, Brass V, Penin F, et al. Nonstructural protein 3-4A: the Swiss army knife of hepatitis C virus. J Viral Hepat. 2011;18(5):305-15. Epub 2011/04/08.

266. Lin C, Kwong AD, Perni RB. Discovery and development of VX-950, a novel, covalent, and reversible inhibitor of hepatitis C virus NS3.4A serine protease. Infect Disord Drug Targets. 2006;6(1):3-16. Epub 2006/06/22.

267. Venkatraman S, Bogen SL, Arasappan A, Bennett F, Chen K, Jao E, et al. Discovery of (1R,5S)-N-[3-amino-1-(cyclobutylmethyl)-2,3-dioxopropyl]- 3-[2(S)-[[[(1,1-dimethylethyl)amino]carbonyl]amino]-3,3-dimethyl-1-oxobutyl]- 6,6-dimethyl-3-azabicyclo[3.1.0]hexan-2(S)-carboxamide (SCH 503034), a selective, potent, orally bioavailable hepatitis C virus NS3 protease inhibitor: a potential therapeutic agent for the treatment of hepatitis C infection. J Med Chem. 2006;49(20):6074-86. Epub 2006/09/29.

268. Prabu-Jeyabalan M, Nalivaika EA, King NM, Schiffer CA. Viability of a drug-resistant human immunodeficiency virus type 1 protease variant: structural insights for better antiviral therapy. Journal of virology. 2003;77(2):1306-15. Epub 2002/12/28.

269. Nalam MN, Schiffer CA. New approaches to HIV protease inhibitor drug design II: testing the substrate envelope hypothesis to avoid drug resistance and discover robust inhibitors. Curr Opin HIV AIDS. 2008;3(6):642-6. Epub 2009/04/18.

270. King NM, Prabu-Jeyabalan M, Nalivaika EA, Schiffer CA. Combating susceptibility to drug resistance: lessons from HIV-1 protease. Chem Biol. 2004;11(10):1333-8. Epub 2004/10/19.

271. Wolk B, Sansonno D, Krausslich HG, Dammacco F, Rice CM, Blum HE, et al. Subcellular localization, stability, and trans-cleavage competence of the hepatitis C virus NS3-NS4A complex expressed in tetracycline-regulated cell lines. Journal of virology. 2000;74(5):2293-304. Epub 2000/02/09.

272. Frick DN. The hepatitis C virus NS3 protein: a model RNA helicase and potential drug target. Curr Issues Mol Biol. 2007;9(1):1-20. Epub 2007/02/01.

273. Gu M, Rice CM. Three conformational snapshots of the hepatitis C virus NS3 helicase reveal a ratchet translocation mechanism. Proceedings of the National Academy of Sciences of the United States of America. 2010;107(2):521-8. Epub 2010/01/19.

274. Aizaki H, Lee KJ, Sung VM, Ishiko H, Lai MM. Characterization of the hepatitis C virus RNA replication complex associated with lipid rafts. Virology. 2004;324(2):450-61. Epub 2004/06/23.

275. Hugle T, Fehrmann F, Bieck E, Kohara M, Krausslich HG, Rice CM, et al. The hepatitis C virus nonstructural protein 4B is an integral endoplasmic reticulum membrane protein. Virology. 2001;284(1):70-81. Epub 2001/05/16.

276. Lundin M, Monne M, Widell A, Von Heijne G, Persson MA. Topology of the membrane-associated hepatitis C virus protein NS4B. J Virol. 2003;77(9):5428-38. Epub 2003/04/15.

277. Elazar M, Liu P, Rice CM, Glenn JS. An N-terminal amphipathic helix in hepatitis C virus (HCV) NS4B mediates membrane association, correct localization of replication

complex proteins, and HCV RNA replication. Journal of virology. 2004;78(20):11393-400. Epub 2004/09/29.

278. Gouttenoire J, Montserret R, Kennel A, Penin F, Moradpour D. An amphipathic alpha-helix at the C terminus of hepatitis C virus nonstructural protein 4B mediates membrane association. Journal of virology. 2009;83(21):11378-84. Epub 2009/08/21.

279. Gosert R, Egger D, Lohmann V, Bartenschlager R, Blum HE, Bienz K, et al. Identification of the hepatitis C virus RNA replication complex in Huh-7 cells harboring subgenomic replicons. J Virol. 2003;77(9):5487-92. Epub 2003/04/15.

280. Egger D, Wolk B, Gosert R, Bianchi L, Blum HE, Moradpour D, et al. Expression of hepatitis C virus proteins induces distinct membrane alterations including a candidate viral replication complex. Journal of virology. 2002;76(12):5974-84. Epub 2002/05/22.

281. Einav S, Elazar M, Danieli T, Glenn JS. A nucleotide binding motif in hepatitis C virus (HCV) NS4B mediates HCV RNA replication. Journal of virology. 2004;78(20):11288-95. Epub 2004/09/29.

282. Park JS, Yang JM, Min MK. Hepatitis C virus nonstructural protein NS4B transforms NIH3T3 cells in cooperation with the Ha-ras oncogene. Biochem Biophys Res Commun. 2000;267(2):581-7. Epub 2000/01/13.

283. Piccininni S, Varaklioti A, Nardelli M, Dave B, Raney KD, McCarthy JE. Modulation of the hepatitis C virus RNA-dependent RNA polymerase activity by the non-structural (NS) 3 helicase and the NS4B membrane protein. The Journal of biological chemistry. 2002;277(47):45670-9. Epub 2002/09/18.

284. Tellinghuisen TL, Marcotrigiano J, Gorbalenya AE, Rice CM. The NS5A protein of hepatitis C virus is a zinc metalloprotein. J Biol Chem. 2004;279(47):48576-87. Epub 2004/09/02.

285. Tanji Y, Kaneko T, Satoh S, Shimotohno K. Phosphorylation of hepatitis C virus-encoded nonstructural protein NS5A. J Virol. 1995;69(7):3980-6. Epub 1995/07/01.

286. Huang L, Hwang J, Sharma SD, Hargittai MR, Chen Y, Arnold JJ, et al. Hepatitis C virus nonstructural protein 5A (NS5A) is an RNA-binding protein. The Journal of biological chemistry. 2005;280(43):36417-28. Epub 2005/08/30.

287. Elazar M, Cheong KH, Liu P, Greenberg HB, Rice CM, Glenn JS. Amphipathic helix-dependent localization of NS5A mediates hepatitis C virus RNA replication. Journal of virology. 2003;77(10):6055-61. Epub 2003/04/30.

288. Ide Y, Zhang L, Chen M, Inchauspe G, Bahl C, Sasaguri Y, et al. Characterization of the nuclear localization signal and subcellular distribution of hepatitis C virus nonstructural protein NS5A. Gene. 1996;182(1-2):203-11. Epub 1996/12/05.

289. Tellinghuisen TL, Marcotrigiano J, Rice CM. Structure of the zinc-binding domain of an essential component of the hepatitis C virus replicase. Nature. 2005;435(7040):374-9. Epub 2005/05/20.

290. Liang Y, Ye H, Kang CB, Yoon HS. Domain 2 of nonstructural protein 5A (NS5A) of hepatitis C virus is natively unfolded. Biochemistry. 2007;46(41):11550-8. Epub 2007/09/21.

291. Tompa P. Intrinsically unstructured proteins. Trends Biochem Sci. 2002;27(10):527-33. Epub 2002/10/09.

292. Dyson HJ, Wright PE. Insights into the structure and dynamics of unfolded proteins from nuclear magnetic resonance. Adv Protein Chem. 2002;62:311-40. Epub 2002/11/07.

293. Pflugheber J, Fredericksen B, Sumpter R, Jr., Wang C, Ware F, Sodora DL, et al. Regulation of PKR and IRF-1 during hepatitis C virus RNA replication. Proceedings of the National Academy of Sciences of the United States of America. 2002;99(7):4650-5. Epub 2002/03/21.

294. Witherell GW, Beineke P. Statistical analysis of combined substitutions in nonstructural 5A region of hepatitis C virus and interferon response. J Med Virol. 2001;63(1):8-16. Epub 2000/12/29.

295. Pascu M, Martus P, Hohne M, Wiedenmann B, Hopf U, Schreier E, et al. Sustained virological response in hepatitis C virus type 1b infected patients is predicted by the number of mutations within the NS5A-ISDR: a meta-analysis focused on geographical differences. Gut. 2004;53(9):1345-51. Epub 2004/08/13.

296. Gale MJ, Jr., Korth MJ, Tang NM, Tan SL, Hopkins DA, Dever TE, et al. Evidence that hepatitis C virus resistance to interferon is mediated through repression of the PKR protein kinase by the nonstructural 5A protein. Virology. 1997;230(2):217-27. Epub 1997/04/14.

297. Tellinghuisen TL, Foss KL, Treadaway JC, Rice CM. Identification of residues required for RNA replication in domains II and III of the hepatitis C virus NS5A protein. Journal of virology. 2008;82(3):1073-83. Epub 2007/11/23.

298. Hanoulle X, Verdegem D, Badillo A, Wieruszeski JM, Penin F, Lippens G. Domain 3 of non-structural protein 5A from hepatitis C virus is natively unfolded. Biochem Biophys Res Commun. 2009;381(4):634-8. Epub 2009/03/03.

299. Appel N, Pietschmann T, Bartenschlager R. Mutational analysis of hepatitis C virus nonstructural protein 5A: potential role of differential phosphorylation in RNA replication and identification of a genetically flexible domain. Journal of virology. 2005;79(5):3187-94. Epub 2005/02/15.

300. Lohmann V, Hoffmann S, Herian U, Penin F, Bartenschlager R. Viral and cellular determinants of hepatitis C virus RNA replication in cell culture. Journal of virology. 2003;77(5):3007-19. Epub 2003/02/14.

301. Neddermann P, Quintavalle M, Di Pietro C, Clementi A, Cerretani M, Altamura S, et al. Reduction of hepatitis C virus NS5A hyperphosphorylation by selective inhibition of cellular kinases activates viral RNA replication in cell culture. J Virol. 2004;78(23):13306-14. Epub 2004/11/16.

302. Tan SL, Nakao H, He Y, Vijaysri S, Neddermann P, Jacobs BL, et al. NS5A, a nonstructural protein of hepatitis C virus, binds growth factor receptor-bound protein 2 adaptor protein in a Src homology 3 domain/ligand-dependent manner and perturbs mitogenic signaling. Proceedings of the National Academy of Sciences of the United States of America. 1999;96(10):5533-8. Epub 1999/05/13.

303. Macdonald A, Crowder K, Street A, McCormick C, Saksela K, Harris M. The hepatitis C virus non-structural NS5A protein inhibits activating protein-1 function by perturbing ras-ERK pathway signaling. The Journal of biological chemistry. 2003;278(20):17775-84. Epub 2003/03/07.

304. Majumder M, Ghosh AK, Steele R, Zhou XY, Phillips NJ, Ray R, et al. Hepatitis C virus NS5A protein impairs TNF-mediated hepatic apoptosis, but not by an anti-FAS antibody, in transgenic mice. Virology. 2002;294(1):94-105. Epub 2002/03/12.

305. Miyasaka Y, Enomoto N, Kurosaki M, Sakamoto N, Kanazawa N, Kohashi T, et al. Hepatitis C virus nonstructural protein 5A inhibits tumor necrosis factor-alpha-mediated apoptosis in Huh7 cells. J Infect Dis. 2003;188(10):1537-44. Epub 2003/11/19.

306. Chung YL, Sheu ML, Yen SH. Hepatitis C virus NS5A as a potential viral Bcl-2 homologue interacts with Bax and inhibits apoptosis in hepatocellular carcinoma. International journal of cancer Journal international du cancer. 2003;107(1):65-73. Epub 2003/08/20.

307. Lan KH, Sheu ML, Hwang SJ, Yen SH, Chen SY, Wu JC, et al. HCV NS5A interacts with p53 and inhibits p53-mediated apoptosis. Oncogene. 2002;21(31):4801-11. Epub 2002/07/09.

308. He Y, Nakao H, Tan SL, Polyak SJ, Neddermann P, Vijaysri S, et al. Subversion of cell signaling pathways by hepatitis C virus nonstructural 5A protein via interaction with Grb2 and P85 phosphatidylinositol 3-kinase. Journal of virology. 2002;76(18):9207-17. Epub 2002/08/21.

309. Street A, Macdonald A, Crowder K, Harris M. The Hepatitis C virus NS5A protein activates a phosphoinositide 3-kinase-dependent survival signaling cascade. The Journal of biological chemistry. 2004;279(13):12232-41. Epub 2004/01/08.

310. Behrens SE, Tomei L, De Francesco R. Identification and properties of the RNA-dependent RNA polymerase of hepatitis C virus. EMBO J. 1996;15(1):12-22. Epub 1996/01/02.

311. Hwang SB, Park KJ, Kim YS, Sung YC, Lai MM. Hepatitis C virus NS5B protein is a membrane-associated phosphoprotein with a predominantly perinuclear localization. Virology. 1997;227(2):439-46. Epub 1997/01/20.

312. Ago H, Adachi T, Yoshida A, Yamamoto M, Habuka N, Yatsunami K, et al. Crystal structure of the RNA-dependent RNA polymerase of hepatitis C virus. Structure. 1999;7(11):1417-26. Epub 1999/11/27.

313. Koonin EV, Mushegian AR, Ryabov EV, Dolja VV. Diverse groups of plant RNA and DNA viruses share related movement proteins that may possess chaperone-like activity. J Gen Virol. 1991;72 (Pt 12):2895-903. Epub 1991/12/01.

314. Lesburg CA, Cable MB, Ferrari E, Hong Z, Mannarino AF, Weber PC. Crystal structure of the RNA-dependent RNA polymerase from hepatitis C virus reveals a fully encircled active site. Nat Struct Biol. 1999;6(10):937-43. Epub 1999/10/03.

315. Gao G, Orlova M, Georgiadis MM, Hendrickson WA, Goff SP. Conferring RNA polymerase activity to a DNA polymerase: a single residue in reverse transcriptase controls substrate selection. Proceedings of the National Academy of Sciences of the United States of America. 1997;94(2):407-11. Epub 1997/01/21.

316. Beese LS, Steitz TA. Structural basis for the 3'-5' exonuclease activity of Escherichia coli DNA polymerase I: a two metal ion mechanism. EMBO J. 1991;10(1):25-33. Epub 1991/01/01.

317. Bressanelli S, Tomei L, Roussel A, Incitti I, Vitale RL, Mathieu M, et al. Crystal structure of the RNA-dependent RNA polymerase of hepatitis C virus. Proceedings of the National Academy of Sciences of the United States of America. 1999;96(23):13034-9. Epub 1999/11/11.

318. Hansen JL, Long AM, Schultz SC. Structure of the RNA-dependent RNA polymerase of poliovirus. Structure. 1997;5(8):1109-22. Epub 1997/08/15.

319. Schmidt-Mende J, Bieck E, Hugle T, Penin F, Rice CM, Blum HE, et al. Determinants for membrane association of the hepatitis C virus RNA-dependent RNA polymerase. The Journal of biological chemistry. 2001;276(47):44052-63. Epub 2001/09/15.

320. Ivashkina N, Wolk B, Lohmann V, Bartenschlager R, Blum HE, Penin F, et al. The hepatitis C virus RNA-dependent RNA polymerase membrane insertion sequence is a transmembrane segment. Journal of virology. 2002;76(24):13088-93. Epub 2002/11/20.

321. Moradpour D, Brass V, Bieck E, Friebe P, Gosert R, Blum HE, et al. Membrane association of the RNA-dependent RNA polymerase is essential for hepatitis C virus RNA replication. Journal of virology. 2004;78(23):13278-84. Epub 2004/11/16.

322. Lyle JM, Bullitt E, Bienz K, Kirkegaard K. Visualization and functional analysis of RNA-dependent RNA polymerase lattices. Science. 2002;296(5576):2218-22. Epub 2002/06/22.

323. Schwartz M, Chen J, Janda M, Sullivan M, den Boon J, Ahlquist P. A positive-strand RNA virus replication complex parallels form and function of retrovirus capsids. Mol Cell. 2002;9(3):505-14. Epub 2002/04/05.

324. Wu SX, Ahlquist P, Kaesberg P. Active complete in vitro replication of nodavirus RNA requires glycerophospholipid. Proceedings of the National Academy of Sciences of the United States of America. 1992;89(23):11136-40. Epub 1992/12/01.

325. Shi ST, Lee KJ, Aizaki H, Hwang SB, Lai MM. Hepatitis C virus RNA replication occurs on a detergent-resistant membrane that cofractionates with caveolin-2. Journal of virology. 2003;77(7):4160-8. Epub 2003/03/14.

326. Wang C, Gale M, Jr., Keller BC, Huang H, Brown MS, Goldstein JL, et al. Identification of FBL2 as a geranylgeranylated cellular protein required for hepatitis C virus RNA replication. Mol Cell. 2005;18(4):425-34. Epub 2005/05/17.

327. Tu H, Gao L, Shi ST, Taylor DR, Yang T, Mircheff AK, et al. Hepatitis C virus RNA polymerase and NS5A complex with a SNARE-like protein. Virology. 1999;263(1):30-41. Epub 1999/11/02.

328. Gao L, Aizaki H, He JW, Lai MM. Interactions between viral nonstructural proteins and host protein hVAP-33 mediate the formation of hepatitis C virus RNA replication complex on lipid raft. Journal of virology. 2004;78(7):3480-8. Epub 2004/03/16.

329. Reiss S, Rebhan I, Backes P, Romero-Brey I, Erfle H, Matula P, et al. Recruitment and activation of a lipid kinase by hepatitis C virus NS5A is essential for integrity of the membranous replication compartment. Cell Host Microbe. 2011;9(1):32-45. Epub 2011/01/18.

330. Amako Y, Sarkeshik A, Hotta H, Yates J, 3rd, Siddiqui A. Role of oxysterol binding protein in hepatitis C virus infection. Journal of virology. 2009;83(18):9237-46. Epub 2009/07/03.

331. Okamoto T, Nishimura Y, Ichimura T, Suzuki K, Miyamura T, Suzuki T, et al. Hepatitis C virus RNA replication is regulated by FKBP8 and Hsp90. EMBO J. 2006;25(20):5015-25. Epub 2006/10/07.

332. Kaul A, Stauffer S, Berger C, Pertel T, Schmitt J, Kallis S, et al. Essential role of cyclophilin A for hepatitis C virus replication and virus production and possible link to polyprotein cleavage kinetics. PLoS Pathog. 2009;5(8):e1000546. Epub 2009/08/15.

333. Bartenschlager R, Cosset FL, Lohmann V. Hepatitis C virus replication cycle. J Hepatol. 2010;53(3):583-5. Epub 2010/06/29.

334. Thomssen R, Bonk S, Propfe C, Heermann KH, Kochel HG, Uy A. Association of hepatitis C virus in human sera with beta-lipoprotein. Medical microbiology and immunology. 1992;181(5):293-300. Epub 1992/01/01.

335. Thomssen R, Bonk S, Thiele A. Density heterogeneities of hepatitis C virus in human sera due to the binding of beta-lipoproteins and immunoglobulins. Med Microbiol Immunol. 1993;182(6):329-34. Epub 1993/12/01.

336. Bradley D, McCaustland K, Krawczynski K, Spelbring J, Humphrey C, Cook EH. Hepatitis C virus: buoyant density of the factor VIII-derived isolate in sucrose. J Med Virol. 1991;34(3):206-8. Epub 1991/07/01.

337. Molina S, Castet V, Fournier-Wirth C, Pichard-Garcia L, Avner R, Harats D, et al. The low-density lipoprotein receptor plays a role in the infection of primary human hepatocytes by hepatitis C virus. J Hepatol. 2007;46(3):411-9. Epub 2006/12/13.

338. Albecka A, Belouzard S, Op de Beeck A, Descamps V, Goueslain L, Bertrand-Michel J, et al. Role of low-density lipoprotein receptor in the hepatitis C virus life cycle. Hepatology. 2012;55(4):998-1007. Epub 2011/11/29.

339. Agnello V, Abel G, Elfahal M, Knight GB, Zhang QX. Hepatitis C virus and other flaviviridae viruses enter cells via low density lipoprotein receptor. Proceedings of the National Academy of Sciences of the United States of America. 1999;96(22):12766-71. Epub 1999/10/27.

340. Monazahian M, Bohme I, Bonk S, Koch A, Scholz C, Grethe S, et al. Low density lipoprotein receptor as a candidate receptor for hepatitis C virus. J Med Virol. 1999;57(3):223-9. Epub 1999/02/18.

341. Bartosch B, Vitelli A, Granier C, Goujon C, Dubuisson J, Pascale S, et al. Cell entry of hepatitis C virus requires a set of co-receptors that include the CD81 tetraspanin and the SR-B1 scavenger receptor. The Journal of biological chemistry. 2003;278(43):41624-30. Epub 2003/08/13.

342. Lavillette D, Morice Y, Germanidis G, Donot P, Soulier A, Pagkalos E, et al. Human serum facilitates hepatitis C virus infection, and neutralizing responses inversely correlate with viral replication kinetics at the acute phase of hepatitis C virus infection. J Virol. 2005;79(10):6023-34. Epub 2005/04/29.

343. Lavillette D, Tarr AW, Voisset C, Donot P, Bartosch B, Bain C, et al. Characterization of host-range and cell entry properties of the major genotypes and subtypes of hepatitis C virus. Hepatology. 2005;41(2):265-74. Epub 2005/01/22.

344. Catanese MT, Graziani R, von Hahn T, Moreau M, Huby T, Paonessa G, et al. High-avidity monoclonal antibodies against the human scavenger class B type I receptor efficiently block hepatitis C virus infection in the presence of high-density lipoprotein. Journal of virology. 2007;81(15):8063-71. Epub 2007/05/18.

345. Barth H, Schafer C, Adah MI, Zhang F, Linhardt RJ, Toyoda H, et al. Cellular binding of hepatitis C virus envelope glycoprotein E2 requires cell surface heparan sulfate. The Journal of biological chemistry. 2003;278(42):41003-12. Epub 2003/07/18.

346. Barth H, Schnober EK, Zhang F, Linhardt RJ, Depla E, Boson B, et al. Viral and cellular determinants of the hepatitis C virus envelope-heparan sulfate interaction. Journal of virology. 2006;80(21):10579-90. Epub 2006/08/25.

347. Basu A, Kanda T, Beyene A, Saito K, Meyer K, Ray R. Sulfated homologues of heparin inhibit hepatitis C virus entry into mammalian cells. Journal of virology. 2007;81(8):3933-41. Epub 2007/02/09.

348. Maillard P, Walic M, Meuleman P, Roohvand F, Huby T, Le Goff W, et al. Lipoprotein lipase inhibits hepatitis C virus (HCV) infection by blocking virus cell entry. PloS one. 2011;6(10):e26637. Epub 2011/11/01.

349. Barba G, Harper F, Harada T, Kohara M, Goulinet S, Matsuura Y, et al. Hepatitis C virus core protein shows a cytoplasmic localization and associates to cellular lipid storage droplets. Proceedings of the National Academy of Sciences of the United States of America. 1997;94(4):1200-5. Epub 1997/02/18.

350. Rouille Y, Helle F, Delgrange D, Roingeard P, Voisset C, Blanchard E, et al. Subcellular localization of hepatitis C virus structural proteins in a cell culture system that efficiently replicates the virus. J Virol. 2006;80(6):2832-41. Epub 2006/02/28.

351. Asselah T, Rubbia-Brandt L, Marcellin P, Negro F. Steatosis in chronic hepatitis C: why does it really matter? Gut. 2006;55(1):123-30. Epub 2005/12/14.

352. Miyamoto H, Okamoto H, Sato K, Tanaka T, Mishiro S. Extraordinarily low density of hepatitis C virus estimated by sucrose density gradient centrifugation and the polymerase chain reaction. J Gen Virol. 1992;73 (Pt 3):715-8. Epub 1992/03/01.

353. Kanto T, Hayashi N, Takehara T, Hagiwara H, Mita E, Naito M, et al. Buoyant density of hepatitis C virus recovered from infected hosts: two different features in sucrose equilibrium density-gradient centrifugation related to degree of liver inflammation. Hepatology. 1994;19(2):296-302. Epub 1994/02/01.

354. Carrick RJ, Schlauder GG, Peterson DA, Mushahwar IK. Examination of the buoyant density of hepatitis C virus by the polymerase chain reaction. J Virol Methods. 1992;39(3):279-89. Epub 1992/09/01.

355. Choo SH, So HS, Cho JM, Ryu WS. Association of hepatitis C virus particles with immunoglobulin: a mechanism for persistent infection. J Gen Virol. 1995;76 (Pt 9):2337-41. Epub 1995/09/01.

356. Hijikata M, Shimizu YK, Kato H, Iwamoto A, Shih JW, Alter HJ, et al. Equilibrium centrifugation studies of hepatitis C virus: evidence for circulating immune complexes. Journal of virology. 1993;67(4):1953-8. Epub 1993/04/01.

357. Kanto T, Hayashi N, Takehara T, Hagiwara H, Mita E, Oshita M, et al. Serial density analysis of hepatitis C virus particle populations in chronic hepatitis C patients treated with interferon-alpha. Journal of medical virology. 1995;46(3):230-7. Epub 1995/07/01.

358. Pumeechockchai W, Bevitt D, Agarwal K, Petropoulou T, Langer BC, Belohradsky B, et al. Hepatitis C virus particles of different density in the blood of chronically infected immunocompetent and immunodeficient patients: Implications for virus clearance by antibody. J Med Virol. 2002;68(3):335-42. Epub 2002/09/13.

359. Hoofnagle AN, Heinecke JW. Lipoproteomics: using mass spectrometry-based proteomics to explore the assembly, structure, and function of lipoproteins. Journal of lipid research. 2009;50(10):1967-75. Epub 2009/09/10.

360. Mahley RW, Innerarity TL, Rall SC, Jr., Weisgraber KH. Plasma lipoproteins: apolipoprotein structure and function. Journal of lipid research. 1984;25(12):1277-94. Epub 1984/12/01.

361. Salter AM, Brindley DN. The biochemistry of lipoproteins. J Inherit Metab Dis. 1988;11 Suppl 1:4-17. Epub 1988/01/01.

362. Xiao C, Hsieh J, Adeli K, Lewis GF. Gut-liver interaction in triglyceride-rich lipoprotein metabolism. American journal of physiology Endocrinology and metabolism. 2011;301(3):E429-46. Epub 2011/06/23.

363. Mjos OD, Faergeman O, Hamilton RL, Havel RJ. Characterization of remnants produced during the metabolism of triglyceride-rich lipoproteins of blood plasma and intestinal lymph in the rat. J Clin Invest. 1975;56(3):603-15. Epub 1975/09/01.

364. Chappell DA, Medh JD. Receptor-mediated mechanisms of lipoprotein remnant catabolism. Progress in lipid research. 1998;37(6):393-422. Epub 1999/04/21.

365. Goodman DS. Cholesterol ester metabolism. Physiol Rev. 1965;45(4):747-839. Epub 1965/10/01.

366. French JE, Morris B, Robinson DS. Removal of lipids from the blood stream. Br Med Bull. 1958;14(3):234-8. Epub 1958/09/01.

367. Bragdon JH, Gordon RS, Jr. Tissue distribution of C14 after the intravenous injection of labeled chylomicrons and unesterified fatty acids in the rat. J Clin Invest. 1958;37(4):574-8. Epub 1958/04/01.

368. Hussain MM, Mahley RW, Boyles JK, Lindquist PA, Brecht WJ, Innerarity TL. Chylomicron metabolism. Chylomicron uptake by bone marrow in different animal species. The Journal of biological chemistry. 1989;264(30):17931-8. Epub 1989/10/25.

369. Olivecrona T, Belfrage P. Mechanisms for Removal of Chyle Triglyceride from the Circulating Blood as Studied with (14c)Glycerol and (3h)Palmitic Acid- Labeled Chyle. Biochimica et biophysica acta. 1965;98:81-93. Epub 1965/02/01.

370. Fraser R, Dobbs BR, Rogers GW. Lipoproteins and the liver sieve: the role of the fenestrated sinusoidal endothelium in lipoprotein metabolism, atherosclerosis, and cirrhosis. Hepatology. 1995;21(3):863-74. Epub 1995/03/01.

371. Wisse E, De Zanger RB, Charels K, Van Der Smissen P, McCuskey RS. The liver sieve: considerations concerning the structure and function of endothelial fenestrae, the sinusoidal wall and the space of Disse. Hepatology. 1985;5(4):683-92. Epub 1985/07/01.

372. Knott TJ, Wallis SC, Robertson ME, Priestley LM, Urdea M, Rall LB, et al. The human apolipoprotein AII gene: structural organization and sites of expression. Nucleic Acids Res. 1985;13(17):6387-98. Epub 1985/09/11.

373. Boren J, Lee I, Zhu W, Arnold K, Taylor S, Innerarity TL. Identification of the low density lipoprotein receptor-binding site in apolipoprotein B100 and the modulation of its binding activity by the carboxyl terminus in familial defective apo-B100. J Clin Invest. 1998;101(5):1084-93. Epub 1998/04/16.

374. Herz J, Hamann U, Rogne S, Myklebost O, Gausepohl H, Stanley KK. Surface location and high affinity for calcium of a 500-kd liver membrane protein closely related to the LDL-receptor suggest a physiological role as lipoprotein receptor. EMBO J. 1988;7(13):4119-27. Epub 1988/12/20.

375. Kanto T, Hayashi N, Takehara T, Hagiwara H, Mita E, Naito M, et al. Density analysis of hepatitis C virus particle population in the circulation of infected hosts: implications for virus neutralization or persistence. J Hepatol. 1995;22(4):440-8. Epub 1995/04/01.

376. Ishida S, Kaito M, Kohara M, Tsukiyama-Kohora K, Fujita N, Ikoma J, et al. Hepatitis C virus core particle detected by immunoelectron microscopy and optical rotation technique. Hepatol Res. 2001;20(3):335-47. Epub 2001/06/19.

377. Trestard A, Bacq Y, Buzelay L, Dubois F, Barin F, Goudeau A, et al. Ultrastructural and physicochemical characterization of the hepatitis C virus recovered from the serum of an agammaglobulinemic patient. Arch Virol. 1998;143(11):2241-5. Epub 1998/12/18.

378. Maillard P, Krawczynski K, Nitkiewicz J, Bronnert C, Sidorkiewicz M, Gounon P, et al. Nonenveloped nucleocapsids of hepatitis C virus in the serum of infected patients. Journal of virology. 2001;75(17):8240-50. Epub 2001/08/03.

379. Okada K, Takishita Y, Shimomura H, Tsuji T, Miyamura T, Kuhara T, et al. Detection of hepatitis C virus core protein in the glomeruli of patients with membranous glomerulonephritis. Clinical nephrology. 1996;45(2):71-6. Epub 1996/02/01.

380. Andre P, Komurian-Pradel F, Deforges S, Perret M, Berland JL, Sodoyer M, et al. Characterization of low- and very-low-density hepatitis C virus RNA-containing particles. Journal of virology. 2002;76(14):6919-28. Epub 2002/06/20.

381. Diaz O, Delers F, Maynard M, Demignot S, Zoulim F, Chambaz J, et al. Preferential association of Hepatitis C virus with apolipoprotein B48-containing lipoproteins. J Gen Virol. 2006;87(Pt 10):2983-91. Epub 2006/09/12.

382. Deforges S, Evlashev A, Perret M, Sodoyer M, Pouzol S, Scoazec JY, et al. Expression of hepatitis C virus proteins in epithelial intestinal cells in vivo. J Gen Virol. 2004;85(Pt 9):2515-23. Epub 2004/08/11.

383. Chang KS, Jiang J, Cai Z, Luo G. Human apolipoprotein e is required for infectivity and production of hepatitis C virus in cell culture. Journal of virology. 2007;81(24):13783-93. Epub 2007/10/05.

384. Lindenbach BD, Meuleman P, Ploss A, Vanwolleghem T, Syder AJ, McKeating JA, et al. Cell culture-grown hepatitis C virus is infectious in vivo and can be recultured in vitro. Proc Natl Acad Sci U S A. 2006;103(10):3805-9. Epub 2006/02/18.

385. Bartenschlager R, Penin F, Lohmann V, Andre P. Assembly of infectious hepatitis C virus particles. Trends Microbiol. 2011;19(2):95-103. Epub 2010/12/15.

386. Drummer HE, Wilson KA, Poumbourios P. Determinants of CD81 dimerization and interaction with hepatitis C virus glycoprotein E2. Biochem Biophys Res Commun. 2005;328(1):251-7. Epub 2005/01/27.

387. Petracca R, Falugi F, Galli G, Norais N, Rosa D, Campagnoli S, et al. Structure-function analysis of hepatitis C virus envelope-CD81 binding. Journal of virology. 2000;74(10):4824-30. Epub 2000/04/25.

388. Pileri P, Uematsu Y, Campagnoli S, Galli G, Falugi F, Petracca R, et al. Binding of hepatitis C virus to CD81. Science. 1998;282(5390):938-41. Epub 1998/10/30.

389. Cormier EG, Tsamis F, Kajumo F, Durso RJ, Gardner JP, Dragic T. CD81 is an entry coreceptor for hepatitis C virus. Proceedings of the National Academy of Sciences of the United States of America. 2004;101(19):7270-4. Epub 2004/05/05.

390. Zhang J, Randall G, Higginbottom A, Monk P, Rice CM, McKeating JA. CD81 is required for hepatitis C virus glycoprotein-mediated viral infection. Journal of virology. 2004;78(3):1448-55. Epub 2004/01/15.

391. Hsu M, Zhang J, Flint M, Logvinoff C, Cheng-Mayer C, Rice CM, et al. Hepatitis C virus glycoproteins mediate pH-dependent cell entry of pseudotyped retroviral particles. Proceedings of the National Academy of Sciences of the United States of America. 2003;100(12):7271-6. Epub 2003/05/23.

392. Drummer HE, Wilson KA, Poumbourios P. Identification of the hepatitis C virus E2 glycoprotein binding site on the large extracellular loop of CD81. Journal of virology. 2002;76(21):11143-7. Epub 2002/10/09.

393. Brazzoli M, Bianchi A, Filippini S, Weiner A, Zhu Q, Pizza M, et al. CD81 is a central regulator of cellular events required for hepatitis C virus infection of human hepatocytes. Journal of virology. 2008;82(17):8316-29. Epub 2008/06/27.

394. Lupberger J, Zeisel MB, Xiao F, Thumann C, Fofana I, Zona L, et al. EGFR and EphA2 are host factors for hepatitis C virus entry and possible targets for antiviral therapy. Nat Med. 2011;17(5):589-95. Epub 2011/04/26.

395. Rosa D, Saletti G, De Gregorio E, Zorat F, Comar C, D'Oro U, et al. Activation of naive B lymphocytes via CD81, a pathogenetic mechanism for hepatitis C virus-associated B lymphocyte disorders. Proceedings of the National Academy of Sciences of the United States of America. 2005;102(51):18544-9. Epub 2005/12/13.

396. Machida K, Cheng KT, Pavio N, Sung VM, Lai MM. Hepatitis C virus E2-CD81 interaction induces hypermutation of the immunoglobulin gene in B cells. Journal of virology. 2005;79(13):8079-89. Epub 2005/06/16.

397. Connelly MA, Williams DL. SR-BI and cholesterol uptake into steroidogenic cells. Trends Endocrinol Metab. 2003;14(10):467-72. Epub 2003/12/03.

398. Murao K, Imachi H, Yu X, Cao WM, Nishiuchi T, Chen K, et al. Interferon alpha decreases expression of human scavenger receptor class BI, a possible HCV receptor in hepatocytes. Gut. 2008;57(5):664-71. Epub 2007/11/14.

399. Bartosch B, Verney G, Dreux M, Donot P, Morice Y, Penin F, et al. An interplay between hypervariable region 1 of the hepatitis C virus E2 glycoprotein, the scavenger receptor BI, and high-density lipoprotein promotes both enhancement of infection and protection against neutralizing antibodies. Journal of virology. 2005;79(13):8217-29. Epub 2005/06/16.

400. von Hahn T, Lindenbach BD, Boullier A, Quehenberger O, Paulson M, Rice CM, et al. Oxidized low-density lipoprotein inhibits hepatitis C virus cell entry in human hepatoma cells. Hepatology. 2006;43(5):932-42. Epub 2006/04/22.

401. Bernfield M, Gotte M, Park PW, Reizes O, Fitzgerald ML, Lincecum J, et al. Functions of cell surface heparan sulfate proteoglycans. Annu Rev Biochem. 1999;68:729-77. Epub 2000/06/29.

402. Esko JD, Lindahl U. Molecular diversity of heparan sulfate. J Clin Invest. 2001;108(2):169-73. Epub 2001/07/18.

403. Jiang J, Cun W, Wu X, Shi Q, Tang H, Luo G. Hepatitis C virus attachment mediated by apolipoprotein E binding to cell surface heparan sulfate. Journal of virology. 2012;86(13):7256-67. Epub 2012/04/26.

404. Feinberg H, Mitchell DA, Drickamer K, Weis WI. Structural basis for selective recognition of oligosaccharides by DC-SIGN and DC-SIGNR. Science. 2001;294(5549):2163-6. Epub 2001/12/12.

405. Figdor CG, van Kooyk Y, Adema GJ. C-type lectin receptors on dendritic cells and Langerhans cells. Nat Rev Immunol. 2002;2(2):77-84. Epub 2002/03/26.

406. Curtis BM, Scharnowske S, Watson AJ. Sequence and expression of a membrane-associated C-type lectin that exhibits CD4-independent binding of human immunodeficiency virus envelope glycoprotein gp120. Proceedings of the National Academy of Sciences of the United States of America. 1992;89(17):8356-60. Epub 1992/09/01.

407. Geijtenbeek TB, Kwon DS, Torensma R, van Vliet SJ, van Duijnhoven GC, Middel J, et al. DC-SIGN, a dendritic cell-specific HIV-1-binding protein that enhances trans-infection of T cells. Cell. 2000;100(5):587-97. Epub 2000/03/18.

408. Gardner JP, Durso RJ, Arrigale RR, Donovan GP, Maddon PJ, Dragic T, et al. L-SIGN (CD 209L) is a liver-specific capture receptor for hepatitis C virus. Proceedings of the National Academy of Sciences of the United States of America. 2003;100(8):4498-503. Epub 2003/04/05.

409. Lozach PY, Lortat-Jacob H, de Lacroix de Lavalette A, Staropoli I, Foung S, Amara A, et al. DC-SIGN and L-SIGN are high affinity binding receptors for hepatitis C virus glycoprotein E2. The Journal of biological chemistry. 2003;278(22):20358-66. Epub 2003/03/01.

410. Bartosch B, Dubuisson J. Recent advances in hepatitis C virus cell entry. Viruses. 2010;2(3):692-709. Epub 2010/03/01.

411. Evans MJ, von Hahn T, Tscherne DM, Syder AJ, Panis M, Wolk B, et al. Claudin-1 is a hepatitis C virus co-receptor required for a late step in entry. Nature. 2007;446(7137):801-5. Epub 2007/02/28.

412. Zheng A, Yuan F, Li Y, Zhu F, Hou P, Li J, et al. Claudin-6 and claudin-9 function as additional coreceptors for hepatitis C virus. J Virol. 2007;81(22):12465-71. Epub 2007/09/07.

413. Furuse M, Fujita K, Hiiragi T, Fujimoto K, Tsukita S. Claudin-1 and -2: novel integral membrane proteins localizing at tight junctions with no sequence similarity to occludin. J Cell Biol. 1998;141(7):1539-50. Epub 1998/07/01.

414. Hewitt KJ, Agarwal R, Morin PJ. The claudin gene family: expression in normal and neoplastic tissues. BMC Cancer. 2006;6:186. Epub 2006/07/14.

415. Krause G, Winkler L, Mueller SL, Haseloff RF, Piontek J, Blasig IE. Structure and function of claudins. Biochimica et biophysica acta. 2008;1778(3):631-45. Epub 2007/11/27.

416. Colegio OR, Van Itallie CM, McCrea HJ, Rahner C, Anderson JM. Claudins create charge-selective channels in the paracellular pathway between epithelial cells. Am J Physiol Cell Physiol. 2002;283(1):C142-7. Epub 2002/06/11.

417. Angelow S, Ahlstrom R, Yu AS. Biology of claudins. Am J Physiol Renal Physiol. 2008;295(4):F867-76. Epub 2008/05/16.

418. Piontek J, Winkler L, Wolburg H, Muller SL, Zuleger N, Piehl C, et al. Formation of tight junction: determinants of homophilic interaction between classic claudins. FASEB J. 2008;22(1):146-58. Epub 2007/09/01.

419. Roh MH, Liu CJ, Laurinec S, Margolis B. The carboxyl terminus of zona occludens-3 binds and recruits a mammalian homologue of discs lost to tight junctions. The Journal of biological chemistry. 2002;277(30):27501-9. Epub 2002/05/22.

420. Itoh M, Furuse M, Morita K, Kubota K, Saitou M, Tsukita S. Direct binding of three tight junction-associated MAGUKs, ZO-1, ZO-2, and ZO-3, with the COOH termini of claudins. J Cell Biol. 1999;147(6):1351-63. Epub 1999/12/22.

421. Gonzalez-Mariscal L, Tapia R, Chamorro D. Crosstalk of tight junction components with signaling pathways. Biochimica et biophysica acta. 2008;1778(3):729-56. Epub 2007/10/24.

422. Van Itallie CM, Gambling TM, Carson JL, Anderson JM. Palmitoylation of claudins is required for efficient tight-junction localization. J Cell Sci. 2005;118(Pt 7):1427-36. Epub 2005/03/17.

423. Meertens L, Bertaux C, Cukierman L, Cormier E, Lavillette D, Cosset FL, et al. The tight junction proteins claudin-1, -6, and -9 are entry cofactors for hepatitis C virus. Journal of virology. 2008;82(7):3555-60. Epub 2008/02/01.

424. Feldman GJ, Mullin JM, Ryan MP. Occludin: structure, function and regulation. Adv Drug Deliv Rev. 2005;57(6):883-917. Epub 2005/04/12.

425. Bamforth SD, Kniesel U, Wolburg H, Engelhardt B, Risau W. A dominant mutant of occludin disrupts tight junction structure and function. J Cell Sci. 1999;112 (Pt 12):1879-88. Epub 1999/05/26.

426. Liu S, Yang W, Shen L, Turner JR, Coyne CB, Wang T. Tight junction proteins claudin-1 and occludin control hepatitis C virus entry and are downregulated during infection to prevent superinfection. Journal of virology. 2009;83(4):2011-4. Epub 2008/12/05.

427. Ploss A, Evans MJ, Gaysinskaya VA, Panis M, You H, de Jong YP, et al. Human occludin is a hepatitis C virus entry factor required for infection of mouse cells. Nature. 2009;457(7231):882-6. Epub 2009/02/03.

428. Russell DW, Schneider WJ, Yamamoto T, Luskey KL, Brown MS, Goldstein JL. Domain map of the LDL receptor: sequence homology with the epidermal growth factor precursor. Cell. 1984;37(2):577-85. Epub 1984/06/01.

429. Yamamoto T, Davis CG, Brown MS, Schneider WJ, Casey ML, Goldstein JL, et al. The human LDL receptor: a cysteine-rich protein with multiple Alu sequences in its mRNA. Cell. 1984;39(1):27-38. Epub 1984/11/01.

430. Sudhof TC, Russell DW, Goldstein JL, Brown MS, Sanchez-Pescador R, Bell GI. Cassette of eight exons shared by genes for LDL receptor and EGF precursor. Science. 1985;228(4701):893-5. Epub 1985/05/17.

431. Sudhof TC, Goldstein JL, Brown MS, Russell DW. The LDL receptor gene: a mosaic of exons shared with different proteins. Science. 1985;228(4701):815-22. Epub 1985/05/17.

432. Stanley KK, Kocher HP, Luzio JP, Jackson P, Tschopp J. The sequence and topology of human complement component C9. EMBO J. 1985;4(2):375-82. Epub 1985/02/01.

433. Haefliger JA, Tschopp J, Nardelli D, Wahli W, Kocher HP, Tosi M, et al. Complementary DNA cloning of complement C8 beta and its sequence homology to C9. Biochemistry. 1987;26(12):3551-6. Epub 1987/06/16.

434. Springer TA. An extracellular beta-propeller module predicted in lipoprotein and scavenger receptors, tyrosine kinases, epidermal growth factor precursor, and extracellular matrix components. J Mol Biol. 1998;283(4):837-62. Epub 1998/10/29.

435. Jeon H, Meng W, Takagi J, Eck MJ, Springer TA, Blacklow SC. Implications for familial hypercholesterolemia from the structure of the LDL receptor YWTD-EGF domain pair. Nat Struct Biol. 2001;8(6):499-504. Epub 2001/05/25.

436. Cummings RD, Kornfeld S, Schneider WJ, Hobgood KK, Tolleshaug H, Brown MS, et al. Biosynthesis of N- and O-linked oligosaccharides of the low density lipoprotein receptor. The Journal of biological chemistry. 1983;258(24):15261-73. Epub 1983/12/25.

437. Davis CG, Lehrman MA, Russell DW, Anderson RG, Brown MS, Goldstein JL. The J.D. mutation in familial hypercholesterolemia: amino acid substitution in cytoplasmic domain impedes internalization of LDL receptors. Cell. 1986;45(1):15-24. Epub 1986/04/11.

438. Yokode M, Pathak RK, Hammer RE, Brown MS, Goldstein JL, Anderson RG. Cytoplasmic sequence required for basolateral targeting of LDL receptor in livers of transgenic mice. J Cell Biol. 1992;117(1):39-46. Epub 1992/04/01.

439. Russell DW, Brown MS, Goldstein JL. Different combinations of cysteine-rich repeats mediate binding of low density lipoprotein receptor to two different proteins. The Journal of biological chemistry. 1989;264(36):21682-8. Epub 1989/12/25.

440. Esser V, Limbird LE, Brown MS, Goldstein JL, Russell DW. Mutational analysis of the ligand binding domain of the low density lipoprotein receptor. The Journal of biological chemistry. 1988;263(26):13282-90. Epub 1988/09/15.

441. Davis CG, Goldstein JL, Sudhof TC, Anderson RG, Russell DW, Brown MS. Acid-dependent ligand dissociation and recycling of LDL receptor mediated by growth factor homology region. Nature. 1987;326(6115):760-5. Epub 1987/04/23.

442. He G, Gupta S, Yi M, Michaely P, Hobbs HH, Cohen JC. ARH is a modular adaptor protein that interacts with the LDL receptor, clathrin, and AP-2. The Journal of biological chemistry. 2002;277(46):44044-9. Epub 2002/09/11.

443. Mishra SK, Watkins SC, Traub LM. The autosomal recessive hypercholesterolemia (ARH) protein interfaces directly with the clathrin-coat machinery. Proceedings of the National Academy of Sciences of the United States of America. 2002;99(25):16099-104. Epub 2002/11/27.

444. Bartosch B, Dubuisson J, Cosset FL. Infectious hepatitis C virus pseudo-particles containing functional E1-E2 envelope protein complexes. J Exp Med. 2003;197(5):633-42. Epub 2003/03/05.

445. Mead JR, Irvine SA, Ramji DP. Lipoprotein lipase: structure, function, regulation, and role in disease. J Mol Med (Berl). 2002;80(12):753-69. Epub 2002/12/17.

446. Williams KJ, Fless GM, Petrie KA, Snyder ML, Brocia RW, Swenson TL. Mechanisms by which lipoprotein lipase alters cellular metabolism of lipoprotein(a), low density lipoprotein, and nascent lipoproteins. Roles for low density lipoprotein receptors and heparan sulfate proteoglycans. The Journal of biological chemistry. 1992;267(19):13284-92. Epub 1992/07/05.

447. Shimizu Y, Hishiki T, Sugiyama K, Ogawa K, Funami K, Kato A, et al. Lipoprotein lipase and hepatic triglyceride lipase reduce the infectivity of hepatitis C virus (HCV) through their catalytic activities on HCV-associated lipoproteins. Virology. 2010;407(1):152-9. Epub 2010/09/09.

448. Davies JP, Levy B, Ioannou YA. Evidence for a Niemann-pick C (NPC) gene family: identification and characterization of NPC1L1. Genomics. 2000;65(2):137-45. Epub 2000/04/28.

449. Carstea ED, Morris JA, Coleman KG, Loftus SK, Zhang D, Cummings C, et al. Niemann-Pick C1 disease gene: homology to mediators of cholesterol homeostasis. Science. 1997;277(5323):228-31. Epub 1997/07/11.

450. Yu L. The structure and function of Niemann-Pick C1-like 1 protein. Curr Opin Lipidol. 2008;19(3):263-9. Epub 2008/05/08.

451. Temel RE, Tang W, Ma Y, Rudel LL, Willingham MC, Ioannou YA, et al. Hepatic Niemann-Pick C1-like 1 regulates biliary cholesterol concentration and is a target of ezetimibe. J Clin Invest. 2007;117(7):1968-78. Epub 2007/06/16.

452. Yu L, Bharadwaj S, Brown JM, Ma Y, Du W, Davis MA, et al. Cholesterol-regulated translocation of NPC1L1 to the cell surface facilitates free cholesterol uptake. The Journal of biological chemistry. 2006;281(10):6616-24. Epub 2006/01/13.

453. Sainz B, Jr., Barretto N, Martin DN, Hiraga N, Imamura M, Hussain S, et al. Identification of the Niemann-Pick C1-like 1 cholesterol absorption receptor as a new hepatitis C virus entry factor. Nat Med. 2012;18(2):281-5. Epub 2012/01/11.

454. Gibbons GF, Islam K, Pease RJ. Mobilisation of triacylglycerol stores. Biochimica et biophysica acta. 2000;1483(1):37-57. Epub 1999/12/22.

455. Rubbia-Brandt L, Quadri R, Abid K, Giostra E, Male PJ, Mentha G, et al. Hepatocyte steatosis is a cytopathic effect of hepatitis C virus genotype 3. J Hepatol. 2000;33(1):106-15. Epub 2000/07/25.

456. Czaja AJ, Carpenter HA, Santrach PJ, Moore SB. Host- and disease-specific factors affecting steatosis in chronic hepatitis C. J Hepatol. 1998;29(2):198-206. Epub 1998/08/29.

457. Lonardo A, Adinolfi LE, Loria P, Carulli N, Ruggiero G, Day CP. Steatosis and hepatitis C virus: mechanisms and significance for hepatic and extrahepatic disease. Gastroenterology. 2004;126(2):586-97. Epub 2004/02/06.

458. Patton HM, Patel K, Behling C, Bylund D, Blatt LM, Vallee M, et al. The impact of steatosis on disease progression and early and sustained treatment response in chronic hepatitis C patients. J Hepatol. 2004;40(3):484-90. Epub 2004/05/05.

459. Poynard T, Ratziu V, McHutchison J, Manns M, Goodman Z, Zeuzem S, et al. Effect of treatment with peginterferon or interferon alfa-2b and ribavirin on steatosis in patients infected with hepatitis C. Hepatology. 2003;38(1):75-85. Epub 2003/06/28.

460. Chern CL, Huang RF, Chen YH, Cheng JT, Liu TZ. Folate deficiency-induced oxidative stress and apoptosis are mediated via homocysteine-dependent overproduction of hydrogen peroxide and enhanced activation of NF-kappaB in human Hep G2 cells. Biomed Pharmacother. 2001;55(8):434-42. Epub 2001/11/01.

461. Tong L. Acetyl-coenzyme A carboxylase: crucial metabolic enzyme and attractive target for drug discovery. Cell Mol Life Sci. 2005;62(16):1784-803. Epub 2005/06/22.

462. Abu-Elheiga L, Jayakumar A, Baldini A, Chirala SS, Wakil SJ. Human acetyl-CoA carboxylase: characterization, molecular cloning, and evidence for two isoforms. Proceedings of the National Academy of Sciences of the United States of America. 1995;92(9):4011-5. Epub 1995/04/25.

463. Mycielska ME, Patel A, Rizaner N, Mazurek MP, Keun H, Patel A, et al. Citrate transport and metabolism in mammalian cells: prostate epithelial cells and prostate cancer. BioEssays : news and reviews in molecular, cellular and developmental biology. 2009;31(1):10-20. Epub 2009/01/21.

464. Abu-Elheiga L, Matzuk MM, Kordari P, Oh W, Shaikenov T, Gu Z, et al. Mutant mice lacking acetyl-CoA carboxylase 1 are embryonically lethal. Proceedings of the National Academy of Sciences of the United States of America. 2005;102(34):12011-6. Epub 2005/08/17.

465. Abu-Elheiga L, Matzuk MM, Abo-Hashema KA, Wakil SJ. Continuous fatty acid oxidation and reduced fat storage in mice lacking acetyl-CoA carboxylase 2. Science. 2001;291(5513):2613-6. Epub 2001/04/03.

466. Brownsey RW, Boone AN, Elliott JE, Kulpa JE, Lee WM. Regulation of acetyl-CoA carboxylase. Biochem Soc Trans. 2006;34(Pt 2):223-7. Epub 2006/03/21.

467. Wakil SJ. Fatty acid synthase, a proficient multifunctional enzyme. Biochemistry. 1989;28(11):4523-30. Epub 1989/05/30.

468. Libertini LJ, Smith S. Purification and properties of a thioesterase from lactating rat mammary gland which modifies the product specificity of fatty acid synthetase. The Journal of biological chemistry. 1978;253(5):1393-401. Epub 1978/03/10.

469. Rangan VS, Smith S. Alteration of the substrate specificity of the malonyl-CoA/acetyl-CoA:acyl carrier protein S-acyltransferase domain of the multifunctional fatty acid synthase by mutation of a single arginine residue. The Journal of biological chemistry. 1997;272(18):11975-8. Epub 1997/05/02.

470. Misra S, Sakamoto K, Moustaid N, Sul HS. Localization of sequences for the basal and insulin-like growth factor-I inducible activity of the fatty acid synthase promoter in 3T3-L1 fibroblasts. The Biochemical journal. 1994;298 Pt 3:575-8. Epub 1994/03/15.

471. Moustaid N, Beyer RS, Sul HS. Identification of an insulin response element in the fatty acid synthase promoter. J Biol Chem. 1994;269(8):5629-34. Epub 1994/02/25.

472. Latasa MJ, Moon YS, Kim KH, Sul HS. Nutritional regulation of the fatty acid synthase promoter in vivo: sterol regulatory element binding protein functions through an upstream region containing a sterol regulatory element. Proceedings of the National Academy of Sciences of the United States of America. 2000;97(19):10619-24. Epub 2000/08/30.

473. Sul HS, Latasa MJ, Moon Y, Kim KH. Regulation of the fatty acid synthase promoter by insulin. J Nutr. 2000;130(2S Suppl):315S-20S. Epub 2000/03/18.

474. Latasa MJ, Griffin MJ, Moon YS, Kang C, Sul HS. Occupancy and function of the -150 sterol regulatory element and -65 E-box in nutritional regulation of the fatty acid synthase gene in living animals. Molecular and cellular biology. 2003;23(16):5896-907. Epub 2003/08/05.

475. Goldstein JL, DeBose-Boyd RA, Brown MS. Protein sensors for membrane sterols. Cell. 2006;124(1):35-46. Epub 2006/01/18.

476. Brown MS, Goldstein JL. The SREBP pathway: regulation of cholesterol metabolism by proteolysis of a membrane-bound transcription factor. Cell. 1997;89(3):331-40. Epub 1997/05/02.

477. Schultz JR, Tu H, Luk A, Repa JJ, Medina JC, Li L, et al. Role of LXRs in control of lipogenesis. Genes & development. 2000;14(22):2831-8. Epub 2000/11/23.

478. Yoshikawa T, Shimano H, Amemiya-Kudo M, Yahagi N, Hasty AH, Matsuzaka T, et al. Identification of liver X receptor-retinoid X receptor as an activator of the sterol regulatory element-binding protein 1c gene promoter. Molecular and cellular biology. 2001;21(9):2991-3000. Epub 2001/04/05.

479. Joseph SB, Laffitte BA, Patel PH, Watson MA, Matsukuma KE, Walczak R, et al. Direct and indirect mechanisms for regulation of fatty acid synthase gene expression by liver X receptors. The Journal of biological chemistry. 2002;277(13):11019-25. Epub 2002/01/16.

480. Koo SH, Dutcher AK, Towle HC. Glucose and insulin function through two distinct transcription factors to stimulate expression of lipogenic enzyme genes in liver. The Journal of biological chemistry. 2001;276(12):9437-45. Epub 2000/12/22.

481. Shih HM, Liu Z, Towle HC. Two CACGTG motifs with proper spacing dictate the carbohydrate regulation of hepatic gene transcription. The Journal of biological chemistry. 1995;270(37):21991-7. Epub 1995/09/15.

482. Rufo C, Teran-Garcia M, Nakamura MT, Koo SH, Towle HC, Clarke SD. Involvement of a unique carbohydrate-responsive factor in the glucose regulation of rat liver fatty-acid synthase gene transcription. The Journal of biological chemistry. 2001;276(24):21969-75. Epub 2001/03/30.

483. O'Callaghan BL, Koo SH, Wu Y, Freake HC, Towle HC. Glucose regulation of the acetyl-CoA carboxylase promoter PI in rat hepatocytes. The Journal of biological chemistry. 2001;276(19):16033-9. Epub 2001/05/08.

484. Stoeckman AK, Ma L, Towle HC. Mlx is the functional heteromeric partner of the carbohydrate response element-binding protein in glucose regulation of lipogenic enzyme genes. The Journal of biological chemistry. 2004;279(15):15662-9. Epub 2004/01/27.

485. Kabashima T, Kawaguchi T, Wadzinski BE, Uyeda K. Xylulose 5-phosphate mediates glucose-induced lipogenesis by xylulose 5-phosphate-activated protein phosphatase in rat liver. Proceedings of the National Academy of Sciences of the United States of America. 2003;100(9):5107-12. Epub 2003/04/10.

486. Xu J, Teran-Garcia M, Park JH, Nakamura MT, Clarke SD. Polyunsaturated fatty acids suppress hepatic sterol regulatory element-binding protein-1 expression by accelerating transcript decay. The Journal of biological chemistry. 2001;276(13):9800-7. Epub 2001/01/02.

487. Botolin D, Wang Y, Christian B, Jump DB. Docosahexaneoic acid (22:6,n-3) regulates rat hepatocyte SREBP-1 nuclear abundance by Erk- and 26S proteasome-dependent pathways. Journal of lipid research. 2006;47(1):181-92. Epub 2005/10/14.

488. Fukasawa M, Tanaka Y, Sato S, Ono Y, Nitahara-Kasahara Y, Suzuki T, et al. Enhancement of de novo fatty acid biosynthesis in hepatic cell line Huh7 expressing hepatitis C virus core protein. Biological & pharmaceutical bulletin. 2006;29(9):1958-61. Epub 2006/09/02.

489. Lima-Cabello E, Garcia-Mediavilla MV, Miquilena-Colina ME, Vargas-Castrillon J, Lozano-Rodriguez T, Fernandez-Bermejo M, et al. Enhanced expression of pro-inflammatory mediators and liver X-receptor-regulated lipogenic genes in non-alcoholic fatty liver disease and hepatitis C. Clin Sci (Lond). 2011;120(6):239-50. Epub 2010/10/12.

490. Fujino T, Nakamuta M, Yada R, Aoyagi Y, Yasutake K, Kohjima M, et al. Expression profile of lipid metabolism-associated genes in hepatitis C virus-infected human liver. Hepatology research : the official journal of the Japan Society of Hepatology. 2010;40(9):923-9. Epub 2010/10/05.

491. Ryan MC, Desmond PV, Slavin JL, Congiu M. Expression of genes involved in lipogenesis is not increased in patients with HCV genotype 3 in human liver. J Viral Hepat. 2011;18(1):53-60. Epub 2010/03/04.

492. McPherson S, Jonsson JR, Barrie HD, O'Rourke P, Clouston AD, Powell EE. Investigation of the role of SREBP-1c in the pathogenesis of HCV-related steatosis. J Hepatol. 2008;49(6):1046-54. Epub 2008/08/30.

493. Wu C, Gilroy R, Taylor R, Olyaee M, Abdulkarim B, Forster J, et al. Alteration of hepatic nuclear receptor-mediated signaling pathways in hepatitis C virus patients with and without a history of alcohol drinking. Hepatology. 2011;54(6):1966-74. Epub 2011/09/08.

494. Jackel-Cram C, Babiuk LA, Liu Q. Up-regulation of fatty acid synthase promoter by hepatitis C virus core protein: genotype-3a core has a stronger effect than genotype-1b core. J Hepatol. 2007;46(6):999-1008. Epub 2006/12/26.

495. Jackel-Cram C, Qiao L, Xiang Z, Brownlie R, Zhou Y, Babiuk L, et al. Hepatitis C virus genotype-3a core protein enhances sterol regulatory element-binding protein-1 activity through the phosphoinositide 3-kinase-Akt-2 pathway. J Gen Virol. 2010;91(Pt 6):1388-95. Epub 2010/02/05.

496. Moriishi K, Mochizuki R, Moriya K, Miyamoto H, Mori Y, Abe T, et al. Critical role of PA28gamma in hepatitis C virus-associated steatogenesis and hepatocarcinogenesis. Proceedings of the National Academy of Sciences of the United States of America. 2007;104(5):1661-6. Epub 2007/01/20.

497. Oem JK, Jackel-Cram C, Li YP, Zhou Y, Zhong J, Shimano H, et al. Activation of sterol regulatory element-binding protein 1c and fatty acid synthase transcription by hepatitis C virus non-structural protein 2. J Gen Virol. 2008;89(Pt 5):1225-30. Epub 2008/04/19.

498. Xiang Z, Qiao L, Zhou Y, Babiuk LA, Liu Q. Hepatitis C virus nonstructural protein-5A activates sterol regulatory element-binding protein-1c through transcription factor Sp1. Biochem Biophys Res Commun. 2010;402(3):549-53. Epub 2010/10/26.

499. Park CY, Jun HJ, Wakita T, Cheong JH, Hwang SB. Hepatitis C virus nonstructural 4B protein modulates sterol regulatory element-binding protein signaling via the AKT pathway. The Journal of biological chemistry. 2009;284(14):9237-46. Epub 2009/02/11.

500. Waris G, Felmlee DJ, Negro F, Siddiqui A. Hepatitis C virus induces proteolytic cleavage of sterol regulatory element binding proteins and stimulates their phosphorylation via oxidative stress. Journal of virology. 2007;81(15):8122-30. Epub 2007/05/18.

501. Garcia-Mediavilla MV, Pisonero-Vaquero S, Lima-Cabello E, Benedicto I, Majano PL, Jorquera F, et al. Liver X receptor alpha-mediated regulation of lipogenesis by core and NS5A proteins contributes to HCV-induced liver steatosis and HCV replication. Lab Invest. 2012;92(8):1191-202. Epub 2012/05/30.

502. Zeng J, Wu Y, Liao Q, Li L, Chen X, Chen X. Liver X receptors agonists impede hepatitis C virus infection in an Idol-dependent manner. Antiviral Res. 2012;95(3):245-56. Epub 2012/06/21.

503. van der Poorten D, Shahidi M, Tay E, Sesha J, Tran K, McLeod D, et al. Hepatitis C virus induces the cannabinoid receptor 1. PloS one. 2010;5(9). Epub 2010/09/24.

504. Kapadia SB, Chisari FV. Hepatitis C virus RNA replication is regulated by host geranylgeranylation and fatty acids. Proceedings of the National Academy of Sciences of the United States of America. 2005;102(7):2561-6. Epub 2005/02/09.

505. Olmstead AD, Knecht W, Lazarov I, Dixit SB, Jean F. Human subtilase SKI-1/S1P is a master regulator of the HCV Lifecycle and a potential host cell target for developing indirect-acting antiviral agents. PLoS Pathog. 2012;8(1):e1002468. Epub 2012/01/14.

506. Yang W, Hood BL, Chadwick SL, Liu S, Watkins SC, Luo G, et al. Fatty acid synthase is up-regulated during hepatitis C virus infection and regulates hepatitis C virus entry and production. Hepatology. 2008;48(5):1396-403. Epub 2008/10/03.

507. Kennedy EP. Metabolism of lipides. Annu Rev Biochem. 1957;26:119-48. Epub 1957/01/01.

508. Kayden HJ, Senior JR, Mattson FH. The monoglyceride pathway of fat absorption in man. J Clin Invest. 1967;46(11):1695-703. Epub 1967/11/01.

509. Bell RM, Coleman RA. Enzymes of glycerolipid synthesis in eukaryotes. Annu Rev Biochem. 1980;49:459-87. Epub 1980/01/01.

510. Coleman RA, Mashek DG. Mammalian triacylglycerol metabolism: synthesis, lipolysis, and signaling. Chemical reviews. 2011;111(10):6359-86. Epub 2011/06/02.

511. Lewin TM, de Jong H, Schwerbrock NJ, Hammond LE, Watkins SM, Combs TP, et al. Mice deficient in mitochondrial glycerol-3-phosphate acyltransferase-1 have diminished myocardial triacylglycerol accumulation during lipogenic diet and altered phospholipid fatty acid composition. Biochimica et biophysica acta. 2008;1781(6-7):352-8. Epub 2008/06/05.

512. Coleman RA, Lee DP. Enzymes of triacylglycerol synthesis and their regulation. Progress in lipid research. 2004;43(2):134-76. Epub 2003/12/05.

513. Lewin TM, Granger DA, Kim JH, Coleman RA. Regulation of mitochondrial sn-glycerol-3-phosphate acyltransferase activity: response to feeding status is unique in various rat tissues and is discordant with protein expression. Archives of biochemistry and biophysics. 2001;396(1):119-27. Epub 2001/11/22.

514. Hammond LE, Neschen S, Romanelli AJ, Cline GW, Ilkayeva OR, Shulman GI, et al. Mitochondrial glycerol-3-phosphate acyltransferase-1 is essential in liver for the metabolism of excess acyl-CoAs. J Biol Chem. 2005;280(27):25629-36. Epub 2005/05/10.

515. Igal RA, Wang S, Gonzalez-Baro M, Coleman RA. Mitochondrial glycerol phosphate acyltransferase directs the incorporation of exogenous fatty acids into triacylglycerol. J Biol Chem. 2001;276(45):42205-12. Epub 2001/09/08.

516. Nagle CA, An J, Shiota M, Torres TP, Cline GW, Liu ZX, et al. Hepatic overexpression of glycerol-sn-3-phosphate acyltransferase 1 in rats causes insulin resistance. J Biol Chem. 2007;282(20):14807-15. Epub 2007/03/29.

517. Xu H, Wilcox D, Nguyen P, Voorbach M, Suhar T, Morgan SJ, et al. Hepatic knockdown of mitochondrial GPAT1 in ob/ob mice improves metabolic profile. Biochem Biophys Res Commun. 2006;349(1):439-48. Epub 2006/08/29.

518. Hammond LE, Albright CD, He L, Rusyn I, Watkins SM, Doughman SD, et al. Increased oxidative stress is associated with balanced increases in hepatocyte apoptosis and proliferation in glycerol-3-phosphate acyltransferase-1 deficient mice. Exp Mol Pathol. 2007;82(2):210-9. Epub 2007/01/30.

519. Linden D, William-Olsson L, Rhedin M, Asztely AK, Clapham JC, Schreyer S. Overexpression of mitochondrial GPAT in rat hepatocytes leads to decreased fatty acid oxidation and increased glycerolipid biosynthesis. Journal of lipid research. 2004;45(7):1279-88. Epub 2004/04/23.

520. Gonzalez-Baro MR, Granger DA, Coleman RA. Mitochondrial glycerol phosphate acyltransferase contains two transmembrane domains with the active site in the N-terminal domain facing the cytosol. The Journal of biological chemistry. 2001;276(46):43182-8. Epub 2001/09/15.

521. Lewin TM, Schwerbrock NM, Lee DP, Coleman RA. Identification of a new glycerol-3-phosphate acyltransferase isoenzyme, mtGPAT2, in mitochondria. J Biol Chem. 2004;279(14):13488-95. Epub 2004/01/16.

522. Wang S, Lee DP, Gong N, Schwerbrock NM, Mashek DG, Gonzalez-Baro MR, et al. Cloning and functional characterization of a novel mitochondrial N-ethylmaleimide-sensitive glycerol-3-phosphate acyltransferase (GPAT2). Archives of biochemistry and biophysics. 2007;465(2):347-58. Epub 2007/08/11.

523. Cao J, Li JL, Li D, Tobin JF, Gimeno RE. Molecular identification of microsomal acyl-CoA:glycerol-3-phosphate acyltransferase, a key enzyme in de novo triacylglycerol synthesis. Proceedings of the National Academy of Sciences of the United States of America. 2006;103(52):19695-700. Epub 2006/12/16.

524. Shan D, Li JL, Wu L, Li D, Hurov J, Tobin JF, et al. GPAT3 and GPAT4 are regulated by insulin-stimulated phosphorylation and play distinct roles in adipogenesis. Journal of lipid research. 2010;51(7):1971-81. Epub 2010/02/26.

525. Vaughan M, Berger JE, Steinberg D. Hormone-Sensitive Lipase and Monoglyceride Lipase Activities in Adipose Tissue. The Journal of biological chemistry. 1964;239:401-9. Epub 1964/02/01.

526. Nagle CA, Vergnes L, Dejong H, Wang S, Lewin TM, Reue K, et al. Identification of a novel sn-glycerol-3-phosphate acyltransferase isoform, GPAT4, as the enzyme deficient in Agpat6-/- mice. Journal of lipid research. 2008;49(4):823-31. Epub 2008/01/15.

527. Vergnes L, Beigneux AP, Davis R, Watkins SM, Young SG, Reue K. Agpat6 deficiency causes subdermal lipodystrophy and resistance to obesity. Journal of lipid research. 2006;47(4):745-54. Epub 2006/01/27.

528. Chen YQ, Kuo MS, Li S, Bui HH, Peake DA, Sanders PE, et al. AGPAT6 is a novel microsomal glycerol-3-phosphate acyltransferase. The Journal of biological chemistry. 2008;283(15):10048-57. Epub 2008/02/02.

529. Kume K, Shimizu T. cDNA cloning and expression of murine 1-acyl-sn-glycerol-3-phosphate acyltransferase. Biochem Biophys Res Commun. 1997;237(3):663-6. Epub 1997/08/28.

530. West J, Tompkins CK, Balantac N, Nudelman E, Meengs B, White T, et al. Cloning and expression of two human lysophosphatidic acid acyltransferase cDNAs that enhance cytokine-induced signaling responses in cells. DNA and cell biology. 1997;16(6):691-701. Epub 1997/06/01.

531. Eberhardt C, Gray PW, Tjoelker LW. Human lysophosphatidic acid acyltransferase. cDNA cloning, expression, and localization to chromosome 9q34.3. J Biol Chem. 1997;272(32):20299-305. Epub 1997/08/08.

532. Hollenback D, Bonham L, Law L, Rossnagle E, Romero L, Carew H, et al. Substrate specificity of lysophosphatidic acid acyltransferase beta -- evidence from membrane and whole cell assays. Journal of lipid research. 2006;47(3):593-604. Epub 2005/12/22.

533. Ruan H, Pownall HJ. Overexpression of 1-acyl-glycerol-3-phosphate acyltransferase-alpha enhances lipid storage in cellular models of adipose tissue and skeletal muscle. Diabetes. 2001;50(2):233-40. Epub 2001/03/29.

534. Lu B, Jiang YJ, Zhou Y, Xu FY, Hatch GM, Choy PC. Cloning and characterization of murine 1-acyl-sn-glycerol 3-phosphate acyltransferases and their regulation by PPARalpha in murine heart. The Biochemical journal. 2005;385(Pt 2):469-77. Epub 2004/09/16.

535. Cortes VA, Curtis DE, Sukumaran S, Shao X, Parameswara V, Rashid S, et al. Molecular mechanisms of hepatic steatosis and insulin resistance in the AGPAT2-deficient mouse model of congenital generalized lipodystrophy. Cell Metab. 2009;9(2):165-76. Epub 2009/02/04.

536. Eberhardt C, Gray PW, Tjoelker LW. cDNA cloning, expression and chromosomal localization of two human lysophosphatidic acid acyltransferases. Adv Exp Med Biol. 1999;469:351-6. Epub 2000/02/10.

537. Agarwal AK, Arioglu E, De Almeida S, Akkoc N, Taylor SI, Bowcock AM, et al. AGPAT2 is mutated in congenital generalized lipodystrophy linked to chromosome 9q34. Nat Genet. 2002;31(1):21-3. Epub 2002/04/23.

538. Agarwal AK, Barnes RI, Garg A. Functional characterization of human 1-acylglycerol-3-phosphate acyltransferase isoform 8: cloning, tissue distribution, gene structure, and enzymatic activity. Archives of biochemistry and biophysics. 2006;449(1-2):64-76. Epub 2006/04/20.

539. Simha V, Garg A. Phenotypic heterogeneity in body fat distribution in patients with congenital generalized lipodystrophy caused by mutations in the AGPAT2 or seipin genes. J Clin Endocrinol Metab. 2003;88(11):5433-7. Epub 2003/11/07.

540. Carman GM, Han GS. Roles of phosphatidate phosphatase enzymes in lipid metabolism. Trends Biochem Sci. 2006;31(12):694-9. Epub 2006/11/03.

541. Brindley DN, Waggoner DW. Mammalian lipid phosphate phosphohydrolases. The Journal of biological chemistry. 1998;273(38):24281-4. Epub 1998/09/12.

542. Brindley DN. Lipid phosphate phosphatases and related proteins: signaling functions in development, cell division, and cancer. J Cell Biochem. 2004;92(5):900-12. Epub 2004/07/20.

543. Han GS, Wu WI, Carman GM. The Saccharomyces cerevisiae Lipin homolog is a Mg2+-dependent phosphatidate phosphatase enzyme. The Journal of biological chemistry. 2006;281(14):9210-8. Epub 2006/02/10.

544. Wendel AA, Li LO, Li Y, Cline GW, Shulman GI, Coleman RA. Glycerol-3-phosphate acyltransferase 1 deficiency in ob/ob mice diminishes hepatic steatosis but does not protect against insulin resistance or obesity. Diabetes. 2010;59(6):1321-9. Epub 2010/03/05.

545. Magre J, Delepine M, Van Maldergem L, Robert JJ, Maassen JA, Meier M, et al. Prevalence of mutations in AGPAT2 among human lipodystrophies. Diabetes. 2003;52(6):1573-8. Epub 2003/05/27.

546. Peterfy M, Phan J, Xu P, Reue K. Lipodystrophy in the fld mouse results from mutation of a new gene encoding a nuclear protein, lipin. Nat Genet. 2001;27(1):121-4. Epub 2001/01/04.

547. Phan J, Peterfy M, Reue K. Lipin expression preceding peroxisome proliferator-activated receptor-gamma is critical for adipogenesis in vivo and in vitro. The Journal of biological chemistry. 2004;279(28):29558-64. Epub 2004/05/05.

548. Reue K, Xu P, Wang XP, Slavin BG. Adipose tissue deficiency, glucose intolerance, and increased atherosclerosis result from mutation in the mouse fatty liver dystrophy (fld) gene. Journal of lipid research. 2000;41(7):1067-76. Epub 2000/07/07.

549. Phan J, Reue K. Lipin, a lipodystrophy and obesity gene. Cell metabolism. 2005;1(1):73-83. Epub 2005/08/02.

550. Xu J, Lee WN, Phan J, Saad MF, Reue K, Kurland IJ. Lipin deficiency impairs diurnal metabolic fuel switching. Diabetes. 2006;55(12):3429-38. Epub 2006/11/30.

551. Donkor J, Sariahmetoglu M, Dewald J, Brindley DN, Reue K. Three mammalian lipins act as phosphatidate phosphatases with distinct tissue expression patterns. The Journal of biological chemistry. 2007;282(6):3450-7. Epub 2006/12/13.

552. Grimsey N, Han GS, O'Hara L, Rochford JJ, Carman GM, Siniossoglou S. Temporal and spatial regulation of the phosphatidate phosphatases lipin 1 and 2. The Journal of biological chemistry. 2008;283(43):29166-74. Epub 2008/08/13.

553. Cases S, Smith SJ, Zheng YW, Myers HM, Lear SR, Sande E, et al. Identification of a gene encoding an acyl CoA:diacylglycerol acyltransferase, a key enzyme in triacylglycerol synthesis. Proceedings of the National Academy of Sciences of the United States of America. 1998;95(22):13018-23. Epub 1998/10/28.

554. Yen CL, Monetti M, Burri BJ, Farese RV, Jr. The triacylglycerol synthesis enzyme DGAT1 also catalyzes the synthesis of diacylglycerols, waxes, and retinyl esters. Journal of lipid research. 2005;46(7):1502-11. Epub 2005/04/19.

555. Yen CL, Stone SJ, Koliwad S, Harris C, Farese RV, Jr. Thematic review series: glycerolipids. DGAT enzymes and triacylglycerol biosynthesis. Journal of lipid research. 2008;49(11):2283-301. Epub 2008/09/02.

556. Weselake RJ, Madhavji M, Szarka SJ, Patterson NA, Wiehler WB, Nykiforuk CL, et al. Acyl-CoA-binding and self-associating properties of a recombinant 13.3 kDa N-terminal fragment of diacylglycerol acyltransferase-1 from oilseed rape. BMC Biochem. 2006;7:24. Epub 2006/12/29.

557. Siloto RM, Madhavji M, Wiehler WB, Burton TL, Boora PS, Laroche A, et al. An N-terminal fragment of mouse DGAT1 binds different acyl-CoAs with varying affinity. Biochem Biophys Res Commun. 2008;373(3):350-4. Epub 2008/06/24.

558. Lardizabal KD, Mai JT, Wagner NW, Wyrick A, Voelker T, Hawkins DJ. DGAT2 is a new diacylglycerol acyltransferase gene family: purification, cloning, and expression in insect cells of two polypeptides from Mortierella ramanniana with diacylglycerol acyltransferase activity. J Biol Chem. 2001;276(42):38862-9. Epub 2001/08/02.

559. Cases S, Stone SJ, Zhou P, Yen E, Tow B, Lardizabal KD, et al. Cloning of DGAT2, a second mammalian diacylglycerol acyltransferase, and related family members. J Biol Chem. 2001;276(42):38870-6. Epub 2001/08/02.

560. Stone SJ, Levin MC, Farese RV, Jr. Membrane topology and identification of key functional amino acid residues of murine acyl-CoA:diacylglycerol acyltransferase-2. The Journal of biological chemistry. 2006;281(52):40273-82. Epub 2006/10/13.

561. Au-Young J, Fielding CJ. Synthesis and secretion of wild-type and mutant human plasma cholesteryl ester transfer protein in baculovirus-transfected insect cells: the carboxyl-terminal region is required for both lipoprotein binding and catalysis of transfer. Proceedings of the National Academy of Sciences of the United States of America. 1992;89(9):4094-8. Epub 1992/05/01.

562. Stone SJ, Myers HM, Watkins SM, Brown BE, Feingold KR, Elias PM, et al. Lipopenia and skin barrier abnormalities in DGAT2-deficient mice. J Biol Chem. 2004;279(12):11767-76. Epub 2003/12/12.

563. Smith SJ, Cases S, Jensen DR, Chen HC, Sande E, Tow B, et al. Obesity resistance and multiple mechanisms of triglyceride synthesis in mice lacking Dgat. Nature genetics. 2000;25(1):87-90. Epub 2000/05/10.

564. Waterman IJ, Price NT, Zammit VA. Distinct ontogenic patterns of overt and latent DGAT activities of rat liver microsomes. Journal of lipid research. 2002;43(9):1555-62. Epub 2002/09/18.

565. Owen MR, Corstorphine CC, Zammit VA. Overt and latent activities of diacylglycerol acytransferase in rat liver microsomes: possible roles in very-low-density lipoprotein triacylglycerol secretion. The Biochemical journal. 1997;323 (Pt 1):17-21. Epub 1997/04/01.

566. Abo-Hashema KA, Cake MH, Power GW, Clarke D. Evidence for triacylglycerol synthesis in the lumen of microsomes via a lipolysis-esterification pathway involving carnitine acyltransferases. The Journal of biological chemistry. 1999;274(50):35577-82. Epub 1999/12/10.

567. Ganji SH, Tavintharan S, Zhu D, Xing Y, Kamanna VS, Kashyap ML. Niacin noncompetitively inhibits DGAT2 but not DGAT1 activity in HepG2 cells. Journal of lipid research. 2004;45(10):1835-45. Epub 2004/07/20.

568. Man WC, Miyazaki M, Chu K, Ntambi J. Colocalization of SCD1 and DGAT2: implying preference for endogenous monounsaturated fatty acids in triglyceride synthesis. Journal of lipid research. 2006;47(9):1928-39. Epub 2006/06/06.

569. Liang JJ, Oelkers P, Guo C, Chu PC, Dixon JL, Ginsberg HN, et al. Overexpression of human diacylglycerol acyltransferase 1, acyl-coa:cholesterol acyltransferase 1, or acyl-CoA:cholesterol acyltransferase 2 stimulates secretion of apolipoprotein B-containing lipoproteins in McA-RH7777 cells. The Journal of biological chemistry. 2004;279(43):44938-44. Epub 2004/08/17.

570. Millar JS, Stone SJ, Tietge UJ, Tow B, Billheimer JT, Wong JS, et al. Short-term overexpression of DGAT1 or DGAT2 increases hepatic triglyceride but not VLDL triglyceride or apoB production. Journal of lipid research. 2006;47(10):2297-305. Epub 2006/08/01.

571. Chen HC, Smith SJ, Ladha Z, Jensen DR, Ferreira LD, Pulawa LK, et al. Increased insulin and leptin sensitivity in mice lacking acyl CoA:diacylglycerol acyltransferase 1. J Clin Invest. 2002;109(8):1049-55. Epub 2002/04/17.

572. Buhman KK, Smith SJ, Stone SJ, Repa JJ, Wong JS, Knapp FF, Jr., et al. DGAT1 is not essential for intestinal triacylglycerol absorption or chylomicron synthesis. The Journal of biological chemistry. 2002;277(28):25474-9. Epub 2002/04/18.

573. Chen HC, Ladha Z, Smith SJ, Farese RV, Jr. Analysis of energy expenditure at different ambient temperatures in mice lacking DGAT1. American journal of physiology Endocrinology and metabolism. 2003;284(1):E213-8. Epub 2002/10/22.

574. Ranganathan G, Unal R, Pokrovskaya I, Yao-Borengasser A, Phanavanh B, Lecka-Czernik B, et al. The lipogenic enzymes DGAT1, FAS, and LPL in adipose tissue: effects of obesity, insulin resistance, and TZD treatment. Journal of lipid research. 2006;47(11):2444-50. Epub 2006/08/09.

575. Payne VA, Au WS, Gray SL, Nora ED, Rahman SM, Sanders R, et al. Sequential regulation of diacylglycerol acyltransferase 2 expression by CAAT/enhancer-binding protein beta (C/EBPbeta) and C/EBPalpha during adipogenesis. The Journal of biological chemistry. 2007;282(29):21005-14. Epub 2007/05/17.

576. Lee AH, Scapa EF, Cohen DE, Glimcher LH. Regulation of hepatic lipogenesis by the transcription factor XBP1. Science. 2008;320(5882):1492-6. Epub 2008/06/17.

577. Hirata T, Unoki H, Bujo H, Ueno K, Saito Y. Activation of diacylglycerol O-acyltransferase 1 gene results in increased tumor necrosis factor-alpha gene expression in 3T3-L1 adipocytes. FEBS Lett. 2006;580(21):5117-21. Epub 2006/09/08.

578. Lau TE, Rodriguez MA. A protein tyrosine kinase associated with the ATP-dependent inactivation of adipose diacylglycerol acyltransferase. Lipids. 1996;31(3):277-83. Epub 1996/03/01.

579. Sooranna SR, Saggerson ED. A decrease in diacylglycerol acyltransferase after treatment of rat adipocytes with adrenaline. FEBS Lett. 1978;95(1):85-7. Epub 1978/11/01.

580. Schoonderwoerd K, Broekhoven-Schokker S, Hulsmann WC, Stam H. Properties of phosphatidate phosphohydrolase and diacylglycerol acyltransferase activities in the isolated rat heart. Effect of glucagon, ischaemia and diabetes. The Biochemical journal. 1990;268(2):487-92. Epub 1990/06/01.

581. Haagsman HP, de Haas CG, Geelen MJ, van Golde LM. Regulation of triacylglycerol synthesis in the liver. Modulation of diacylglycerol acyltransferase activity in vitro. The Journal of biological chemistry. 1982;257(18):10593-8. Epub 1982/09/25.

582. Herker E, Harris C, Hernandez C, Carpentier A, Kaehlcke K, Rosenberg AR, et al. Efficient hepatitis C virus particle formation requires diacylglycerol acyltransferase-1. Nat Med. 2010;16(11):1295-8. Epub 2010/10/12.

583. Martin S, Parton RG. Lipid droplets: a unified view of a dynamic organelle. Nat Rev Mol Cell Biol. 2006;7(5):373-8. Epub 2006/03/22.

584. Brown DA. Lipid droplets: proteins floating on a pool of fat. Curr Biol. 2001;11(11):R446-9. Epub 2001/08/23.

585. Marchesan D, Rutberg M, Andersson L, Asp L, Larsson T, Boren J, et al. A phospholipase D-dependent process forms lipid droplets containing caveolin, adipocyte differentiation-related protein, and vimentin in a cell-free system. The Journal of biological chemistry. 2003;278(29):27293-300. Epub 2003/05/06.

586. Bostrom P, Rutberg M, Ericsson J, Holmdahl P, Andersson L, Frohman MA, et al. Cytosolic lipid droplets increase in size by microtubule-dependent complex formation. Arteriosclerosis, thrombosis, and vascular biology. 2005;25(9):1945-51. Epub 2005/07/30.

587. Andersson L, Bostrom P, Ericson J, Rutberg M, Magnusson B, Marchesan D, et al. PLD1 and ERK2 regulate cytosolic lipid droplet formation. J Cell Sci. 2006;119(Pt 11):2246-57. Epub 2006/05/26.

588. Wiggins D, Gibbons GF. The lipolysis/esterification cycle of hepatic triacylglycerol. Its role in the secretion of very-low-density lipoprotein and its response to hormones and sulphonylureas. The Biochemical journal. 1992;284 (Pt 2):457-62. Epub 1992/06/01.

589. Salter AM, Wiggins D, Sessions VA, Gibbons GF. The intracellular triacylglycerol/fatty acid cycle: a comparison of its activity in hepatocytes which secrete exclusively apolipoprotein (apo) B100 very-low-density lipoprotein (VLDL) and in those which secrete predominantly apoB48 VLDL. The Biochemical journal. 1998;332 (Pt 3):667-72. Epub 1998/06/11.

590. Londos C, Brasaemle DL, Schultz CJ, Segrest JP, Kimmel AR. Perilipins, ADRP, and other proteins that associate with intracellular neutral lipid droplets in animal cells. Seminars in cell & developmental biology. 1999;10(1):51-8. Epub 1999/06/04.

591. Dalen KT, Dahl T, Holter E, Arntsen B, Londos C, Sztalryd C, et al. LSDP5 is a PAT protein specifically expressed in fatty acid oxidizing tissues. Biochimica et biophysica acta. 2007;1771(2):210-27. Epub 2007/01/20.

592. Tai ES, Ordovas JM. The role of perilipin in human obesity and insulin resistance. Curr Opin Lipidol. 2007;18(2):152-6. Epub 2007/03/14.

593. Londos C, Brasaemle DL, Gruia-Gray J, Servetnick DA, Schultz CJ, Levin DM, et al. Perilipin: unique proteins associated with intracellular neutral lipid droplets in adipocytes and steroidogenic cells. Biochem Soc Trans. 1995;23(3):611-5. Epub 1995/08/01.

594. Lu X, Gruia-Gray J, Copeland NG, Gilbert DJ, Jenkins NA, Londos C, et al. The murine perilipin gene: the lipid droplet-associated perilipins derive from tissue-specific, mRNA splice variants and define a gene family of ancient origin. Mamm Genome. 2001;12(9):741-9. Epub 2001/10/20.

595. Martinez-Botas J, Anderson JB, Tessier D, Lapillonne A, Chang BH, Quast MJ, et al. Absence of perilipin results in leanness and reverses obesity in Lepr(db/db) mice. Nat Genet. 2000;26(4):474-9. Epub 2000/12/02.

596. Tansey JT, Sztalryd C, Gruia-Gray J, Roush DL, Zee JV, Gavrilova O, et al. Perilipin ablation results in a lean mouse with aberrant adipocyte lipolysis, enhanced leptin production, and resistance to diet-induced obesity. Proc Natl Acad Sci U S A. 2001;98(11):6494-9. Epub 2001/05/24.

597. Granneman JG, Moore HP, Granneman RL, Greenberg AS, Obin MS, Zhu Z. Analysis of lipolytic protein trafficking and interactions in adipocytes. The Journal of biological chemistry. 2007;282(8):5726-35. Epub 2006/12/26.

598. Brasaemle DL, Rubin B, Harten IA, Gruia-Gray J, Kimmel AR, Londos C. Perilipin A increases triacylglycerol storage by decreasing the rate of triacylglycerol hydrolysis. The Journal of biological chemistry. 2000;275(49):38486-93. Epub 2000/08/19.

599. Lass A, Zimmermann R, Haemmerle G, Riederer M, Schoiswohl G, Schweiger M, et al. Adipose triglyceride lipase-mediated lipolysis of cellular fat stores is activated by CGI-58 and defective in Chanarin-Dorfman Syndrome. Cell Metab. 2006;3(5):309-19. Epub 2006/05/09.

600. Miyoshi H, Perfield JW, 2nd, Souza SC, Shen WJ, Zhang HH, Stancheva ZS, et al. Control of adipose triglyceride lipase action by serine 517 of perilipin A globally regulates protein kinase A-stimulated lipolysis in adipocytes. J Biol Chem. 2007;282(2):996-1002. Epub 2006/11/23.

601. Targett-Adams P, Chambers D, Gledhill S, Hope RG, Coy JF, Girod A, et al. Live cell analysis and targeting of the lipid droplet-binding adipocyte differentiation-related protein. The Journal of biological chemistry. 2003;278(18):15998-6007. Epub 2003/02/20.

602. Dalen KT, Ulven SM, Arntsen BM, Solaas K, Nebb HI. PPARalpha activators and fasting induce the expression of adipose differentiation-related protein in liver. Journal of lipid research. 2006;47(5):931-43. Epub 2006/02/21.

603. Edvardsson U, Ljungberg A, Linden D, William-Olsson L, Peilot-Sjogren H, Ahnmark A, et al. PPARalpha activation increases triglyceride mass and adipose differentiation-related protein in hepatocytes. Journal of lipid research. 2006;47(2):329-40. Epub 2005/11/12.

604. Xu G, Sztalryd C, Lu X, Tansey JT, Gan J, Dorward H, et al. Post-translational regulation of adipose differentiation-related protein by the ubiquitin/proteasome pathway. J Biol Chem. 2005;280(52):42841-7. Epub 2005/08/24.

605. Masuda Y, Itabe H, Odaki M, Hama K, Fujimoto Y, Mori M, et al. ADRP/adipophilin is degraded through the proteasome-dependent pathway during regression of lipid-storing cells. Journal of lipid research. 2006;47(1):87-98. Epub 2005/10/19.

606. Gross DN, Miyoshi H, Hosaka T, Zhang HH, Pino EC, Souza S, et al. Dynamics of lipid droplet-associated proteins during hormonally stimulated lipolysis in engineered adipocytes: stabilization and lipid droplet binding of adipocyte differentiation-related protein/adipophilin. Mol Endocrinol. 2006;20(2):459-66. Epub 2005/10/22.

607. Chang BH, Li L, Paul A, Taniguchi S, Nannegari V, Heird WC, et al. Protection against fatty liver but normal adipogenesis in mice lacking adipose differentiation-related protein. Molecular and cellular biology. 2006;26(3):1063-76. Epub 2006/01/24.

608. Diaz E, Pfeffer SR. TIP47: a cargo selection device for mannose 6-phosphate receptor trafficking. Cell. 1998;93(3):433-43. Epub 1998/05/20.

609. Krise JP, Sincock PM, Orsel JG, Pfeffer SR. Quantitative analysis of TIP47-receptor cytoplasmic domain interactions: implications for endosome-to-trans Golgi network trafficking. The Journal of biological chemistry. 2000;275(33):25188-93. Epub 2000/06/01.

610. Wolins NE, Rubin B, Brasaemle DL. TIP47 associates with lipid droplets. J Biol Chem. 2001;276(7):5101-8. Epub 2000/11/21.

611. Carroll KS, Hanna J, Simon I, Krise J, Barbero P, Pfeffer SR. Role of Rab9 GTPase in facilitating receptor recruitment by TIP47. Science. 2001;292(5520):1373-6. Epub 2001/05/19.

612. Hickenbottom SJ, Kimmel AR, Londos C, Hurley JH. Structure of a lipid droplet protein; the PAT family member TIP47. Structure. 2004;12(7):1199-207. Epub 2004/07/10.

613. Wolins NE, Quaynor BK, Skinner JR, Tzekov A, Croce MA, Gropler MC, et al. OXPAT/PAT-1 is a PPAR-induced lipid droplet protein that promotes fatty acid utilization. Diabetes. 2006;55(12):3418-28. Epub 2006/11/30.

614. Hope RG, McLauchlan J. Sequence motifs required for lipid droplet association and protein stability are unique to the hepatitis C virus core protein. J Gen Virol. 2000;81(Pt 8):1913-25. Epub 2000/07/19.

615. Hope RG, Murphy DJ, McLauchlan J. The domains required to direct core proteins of hepatitis C virus and GB virus-B to lipid droplets share common features with plant oleosin proteins. The Journal of biological chemistry. 2002;277(6):4261-70. Epub 2001/11/14.

616. Targett-Adams P, Hope G, Boulant S, McLauchlan J. Maturation of hepatitis C virus core protein by signal peptide peptidase is required for virus production. The Journal of biological chemistry. 2008;283(24):16850-9. Epub 2008/04/22.

617. McLauchlan J. Lipid droplets and hepatitis C virus infection. Biochimica et biophysica acta. 2009;1791(6):552-9. Epub 2009/01/27.

618. Miyanari Y, Atsuzawa K, Usuda N, Watashi K, Hishiki T, Zayas M, et al. The lipid droplet is an important organelle for hepatitis C virus production. Nat Cell Biol. 2007;9(9):1089-97. Epub 2007/08/28.

619. Appel N, Zayas M, Miller S, Krijnse-Locker J, Schaller T, Friebe P, et al. Essential role of domain III of nonstructural protein 5A for hepatitis C virus infectious particle assembly. PLoS Pathog. 2008;4(3):e1000035. Epub 2008/03/29.

620. Camus G, Herker E, Modi AA, Haas JT, Ramage HR, Farese RV, Jr., et al. Diacylglycerol glycerol acyltransferase-1 localizes hepatitis C virus NS5A protein to lipid droplets and enhances NS5A interaction with the viral capsid core. The Journal of biological chemistry. 2013. Epub 2013/02/20.

621. Nevo-Yassaf I, Yaffe Y, Asher M, Ravid O, Eizenberg S, Henis YI, et al. Role for TBC1D20 and Rab1 in hepatitis C virus replication via interaction with lipid droplet-bound nonstructural protein 5A. Journal of virology. 2012;86(12):6491-502. Epub 2012/04/12.

622. Boulant S, Douglas MW, Moody L, Budkowska A, Targett-Adams P, McLauchlan J. Hepatitis C virus core protein induces lipid droplet redistribution in a microtubule- and dynein-dependent manner. Traffic. 2008;9(8):1268-82. Epub 2008/05/21.

623. Lyn RK, Kennedy DC, Stolow A, Ridsdale A, Pezacki JP. Dynamics of lipid droplets induced by the hepatitis C virus core protein. Biochem Biophys Res Commun. 2010;399(4):518-24. Epub 2010/08/04.

624. Ma Y, Anantpadma M, Timpe JM, Shanmugam S, Singh SM, Lemon SM, et al. Hepatitis C virus NS2 protein serves as a scaffold for virus assembly by interacting with both structural and nonstructural proteins. Journal of virology. 2011;85(1):86-97. Epub 2010/10/22.

625. Popescu CI, Callens N, Trinel D, Roingeard P, Moradpour D, Descamps V, et al. NS2 protein of hepatitis C virus interacts with structural and non-structural proteins towards virus assembly. PLoS Pathog. 2011;7(2):e1001278. Epub 2011/02/25.

626. Boson B, Granio O, Bartenschlager R, Cosset FL. A concerted action of hepatitis C virus p7 and nonstructural protein 2 regulates core localization at the endoplasmic reticulum and virus assembly. PLoS Pathog. 2011;7(7):e1002144. Epub 2011/08/05.

627. Ma Y, Yates J, Liang Y, Lemon SM, Yi M. NS3 helicase domains involved in infectious intracellular hepatitis C virus particle assembly. Journal of virology. 2008;82(15):7624-39. Epub 2008/05/30.

628. Jones DM, Atoom AM, Zhang X, Kottilil S, Russell RS. A genetic interaction between the core and NS3 proteins of hepatitis C virus is essential for production of infectious virus. Journal of virology. 2011;85(23):12351-61. Epub 2011/10/01.

629. Cladaras C, Hadzopoulou-Cladaras M, Nolte RT, Atkinson D, Zannis VI. The complete sequence and structural analysis of human apolipoprotein B-100: relationship between apoB-100 and apoB-48 forms. EMBO J. 1986;5(13):3495-507. Epub 1986/12/20.

630. Knott TJ, Rall SC, Jr., Innerarity TL, Jacobson SF, Urdea MS, Levy-Wilson B, et al. Human apolipoprotein B: structure of carboxyl-terminal domains, sites of gene

expression, and chromosomal localization. Science. 1985;230(4721):37-43. Epub 1985/10/04.

631. Alexander CA, Hamilton RL, Havel RJ. Subcellular localization of B apoprotein of plasma lipoproteins in rat liver. J Cell Biol. 1976;69(2):241-63. Epub 1976/05/01.

632. Borchardt RA, Davis RA. Intrahepatic assembly of very low density lipoproteins. Rate of transport out of the endoplasmic reticulum determines rate of secretion. J Biol Chem. 1987;262(34):16394-402. Epub 1987/12/05.

633. Segrest JP, Jones MK, De Loof H, Dashti N. Structure of apolipoprotein B-100 in low density lipoproteins. Journal of lipid research. 2001;42(9):1346-67. Epub 2001/08/24.

634. Mann CJ, Anderson TA, Read J, Chester SA, Harrison GB, Kochl S, et al. The structure of vitellogenin provides a molecular model for the assembly and secretion of atherogenic lipoproteins. J Mol Biol. 1999;285(1):391-408. Epub 1999/01/08.

635. Jiang ZG, Gantz D, Bullitt E, McKnight CJ. Defining lipid-interacting domains in the N-terminal region of apolipoprotein B. Biochemistry. 2006;45(39):11799-808. Epub 2006/09/28.

636. Dashti N, Gandhi M, Liu X, Lin X, Segrest JP. The N-terminal 1000 residues of apolipoprotein B associate with microsomal triglyceride transfer protein to create a lipid transfer pocket required for lipoprotein assembly. Biochemistry. 2002;41(22):6978-87. Epub 2002/05/30.

637. Carraway M, Herscovitz H, Zannis V, Small DM. Specificity of lipid incorporation is determined by sequences in the N-terminal 37 of apoB. Biochemistry. 2000;39(32):9737-45. Epub 2000/08/10.

638. Hussain MM, Bakillah A, Nayak N, Shelness GS. Amino acids 430-570 in apolipoprotein B are critical for its binding to microsomal triglyceride transfer protein. The Journal of biological chemistry. 1998;273(40):25612-5. Epub 1998/09/25.

639. Liang J, Ginsberg HN. Microsomal triglyceride transfer protein binding and lipid transfer activities are independent of each other, but both are required for secretion of apolipoprotein B lipoproteins from liver cells. The Journal of biological chemistry. 2001;276(30):28606-12. Epub 2001/05/19.

640. Bradbury P, Mann CJ, Kochl S, Anderson TA, Chester SA, Hancock JM, et al. A common binding site on the microsomal triglyceride transfer protein for apolipoprotein B and protein disulfide isomerase. J Biol Chem. 1999;274(5):3159-64. Epub 1999/01/23.

641. Shelness GS, Hou L, Ledford AS, Parks JS, Weinberg RB. Identification of the lipoprotein initiating domain of apolipoprotein B. The Journal of biological chemistry. 2003;278(45):44702-7. Epub 2003/08/28.

642. Wang L, Martin DD, Genter E, Wang J, McLeod RS, Small DM. Surface study of apoB1694-1880, a sequence that can anchor apoB to lipoproteins and make it nonexchangeable. Journal of lipid research. 2009;50(7):1340-52. Epub 2009/03/03.

643. Hospattankar AV, Law SW, Lackner K, Brewer HB, Jr. Identification of low density lipoprotein receptor binding domains of human apolipoprotein B-100: a proposed consensus LDL receptor binding sequence of apoB-100. Biochem Biophys Res Commun. 1986;139(3):1078-85. Epub 1986/09/30.

644. Yang CY, Chen SH, Gianturco SH, Bradley WA, Sparrow JT, Tanimura M, et al. Sequence, structure, receptor-binding domains and internal repeats of human apolipoprotein B-100. Nature. 1986;323(6090):738-42. Epub 1986/10/23.

645. Wang L, Walsh MT, Small DM. Apolipoprotein B is conformationally flexible but anchored at a triolein/water interface: a possible model for lipoprotein surfaces. Proceedings of the National Academy of Sciences of the United States of America. 2006;103(18):6871-6. Epub 2006/04/26.

646. Sturley SL, Talmud PJ, Brasseur R, Culbertson MR, Humphries SE, Attie AD. Human apolipoprotein B signal sequence variants confer a secretion-defective phenotype when expressed in yeast. The Journal of biological chemistry. 1994;269(34):21670-5. Epub 1994/08/26.

647. Alder NN, Johnson AE. Cotranslational membrane protein biogenesis at the endoplasmic reticulum. The Journal of biological chemistry. 2004;279(22):22787-90. Epub 2004/03/19.

648. Rapoport TA. Protein translocation across the eukaryotic endoplasmic reticulum and bacterial plasma membranes. Nature. 2007;450(7170):663-9. Epub 2007/11/30.

649. Yamaguchi J, Conlon DM, Liang JJ, Fisher EA, Ginsberg HN. Translocation efficiency of apolipoprotein B is determined by the presence of beta-sheet domains, not pause transfer sequences. The Journal of biological chemistry. 2006;281(37):27063-71. Epub 2006/07/21.

650. Hussain MM, Shi J, Dreizen P. Microsomal triglyceride transfer protein and its role in apoB-lipoprotein assembly. Journal of lipid research. 2003;44(1):22-32. Epub 2003/01/09.

651. Rashid KA, Hevi S, Chen Y, Le Caherec F, Chuck SL. A proteomic approach identifies proteins in hepatocytes that bind nascent apolipoprotein B. The Journal of biological chemistry. 2002;277(24):22010-7. Epub 2002/04/06.

652. Zhang J, Herscovitz H. Nascent lipidated apolipoprotein B is transported to the Golgi as an incompletely folded intermediate as probed by its association with network of endoplasmic reticulum molecular chaperones, GRP94, ERp72, BiP, calreticulin, and cyclophilin B. The Journal of biological chemistry. 2003;278(9):7459-68. Epub 2002/10/25.

653. Qiu W, Kohen-Avramoglu R, Mhapsekar S, Tsai J, Austin RC, Adeli K. Glucosamine-induced endoplasmic reticulum stress promotes ApoB100 degradation: evidence for Grp78-mediated targeting to proteasomal degradation. Arteriosclerosis, thrombosis, and vascular biology. 2005;25(3):571-7. Epub 2004/12/25.

654. Zhou M, Fisher EA, Ginsberg HN. Regulated Co-translational ubiquitination of apolipoprotein B100. A new paradigm for proteasomal degradation of a secretory protein. J Biol Chem. 1998;273(38):24649-53. Epub 1998/09/12.

655. Fisher EA, Zhou M, Mitchell DM, Wu X, Omura S, Wang H, et al. The degradation of apolipoprotein B100 is mediated by the ubiquitin-proteasome pathway and involves heat shock protein 70. The Journal of biological chemistry. 1997;272(33):20427-34. Epub 1997/08/15.

656. Gusarova V, Caplan AJ, Brodsky JL, Fisher EA. Apoprotein B degradation is promoted by the molecular chaperones hsp90 and hsp70. The Journal of biological chemistry. 2001;276(27):24891-900. Epub 2001/05/03.

657. Schonfeld G. Familial hypobetalipoproteinemia: a review. Journal of lipid research. 2003;44(5):878-83. Epub 2003/03/18.

658. Pontrelli L, Sidiropoulos KG, Adeli K. Translational control of apolipoprotein B mRNA: regulation via cis elements in the 5' and 3' untranslated regions. Biochemistry. 2004;43(21):6734-44. Epub 2004/05/26.

659. Benoist F, Nicodeme E, Grand-Perret T. Microsomal triacylglycerol transfer protein prevents presecretory degradation of apolipoprotein B-100. A dithiothreitol-sensitive protease is involved. Eur J Biochem. 1996;240(3):713-20. Epub 1996/09/15.

660. Benoist F, Grand-Perret T. Co-translational degradation of apolipoprotein B100 by the proteasome is prevented by microsomal triglyceride transfer protein. Synchronized translation studies on HepG2 cells treated with an inhibitor of microsomal triglyceride transfer protein. The Journal of biological chemistry. 1997;272(33):20435-42. Epub 1997/08/15.

661. Siuta-Mangano P, Janero DR, Lane MD. Association and assembly of triglyceride and phospholipid with glycosylated and unglycosylated apoproteins of very low density lipoprotein in the intact liver cell. The Journal of biological chemistry. 1982;257(19):11463-7. Epub 1982/10/10.

662. Vukmirica J, Nishimaki-Mogami T, Tran K, Shan J, McLeod RS, Yuan J, et al. The N-linked oligosaccharides at the amino terminus of human apoB are important for the assembly and secretion of VLDL. Journal of lipid research. 2002;43(9):1496-507. Epub 2002/09/18.

663. Sparks JD, Sparks CE. Insulin modulation of hepatic synthesis and secretion of apolipoprotein B by rat hepatocytes. J Biol Chem. 1990;265(15):8854-62. Epub 1990/05/25.

664. Brewer HB, Jr., Hoeg JM, Beg Z, Fojo SS, Gregg RE. Translational and post-translational processing in apolipoprotein metabolism. Agents Actions Suppl. 1988;26:133. Epub 1988/01/01.

665. Wetterau JR, Zilversmit DB. Purification and characterization of microsomal triglyceride and cholesteryl ester transfer protein from bovine liver microsomes. Chem Phys Lipids. 1985;38(1-2):205-22. Epub 1985/08/30.

666. Wetterau JR, Combs KA, Spinner SN, Joiner BJ. Protein disulfide isomerase is a component of the microsomal triglyceride transfer protein complex. The Journal of biological chemistry. 1990;265(17):9800-7. Epub 1990/06/15.

667. Segrest JP, Jones MK, Dashti N. N-terminal domain of apolipoprotein B has structural homology to lipovitellin and microsomal triglyceride transfer protein: a "lipid pocket" model for self-assembly of apob-containing lipoprotein particles. Journal of lipid research. 1999;40(8):1401-16. Epub 1999/08/03.

668. Sharp D, Blinderman L, Combs KA, Kienzle B, Ricci B, Wager-Smith K, et al. Cloning and gene defects in microsomal triglyceride transfer protein associated with abetalipoproteinaemia. Nature. 1993;365(6441):65-9. Epub 1993/09/02.

669. Berriot-Varoqueaux N, Aggerbeck LP, Samson-Bouma M, Wetterau JR. The role of the microsomal triglygeride transfer protein in abetalipoproteinemia. Annu Rev Nutr. 2000;20:663-97. Epub 2000/08/15.

670. Haghpassand M, Wilder D, Moberly JB. Inhibition of apolipoprotein B and triglyceride secretion in human hepatoma cells (HepG2). Journal of lipid research. 1996;37(7):1468-80. Epub 1996/07/01.

671. Jamil H, Gordon DA, Eustice DC, Brooks CM, Dickson JK, Jr., Chen Y, et al. An inhibitor of the microsomal triglyceride transfer protein inhibits apoB secretion from HepG2 cells. Proc Natl Acad Sci U S A. 1996;93(21):11991-5. Epub 1996/10/15.

672. Gordon DA, Jamil H, Gregg RE, Olofsson SO, Boren J. Inhibition of the microsomal triglyceride transfer protein blocks the first step of apolipoprotein B lipoprotein assembly but not the addition of bulk core lipids in the second step. J Biol Chem. 1996;271(51):33047-53. Epub 1996/12/20.

673. Tietge UJ, Bakillah A, Maugeais C, Tsukamoto K, Hussain M, Rader DJ. Hepatic overexpression of microsomal triglyceride transfer protein (MTP) results in increased in vivo secretion of VLDL triglycerides and apolipoprotein B. Journal of lipid research. 1999;40(11):2134-9. Epub 1999/12/20.

674. Wetterau JR, Zilversmit DB. A triglyceride and cholesteryl ester transfer protein associated with liver microsomes. The Journal of biological chemistry. 1984;259(17):10863-6. Epub 1984/09/10.

675. Bakillah A, Hussain MM. Binding of microsomal triglyceride transfer protein to lipids results in increased affinity for apolipoprotein B: evidence for stable microsomal MTP-lipid complexes. The Journal of biological chemistry. 2001;276(33):31466-73. Epub 2001/06/28.

676. Wang Y, Tran K, Yao Z. The activity of microsomal triglyceride transfer protein is essential for accumulation of triglyceride within microsomes in McA-RH7777 cells. A unified model for the assembly of very low density lipoproteins. The Journal of biological chemistry. 1999;274(39):27793-800. Epub 1999/09/17.

677. Shelness GS, Sellers JA. Very-low-density lipoprotein assembly and secretion. Curr Opin Lipidol. 2001;12(2):151-7. Epub 2001/03/27.

678. Wang H, Gilham D, Lehner R. Proteomic and lipid characterization of apolipoprotein B-free luminal lipid droplets from mouse liver microsomes: implications for very low density lipoprotein assembly. The Journal of biological chemistry. 2007;282(45):33218-26. Epub 2007/09/13.

679. Yang LY, Kuksis A, Myher JJ, Steiner G. Contribution of de novo fatty acid synthesis to very low density lipoprotein triacylglycerols: evidence from mass isotopomer distribution analysis of fatty acids synthesized from [2H6]ethanol. Journal of lipid research. 1996;37(2):262-74. Epub 1996/02/01.

680. Lankester DL, Brown AM, Zammit VA. Use of cytosolic triacylglycerol hydrolysis products and of exogenous fatty acid for the synthesis of triacylglycerol secreted by cultured rat hepatocytes. Journal of lipid research. 1998;39(9):1889-95. Epub 1998/09/19.

681. Gilham D, Ho S, Rasouli M, Martres P, Vance DE, Lehner R. Inhibitors of hepatic microsomal triacylglycerol hydrolase decrease very low density lipoprotein secretion. FASEB journal : official publication of the Federation of American Societies for Experimental Biology. 2003;17(12):1685-7. Epub 2003/09/06.

682. Gibbons GF, Khurana R, Odwell A, Seelaender MC. Lipid balance in HepG2 cells: active synthesis and impaired mobilization. Journal of lipid research. 1994;35(10):1801-8. Epub 1994/10/01.

683. Boren J, Wettesten M, Rustaeus S, Andersson M, Olofsson SO. The assembly and secretion of apoB-100-containing lipoproteins. Biochem Soc Trans. 1993;21(2):487-93. Epub 1993/05/01.

684. Lehner R, Cui Z, Vance DE. Subcellullar localization, developmental expression and characterization of a liver triacylglycerol hydrolase. The Biochemical journal. 1999;338 (Pt 3):761-8. Epub 1999/03/03.

685. Gusarova V, Brodsky JL, Fisher EA. Apolipoprotein B100 exit from the endoplasmic reticulum (ER) is COPII-dependent, and its lipidation to very low density lipoprotein occurs post-ER. The Journal of biological chemistry. 2003;278(48):48051-8. Epub 2003/09/10.

686. Asp L, Magnusson B, Rutberg M, Li L, Boren J, Olofsson SO. Role of ADP ribosylation factor 1 in the assembly and secretion of ApoB-100-containing lipoproteins. Arteriosclerosis, thrombosis, and vascular biology. 2005;25(3):566-70. Epub 2004/12/25.

687. Asp L, Claesson C, Boren J, Olofsson SO. ADP-ribosylation factor 1 and its activation of phospholipase D are important for the assembly of very low density lipoproteins. The Journal of biological chemistry. 2000;275(34):26285-92. Epub 2000/06/14.

688. Tran K, Sun F, Cui Z, Thorne-Tjomsland G, St Germain C, Lapierre LR, et al. Attenuated secretion of very low density lipoproteins from McA-RH7777 cells treated with eicosapentaenoic acid is associated with impaired utilization of triacylglycerol synthesized via phospholipid remodeling. Biochimica et biophysica acta. 2006;1761(4):463-73. Epub 2006/05/06.

689. Tran K, Wang Y, DeLong CJ, Cui Z, Yao Z. The assembly of very low density lipoproteins in rat hepatoma McA-RH7777 cells is inhibited by phospholipase A2 antagonists. The Journal of biological chemistry. 2000;275(32):25023-30. Epub 2000/05/29.

690. Gusarova V, Seo J, Sullivan ML, Watkins SC, Brodsky JL, Fisher EA. Golgi-associated maturation of very low density lipoproteins involves conformational changes in apolipoprotein B, but is not dependent on apolipoprotein E. The Journal of biological chemistry. 2007;282(27):19453-62. Epub 2007/05/15.

691. Ye J, Li JZ, Liu Y, Li X, Yang T, Ma X, et al. Cideb, an ER- and lipid droplet-associated protein, mediates VLDL lipidation and maturation by interacting with apolipoprotein B. Cell Metab. 2009;9(2):177-90. Epub 2009/02/04.

692. Fisher EA, Pan M, Chen X, Wu X, Wang H, Jamil H, et al. The triple threat to nascent apolipoprotein B. Evidence for multiple, distinct degradative pathways. J Biol Chem. 2001;276(30):27855-63. Epub 2001/04/04.

693. Chirieac DV, Davidson NO, Sparks CE, Sparks JD. PI3-kinase activity modulates apo B available for hepatic VLDL production in apobec-1-/- mice. Am J Physiol Gastrointest Liver Physiol. 2006;291(3):G382-8. Epub 2006/06/27.

694. Brodsky JL. The protective and destructive roles played by molecular chaperones during ERAD (endoplasmic-reticulum-associated degradation). The Biochemical journal. 2007;404(3):353-63. Epub 2007/05/25.

695. Nakatsukasa K, Huyer G, Michaelis S, Brodsky JL. Dissecting the ER-associated degradation of a misfolded polytopic membrane protein. Cell. 2008;132(1):101-12. Epub 2008/01/15.

696. Schroder M, Kaufman RJ. The mammalian unfolded protein response. Annu Rev Biochem. 2005;74:739-89. Epub 2005/06/15.

697. Ron D, Walter P. Signal integration in the endoplasmic reticulum unfolded protein response. Nat Rev Mol Cell Biol. 2007;8(7):519-29. Epub 2007/06/15.

698. Pan M, Cederbaum AI, Zhang YL, Ginsberg HN, Williams KJ, Fisher EA. Lipid peroxidation and oxidant stress regulate hepatic apolipoprotein B degradation and VLDL production. J Clin Invest. 2004;113(9):1277-87. Epub 2004/05/05.

699. Holm C, Kirchgessner TG, Svenson KL, Fredrikson G, Nilsson S, Miller CG, et al. Hormone-sensitive lipase: sequence, expression, and chromosomal localization to 19 cent-q13.3. Science. 1988;241(4872):1503-6. Epub 1988/09/16.

700. Langin D, Laurell H, Holst LS, Belfrage P, Holm C. Gene organization and primary structure of human hormone-sensitive lipase: possible significance of a sequence homology with a lipase of Moraxella TA144, an antarctic bacterium. Proceedings of the National Academy of Sciences of the United States of America. 1993;90(11):4897-901. Epub 1993/06/01.

701. Mairal A, Melaine N, Laurell H, Grober J, Holst LS, Guillaudeux T, et al. Characterization of a novel testicular form of human hormone-sensitive lipase. Biochem Biophys Res Commun. 2002;291(2):286-90. Epub 2002/02/16.

702. Mulder H, Holst LS, Svensson H, Degerman E, Sundler F, Ahren B, et al. Hormone-sensitive lipase, the rate-limiting enzyme in triglyceride hydrolysis, is expressed and active in beta-cells. Diabetes. 1999;48(1):228-32. Epub 1999/01/19.

703. Zimmermann R, Strauss JG, Haemmerle G, Schoiswohl G, Birner-Gruenberger R, Riederer M, et al. Fat mobilization in adipose tissue is promoted by adipose triglyceride lipase. Science. 2004;306(5700):1383-6. Epub 2004/11/20.

704. Ong KT, Mashek MT, Bu SY, Greenberg AS, Mashek DG. Adipose triglyceride lipase is a major hepatic lipase that regulates triacylglycerol turnover and fatty acid signaling and partitioning. Hepatology. 2011;53(1):116-26. Epub 2010/10/23.

705. Reid BN, Ables GP, Otlivanchik OA, Schoiswohl G, Zechner R, Blaner WS, et al. Hepatic overexpression of hormone-sensitive lipase and adipose triglyceride lipase promotes fatty acid oxidation, stimulates direct release of free fatty acids, and ameliorates steatosis. The Journal of biological chemistry. 2008;283(19):13087-99. Epub 2008/03/14.

706. Alam M, Ho S, Vance DE, Lehner R. Heterologous expression, purification, and characterization of human triacylglycerol hydrolase. Protein Expr Purif. 2002;24(1):33-42. Epub 2002/01/29.

707. Satoh T, Hosokawa M. The mammalian carboxylesterases: from molecules to functions. Annu Rev Pharmacol Toxicol. 1998;38:257-88. Epub 1998/05/23.

708. Lehner R, Verger R. Purification and characterization of a porcine liver microsomal triacylglycerol hydrolase. Biochemistry. 1997;36(7):1861-8. Epub 1997/02/18.

709. Robbi M, Beaufay H. The COOH terminus of several liver carboxylesterases targets these enzymes to the lumen of the endoplasmic reticulum. The Journal of biological chemistry. 1991;266(30):20498-503. Epub 1991/10/25.

710. Dolinsky VW, Sipione S, Lehner R, Vance DE. The cloning and expression of a murine triacylglycerol hydrolase cDNA and the structure of its corresponding gene. Biochimica et biophysica acta. 2001;1532(3):162-72. Epub 2001/07/27.

711. Alam M, Vance DE, Lehner R. Structure-function analysis of human triacylglycerol hydrolase by site-directed mutagenesis: identification of the catalytic triad and a glycosylation site. Biochemistry. 2002;41(21):6679-87. Epub 2002/05/23.

712. Bencharit S, Morton CL, Howard-Williams EL, Danks MK, Potter PM, Redinbo MR. Structural insights into CPT-11 activation by mammalian carboxylesterases. Nat Struct Biol. 2002;9(5):337-42. Epub 2002/04/23.

713. Bencharit S, Morton CL, Hyatt JL, Kuhn P, Danks MK, Potter PM, et al. Crystal structure of human carboxylesterase 1 complexed with the Alzheimer's drug tacrine: from binding promiscuity to selective inhibition. Chem Biol. 2003;10(4):341-9. Epub 2003/05/03.

714. Bencharit S, Morton CL, Xue Y, Potter PM, Redinbo MR. Structural basis of heroin and cocaine metabolism by a promiscuous human drug-processing enzyme. Nat Struct Biol. 2003;10(5):349-56. Epub 2003/04/08.

715. Wong H, Schotz MC. The lipase gene family. Journal of lipid research. 2002;43(7):993-9. Epub 2002/07/02.

716. Dolinsky VW, Gilham D, Alam M, Vance DE, Lehner R. Triacylglycerol hydrolase: role in intracellular lipid metabolism. Cell Mol Life Sci. 2004;61(13):1633-51. Epub 2004/06/30.

717. Shibata F, Takagi Y, Kitajima M, Kuroda T, Omura T. Molecular cloning and characterization of a human carboxylesterase gene. Genomics. 1993;17(1):76-82. Epub 1993/07/01.

718. Douglas DN, Dolinsky VW, Lehner R, Vance DE. A role for Sp1 in the transcriptional regulation of hepatic triacylglycerol hydrolase in the mouse. J Biol Chem. 2001;276(27):25621-30. Epub 2001/05/05.

719. Dolinsky VW, Gilham D, Hatch GM, Agellon LB, Lehner R, Vance DE. Regulation of triacylglycerol hydrolase expression by dietary fatty acids and peroxisomal proliferator-activated receptors. Biochimica et biophysica acta. 2003;1635(1):20-8. Epub 2003/12/04.

720. Staels B, van Tol A, Chan L, Verhoeven G, Auwerx J. Variable effects of different corticosteroids on plasma lipids, apolipoproteins, and hepatic apolipoprotein mRNA levels in rats. Arterioscler Thromb. 1991;11(3):760-9. Epub 1991/05/01.

721. Dolinsky VW, Douglas DN, Lehner R, Vance DE. Regulation of the enzymes of hepatic microsomal triacylglycerol lipolysis and re-esterification by the glucocorticoid dexamethasone. The Biochemical journal. 2004;378(Pt 3):967-74. Epub 2003/12/10.

722. Hosokawa M, Hattori K, Satoh T. Differential responses of rat hepatic microsomal carboxylesterase isozymes to glucocorticoids and pregnenolone 16 alpha-carbonitrile. Biochem Pharmacol. 1993;45(11):2317-22. Epub 1993/06/09.

723. Zhu W, Song L, Zhang H, Matoney L, LeCluyse E, Yan B. Dexamethasone differentially regulates expression of carboxylesterase genes in humans and rats. Drug Metab Dispos. 2000;28(2):186-91. Epub 2000/01/21.

724. Verine A, Le Petit-Thevenin J, Panicot-Dubois L, Valette A, Lombardo D. Phosphorylation of the oncofetal variant of the human bile salt-dependent lipase. identification of phosphorylation site and relation with secretion process. The Journal of biological chemistry. 2001;276(15):12356-61. Epub 2001/01/20.

725. Lehner R, Vance DE. Cloning and expression of a cDNA encoding a hepatic microsomal lipase that mobilizes stored triacylglycerol. The Biochemical journal. 1999;343 Pt 1:1-10. Epub 1999/09/24.

726. Wei E, Alam M, Sun F, Agellon LB, Vance DE, Lehner R. Apolipoprotein B and triacylglycerol secretion in human triacylglycerol hydrolase transgenic mice. Journal of lipid research. 2007;48(12):2597-606. Epub 2007/09/20.

727. Wei E, Ben Ali Y, Lyon J, Wang H, Nelson R, Dolinsky VW, et al. Loss of TGH/Ces3 in mice decreases blood lipids, improves glucose tolerance, and increases energy expenditure. Cell Metab. 2010;11(3):183-93. Epub 2010/03/04.

728. Lian J, Wei E, Wang SP, Quiroga AD, Li L, Pardo AD, et al. Liver specific inactivation of carboxylesterase 3/triacylglycerol hydrolase decreases blood lipids without causing severe steatosis in mice. Hepatology. 2012;56(6):2154-62. Epub 2012/06/19.

729. Blais DR, Lyn RK, Joyce MA, Rouleau Y, Steenbergen R, Barsby N, et al. Activity-based protein profiling identifies a host enzyme, carboxylesterase 1, which is differentially active during hepatitis C virus replication. The Journal of biological chemistry. 2010;285(33):25602-12. Epub 2010/06/10.

730. Yu MC, Skipper PL, Tannenbaum SR, Chan KK, Ross RK. Arylamine exposures and bladder cancer risk. Mutat Res. 2002;506-507:21-8. Epub 2002/09/28.

731. Probst MR, Beer M, Beer D, Jeno P, Meyer UA, Gasser R. Human liver arylacetamide deacetylase. Molecular cloning of a novel esterase involved in the metabolic activation of arylamine carcinogens with high sequence similarity to hormone-sensitive lipase. J Biol Chem. 1994;269(34):21650-6. Epub 1994/08/26.

732. Kobayashi Y, Fukami T, Higuchi R, Nakajima M, Yokoi T. Metabolic activation by human arylacetamide deacetylase, CYP2E1, and CYP1A2 causes phenacetin-induced methemoglobinemia. Biochem Pharmacol. 2012;84(9):1196-206. Epub 2012/09/04.

733. Watanabe A, Fukami T, Nakajima M, Takamiya M, Aoki Y, Yokoi T. Human arylacetamide deacetylase is a principal enzyme in flutamide hydrolysis. Drug metabolism and disposition: the biological fate of chemicals. 2009;37(7):1513-20. Epub 2009/04/03.

734. Yamazaki K, Kusano K, Tadano K, Tanaka I. Radiation hybrid mapping of human arylacetamide deacetylase (AADAC) locus to chromosome 3. Genomics. 1997;44(2):248-50. Epub 1997/09/23.

735. Trickett JI, Patel DD, Knight BL, Saggerson ED, Gibbons GF, Pease RJ. Characterization of the rodent genes for arylacetamide deacetylase, a putative microsomal lipase, and evidence for transcriptional regulation. The Journal of biological chemistry. 2001;276(43):39522-32. Epub 2001/08/02.

736. Ross MK, Crow JA. Human carboxylesterases and their role in xenobiotic and endobiotic metabolism. J Biochem Mol Toxicol. 2007;21(4):187-96. Epub 2007/10/16.

737. Gibbons GF. Assembly and secretion of hepatic very-low-density lipoprotein. The Biochemical journal. 1990;268(1):1-13. Epub 1990/05/15.

738. Zhang Y, Cheng X, Aleksunes L, Klaassen CD. Transcription factor-mediated regulation of carboxylesterase enzymes in livers of mice. Drug Metab Dispos. 2012;40(6):1191-7. Epub 2012/03/21.

739. Riegler B, Besenboeck C, Bauer R, Nimpf J, Schneider WJ. Enzymes involved in hepatic acylglycerol metabolism in the chicken. Biochem Biophys Res Commun. 2011;406(2):257-61. Epub 2011/02/15.

740. Lo V, Erickson B, Thomason-Hughes M, Ko KW, Dolinsky VW, Nelson R, et al. Arylacetamide deacetylase attenuates fatty-acid-induced triacylglycerol accumulation in rat hepatoma cells. Journal of lipid research. 2010;51(2):368-77. Epub 2009/08/06.

741. Huang H, Sun F, Owen DM, Li W, Chen Y, Gale M, Jr., et al. Hepatitis C virus production by human hepatocytes dependent on assembly and secretion of very low-density lipoproteins. Proceedings of the National Academy of Sciences of the United States of America. 2007;104(14):5848-53. Epub 2007/03/23.

742. Jiang J, Luo G. Apolipoprotein E but not B is required for the formation of infectious hepatitis C virus particles. Journal of virology. 2009;83(24):12680-91. Epub 2009/10/02.

743. Benga WJ, Krieger SE, Dimitrova M, Zeisel MB, Parnot M, Lupberger J, et al. Apolipoprotein E interacts with hepatitis C virus nonstructural protein 5A and determines assembly of infectious particles. Hepatology. 2010;51(1):43-53. Epub 2009/12/17.

744. Cun W, Jiang J, Luo G. The C-terminal alpha-helix domain of apolipoprotein E is required for interaction with nonstructural protein 5A and assembly of hepatitis C virus. Journal of virology. 2010;84(21):11532-41. Epub 2010/08/20.

745. Icard V, Diaz O, Scholtes C, Perrin-Cocon L, Ramiere C, Bartenschlager R, et al. Secretion of hepatitis C virus envelope glycoproteins depends on assembly of apolipoprotein B positive lipoproteins. PloS one. 2009;4(1):e4233. Epub 2009/01/22.

746. Sasaki T, Kishi M, Saito M, Tanaka T, Higuchi N, Kominami E, et al. Inhibitory effect of di- and tripeptidyl aldehydes on calpains and cathepsins. J Enzyme Inhib. 1990;3(3):195-201. Epub 1990/01/01.

747. Gastaminza P, Cheng G, Wieland S, Zhong J, Liao W, Chisari FV. Cellular determinants of hepatitis C virus assembly, maturation, degradation, and secretion. Journal of virology. 2008;82(5):2120-9. Epub 2007/12/14.

748. Lai CK, Jeng KS, Machida K, Lai MM. Hepatitis C virus egress and release depend on endosomal trafficking of core protein. Journal of virology. 2010;84(21):11590-8. Epub 2010/08/27.

749. Coller KE, Heaton NS, Berger KL, Cooper JD, Saunders JL, Randall G. Molecular determinants and dynamics of hepatitis C virus secretion. PLoS Pathog. 2012;8(1):e1002466. Epub 2012/01/14.

750. Chen W, Feng Y, Chen D, Wandinger-Ness A. Rab11 is required for trans-golgi network-to-plasma membrane transport and a preferential target for GDP dissociation inhibitor. Mol Biol Cell. 1998;9(11):3241-57. Epub 1998/11/05.

751. Sollner T, Bennett MK, Whiteheart SW, Scheller RH, Rothman JE. A protein assembly-disassembly pathway in vitro that may correspond to sequential steps of synaptic vesicle docking, activation, and fusion. Cell. 1993;75(3):409-18. Epub 1993/11/05.

752. Bishe B, Syed GH, Field SJ, Siddiqui A. Role of phosphatidylinositol 4-phosphate (PI4P) and its binding protein GOLPH3 in hepatitis C virus secretion. The Journal of biological chemistry. 2012;287(33):27637-47. Epub 2012/06/30.

753. Neveu G, Barouch-Bentov R, Ziv-Av A, Gerber D, Jacob Y, Einav S. Identification and targeting of an interaction between a tyrosine motif within hepatitis C virus core protein and AP2M1 essential for viral assembly. PLoS Pathog. 2012;8(8):e1002845. Epub 2012/08/24.

754. Siagris D, Christofidou M, Theocharis GJ, Pagoni N, Papadimitriou C, Lekkou A, et al. Serum lipid pattern in chronic hepatitis C: histological and virological correlations. J Viral Hepat. 2006;13(1):56-61. Epub 2005/12/21.

755. Serfaty L, Andreani T, Giral P, Carbonell N, Chazouilleres O, Poupon R. Hepatitis C virus induced hypobetalipoproteinemia: a possible mechanism for steatosis in chronic hepatitis C. J Hepatol. 2001;34(3):428-34. Epub 2001/04/27.

756. Hofer H, Bankl HC, Wrba F, Steindl-Munda P, Peck-Radosavljevic M, Osterreicher C, et al. Hepatocellular fat accumulation and low serum cholesterol in patients infected with HCV-3a. Am J Gastroenterol. 2002;97(11):2880-5. Epub 2002/11/12.

757. Petit JM, Benichou M, Duvillard L, Jooste V, Bour JB, Minello A, et al. Hepatitis C virus-associated hypobetalipoproteinemia is correlated with plasma viral load, steatosis, and liver fibrosis. Am J Gastroenterol. 2003;98(5):1150-4.

758. Mirandola S, Realdon S, Iqbal J, Gerotto M, Dal Pero F, Bortoletto G, et al. Liver microsomal triglyceride transfer protein is involved in hepatitis C liver steatosis. Gastroenterology. 2006;130(6):1661-9. Epub 2006/05/16.

759. Yamaguchi A, Tazuma S, Nishioka T, Ohishi W, Hyogo H, Nomura S, et al. Hepatitis C virus core protein modulates fatty acid metabolism and thereby causes lipid accumulation in the liver. Dig Dis Sci. 2005;50(7):1361-71. Epub 2005/07/29.

760. Perlemuter G, Sabile A, Letteron P, Vona G, Topilco A, Chretien Y, et al. Hepatitis C virus core protein inhibits microsomal triglyceride transfer protein activity and very low density lipoprotein secretion: a model of viral-related steatosis. FASEB J. 2002;16(2):185-94. Epub 2002/01/31.

Chapter 2: Hypothesis, Aims and Rational

Hypothesis: Hepatitis C Virus induces steatosis by modulating the host molecular and cellular mechanisms that regulate VLDL assembly and secretion.

Aim 1. Investigate if HCV infection impairs the mass secretion of TG from lipid-loaded Huh7.5 cells.

Rationale: Hepatic steatosis is one of the striking features of chronic HCV (CHC) infection. The prevalence of steatosis in CHC is around 40-80% [table 1 in (1)], about 2-3 times more prevalent than HBV. Steatosis may lead to non-alcoholic steatohepatitis (NASH) and intensifies the process of liver fibrosis and enhances progression to cirrhosis. The etiology of steatosis in CHC is not perfectly known but at least two different types of steatosis have been defined. With genotypes other than 3, steatosis is positively correlated with BMI, therefore is mainly related to metabolic factors (Metabolic Fat), although cytopathic effect of the virus cannot be excluded (2). In genotype-3 steatosis is not correlated with metabolic factors but positively correlated with HCV replication (2), therefore is mainly related to cytopathic effect of virus (Viral Fat).
The possible mechanisms for HCV steatosis were discussed in introduction. As it was indicated before, hepatic steatosis seen in chronic HCV infected patients is often associated with hypobetalipoproteinemia (HBL), defined as low level of apoB-containing lipoprotein (VLDL and its derivatives) in serum (3-6). In addition HBL is resolved in patients treated with anti HCV therapy (3-6). As VLDL is exclusively secreted by the liver and is the only way by which liver exports TG, it is tempting to speculate that this process is impaired during HCV infection. Although enhanced de novo lipogenesis and/or impaired β-oxidation have been suggested as other possible mechanisms of HCV steatosis, these mechanisms are not able to explain the HBL associated with HCV infection. Even if these mechanisms are part of the lipid irregularities that occur in HCV infection, it is likely that they occur in conjunction with impaired VLDL-TG secretion.

Aim 2. Investigate if any cellular processes relevant to VLDL assembly are differentially modulated during HCV infection.

Rationale: VLDL assembly and secretion has been reviewed in the introduction. As it was discussed, a hypothetical two-step model of VLDL assembly and secretion has been widely accepted. ApoB100 is mandatory for formation and secretion of VLDL. ApoB is transcribed at relatively constants levels (7) and the availability of lipid (in particular TG)

for interaction with newly synthesized apoB regulates the amount of apoB (and VLDL) degradation or secretion. In this process, co-translational lipidation of the nascent apoB is the major regulator since poorly lipidated apoB is destined for degradation by the proteasome (7-10). A key role for MTP in early lipidation of apoB100 has been established (11-14). In addition MTP may also be required for the formation of a luminal TG storage droplet from cytosolic lipid pool (15, 16). After initial lipidation of apoB100, dense poorly lipidated VLDL (pre-VLDL) is formed. In the second step the pre-VLDL acquires more lipids to form a low density fully lipidated mature VLDL (17). Although the luminal lipid pool likely is the immediate source for second step of apoB lipidation and maturation, about 70% of VLDL-TG originates from cytosolic lipid droplets (573). As it was discussed in the introduction, this process of lipidation requires lipolysis and re-esterification of luminal lipids and is believed to be mediated by luminal lipases (667). If HCV impairs the VLDL-TG secretion, then it is possible that at least one of the above factors has been affected by HCV.

Aim 1 is expected to demonstrate if impaired VLDL assembly contributes to the cellular accumulation of TG stores. However, it remains a possibility that impaired VLDL production occurs without the accumulation of cellular TG stores. For example, HCV infected cells may secrete the same amount of TG (from pre-formed stores) but this TG may be loaded onto more or less ApoB-containing lipoprotein particles (VLDL). In this case, impaired VLDL production by infected cells may not contribute to steatosis but may be important for the HCV lifecycle. Aim 2 is expected to provide mechanistic insight for the results obtained in Aim1, but is also relevant if cellular TG stores do not accumulate during HCV infection.

Aim 3. Investigate the role of putative TG lipases on VLDL assembly and HCV production by Huh7.5 cells.

Rationale: Two candidate luminal lipases have been suggested to have a role in lipidation of pre-VLDL. Triacylglycerol Hydrolase (TGH) has been widely studied and its role in lipidation of apoB and enhancement of TG secretion has been shown both in vivo and in vitro (18-21). Arylacetamide Deacetylase is a putative serine esterase and its role in VLDL secretion is much less understood. Although some evidences have suggested that it might be involved in VLDL secretion, a recent study in McArdle7777 cells has shown that it hydrolyze TG but directs the fatty acids for β-oxidation rather than re-esterification for secretion with VLDL (22). Both TGH and AADAC have been reported to be absent from HepG2 cells. It is not known if these are present in Huh7.5 cells. We will explore the possibility that these lipases (and/or others) play a role in the recruitment of

cellular TG stores for output as VLDL by Huh7.5 cells and whether or not these lipases are differentially modulated during HCV infection. Since the lipolysis of cellular TG stores is expected to impact HCV production, the role of these lipases in the HCV lifecycle will also be examined.

References

1. Asselah T, Rubbia-Brandt L, Marcellin P, Negro F. Steatosis in chronic hepatitis C: why does it really matter? Gut. 2006;55(1):123-30. Epub 2005/12/14.

2. Rubbia-Brandt L, Quadri R, Abid K, Giostra E, Male PJ, Mentha G, et al. Hepatocyte steatosis is a cytopathic effect of hepatitis C virus genotype 3. J Hepatol. 2000;33(1):106-15. Epub 2000/07/25.

3. Siagris D, Christofidou M, Theocharis GJ, Pagoni N, Papadimitriou C, Lekkou A, et al. Serum lipid pattern in chronic hepatitis C: histological and virological correlations. J Viral Hepat. 2006;13(1):56-61. Epub 2005/12/21.

4. Serfaty L, Andreani T, Giral P, Carbonell N, Chazouilleres O, Poupon R. Hepatitis C virus induced hypobetalipoproteinemia: a possible mechanism for steatosis in chronic hepatitis C. J Hepatol. 2001;34(3):428-34. Epub 2001/04/27.

5. Poynard T, Ratziu V, McHutchison J, Manns M, Goodman Z, Zeuzem S, et al. Effect of treatment with peginterferon or interferon alfa-2b and ribavirin on steatosis in patients infected with hepatitis C. Hepatology. 2003;38(1):75-85. Epub 2003/06/28.

6. Hofer H, Bankl HC, Wrba F, Steindl-Munda P, Peck-Radosavljevic M, Osterreicher C, et al. Hepatocellular fat accumulation and low serum cholesterol in patients infected with HCV-3a. Am J Gastroenterol. 2002;97(11):2880-5. Epub 2002/11/12.

7. Adeli K. Regulated intracellular degradation of apolipoprotein B in semipermeable HepG2 cells. The Journal of biological chemistry. 1994;269(12):9166-75.

8. Yeung SJ, Chen SH, Chan L. Ubiquitin-proteasome pathway mediates intracellular degradation of apolipoprotein B. Biochemistry. 1996;35(43):13843-8.

9. Adeli K, Wettesten M, Asp L, Mohammadi A, Macri J, Olofsson SO. Intracellular assembly and degradation of apolipoprotein B-100-containing lipoproteins in digitonin-permeabilized HEP G2 cells. The Journal of biological chemistry. 1997;272(8):5031-9.

10. Wu X, Sakata N, Lele KM, Zhou M, Jiang H, Ginsberg HN. A two-site model for ApoB degradation in HepG2 cells. The Journal of biological chemistry. 1997;272(17):11575-80.

11. Jamil H, Dickson JK, Jr., Chu CH, Lago MW, Rinehart JK, Biller SA, et al. Microsomal triglyceride transfer protein. Specificity of lipid binding and transport. The Journal of biological chemistry. 1995;270(12):6549-54.

12. Hussain MM, Bakillah A, Nayak N, Shelness GS. Amino acids 430-570 in apolipoprotein B are critical for its binding to microsomal triglyceride transfer protein. The Journal of biological chemistry. 1998;273(40):25612-5. Epub 1998/09/25.

13. Perlemuter G, Letteron P, Carnot F, Zavala F, Pessayre D, Nalpas B, et al. Alcohol and hepatitis C virus core protein additively increase lipid peroxidation and synergistically trigger hepatic cytokine expression in a transgenic mouse model. J Hepatol. 2003;39(6):1020-7. Epub 2003/12/04.

14. Leung GK, Veniant MM, Kim SK, Zlot CH, Raabe M, Bjorkegren J, et al. A deficiency of microsomal triglyceride transfer protein reduces apolipoprotein B secretion. The Journal of biological chemistry. 2000;275(11):7515-20.

15. Wang Y, Tran K, Yao Z. The activity of microsomal triglyceride transfer protein is essential for accumulation of triglyceride within microsomes in McA-RH7777 cells. A unified model for the assembly of very low density lipoproteins. The Journal of biological chemistry. 1999;274(39):27793-800. Epub 1999/09/17.

16. Kulinski A, Rustaeus S, Vance JE. Microsomal triacylglycerol transfer protein is required for lumenal accretion of triacylglycerol not associated with ApoB, as well as for ApoB lipidation. The Journal of biological chemistry. 2002;277(35):31516-25.

17. Shelness GS, Sellers JA. Very-low-density lipoprotein assembly and secretion. Curr Opin Lipidol. 2001;12(2):151-7. Epub 2001/03/27.

18. Gibbons GF, Khurana R, Odwell A, Seelaender MC. Lipid balance in HepG2 cells: active synthesis and impaired mobilization. Journal of lipid research. 1994;35(10):1801-8. Epub 1994/10/01.

19. Boren J, Wettesten M, Rustaeus S, Andersson M, Olofsson SO. The assembly and secretion of apoB-100-containing lipoproteins. Biochem Soc Trans. 1993;21(2):487-93. Epub 1993/05/01.

20. Lehner R, Vance DE. Cloning and expression of a cDNA encoding a hepatic microsomal lipase that mobilizes stored triacylglycerol. The Biochemical journal. 1999;343 Pt 1:1-10. Epub 1999/09/24.

21. Wei E, Ben Ali Y, Lyon J, Wang H, Nelson R, Dolinsky VW, et al. Loss of TGH/Ces3 in mice decreases blood lipids, improves glucose tolerance, and increases energy expenditure. Cell Metab. 2010;11(3):183-93. Epub 2010/03/04.

22. Lo V, Erickson B, Thomason-Hughes M, Ko KW, Dolinsky VW, Nelson R, et al. Arylacetamide deacetylase attenuates fatty-acid-induced triacylglycerol accumulation in rat hepatoma cells. Journal of lipid research. 2010;51(2):368-77. Epub 2009/08/06.

3-Results

The results of our experiments will be presented in two papers.

Paper 1

Entitled: Arylacetamide deacetylase: a novel host factor with important roles in the lipolysis of cellular triacylglycerol stores, VLDL assembly and HCV production.

In this paper, we utilized the Huh7.5/JFH-1 HCV cell culture model to investigate the VLDL secretory pathway in Huh7.5 cells and the impact of HCV infection on this process (Aim 1). The key regulators of VLDL assembly were analyzed using established biochemical approaches (Aim 2). We have shown that infected cells have reduced mobilization of TG from preformed lipid stores for secretion with VLDL and indeed they secreted VLDL with lesser amount of TG in comparison to naïve cells (Aims 1&2). This was partially explained by the absence of a putative TG lipase, AADAC (Aim3), the downregulation of which coincided with the early peak of viral infection. TGH was absent from these cells altogether (Aim3). We have also shown that AADAC is required for HCV production during the acute stages of HCV infection, indicating a role for AADAC in the HCV lifecycle (Aim 3).

Author Contributions

Mahra Nourbakhsh: Designing the project and the strategy to test the hypothesis, writing the manuscript, performing assays and experiments, managing and overseeing technical support, collecting and analyzing the data.

Dr. Donna Douglas: Designing the project and the strategy to test the hypothesis, writing the manuscript and supervision.

Dr. Norman Kneteman: Designing the project and the strategy to test the hypothesis, critical reading, and supervision.

Dr. Richard Lehner: Design the project and strategy to test the hypothesis and critical reading.

Mr. Christopher Hao Pu: Technical support, generation of AADAC overexpression and shRNA knock down of AADAC.

Mr. Jamie Lewis: Technical Support, cell culture and management of viral stocks.

Mr. Randy Nelson: Quantitative RT-PCR of AADAC.

Dr. Toshiyasu Kawahara: Assisting in statistical analysis and discussions.

Dr. Luiz Lisboa: FACS analysis.

Dr. Enhui Wei and Dr. Ariel Quiroga: Thin Layer Chromatography.

Dr. Lok Man John Law and Chao Chen: Analyzing HCV Infectivity titer and HCV growth curve.

Dr. Sonal Asthana: Assisting in lipid droplets staining.

Dr. William R. Addison: Critical reading and discussion.

Dr. Michael Houghton: Critical reading, provision of reagents, academic support.

Arylacetamide deacetylase: a novel host factor with important roles in the lipolysis of cellular triacylglycerol stores, VLDL assembly and HCV production [i]

Mahra Nourbakhsh[1,7*], Donna N. Douglas[1,7*¶], Christopher Hao Pu[1,7], Jamie T. Lewis[1,7], Toshiyasu Kawahara[1,7], Luiz F. Lisboa[6,7], Enhui Wei[1,7], Sonal Asthana[1,7], Ariel D. Quiroga[4], Lok Man John Law[5,7], Chao Chen[5,7], William R. Addison[5,7], Randy Nelson[2], Michael Houghton[5,7], Richard Lehner[3,4], Norman M. Kneteman[1,7]

From the Departments of [1]Surgery, [2]Biochemistry, [3]Cell Biology,

[4]Pediatrics, [5]Med Microbiology & Immunology, [6]Transplant Infectious Diseases, and [7]Li Ka Shing Institute of Virology, University of Alberta, Edmonton, Alberta, T6G 2E1, Canada

* D.N. Douglas and M. Nourbakhsh contributed equally to this work

Address correspondence to:

Donna N. Douglas, PhD

6-010A Katz Group-Rexall Centre,

Department of Surgery, University of Alberta,

Edmonton, Alberta, T6G 2E1, Canada.

Phone: 780-492-7921

FAX: 780-407-7374

E-mail: donnad@ualberta.ca

[i] This paper has been accepted for publication at Journal of Hepatology.

List of abbreviations:

LD	lipid droplet
VLDL	very low density lipoprotein
HCV	Hepatitis C virus
TG	triacylglycerol
ORO	Oil Red O
MTP	microsomal triglyceride transfer protein
ApoB	apolipoprotein B-100
AADAC	arylacetamide deacetylase
E600	diethyl-p-nitrophenyl phosphate
ELISA	enzyme-linked immunosorbent assay
FP	fluorophosphonate
DMEM	Dulbecco's Modified Eagle Medium
FBS	fetal bovine serum
JFH	Japanese fulminant hepatitis
MOI	multiplicity of infection
RNA	ribonucleic acid
qRT-PCR	quantitative reverse transcriptase-polymerase chain reaction
OA	oleic acid
BSA	bovine serum albumin
PBS	phosphate buffered saline
ER	endoplasmic reticulum
TGH	triacylglycerol hydrolase
PDI	protein disulfide isomerase

Financial Support:

Financial support was provided by an operating grant from the Canadian Institute of Health Research (CIHR/IRSC) awarded to Drs. Kneteman, Douglas and Lehner, the National CIHR Research Training Program (NCRTP) in Hepatitis C awarded to Dr. Mahra Nourbakhsh, and a Canada Excellence in Research Chair (CERC) awarded to Dr. Michael Houghton.

Abstract

Background & Aims: Very low density lipoproteins (VLDLs) are triacylglycerol(TG)-rich lipoproteins produced by the liver. The majority of their TG cargo is derived from the lipolysis of TG stored in hepatocellular lipid droplets (LDs). Important roles for LDs and the VLDL secretory pathway in the cell culture production of infectious hepatitis C virus (HCV) have been established. We hypothesized that TG lipolysis and VLDL production are impaired during HCV infection so that these cellular processes can be diverted towards HCV production.

Method: We used an HCV permissive cell culture system (JFH-1/Huh7.5 cells) to examine the relationship between TG lipolysis, VLDL assembly, and the HCV lifecycle using standard biochemical approaches.

Results: Lipolysis of cellular TG and VLDL production were impaired in HCV infected cells during the early peak of viral infection. This was partially explained by an apparent deficiency of a putative TG lipase, arylacetamide deacetylase (AADAC). The re-introduction of AADAC to infected cells restored cellular TG lipolysis, indicating a role for HCV-mediated downregulation of AADAC in this process. Defective lipolysis of cellular TG stores and VLDL production were also observed with Huh7.5 cells stably expressing a short hairpin RNA targeting AADAC expression, proving AADAC-deficiency contributes to these defective pathways. Finally, impaired production of HCV was observed with the AADAC knockdown cells, demonstrating a role for AADAC in the HCV lifecycle.

Conclusions: This insight into the biology of HCV infection and possibly pathogenesis identifies AADAC as a novel and translationally relevant therapeutic target.

Keywords: Hepatitis C virus; very low density lipoprotein; lipid droplet; triacylglycerol hydrolase; activity-based protein profiling; arylacetamide deacetylase; triacylglycerol; apolipoprotein; hepatic lipid metabolism; carboxylesterase; lipase; serine esterase.

Introduction

Lipid metabolism and lipids have been shown to play important roles in various phases of the Hepatitis C virus (HCV) lifecycle (1). The advent of a fully permissive culture system has established a role for hepatocellular lipid droplets (LDs) in the HCV lifecycle, possibly for the early stages of virion assembly, whereas further maturation and release is thought to require the hepatic very low density lipoprotein (VLDL) secretory pathway (1). VLDL assembly/secretion offers the only means by which triacylglycerol (TG) is exported from the liver and the majority (>70%) of TG assembled with VLDL is derived from the TG available in cellular LDs through a lipolysis/re-esterification cycle (2). In this study, we set out to examine the possibility that this VLDL substrate pool gets redirected to support viral production when cells are infected with HCV. The lipolytic mobilization of cellular TG stores and the assembly of TG-rich VLDL were found to be impaired in infected cells during the early peak of viral infection. This was partially explained by a profound reduction in the abundance of a putative TG lipase, arylacetamide deacetylase (AADAC). This study also identified a role for AADAC in the HCV lifecycle during the more acute stages of viral infection. We suggest that AADAC deficiency, which occurs after the initial spread of infection, represents a cellular adaptation to infection that is aimed at limiting viral production.

Materials and Methods

Generation of infected cells – Infected cells were established by inoculation of naïve Huh7.5 cells with viral stocks (MOI=0.01) derived from cells that had been transfected with Japanese Fulminant Hepatitis (JFH)-1 HCV RNA essentially as described (3). Infection in cells was routinely monitored by qRT-PCR for HCV RNA in media and indirect immunofluorescence for HCV core protein in cells, essentially as described (3, 4). These were enrolled into experiments as “infected” cells at 8-14d post infection, when they produced > 10^7 IU of HCV RNA per mg of cellular RNA and had >95% of cells core-positive. “Naïve” cells used in experiments were derived from the same Huh7.5 cell stocks as infected cells.

Mass secretion of TG from cells - The mass secretion of TG from cells after oleic acid (OA)-induced cellular expansion of cellular TG stores was examined as described previously (5). Briefly, cells were incubated in serum-free DMEM supplemented with 0.375 mM OA complexed with 0.5% (w/v) fatty acid-free BSA (OA-BSA) to expand cellular TG stores. For the last 2h of this incubation, the media was replenished with fresh DMEM supplemented with OA-BSA. At the end of this incubation period (t = 0h), cellular and secreted lipids (present in media) were extracted from one half of the culture dishes for analysis of TG mass (see TG analysis in supplemental information) present in cells

and media prior to the withdrawal of OA from the culture media. With the remaining half of the culture dishes, cells were washed and incubated for up to 8h in DMEM (without the OA supplement) to allow for the secretion of TG derived from the lipolysis of TG in preformed cellular stores. In some cases, this media was collected and replenished every 2h (up to 8h). In other cases, this incubation was performed in the presence of a competitive inhibitor of acyl-CoA synthetase, triacsin C (6) (6 μM final) or a pan inhibitor of serine eserases/lipases, E600 (7) (100 μM) in DMSO. The concentration of DMSO was 0.1% (v/v) final. TG mass in media and cells were determined enzymatically as previously described (5).

Materials and all other methods are provided in Supplemental Information.

Results

Lipolysis of cellular TG stores. A mutant line of Huh7 cells (Huh7.5) that supports HCV replication with high efficiency (8) was chosen to examine the hypothesis that cellular LDs are sequestered from VLDL assembly during productive infection with HCV. Infected cells were enrolled into experiments during the early peak of viral RNA production (~8-14d post-infection, MOI=0.01) characterized by spread of infection to >95% of the cells (9). This minimized the contribution to outcomes of non-infected cells present at earlier stages over the course of acute infection.

Huh7 cells have been shown to have a dependency on exogenous oleic acid (OA) for VLDL production (10). This has been attributed to the expansion of cellular TG stores available for lipolytic recruitment into the VLDL secretory pathway following OA-stimulated TG synthesis. These stores continue to supply VLDL with the majority of its TG after fatty acids (i.e. OA) have been removed from the culture media (11). Our preliminary experiments established that Huh7.5 cells also have a dependency on OA-induced expansion of cellular TG stores in order to secrete appreciable amounts of TG in the absence of supplied fatty acids (Fig S1A, OA-BSA vs. FBS and BSA). The LDs that formed during OA-induced expansion of TG stores were larger than those that formed in the absence of supplied OA (Fig S1B, OA-BSA vs. FBS). These larger LDs also formed when OA was supplied to infected cells and the HCV core protein was localized to their surface.

To test if LDs are sequestered from their normal role in VLDL assembly during HCV infection, TG mass secretion from naïve and infected cells were compared (Fig 1A). Less TG was secreted from infected cells when the culture media still contained OA (secreted, 0h), but this did not reach statistical significance until after the OA had been withdrawn from the media (secreted, 2-8h). Overall, infected cells secreted ~30% less TG per mg of

cell protein than naïve cells, despite having similar cellular TG levels prior to OA withdrawal (cellular, 0h). This coincided with an apparent accumulation of TG in infected cells at the end of the secretion period (cellular, 8h). The addition of an acyl-CoA synthetase inhibitor (+triacsin C) (12) to the culture media had no impact on the TG that accumulated in cells during the secretion period (cellular, 8h), ruling out the possibility that TG synthesis or the re-esterification of fatty acids released by lipases contributed to this pool. This was corroborated by pulse/chase experiments in which OA was also supplied to cells in the presence of trace amounts of radiolabeled OA (Fig S1C, pulse). Naïve and infected cells incorporated similar levels of radiolabeled OA into cellular TG (and phospholipids, PL). However, after OA had been withdrawn from the culture media (chase), ~ 36% of these labeled TG stores were turned over in naïve cells whereas no turnover was observed with infected cells. This effect was visualized by fluorescence microscopy of LD morphology using ORO staining (Fig 1B). After receiving the OA supplement, the size (i) and numbers (ii) of LDs present in naïve and infected cells were similar (0h). After the media was replaced with fresh DMEM containing triacsin C to promote TG lipolysis, the LDs in naïve cells underwent remodeling; the average area of individual LDs decreased (i) and the average LD number per cell increased (ii). By 72h, there was a significant reduction in the total LD area (iii, fluorescent area), indicating significant lipolysis. By contrast, no significant changes in the average LD size, numbers, or total LD area were observed with infected cells (see Fig S1D for representative micrographs). These results establish that the lipolysis of preformed cellular TG stores for recruitment into the VLDL assembly pathway is impaired when Huh7.5 cells are infected with HCV.

ApoB Density Profiles. Reduced lipolysis of cellular TG stores for recruitment into the VLDL secretory pathway is expected to impact either the physical properties of VLDL with respect to TG content or the number of VLDL particles produced (10). Determining the buoyant density of apolipoprotein 100 (ApoB) is an established procedure for estimating the TG content of VLDL (10) since the buoyant density of VLDL inversely correlates with TG content and each VLDL particle has just one ApoB constituent. Thus, OA was initially supplied to cell cultures to expand cellular TG stores and then was removed for 8h to allow for the secretion of VLDL in the absence of supplied fatty acids. The density profiles of the ApoB secreted into the media by naïve and infected cells were compared (Fig 1C). The majority of the ApoB secreted from naïve cells were in the 1.019-1.063 g/mL density range and the amount secreted with densities more typical of the VLDL found in human plasma (<1.006 g/ml) was insignificant (<5%). This is consistent with the ApoB density profiles obtained from Huh7 cells (10). Significantly less of the total ApoB secreted from infected cells appeared in the 1.019-1.063 g/mL density range (44.3±6.4% vs.

74.2±6.0%, p=0.0237, n=4), and more appeared with higher densities (i.e. > 1.063 g/mL). Supplying cell cultures with OA did not alter ApoB density profiles (Fig S2Ai, for BSA and FBS). This is consistent with the ApoB density profiles obtained from Huh7 cells that received the OA supplement (10) and is an indication that OA-stimulated expansion of cellular TG stores results in the production of more VLDL particles, as opposed to the production of VLDL with more TG content. Total ApoB (cell-associated plus secreted) were similar between naïve and infected cells, but less of this ApoB was secreted into the media by infected cells (Fig S2Aii, OA-BSA). Thus in addition to producing VLDL with reduced TG content, infected cells also secrete fewer VLDL particles.

A key role for MTP has been established in directing newly synthesized ApoB away from early proteasomal degradation (13). We did not observe any changes in the protein abundance for MTP or its binding partner, protein disulfide isomerase (PDI), but a modest reduction in MTP activity was observed with infected cells (Fig S2B). This did not impact the levels of newly synthesized ApoB (Fig S2C), since these were similar between naïve and infected cells and accumulated in cells when MG132 (a proteasome inhibitor) was included in the labeling media. However, MTP also functions in the smooth regions of the ER where lipoprotein particles containing ApoB have been shown to exhibit lower densities than those associated with the rough ER (13). Therefore, reduced MTP activity may have contributed to the production of fewer ApoB-containing particles in the lower density ranges (i.e. 1.019-1.063 g/mL) by infected cells.

Identification of putative TG lipases. The lipolytic mobilization of cellular TG is a key regulator of hepatic VLDL assembly and hepatic lipolytic activity may also affect the precise amount of TG which is added to a single molecule of ApoB during VLDL assembly (2). So far, two ER-localized lipases have been suggested to play a role in the mobilization of cellular TG stores for VLDL assembly: triacylglycerol hydrolase (TGH) and arylacetamide deacetylase (AADAC) (2). The possibility that infected cells had a lipase deficiency was examined using an established procedure that estimates serine esterase/lipase activity by the release of p-nitrophenol from p-nitrophenyl acetate (14) (Fig 2A). Infected cells had significantly reduced esterase/lipase activities when compared with naïve cells. Activity-dependent labeling of TGH and AADAC with fluorophosphonate (FP)-biotin has already been demonstrated (14) and is based on the binding of FP to the reactive serine within the highly conserved active sites of serine esterases/lipases. The same approach was used to determine if the activity of these lipases (and/or other esterases/lipases) might be altered in infected cells (Fig 2B). A single FP-labeled band appearing in the molecular weight (MW) range of AADAC was observed with naive Huh7.5 cells but was absent when infected cells were used. This

represents a catalytically active serine esterase(s)/lipase(s) since reduced FP labeling of this species was observed when a pan inhibitor of serine esterases/lipases was include in binding reactions (+E600) (14) and when lysates were heat inactivated prior to performing binding reactions (+Heat). Performing binding reactions with lysates derived from AADAC knockdown (AADAC-1, see Fig S3D for derivation) and overexpressing (pAADAC, see Fig S3A for derivation) cells ruled out the possibility that FP labeling in the MW range of AADAC was due to a serine esterase(s) other than AADAC. Immunoblot analysis demonstrated that endogenous AADAC is expressed in naïve cells but is absent from infected cells and that TGH is absent from these cells altogether (Fig 2Ci, left panel). Thus, reduced abundance of AADAC in infected cells is responsible for reduced FP-labeling of AADAC, as opposed to reduced AADAC activity. A transcriptional and/or post-transcriptional mechanism is suggested since AADAC mRNA abundance was reduced to a similar extent (Fig 2Ci, right panel).

Immunoblot analysis was performed over a time course of acute HCV infection (Fig 2Cii); cells sampled during the early peak of infection (2 weeks post-infection, MOI=0.01) had very little AADAC when compared with cells sampled at earlier timepoints. This indicates that the downregulation of AADAC occurs temporally, after the initial spread of infection has taken place. In support of this, very little (if any) AADAC was detected in Huh7-Lunet cells harboring a persistently replicating HCV replicon (Fig 2Ciii). However, AADAC was restored to these cells after they had been cured of the replicon by prolonged treatment with alpha interferon 2b (IFNa2B) (8). This indicates that the nonstructural proteins of HCV, which are expressed in infected cells after initial translation of the viral genome has taken place, are sufficient for the downregulation of AADAC. Flow cytometry was performed as an alternate method for examining AADAC expression specifically in infected cell populations. At 1 week post-infection (MOI=0.01), cell cultures had not yet reached the early peak of infection (Fig 2Diii); ~62% of the cells were found to be core-positive (Q1+Q2) and the majority of these (~84%) still contained AADAC (Q2). In comparison, ~90% of infected cells sampled during the early peak of infection (Fig 2Dii, 2 weeks post-infection) were core-positive and only a minor proportion of these (~5%, Q2) were AADAC-positive. Furthermore, the mean fluorescence intensity (MFI) for AADAC in these infected cells (Q2) was reduced by ~75% when compared with the MFI for AADAC present in cells sampled prior to the early peak of infection (MFI, ii vs. iii), indicating a greater downregulation of AADAC in the more persistently infected cells present during the early peak of infection. Collectively, these data demonstrate that the downregulation of AADAC occurs after the initial spread of infection has taken place, possibly after the initial translation of the viral genome has occurred.

Introduction of AADAC to HCV infected cells. A transient expression approach was used to re-introduce AADAC to infected cells during the early peak of viral infection. Transfection of naïve and infected cells with pAADAC resulted in ectopic expression of AADAC on microsomes with AADAC-dependent increases in cellular lipolytic activities (Fig S3AB). These outcomes were obtained with transfection efficiencies ranging from 35-55% (Fig S3C). The same approach was used to determine if the introduction of AADAC to infected cells during the early peak of HCV infection could restore defective lipolysis of cellular TG stores (Fig 3A). A significant depletion of cellular TG stores was observed in pAADAC transfected cells after OA had been withdrawn from the culture media for 8h (8h vs. 0h) and was prevented when E600 was included in the culture media (+E600 vs. –E600), indicating lipase-mediated hydrolysis. No appreciable depletion of cellular TG was observed in vector control cells. AADAC expression was maintained in pAADAC transfected cells throughout the OA withdrawal period, whereas vector control cells maintained their AADAC-deficient status (Fig 3B). Thus, the introduction of AADAC to infected cells that were otherwise AADAC-deficient was able to restore lipolysis of cellular TG stores to these cells.

Knockdown of AADAC. To our knowledge, there are no specific pharmacological inhibitors for AADAC. To better understand the role of AADAC in lipid metabolism and the HCV lifecycle, five different Huh7.5 cell lines, each stably expressing a different shRNA targeting AADAC, were generated. Knockdown of endogenous AADAC (relative to wild-type Huh7.5 cells) was quantified by immunoblot analysis and densitometry (Fig S3D). The greatest AADAC knockdown (~75%) was seen with AADAC-1 cells. Therefore these cells were used in subsequent studies. AADAC-2 and non-targeting shRNA expressing cells (NT) were used as additional controls since no appreciable AADAC knockdown was observed with these cells.

For TG secretion studies, OA was initially supplied to cells to expand cellular TG stores available for lipolytic recruitment into the VLDL assembly pathway. However, after receiving the OA supplement, cellular TG levels in AADAC-1 cells were significantly lower when compared with NT (or AADAC-2) cells (Fig S3E). It is not known if this was due to AADAC knockdown or the transduction/selection procedure. Therefore, cellular TG stores remaining after 8h of OA withdrawal from the culture media were expressed as a percentage relative to the amount present just prior to OA withdrawal (Fig 3Ci, cellular); these were significantly lower in AADAC-1 cells when compared with controls. AADAC-1 cells also secreted ~35% less VLDL-TG into the media during this same period (secreted). Unlike the ApoB density profiles obtained with infected cells (Fig 1C), the majority of ApoB secreted into the media by AADAC-1 cells were still in the 1.019-1.063

g/mL density range (Fig 3Cii). Consistent with reduced TG secretion by these cells, the ApoB peak density observed for AADAC-1 cells was slightly higher than the peak density of ApoB secreted from NT cells. These data demonstrate that AADAC deficiency, whether induced by HCV infection or by a silencing approach, contributed to the observed reductions in lipolysis of cellular TG stores for VLDL assembly. These data also indicate that additional factors, such as MTP for example, contribute to altered lipidation of nascent VLDL in infected cells.

Having established that AADAC abundance is unchanged in Huh7.5 cells up to 72 h post infection (Fig 2Cii), the impact of AADAC knockdown on infectious virion production over this time course of acute infection was examined. Infection of AADAC-1 cells with Bi-Gluc-J6/JFH resulted in a significant reduction in luciferase production by 48h post-infection compared with controls (Fig 4A), indicating a role for AADAC-1 in the virus replication cycle during the acute phase of infection. AADAC-1 cells also supported lower levels of JFH-1 viral production (Fig 4B), since cellular (i) and secreted (ii) viral RNA were found to be substantially reduced by 72h post infection with a profound reduction in TCID50 (iii) when compared with controls. The density profile of HCV RNA secreted from AADAC-1 and NT cells were similar (Fig 4C), indicating that AADAC does not play a role in the acquisition of lipid by HCV and that this physical aspect (i.e. buoyant density) of HCV does not contribute to the reduced infectivity of HCV produced by AADAC-1 cells. As we did not evaluate infectivity titers of cellular virions, it is not known if defective viral assembly or impaired viral secretion contributed to reduced HCV production by AADAC-1 cells. Collectively, these data demonstrate a role for AADAC in the HCV replication cycle during the acute phase of HCV infection. It is possible that AADAC deficiency, which we have shown occurs later in the more persistently infected cells present during the early peak of viral infection, is aimed at limiting viral production.

Discussion

A role for AADAC in the lipolysis of cellular TG stores and VLDL assembly was initially predicted based on an AADAC deficiency noted in infected cells during the early peak of viral infection. This was validated by two complimentary approaches which took into consideration the lipolysis/re-esterification cycle required for the continued secretion of VLDL-TG derived from preformed cellular TG stores after exogenous fatty acids have been withdrawn from the culture media (2): The re-introduction of AADAC into these infected cells restored lipolysis of preformed cellular TG stores while the knockdown of endogenous AADAC in naïve cells led to defective lipolysis of cellular TG stores and reduced secretion of VLDL-TG. A role for AADAC in the lipolysis of cellular TG stores for VLDL-TG production has been previously demonstrated by the introduction of AADAC to

HepG2 cells (a human hepatoma cell line that does not have endogenous AADAC) (2). To our knowledge, ours is the first study to demonstrate a role for endogenous AADAC in the lipolysis of cellular TG stores and VLDL assembly.

Like HepG2 cells, rat hepatoma (McArdle-RH7777) cells do not express endogenous AADAC. Interestingly, when murine AADAC cDNA was expressed in these cells, AADAC-mediated lipolysis of cellular TG only occurred while exogenous fatty acids were being supplied to the cells. Furthermore, the lipolytic products were channeled towards β-oxidation instead of VLDL-TG production (14). We did not observe an increase in cellular TG stores while fatty acids were being supplied to infected cells that were already AADAC-deficient (Fig 1A, cellular at 0h) or to AADAC knockdown cells, arguing against a role for endogenous AADAC in mobilizing these stores for β-oxidation. Further studies are required to determine if the endogenous AADAC present in Huh7.5 cells also has a role in mobilizing the endogenous TG pool for β-oxidation in the absence of supplied fatty acids. This possibility is intriguing since a role for β-oxidation in HCV replication has already been demonstrated (15).

The current study also uncovered a role for AADAC in the replication cycle of HCV, particularly during the acute phase of infection leading up the early peak of infection. Given that LDs are considered to have important roles in the HCV lifecycle, it is difficult to reconcile AADAC deficiency; a state leading to the cellular accumulation of LDs yet reducing viral production. An interesting model has emerged from a recent study that combined computational modeling with proteomic and lipidomic profiling over a time course of acute HCV infection (16). It was suggested that increases in host biosynthetic and catabolic activities occur early during infection in order to support viral production. As infection progresses and cellular stress increases, a metabolic shift occurs in favor of cell survival, albeit with predictable consequences to the viral life cycle (16). Proteins with known roles in β-oxidation whose abundances increased early after infection and whose decreased abundance coincided with increased cytopathic effects of HCV, were suggested to be key regulators of this metabolic reprogramming. Although AADAC was not among these so-called bottlenecks, its abundance was reported to follow a similar pattern (16). This is consistent with the AADAC deficiency we noted in infected cells during the early peak of viral infection, where variable cytopathic effects of HCV are known to occur (9). Importantly, the AADAC-deficient cells had not yet entered the trough of viral replication that typically precedes a more dynamic persistent infection (9). Cells at these later stages are characterized by fluctuating levels of viral RNA/infection and become more resistant to HCV infection (9).

The model we envision for the mechanism behind the role for AADAC in the viral lifecycle is consistent with the suggested roles for LDs and the VLDL secretory pathway in the early and later stages of virion assembly (1) and is consistent with the metabolic reprogramming suggested to be coincident with cytopathic effects of HCV infection. Thus it is possible that endogenous AADAC increases the efficiency of HCV production by coupling early replication/assembly events dependent on enhanced LD turnover (replication of viral genomes and/or their packaging with capsids (1), for examples) with maturation events that might be dependent on the VLDL secretory pathway (gaining access to the E1/E2 glycoproteins and/or egress (1), for examples). We suspect that AADAC deficiency, which occurs in more persistently infected cells, is one aspect of the host response that contributes to the eventual cellular reprogramming required for achieving viral resistance and therefore cellular survival.

Although aimed at limiting viral production, reduced lipolysis of cellular TG stores and reduced secretion of VLDL-TG were also observed to be cellular consequences of AADAC deficiency. These are established causes for the development of hepatic steatosis, which is a common histological feature of chronic HCV infection. Whether or not AADAC-deficiency contributes to viral-associated steatosis in the clinical setting is the focus of future work.

These studies identify AADAC as a novel host factor important in the biology of HCV infection and possibly pathogenesis. The identification of AADAC provides an attractive potential new target for treating HCV infection.

Acknowledgements

The authors thank Zong Chao Ling and KMT Hepatech for RT-PCR analysis of HCV RNA, Dr. Charles Rice for providing many of the key reagents that made this study possible (Huh7.5 cells, pJFH-1, Bi-Gluc-J6/JFH, and anti-NS5A 9E10), Dr. Ralph Bartenschlager for providing Huh7-Lunet replicon cells, and Dr. Aviad Levin, Dr. Deanna Santer and Karl Fischer for helpful discussions throughout these studies.

References

1. Alvisi G, Madan V, Bartenschlager R. Hepatitis C virus and host cell lipids: an intimate connection. RNA Biol. 2011;8(2):258-69. Epub 2011/05/20.

2. Gibbons GF, Islam K, Pease RJ. Mobilisation of triacylglycerol stores. Biochimica et biophysica acta. 2000;1483(1):37-57. Epub 1999/12/22.

3. Kato T, Date T, Murayama A, Morikawa K, Akazawa D, Wakita T. Cell culture and infection system for hepatitis C virus. Nat Protoc. 2006;1(5):2334-9. Epub 2007/04/05.

4. Kneteman NM, Asthana S, Lewis J, Dibben C, Douglas D, Nourbakhsh M, et al. Impact of calcineurin inhibitors with or without interferon on hepatitis C virus titers in a chimeric mouse model of hepatitis C virus infection. Liver Transpl. 2012;18(1):38-44. Epub 2011/08/13.

5. Lehner R, Vance DE. Cloning and expression of a cDNA encoding a hepatic microsomal lipase that mobilizes stored triacylglycerol. The Biochemical journal. 1999;343 Pt 1:1-10. Epub 1999/09/24.

6. Brasaemle DL, Rubin B, Harten IA, Gruia-Gray J, Kimmel AR, Londos C. Perilipin A increases triacylglycerol storage by decreasing the rate of triacylglycerol hydrolysis. The Journal of biological chemistry. 2000;275(49):38486-93. Epub 2000/08/19.

7. Gilham D, Ho S, Rasouli M, Martres P, Vance DE, Lehner R. Inhibitors of hepatic microsomal triacylglycerol hydrolase decrease very low density lipoprotein secretion. FASEB J. 2003;17(12):1685-7. Epub 2003/09/06.

8. Blight KJ, McKeating JA, Rice CM. Highly permissive cell lines for subgenomic and genomic hepatitis C virus RNA replication. Journal of virology. 2002;76(24):13001-14. Epub 2002/11/20.

9. Zhong J, Gastaminza P, Chung J, Stamataki Z, Isogawa M, Cheng G, et al. Persistent hepatitis C virus infection in vitro: coevolution of virus and host. Journal of virology. 2006;80(22):11082-93. Epub 2006/09/08.

10. Meex SJ, Andreo U, Sparks JD, Fisher EA. Huh-7 or HepG2 cells: which is the better model for studying human apolipoprotein-B100 assembly and secretion? Journal of lipid research. 2011;52(1):152-8. Epub 2010/10/20.

11. Wiggins D, Gibbons GF. The lipolysis/esterification cycle of hepatic triacylglycerol. Its role in the secretion of very-low-density lipoprotein and its response to hormones and sulphonylureas. The Biochemical journal. 1992;284 (Pt 2):457-62. Epub 1992/06/01.

12. Fujimoto Y, Itabe H, Kinoshita T, Homma KJ, Onoduka J, Mori M, et al. Involvement of ACSL in local synthesis of neutral lipids in cytoplasmic lipid droplets in human hepatocyte HuH7. Journal of lipid research. 2007;48(6):1280-92. Epub 2007/03/24.

13. Fisher EA, Ginsberg HN. Complexity in the secretory pathway: the assembly and secretion of apolipoprotein B-containing lipoproteins. The Journal of biological chemistry. 2002;277(20):17377-80.

14. Lo V, Erickson B, Thomason-Hughes M, Ko KW, Dolinsky VW, Nelson R, et al. Arylacetamide deacetylase attenuates fatty-acid-induced triacylglycerol accumulation in rat hepatoma cells. Journal of lipid research. 2010;51(2):368-77. Epub 2009/08/06.

15. Rasmussen AL, Diamond DL, McDermott JE, Gao X, Metz TO, Matzke MM, et al. Systems virology identifies a mitochondrial fatty acid oxidation enzyme, dodecenoyl coenzyme A delta isomerase, required for hepatitis C virus replication and likely pathogenesis. Journal of virology. 2011;85(22):11646-54. Epub 2011/09/16.

16. Diamond DL, Syder AJ, Jacobs JM, Sorensen CM, Walters KA, Proll SC, et al. Temporal proteome and lipidome profiles reveal hepatitis C virus-associated reprogramming of hepatocellular metabolism and bioenergetics. PLoS Pathog. 2010;6(1):e1000719. Epub 2010/01/12.

Fig. 1. Reduced lipolysis of cellular TG stores for VLDL assembly/secretion by infected cells. Cells were incubated in DMEM supplemented with OA-BSA for 14h to increase cellular TG stores. **(A)** For the last 2h of this incubation period, the media was replaced with fresh DMEM supplemented with OA-BSA. TG analysis was performed with cells (cellular) and media (secreted) collected from half of the dishes (0h). For remaining dishes, media was replaced (and replenished every 2h) with DMEM (or DMEM+Triacsin C) for 8h prior to TG analysis (2-8h). **(B)** Media was replaced with DMEM+Triacsin C for up to 72h prior to analysis of LD morphology. **(C)** Media was replaced with DMEM for 8h and the density profile of ApoB secreted into this media was determined. Each symbol denotes a separate experiment. The mean percentage of total ApoB appearing within a given density range is also shown.

Fig. 2. Infected cells have reduced abundance of a putative TG lipase (AADAC). (A) Lipolytic activities in cellular lysates obtained from naïve and infected cells were estimated by the release of *p*-nitrophenol from p-nitrophenyl acetate. Data were normalized to cellular protein. **(B)** Activity-based protein profiling of cellular proteins based on bound FP-biotin (+FP-biotin). Lysates used were obtained from naïve, infected, AADAC knockdown (AADAC-1), AADAC overexpressing (pAADAC) Huh7.5 cells and human hepatocytes (HH). In some cases, E600 was included in binding reactions (+/- E600) or lysates were heat inactivated (+/- Heat) prior to performing binding reactions. Binding reactions were also performed without FP-biotin (-FP-biotin). TGH, triacylglycerol hydrolase; AADAC, arylacetamide deacetylase. **(C)** Immunoblot analysis for AADAC in lysates used in B (i, left) and AADAC mRNA levels (normalized to actin) in naïve and infected cells during the early peak of viral infection (i, right). Immunblot analysis for AADAC was also performed with infected cells sampled over a time course of acute infection (ii) and with cells harboring a persistently replicating HCV replicon (iii) before and after 72h treatment with IFNa2b (IFN). In some cases, cells were cultured for an additional 48h in the absence of IFN (recovery from IFN). **(D)** Cellular AADAC in infected cells was examined by flow cytometry using dual indirect intracellular labeling for AADAC (AF488) and core (AF594) using distinct lasers. Infected cells sampled during the early peak of viral infection (ii) were compared with infected cells sampled before the early peak of viral infection had been reached (iii). Single cells were included in the analysis based on their characteristics on light scatter channels. A biexponential transform was applied to data and presented as 5% probability contour plots with gates based on both isotype controls present during the primary incubation for cells sampled during the early peak of infection (i). The mean fluorescence intensity (MFI) for AADAC in core-positive cells (Q2) is also shown.

Fig. 3. AADAC mediates the lipolysis of cellular TG stores. (A) Infected Huh7.5 cells that were already AADAC deficient were transfected with pAADAC (or vector). At 24h post-transfection, cells were incubated for 14h with DMEM+OA-BSA prior to collecting cells for TG analysis (0h) or incubating them for an additional 8h in DMEM (±E600; secretion period) prior to collecting cells for TG analysis (8h). Untransfected naïve cells (naïve) were also included for comparison. **(B)** Expression of AADAC (and core and actin) for cells collected at 0h and 8h (see A) was detected by immunoblot analysis and quantified by densitometry. The immunoblot is representative of 4 experiments. **(C)** Mass secretion of TG from AADAC knockdown (AADAC-1) cells during 8h of OA withdrawal from the culture media (secreted) was determined after OA-stimulated expansion of cellular TG stores (i). The TG that remained in cells at the end of the secretion period (cellular) is expressed as a percentage of the TG present prior to OA withdrawal. AADAC-1 and NT cells were included as controls. Density profiles of the ApoB secreted from AADAC-1 and NT cells during the 8h secretion period are also shown (ii). Each symbol denotes a separate experiment.

Fig. 4. HCV production by AADAC knockdown cells. (A) HCV growth curves were titrated at days 1, 2 and 3 post-infection of AADAC-1 cells with Bi-Gluc-J6/JFH (MOI=0.02). **(B)** Viral RNA titers (i, ii) and TCID50s (iii) were determined after 72h post-infection of AADAC-1 cells with JFH-1 (MOI=0.5). AADAC-2 and NT were included in A and B as controls. **(C)** The buoyant density profile of HCV RNA secreted from AADAC-1 (and NT) cells after 72h post-infection with JFH-1 (MOI=0.5) are shown.

Figure 1A

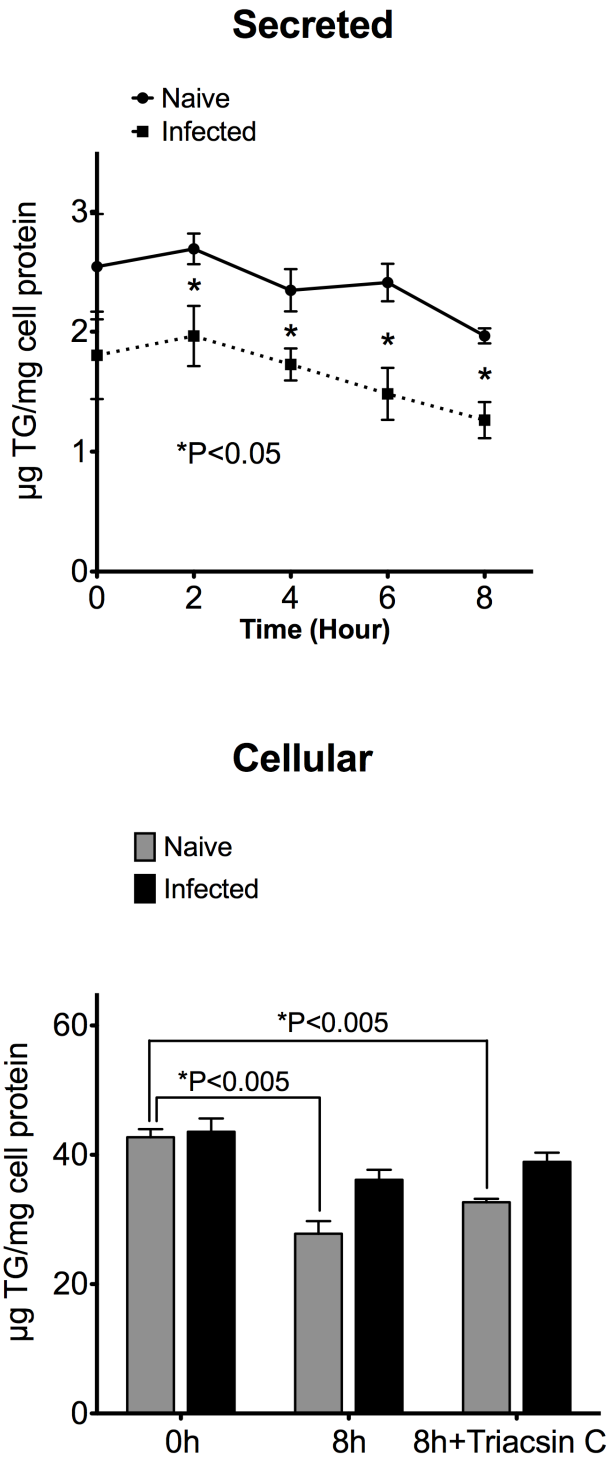
Secreted
Naive
Infected
µg TG/mg cell protein
3
2
1
0
*P<0.05
0
2
4
6
8
Time (Hour)
Cellular
Naive
Infected
µg TG/mg cell protein
60
40
20
0
*P<0.005
*P<0.005
0h
8h
8h+Triacsin C

Figure 1B

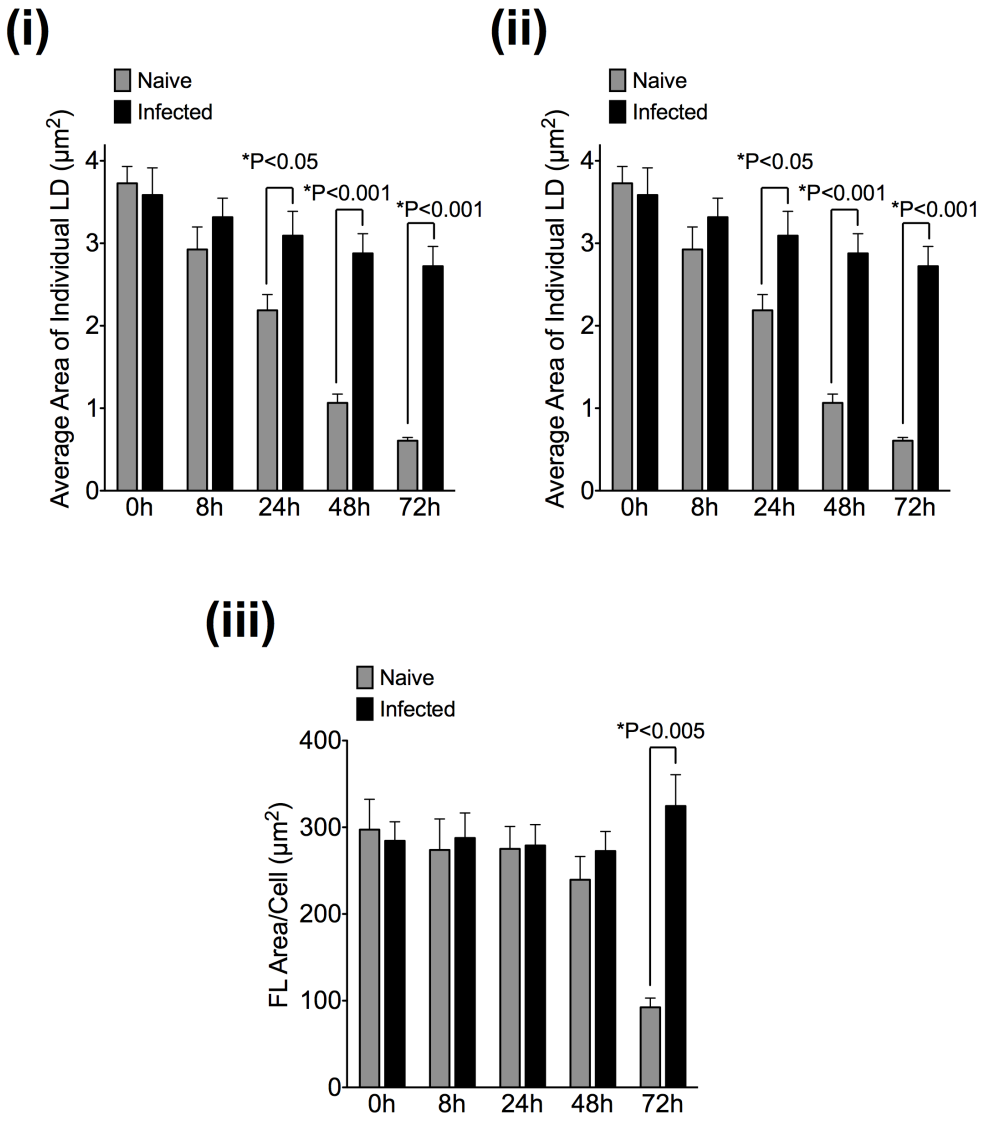
(i)
Naive
Infected
Average Area of Individual LD (μm²)
*P<0.05
*P<0.001
*P<0.001
0h
8h
24h
48h
72h
(ii)
Naive
Infected
Average Area of Individual LD (μm²)
*P<0.05
*P<0.001
*P<0.001
0h
8h
24h
48h
72h
(iii)
Naive
Infected
FL Area/Cell (μm²)
*P<0.005
0h
8h
24h
48h
72h

Figure 1C

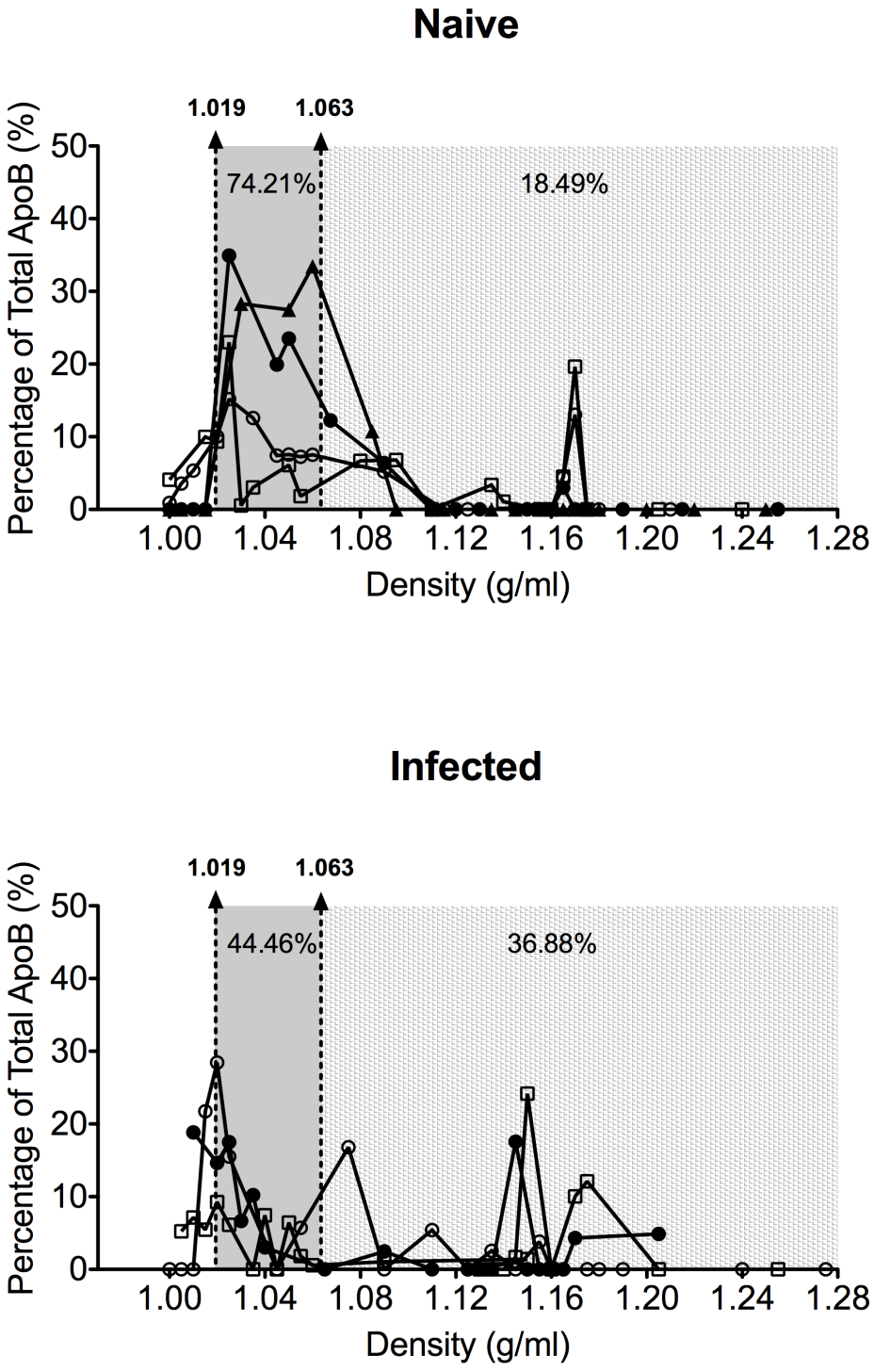
Naive
1.019
1.063
74.21%
18.49%
Percentage of Total ApoB (%)
0
10
20
30
40
50
1.00
1.04
1.08
1.12
1.16
1.20
1.24
1.28
Density (g/ml)
Infected
1.019
1.063
44.46%
36.88%
Percentage of Total ApoB (%)
0
10
20
30
40
50
1.00
1.04
1.08
1.12
1.16
1.20
1.24
1.28
Density (g/ml)

Figure 2A and 2B

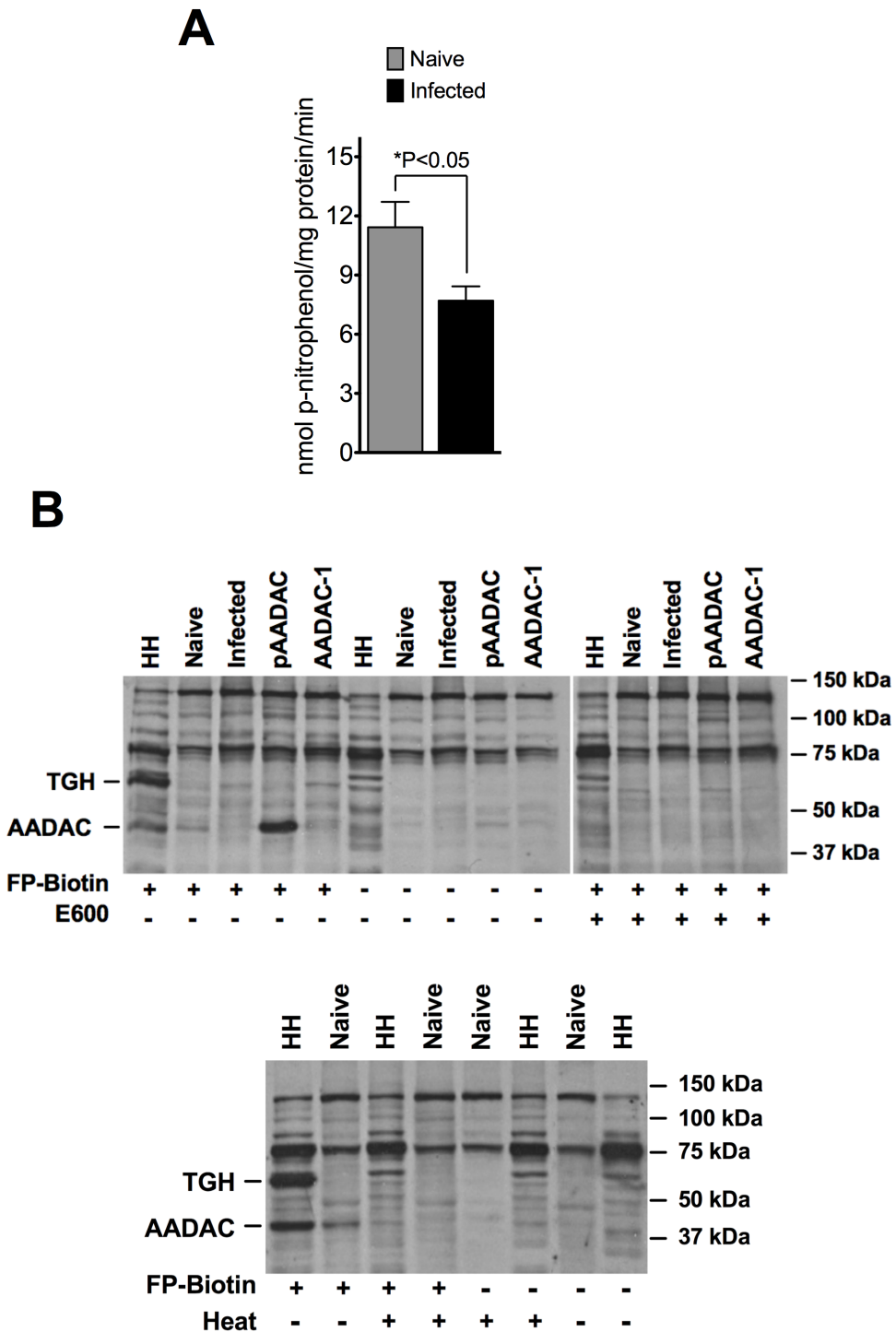

Figure 2C

(i)

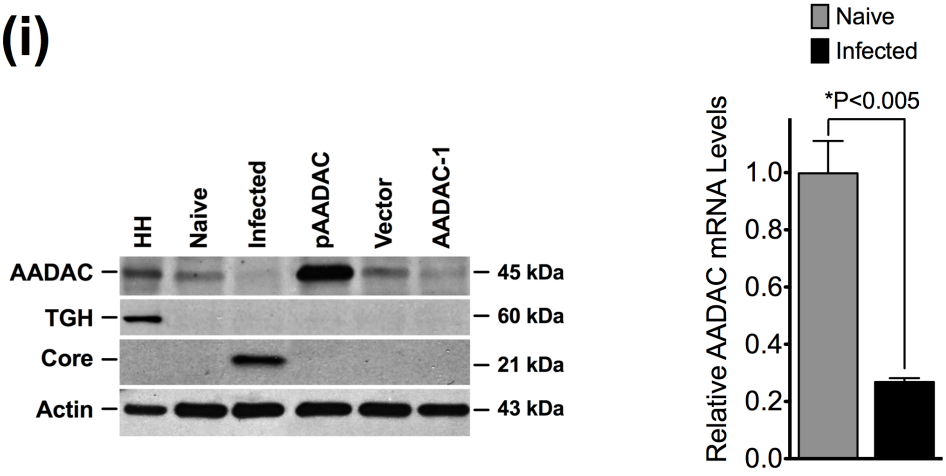

(ii)

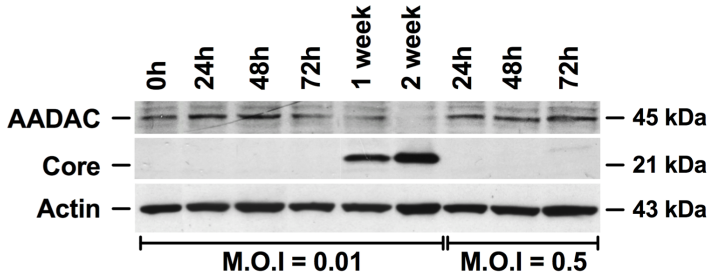

(iii)

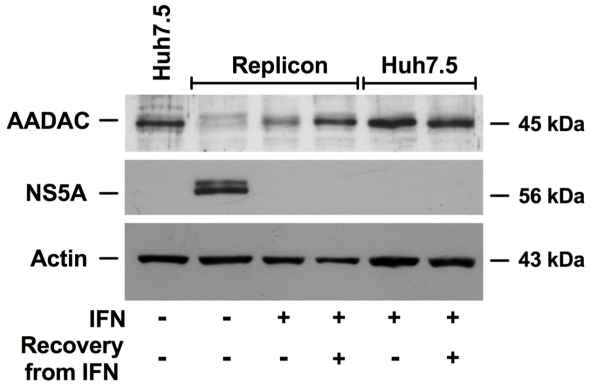

Figure 2D

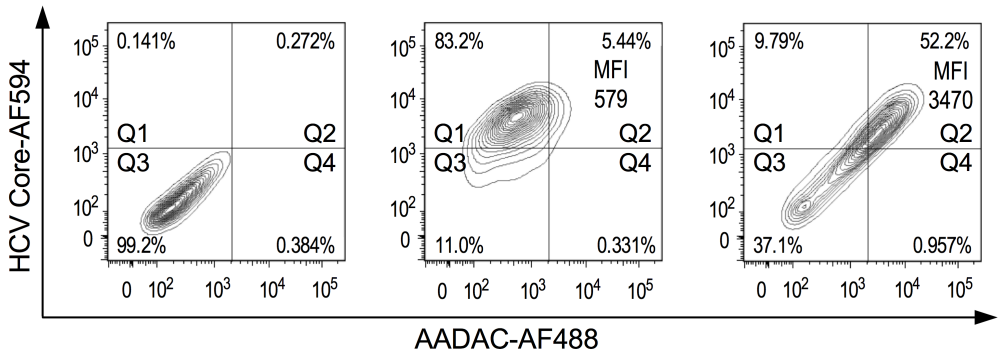
HCV Core-AF594
AADAC-AF488
0.141%
0.272%
Q1
Q2
Q3
Q4
99.2%
0.384%
83.2%
5.44%
MFI
579
11.0%
0.331%
9.79%
52.2%
MFI
3470
37.1%
0.957%
0
10^2
10^3
10^4
10^5

Figure 3A and 3B

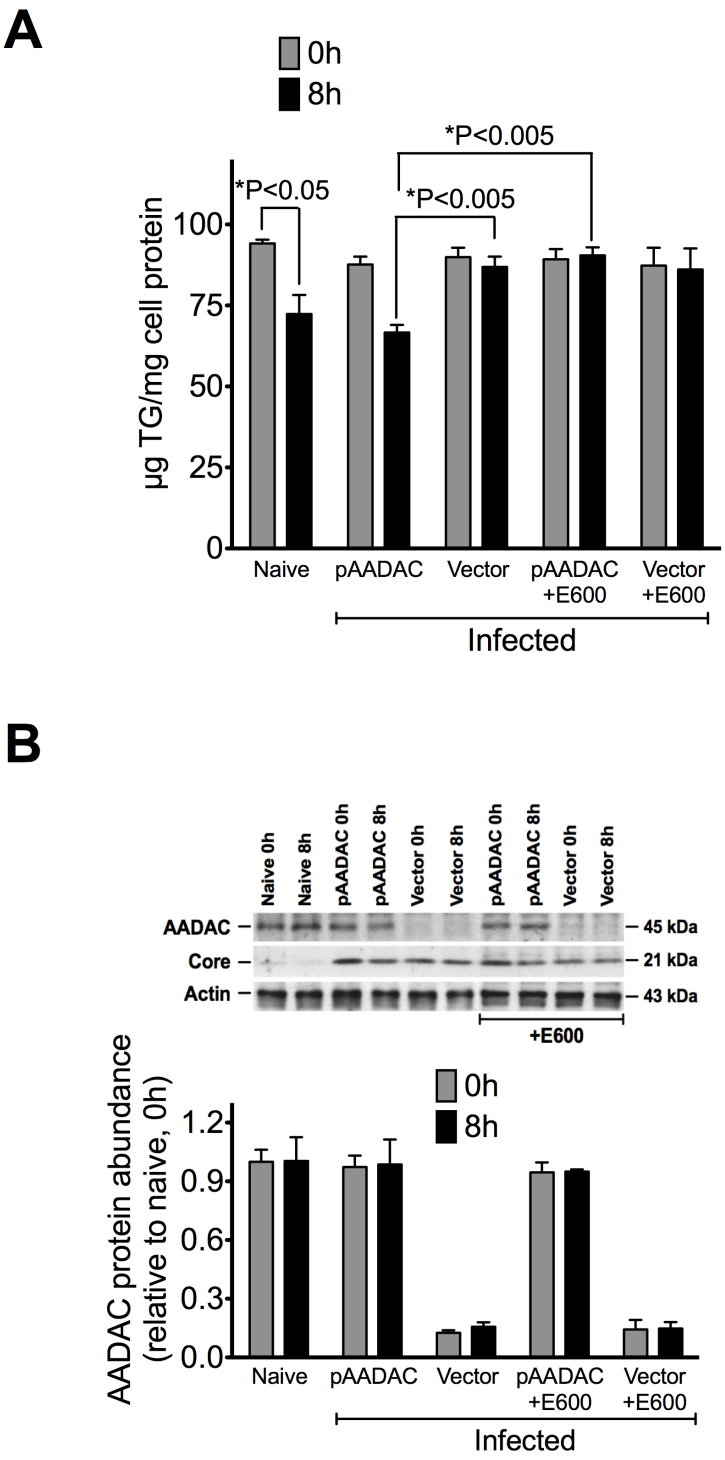

Figure 3C

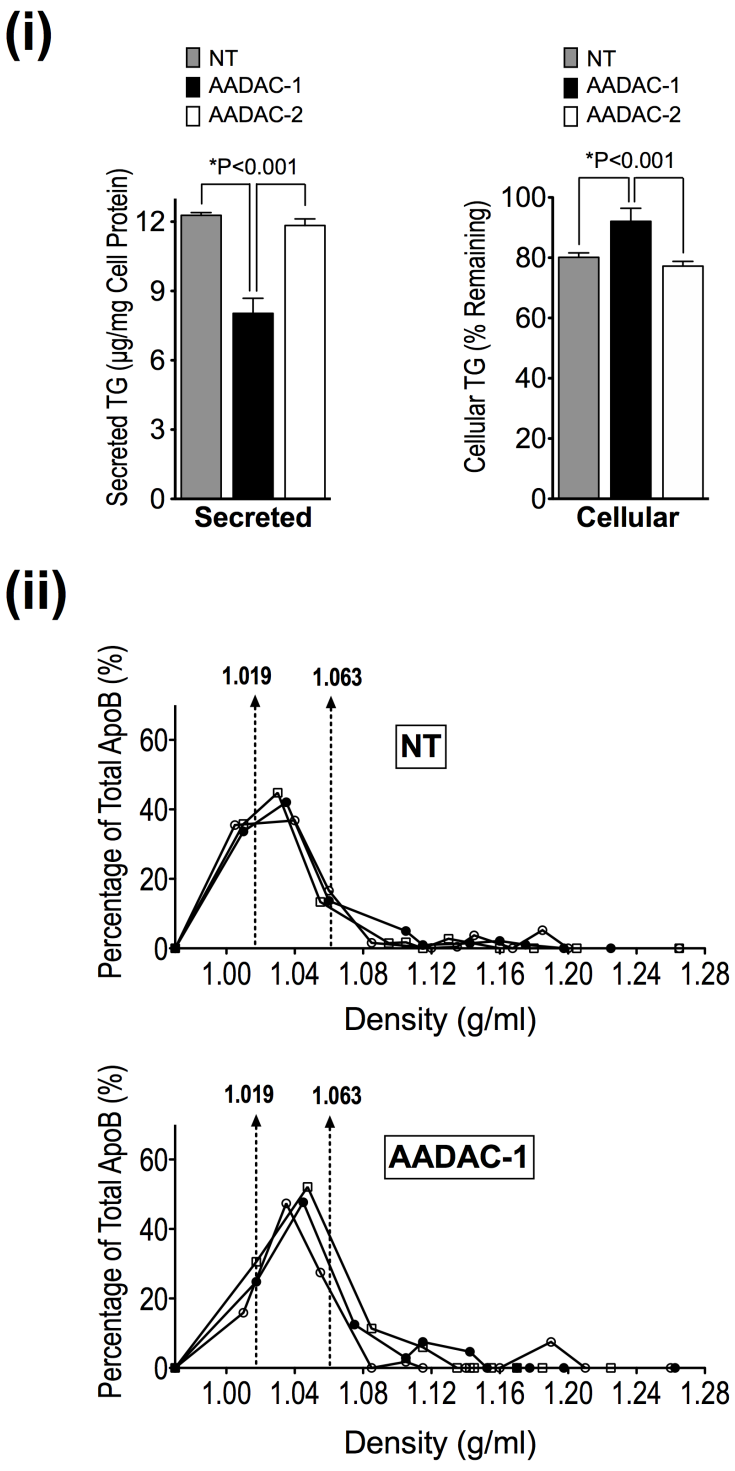
(i)
NT
AADAC-1
AADAC-2
*P<0.001
Secreted TG (µg/mg Cell Protein)
0
3
6
9
12
Secreted
NT
AADAC-1
AADAC-2
*P<0.001
Cellular TG (% Remaining)
0
20
40
60
80
100
Cellular
(ii)
1.019
1.063
NT
Percentage of Total ApoB (%)
0
20
40
60
1.00 1.04 1.08 1.12 1.16 1.20 1.24 1.28
Density (g/ml)
1.019
1.063
AADAC-1
Percentage of Total ApoB (%)
0
20
40
60
1.00 1.04 1.08 1.12 1.16 1.20 1.24 1.28
Density (g/ml)

Figure 4

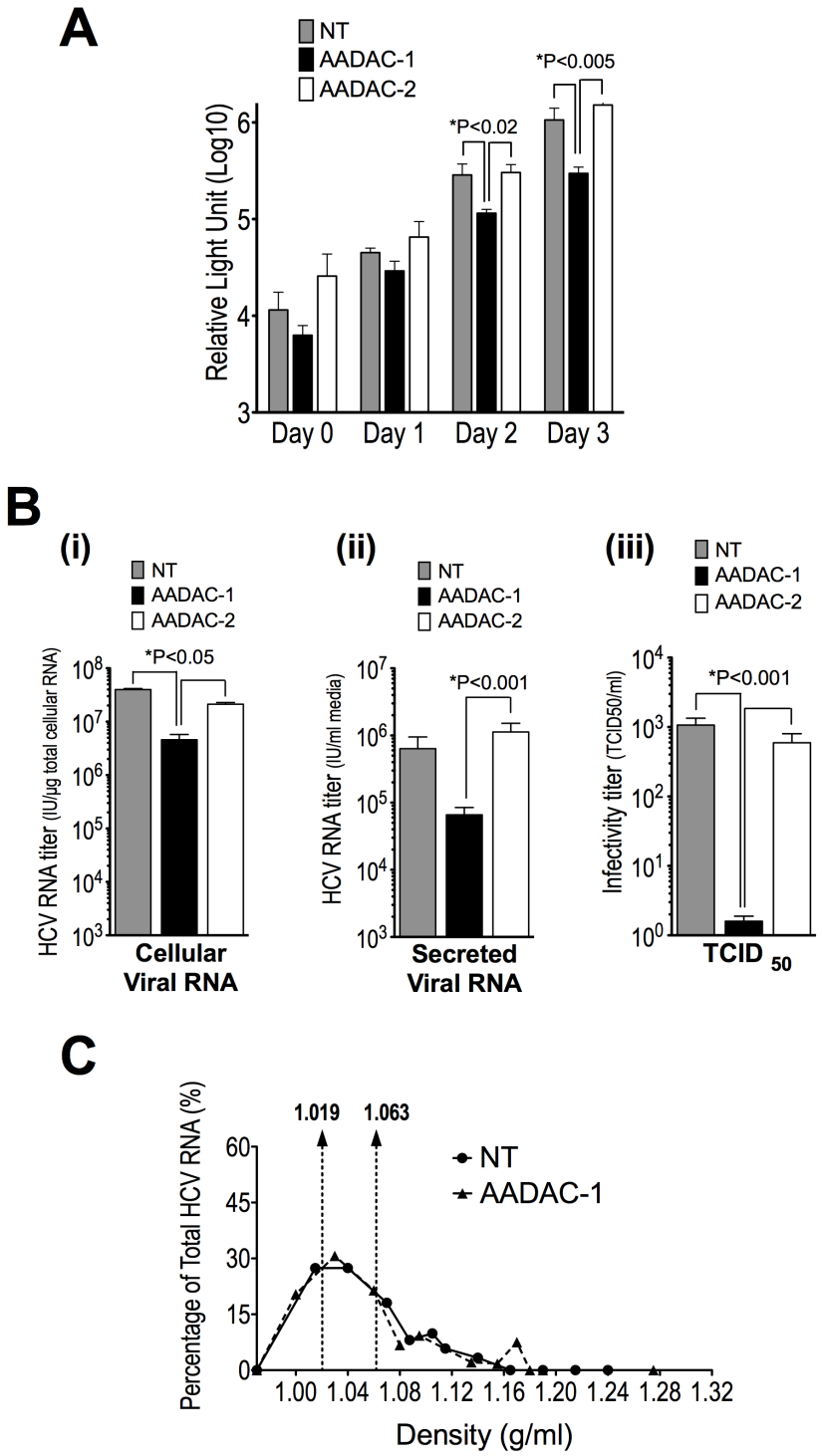
A
NT
AADAC-1
AADAC-2
*P<0.005
*P<0.02
Relative Light Unit (Log10)
Day 0
Day 1
Day 2
Day 3
B
(i)
(ii)
(iii)
*P<0.05
*P<0.001
*P<0.001
HCV RNA titer (IU/μg total cellular RNA)
HCV RNA titer (IU/ml media)
Infectivity titer (TCID50/ml)
Cellular Viral RNA
Secreted Viral RNA
TCID 50
C
1.019
1.063
Percentage of Total HCV RNA (%)
Density (g/ml)

SUPPLEMENTAL INFORMATION

Materials - Serum Triacylglycerol Determination Kit (Cat. No. TR0100), Iodixanol (OptiPrep Density Gradient Medium), Oil Red O (ORO) and diethyl-p-nitrophenyl phosphate (E600), benzamidine, fatty acid free-bovine serum albumin (BSA), oleic acid (OA), glycerol, leupeptin, phenylmethanesulfonyl fluoride (PMSF), protease inhibitor cocktail, protein A-sepharose, Z-Leu-Leu-Leu-al (MG132), p-nitrophenol and p-nitrophenyl acetate, glycerol trioleate, cholesteryl oleate, L-a-phosphatidylcholine, heptane, isopropyl ether, MISSION® Lentiviral Transduction Particles, polybrene and puromycin were obtained from Sigma-Aldrich (Oakville, ON). ELISA kit for human Apolipoprotein B was from Mabtech (Cincinnati, OH); MTP activity assay kit was obtained from Roar Biomedical, (New York, NY). Biotinylated fluorophosphonate (FP-biotin) was obtained from Toronto research center (Toronto, ON). A mammalian expression vector (pAADAC) containing the coding region for human AADAC (I.M.A.G.E Clone ID: 5185099) was purchased from ATCC (VA, USA). Thin layer chromatography plates (cat#WHT4860-820) were from Fisher Scientific. Dulbecco's Modified Eagles Medium (DMEM), TRIzol LS, Platinum Quantitative PCR SuperMix-UDG, cysteine-methionine free DMEM, penicillin-streptomycin mixture and Lipofectamine 2000 were purchased from Invitrogen (Burlington, ON). The antibodies were obtained from the following sources: goat anti human ApoB was from Chemicon (Billerica, MA); mouse anti-core C7-50 monoclonal antibody was from Affinity BioReagents (Rockford, IL); mouse anti-NS5A 9E10 monoclonal antibody was provided by Dr. Charles M. Rice (Rockefeller University, NY); goat anti human microsomal triglyceride transfer protein (anti-MTP) polyclonal antibody and goat anti human arylacetamide deacetylase (anti-AADAC) polyclonal antibody (sc-99249: clone K-12) were from Santa Cruz Biotech (Santa Cruz, CA); rabbit anti human triacylglycerol hydrolase (anti-TGH) polyclonal antibody was obtained as described previously(1); mouse anti actin clone C4 (anti-actin) monoclonal antibody was from Millipore (Billerica, MA); mouse anti human protein disulfide isomerase (anti-PDI) monoclonal antibody was from Stressgen Biotechnologies (Victoria, BC); HRP-conjugated rabbit anti-goat IgG antibody was from Pierce Biotechnology Inc. (Rockford, IL); HRP-conjugated anti mouse IgG antibody was from MP Biomedical (Solon, OH); HRP-conjugated donkey anti rabbit IgG was from Jackson Immunoresearch (West Grove, PA); HRP conjugated sheep anti-mouse IgG antibody was from GE Healthcare Amersham (Milwaukee, WI); Alexa fluor 488 donkey anti goat IgG, Alexa fluor 488 and 594 goat anti mouse IgG were from Invitrogen (Burlington, ON). Goat and mouse IgG (isotype controls) were from Cedarlane (Burlington, ON). Micro BCA Protein Assay Reagent Kit was obtained from Pierce Biotechnology (Rockford, IL). MEGAscript® T7 kit was obtained from Ambion/Applied Biosystems (Streetsville, ON). EasyTag™ EXPRESS

^{35}S-Protein Labeling Mix and [9,10(*n*)-^{3}H]oleic acid were obtained from PerkinElmer (Woodbridge, ON). DAB substrate kit was from DAKO (Burlington, ON). ECL™ Western Blotting Detection Reagents and Hyperfilm™ ECL were from GE Healthcare Amersham (Milwaukee, WI). qScript cDNA SuperMix was from Quanta Biosciences (Gaithersburg, MD). Renilla Luciferase assay system was from Promega (Madison, WI). All DNA primer synthesis was performed by IDT (Coralville, IA).

Cells and Cell Culture - Huh7.5 cells, a mutant line of Huh7 cells that support HCV replication with high efficiency(2), and pJFH-1 used to transfect Huh7.5 cells in order to generate infectious virus stocks, were generously provided by Dr. Charles M. Rice (Rockefeller University, NY). HepG2 cells were obtained from ATCC (Manassas, VA**)** and human hepatocytes were obtained in site using procedures we have previously described(3). Huh7-Lunet cells harboring a stable replicon (Luc-ubi-neo-SG-JFH1) based on pFK-I389/NS3-3'/5.1(4)) were provided by Dr. Ralph Bartenschlager (Heidelberg University). Cell cultures were maintained in Dulbecco's modified Eagle's medium (DMEM) containing 10% fetal bovine serum (FBS), 100 U/ml penicillin and 100 μg/ml streptomycin at 37ºC in humidified air containing 5% CO_2. Replicon cells were also cultured in the presence of G418 (1mg/mL). The method used to cure replicon cells of HCV RNA replication has been described previously(2).

TG analysis – Briefly, lipids from cells (sonicated in 1 ml of phosphate buffered saline, PBS) and media were extracted with 4 ml of chloroform/methanol (2:1, v/v), dried under nitrogen, and resuspended in 20 µl of ethanol for the enzymatic determination of TG content using a Serum Triacylglycerol Determination Kit according to the supplied instructions.

Incorporation of OA into TG and PL - Cells were incubated for 4h with OA-BSA containing 2.5 µCi/ml of [9,10(n)-^{3}H]OA as radiolabeled tracer (pulse period) (5). Media was aspirated and cells were washed three times with PBS containing 0.5% fatty acid free BSA. Half of the cell cultures were harvested for lipid analysis (pulse). The remaining cell cultures were incubated for 4h with DMEM before harvesting the cells for lipid analysis (chase). For lipid analysis, all cells were washed with ice-cold PBS, harvested in the same buffer, and disrupted by sonication. Cellular lipids were extracted with chloroform/methanol (2:1, v/v) in the presence of nonradioactive lipid carriers (phoshatidylcholine [PC], and trioleoylglycerol). The chloroform phase containing lipids was dried under nitrogen, redissolved in a small volume of chloroform, and applied to silica gel H thin-layer chromatography plates. The plates were developed in heptane/isopropyl ether/acetic acid (60:40:4, v/v/v) to separate neutral lipids from

phospholipids. The lipid classes were visualized by exposure to iodine vapor, the bands were scraped, and the associated radioactivity was determined by scintillation counting.

Oil Red O (ORO) staining and fluorescence microscopy of cellular LDs - The methods used to detect cellular LDs have been described previously(6).

Analysis of LD morphology – OA was supplied to naïve and infected cells for 14h to expand cellular TG stores, then up to 72 h in DMEM containing 6μM Triacsin C for their lipolysis. LDs were observed by fluorescence microscopy after ORO staining. LD size, numbers and fluorescence area were quantified essentially as described previously(7). A total of 100 images (25 random cells per experiment, for 4 experiments) were captured for analysis of average area of individual LDs, number of LDs per cell, and total area of LDs per cell using Meta- Morph, version 7.5 software (Molecular Devices).

ApoB and HCV density profiles - Media samples (1 ml) were applied to the top of 6-54% (w,v) iodixanol gradients [prepared as described previously(8)] and centrifuged for 10h in a Beckman Optima L100 XP ultracentrifuge at 41000 rpm and 4°C in an SW41 rotor. The gradient was harvested from the top and collected into 23 fractions (0.5 ml each) or 11 fractions (1 ml each). Densities of each fraction were determined by measuring the weight of 200 ml. The ApoB concentration in each fraction was determined using an ELISA for human ApoB (Mabtech, Cincinnati, OH) according to the protocol provided by the supplier. The HCV RNA concentration in each fraction was determined by qRT-PCR.

Esterase/lipase assay and activity-based protein profiling - Esterase/lipase activities present in cellular lysates or microsomal membranes were estimated using an established procedure based on the production of p-nitrophenol from p-nitrophenyl acetate(9) essentially as described previously(10). Activity-based protein profiling based on the reaction of FP-biotin with the catalytic serine residue in lipases and serine hydrolases was performed as described previously(5). Briefly, cells were lysed in 20 mM Tris, pH 7.0, 150 mM NaCl, 1mM EDTA adjusted to 1.5 mM (0.07%) Triton X-100. Cellular lysates (30 mg protein) were incubated with 100 μM FP-biotin (added from a 10 mM stock solution in dimethyl sulfoxide) for 30 min at room temperature. Samples were then boiled in SDS-PAGE loading buffer and proteins resolved on 10% polyacrylamide gels under denaturing conditions. The proteins were transferred to a nitrocellulose membrane and proteins bound to FP-biotin were detected by probing with avidin-HRP (1:15000, v/v) followed by enhanced chemiluminescence (ECL) detection with Amersham Hyperfilm^{TM} ECL.

MTP activity assay - MTP transfer activity was measured using the Roar MTP Activity Assay Kit according to the manufacturer's instructions and is based on MTP-mediated transfer of fluorescence between donor and acceptor particles. In brief, cells were sonicated in 200 µl ice-cold homogenization buffer (10 mM Tris, 150mM NaCl, 1 mM EDTA, pH=7.4, 20 µg/ml leupeptin and 500µM PMSF). Cellular homogenate (100 µg protein) was combined with donor (5 µl) and acceptor (5 µl) vesicles in a total volume of 200 µl of assay buffer, then incubated at 37°C for 240 min. MTP activity was calculated by measuring fluorescence at the excitation wavelength of 465 nm and emission wavelength of 535 nm (Spectramax Gemini, Molecular Devices).

Determination of levels of newly synthesized ApoB - The methods used to quantify the levels of newly synthesized (labeled) ApoB in cellular lysates and media were described previously(11). In brief, cells were incubated for 14 h in serum-free DMEM supplemented with OA-BSA to increase intracellular TG stores, then in 2 ml of methionine/cysteine-free DMEM supplemented with 50 µCi/ml ^{35}S-labeled methionine and cysteine ± 25 µM MG132 (proteasome inhibitor) for 2 h. Cells were washed and scraped in 1 × immunoprecipitation (IP) buffer (150 mM NaCl, 50 mM Tris/HCL, pH=7.4, 5 mM EDTA, 0.5% v/v Triton X-100, 0.1% w/v SDS) containing 1mM benzamidine and were homogenized by sonication, and protein concentration was determined. Collected media were briefly centrifuged to remove cellular debris and adjusted with 10 × IP buffer containing 1mM final concentration of benzamidine. Then 10 µl of goat anti-human ApoB IgG was added to 1 ml of cell sonicates or culture media and the mixture was incubated on a rotating rack for 12 h at 4°C, after which 25 µl of protein A-Sepharose was added and the mixture was incubated on a rotating rack for 3 h at 4°C. The beads were pelleted by brief centrifugation and were washed three times with excess 1 × IP buffer. Denaturing electrophoresis sample buffer was added, samples were boiled and underwent electrophoresis using 5% polyacrylamide gels. Gels were dried and exposed to Kodak BioMax MR Film for 4 weeks at -80ºC. Bands corresponding to labeled ApoB were quantified by densitometry using Bio-Rad Quantity One software.

Quantitative RT-PCR for AADAC and actin – Primer sequences were as follows: hAADAC-F, 5'-CAAAATATG GTGTGAACCCTGA-3'; hAADAC-R, 5'-GAAGGGCAGGATAAATTAAAGA-3'; hbetaActin-F, 5'-CCAACCGCGAGAAGATGA-3'; hbetaActin-R, 5'-TCCATCACGATGCCAGTG-3'. Total RNA was isolated using Trizol LS reagent and reverse transcribed with a mixture of random hexamers and oligo(dT) using qScript cDNA SuperMix according to manufacturer's instructions. AADAC (primers hAADAC-F/hAADAC-R) and beta-actin (primers hbetaActin-F/hbetaActin-R) transcripts were detected by real-time PCR using a Qiagen RotorGene 3000 instrument. Reaction

mixtures contained Platinum Quantitative PCR SuperMix-UDG with 400nM concentrations for each primer in a total volume of 20 ml. Following a 3 minute initial denaturation at 94°C, PCR amplification of AADAC proceeded for 40 PCR cycles of 95°C for 20 s, 56°C for 20 s then 72°C for 20 s. For beta-actin, samples were amplified for 35 cycles of 95°C for 20 s, 60°C for 20 s; 72°C for 20 s. Data analysis was performed with the Corbett Rotor Gene software using the standard curves method. All AADAC values were normalized to beta-actin.

Preparation of microsomal membranes - Cells from culture dishes were harvested into 20 mM Tris/HCl, pH7.5, containing 250 mM sucrose and 5 mM EDTA then homogenized with a Polytron. The microsomal membranes were isolated by ultracentrifugation of the post-mitochondrial supernatant(12).

Immunoblot analysis - Cellular and microsomal proteins were separated on SDS-PAGE, transferred to nitrocellulose membranes and blocked with PBS containing 0.1% Tween 20 (v/v) and 5% non-fat dry milk powder (w/v). Membranes were then incubated for 1 h at room temperature with appropriate dilutions of primary antibodies (1:3000 of anti-MTP, 1:5000 anti-PDI, 1:500 anti-AADAC, 1:5000 anti-TGH, 1:1000 anti-core, 1:20000 anti-NS5A, or 1:10000 anti-actin) followed by 1:10000 appropriate secondary HRP-conjugated IgG antibodies. All immunoreactive bands were detected using Amersham ECL™ Western Blotting Detection Reagents with Amersham Hyperfilm™ ECL.

Indirect immunofluorescence detection of HCV core and AADAC - Dual staining for AADAC and HCV core was achieved using the same indirect immunofluorescence procedure described for HCV core(13), except primary incubations also contained anti-AADAC and the secondary incubations also contained Alexa fluor 488 donkey anti goat IgG.

Flow cytometry - Intracellular indirect dual labeling of AADAC and HCV core protein utilized anti-AADAC and anti-core (C7-50) antibodies in primary incubations followed by their corresponding Alexa fluor 488 donkey anti goat IgG and Alexa fluor 594 goat anti mouse IgG, respectively, in secondary incubations. Nonlabeled cells and labeling due to isotype controls present during primary incubations (instead of primary antibodies) served as controls. Data were acquired utilizing distinct lasers for excitation of the fluorophores (488 and 561 nm) on a BD LSRFortessa (BD Biosciences, San Jose, CA) and analyzed with FlowJo 7.6.5 (Tree Star, Ashland, OR).

Transient expression of AADAC in Huh7.5 cells - For expression studies, naïve and HCV infected Huh7.5 cells were transiently transfected with pAADAC using

Lipofectamine 2000 according to the supplied protocol. Transfections were also performed in parallel using a control vector that did not contain the AADAC coding region.

Generation of stable short hairpin RNA (shRNA)-expressing Huh7.5 cells - MISSION® Lentiviral Transduction Particles expressing shRNAs targeting human AADAC and a non-targeting (NT) shRNA that does not target any known human transcripts (5'-CAACAAGATGAAGAGCACCAA-3') were used to generate stable shRNA-expressing Huh7.5 cells. The following sequences in AADAC were targeted: AADAC-1 (5′-GCCATGCTTTCCAGACAACAT-3′), AADAC-2 (5′-GCTCCCTGAGAGGTTTATAAA-3′), AADAC-3 (5′-GCCATGCTTTCCAGACAACAT-3′), AADAC-4 (5'-CGTATCAACCAAC TACAGATT-3'), and AADAC-5 (5'- CTGTGGGATTTCATTTCAATT-3'). Huh7.5 cells were transduced at a MOI of 5 with shRNA-expressing lentiviruses and Polybrene (8 µg/ml). After 48-h incubation with lentiviruses, fresh medium containing puromycin (10 µg/ml) was applied. After 3 weeks of drug selection, target protein knockdown was evaluated by immunoblot analysis. Stable knockdown cell lines were routinely maintained in medium containing puromycin (2 µg/ml).

Titration of HCV growth curves - A recombinant HCV encoding for a secreted luciferase upon HCV replication (Bi-Gluc-J6/JFH) was kindly provided by Dr. Charles Rice (Rockefeller University, NY) and was used to monitor virus growth(14). Growth curves were set up in general by plating 8×10^3 cells per well in poly-L-lysine-coated 96-well plates 24h prior inoculation with 100 ml of a viral stock containing Bi-Gluc-J6/JFH at an MOI of 0.02. At time points, 6, 24, 48 and 72 hours post-infection, 10 ml supernatant was collected to measure the amount of secreted luciferase with the Renilla luciferase assay system. Briefly, 10 ml Renilla lysis buffer and 10 ml cell culture supernatant were mixed in a white polystyrene assay plate, followed by addition of 50 ml Renilla luciferase substrate to initiate the reaction. The resultant luminescence was measured with the Enspire 2300 Multilabel Reader (PerkinElmer).

Determination of HCV infectivity titer - Limiting dilution assays were used to quantify HCV infectivity between samples as median tissue culture infectious units per milliliter (TCID50/ml). The TCID50 is the dilution that infects 50% of replicate cell cultures and was determined essentially as described(15). Briefly, Huh 7.5 cells were seeded on poly-lysine coated 96 well plates (6×10^3 cells/well). At 24h post-seeding, cells were infected with 10 fold serially diluted cell culture supernatants (8 wells per dilution). Cell culture media was replaced with fresh media at 16h post-infection, then cells fixed in methanol at 72h post-infection. HCV infected cells were detected by immunostaining using anti-NS5A antibody (9E10) with HRP conjugated sheep anti-mouse IgG secondary antibody and

subsequently visualized with a DAB substrate kit (DAKO). TCID50 was calculated, based on the NS5A positive wells, according to the method of Reed and Muench(16).

Statistical analysis – Means +/- SEM were determined for N=4 independent experiments. The results were statistically analyzed by the Student *t* test of means and one-way ANOVA or non-parametric tests, Kruskal-Wallis and Mann Whitney U tests. *P* values less than 0.05 were considered to be significant. Calculations were performed using SPSS 20.0 software (Chicago, IL).

Other methods - Protein concentrations were determined by the Pierce Micro BCA Assay Kit.

Legends for Supplemental Figures

Fig S1. The secretion of TG derived from preformed cellular TG stores (A) Huh7.5 cells were cultured for 14h in DMEM supplemented with OA-BSA (OA-BSA) to increase cellular TG stores or in DMEM containing 10% FBS (FBS) or containing just BSA (BSA). Cells were washed and collected for analysis of cellular TG mass (cellular) or the media was replaced with fresh DMEM for 2h to allow for secretion of TG (as VLDL-TG) derived from preformed cellular TG stores prior to collecting the media for analysis of TG mass (secreted). **(B)** Naïve and infected cells (during the early peak of viral infection) were cultured for 14 h in DMEM supplemented with OA-BSA (OA-BSA) or in DMEM containing 10% FBS (FBS) prior to fixing cells and staining LDs with Oil red O (ORO), nuclei with DAPI, and HCV core protein by indirect immunofluorescence. **(C)** Naïve and infected cells (during the early peak of viral infection) were incubated for 4h in DMEM supplemented with OA-BSA and trace amounts of [9,10(n)-^{3}H]OA (pulse period). At the end of the pulse period, cells were washed with PBS containing 0.5% fatty acid free BSA to remove residual labeled substrate that had not been taken up by the cells and lipids were extracted from cells for lipid analysis (pulse) or fresh media (DMEM) was added and cells were incubated for an additional 4h to allow for TG secretion from preformed stores (chase period) prior to extracting lipids from cells for lipid analysis by TLC (chase). Radioactivity associated with cellular phospholipids (PL) and TG at the end of the pulse and chase periods were determined by TLC and is expressed as dpm×10^{-3}/mg cellular protein. **(D)** Naïve and infected cells (during the early peak of viral infection) were incubated for 14h with DMEM containing OA-BSA to increase cellular TG stores, then in DMEM (+triacsin C) for up to 72h. Cells were collected for examination of LD morphology by ORO staining and fluorescence microscopy.

Fig S2. ApoB density profiles/mass, MTP activity and ApoB synthesis. (A) ApoB density profiles were obtained as described for Fig 1C except cells were incubated with DMEM containing BSA alone (i.e. without the OA supplement) or 10% FBS for 14 h prior to the 8h secretion period (i). Naïve and infected cells (during the early peak of viral infection) were incubated with DMEM containing OA-BSA or 10% FBS for 14h. Media was replaced with fresh DMEM for 8h before collecting media and cells for determination of cell-associated (cellular) and secreted ApoB mass (ii). When compared with cells that were incubated with DMEM containing 10% FBS, no significant changes in ApoB mass was observed with cells that were incubated with DMEM containing BSA alone (not shown). **(B)** MTP transfer activity was measured in cellular lysates prepared from naïve and infected cells (collected during the early peak of viral infection) using the Roar MTP Activity Assay Kit as described under “Experimental Procedures” and is expressed as

pmol substrate transferred/mg protein. MTP expression levels were evaluated by immunoblot analysis and then the same nitrocellulose membrane was sequentially stripped and re-probed with antibodies for the detection of protein disulfide isomerase (PDI), HCV core, and actin. The immunoblots shown are representative of 4 independent experiments. **(C)** Naïve and infected cells (during the early peak of viral infection) were incubated for 14h in DMEM supplemented with OA-BSA to increase intracellular TG stores available for VLDL assembly. Cells were washed then incubated for 2h in methionine- and cysteine-free DMEM containing ^{35}S-methionine and -cysteine ± 25μM MG132 (-/+ MG132 as indicated) to label the endogenous pool of newly synthesized proteins and allow for the secretion of VLDL containing labeled ApoB. The levels of ^{35}S-labeled ApoB present in media and cellular lysates were determined as described under "Experimental Procedures". Values are Means ± SEM for N=4 independent experiments (*P<0.001).

Fig. S3. AADAC expression in infected cells and AADAC knockdown cells (A) Naive cells were transfected with pAADAC (or vector). Microsomes were prepared at 48h post transfection for the determination of lipolytic activities (and AADAC and PDI expression, inset). **(B)** Infected cells (during the early peak of viral infection) were transfected with pAADAC (or vector). Cellular lysates were prepared at 48h post transfection for the determination of lipolytic activities (and AADAC and PDI expression in microsomes, inset). E600 (100 mM, +/- as indicated) was added to the culture media of half of the culture dishes at 24 h post-transfection. **(C)** The abundance of AADAC in infected cells (described in B) that had undergone the transfection procedure was also evaluated by indirect immunofluorescence microscopy. The HCV core protein was readily detected in the majority of cells (>90%) that had undergone the transfection procedure. AADAC was detected in infected cells that had been transfected with pAADAC with an estimated transfection efficiency of 35-50%. By contrast, vector control cells had no detectable AADAC by this method. Nuclei were stained with DAPI. **(D)** Immunoblot analysis showing AADAC expression in Huh7.5 cells bearing stable short hairpin RNA (shRNA)-expressing lentiviral constructs targeting AADAC (1-5) or a non-targeting control (NT). The same membrane was stripped and re-probed for actin to control for loading. Intensities of bands were determined by densitometry using BioRad Quantity One software. The percentage of AADAC (normalized to actin) relative to Huh7.5 cells (100%) is shown. **(E)** AADAC-1, AADAC-2, and NT cells were incubated in DMEM containing OA-BSA for 14h prior to collecting cells for TG analysis. Values are Means ± SEM from N=4 independent experiments.

Figure S1A and S1B

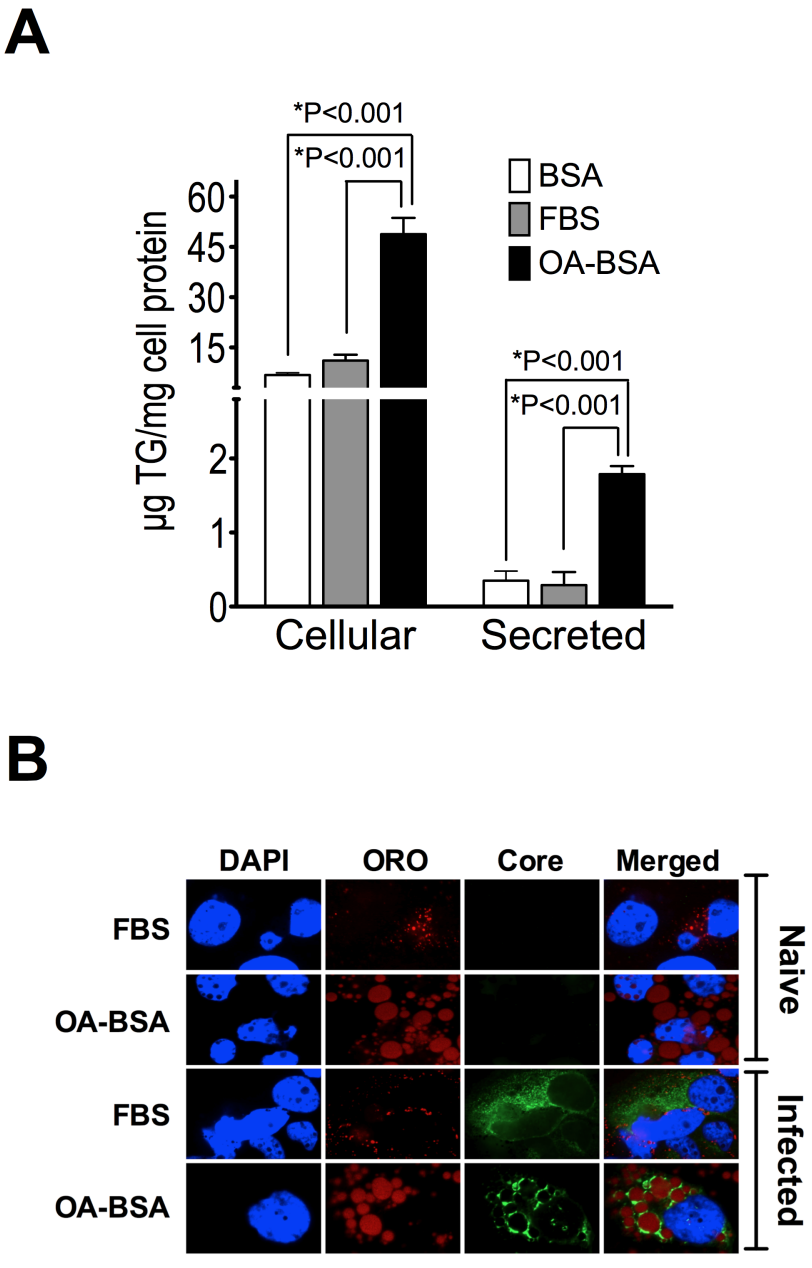

Figure S1C and S1D

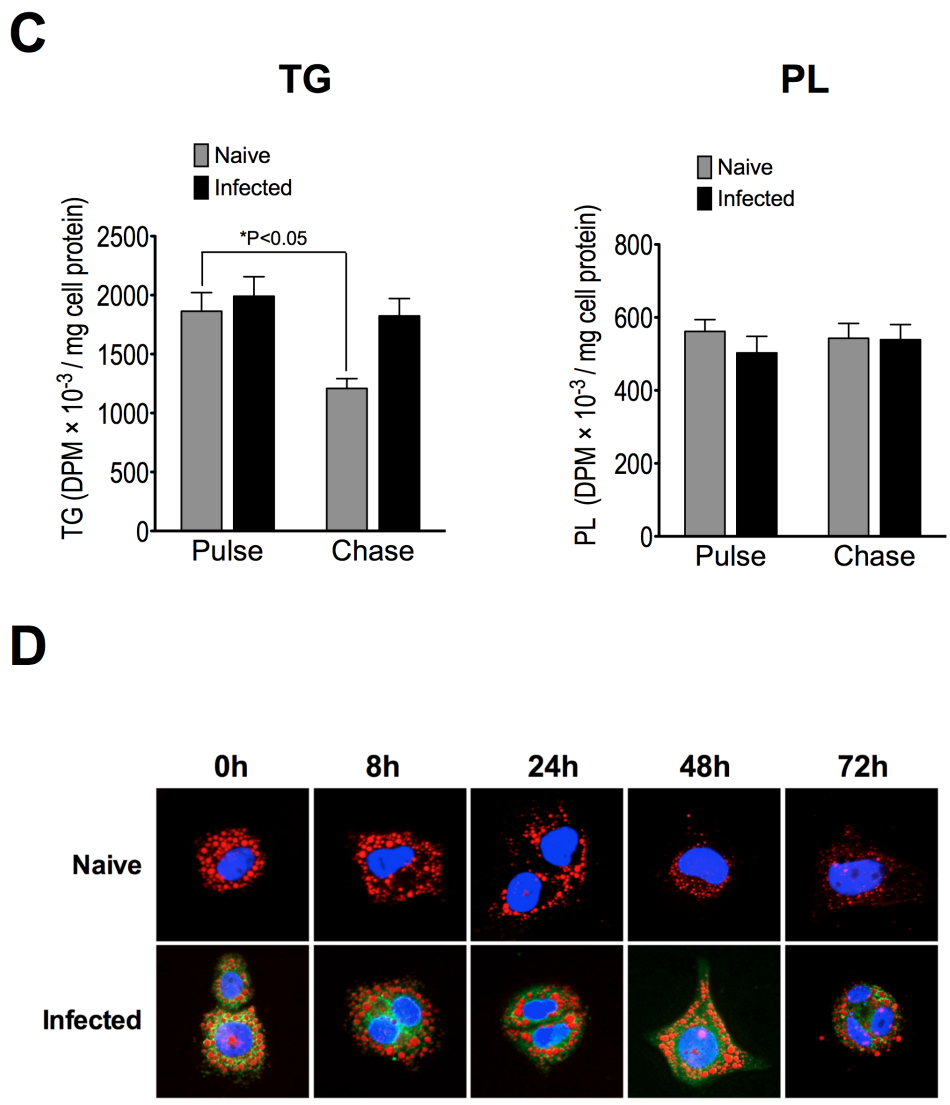

Figure S2A

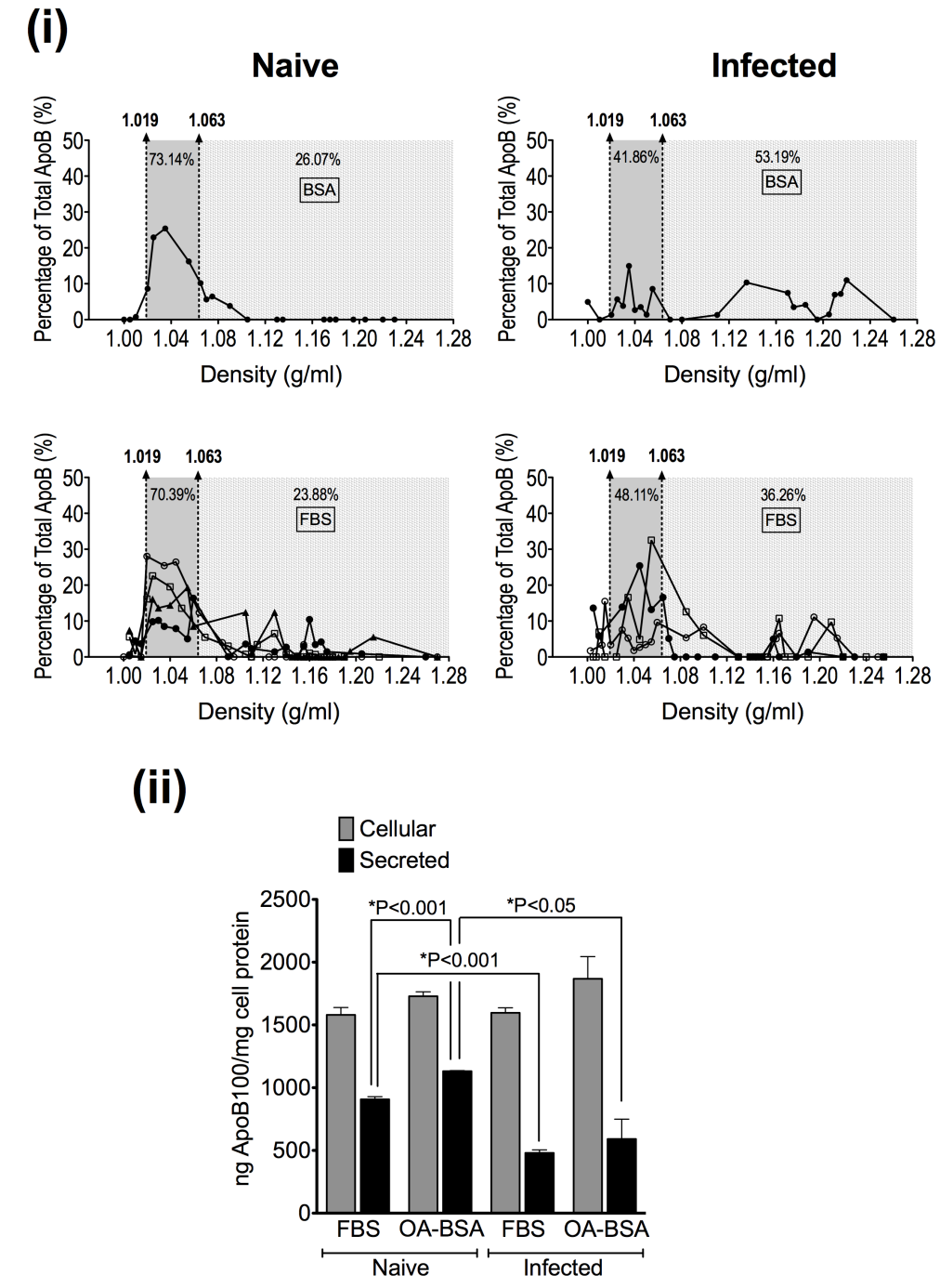
(i)
Naive
Infected
1.019
1.063
73.14%
26.07%
BSA
41.86%
53.19%
70.39%
23.88%
FBS
48.11%
36.26%
Percentage of Total ApoB (%)
Density (g/ml)
(ii)
Cellular
Secreted
*P<0.001
*P<0.05
*P<0.001
ng ApoB100/mg cell protein
FBS
OA-BSA
FBS
OA-BSA
Naive
Infected

Figure S2B and S2C

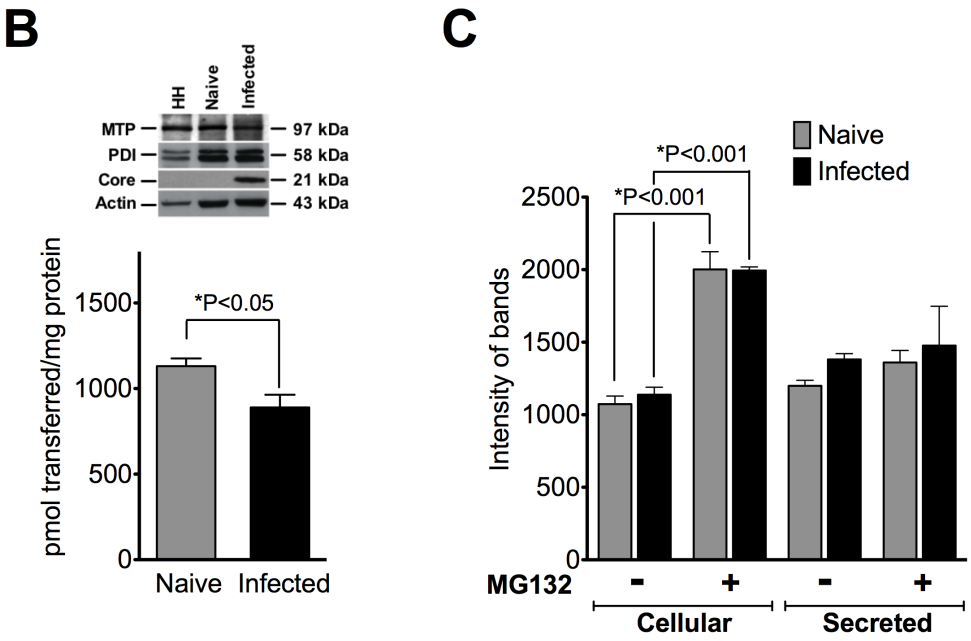

Figure S3A, S3B and S3C

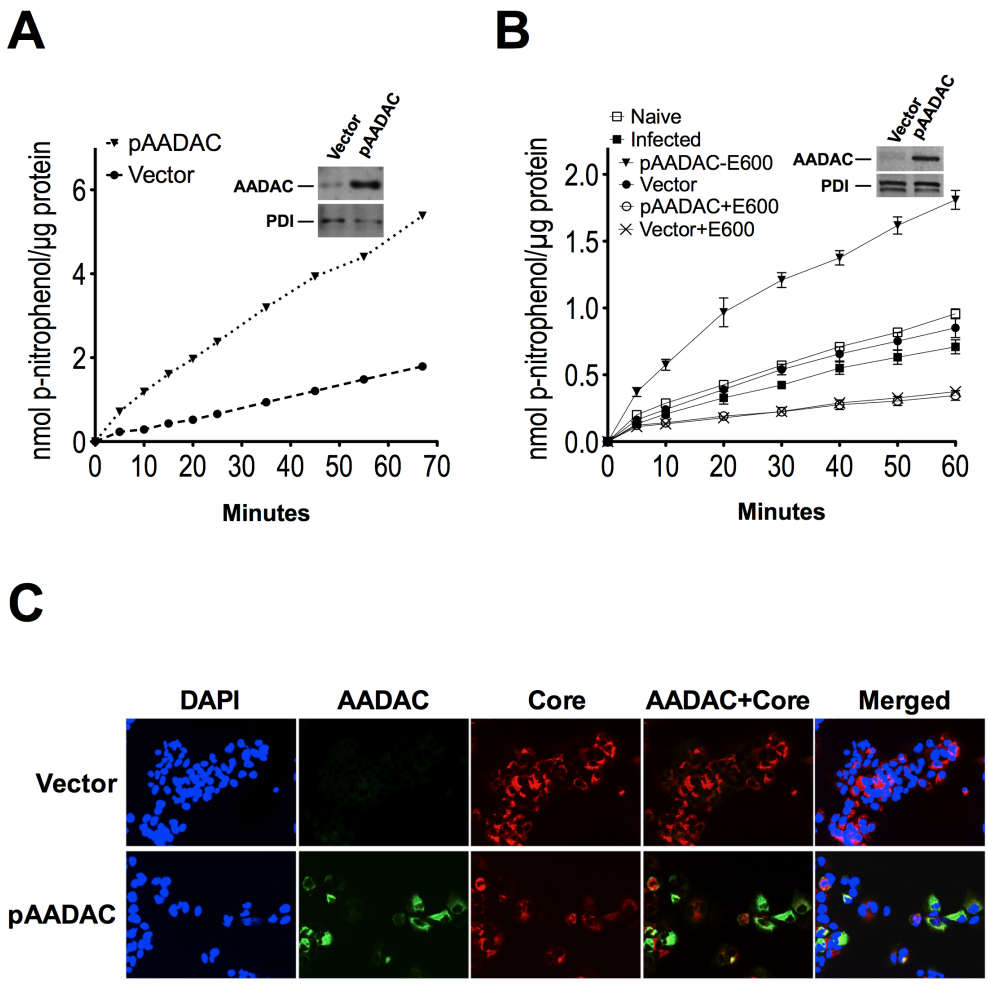

Figure S3D and S3E

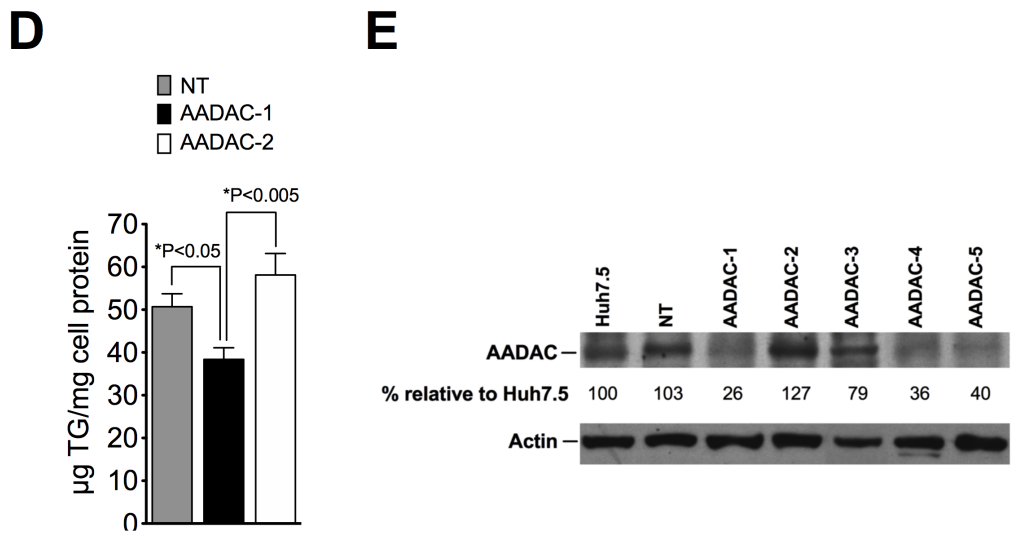

References

1. Wei E, Alam M, Sun F, Agellon LB, Vance DE, Lehner R. Apolipoprotein B and triacylglycerol secretion in human triacylglycerol hydrolase transgenic mice. Journal of lipid research. 2007;48(12):2597-606. Epub 2007/09/20.

2. Blight KJ, McKeating JA, Rice CM. Highly permissive cell lines for subgenomic and genomic hepatitis C virus RNA replication. Journal of virology. 2002;76(24):13001-14. Epub 2002/11/20.

3. Kawahara T, Toso C, Douglas DN, Nourbakhsh M, Lewis JT, Tyrrell DL, et al. Factors affecting hepatocyte isolation, engraftment, and replication in an in vivo model. Liver Transpl. 2010;16(8):974-82. Epub 2010/08/03.

4. Vrolijk JM, Kaul A, Hansen BE, Lohmann V, Haagmans BL, Schalm SW, et al. A replicon-based bioassay for the measurement of interferons in patients with chronic hepatitis C. J Virol Methods. 2003;110(2):201-9. Epub 2003/06/12.

5. Lo V, Erickson B, Thomason-Hughes M, Ko KW, Dolinsky VW, Nelson R, et al. Arylacetamide deacetylase attenuates fatty-acid-induced triacylglycerol accumulation in rat hepatoma cells. J Lipid Res. 2010;51(2):368-77. Epub 2009/08/06.

6. Abid K, Pazienza V, de Gottardi A, Rubbia-Brandt L, Conne B, Pugnale P, et al. An in vitro model of hepatitis C virus genotype 3a-associated triglycerides accumulation. J Hepatol. 2005;42(5):744-51.

7. Wang H, Wei E, Quiroga AD, Sun X, Touret N, Lehner R. Altered lipid droplet dynamics in hepatocytes lacking triacylglycerol hydrolase expression. Mol Biol Cell. 2010;21(12):1991-2000. Epub 2010/04/23.

8. Nielsen SU, Bassendine MF, Burt AD, Martin C, Pumeechockchai W, Toms GL. Association between hepatitis C virus and very-low-density lipoprotein (VLDL)/LDL analyzed in iodixanol density gradients. Journal of virology. 2006;80(5):2418-28. Epub 2006/02/14.

9. Gilham D, Lehner R. Techniques to measure lipase and esterase activity in vitro. Methods. 2005;36(2):139-47. Epub 2005/05/17.

10. Lehner R, Vance DE. Cloning and expression of a cDNA encoding a hepatic microsomal lipase that mobilizes stored triacylglycerol. Biochem J. 1999;343 Pt 1:1-10.

11. Gilham D, Ho S, Rasouli M, Martres P, Vance DE, Lehner R. Inhibitors of hepatic microsomal triacylglycerol hydrolase decrease very low density lipoprotein secretion. Faseb J. 2003;17(12):1685-7.

12. Lehner R, Kuksis A. Purification of an acyl-CoA hydrolase from rat intestinal microsomes. A candidate acyl-enzyme intermediate in glycerolipid acylation. The Journal of biological chemistry. 1993;268(33):24726-33. Epub 1993/11/25.

13. Kato T, Date T, Murayama A, Morikawa K, Akazawa D, Wakita T. Cell culture and infection system for hepatitis C virus. Nat Protoc. 2006;1(5):2334-9.

14. Reyes-Del Valle J, de la Fuente C, Turner MA, Springfeld C, Apte-Sengupta S, Frenzke ME, et al. Broad neutralizing immune responses against hepatitis C virus induced by vectored measles viruses and a recombinant envelope protein boost. J Virol. 2012. Epub 2012/08/17.

15. Lindenbach BD, Evans MJ, Syder AJ, Wolk B, Tellinghuisen TL, Liu CC, et al. Complete replication of hepatitis C virus in cell culture. Science. 2005;309(5734):623-6. Epub 2005/06/11.

16. Reed LJ, & Muench, H. . A simple method of estimating fifty percent endpoints. Am J Hygiene. 1938;27:493-7.

Paper 2

Entitled: Characterization of VLDL and HCV production by hepatoma cells after the introduction of triacylglycerol hydrolase.

In this paper, we have investigated the role of triacylglycerol hydrolase (TGH) in the mobilization of cellular TG stores for VLDL secretion and on HCV production (Aim 3). We have shown that Huh7.5 cells are deficient in TGH and this deficiency is associated with impaired mobilization of TG for secretion with VLDL. The introduction of TGH to huh7.5 cells by stable transfection was associated with enhanced cellular lipolytic activity, enhanced mobilization of preformed cellular TG stores for secretion with VLDL and enhanced apoB secretion. These results were TGH dependent since treating cells with GR148672X, a specific inhibitor of TGH, obliterated these changes.

Similar to what we observed with wild-type Huh7.5 cells (previous manuscript), infection of Huh7.5 cells that express TGH resulted in reduced lipolytic recruitment of cellular TG stores for VLDL assembly and were AADAC deficient (Aims 1-3). Thus, the introduction of TGH to these cells does not substitute for AADAC's role in this process. When HCV infection was established in TGH expressing cells, there was a modest increase in viral RNA secretion but these cultures still produced similar levels of infectious virions as wild-type cells (Aim 3).

Author Contributions

Mahra Nourbakhsh: Designing the project and the strategy to test the hypothesis, writing the manuscript, performing the assays and experiments, managing and overseeing technical support, collecting and analyzing the data.

Dr. Donna Douglas: Designing the project and the strategy to test the hypothesis, writing the manuscript and supervision.

Dr. Norman Kneteman: Designing the project and the strategy to test the hypothesis, critical reading, and supervision.

Dr. Richard Lehner: Designing the project and strategy to test the hypothesis and critical reading.

Mr. Christopher Hao Pu: Technical support.

Mr. Jamie Lewis: Technical Support, cell culture and management of viral stocks

Mrs. Chelcey Buck: Technical Support.

Mr. Randy Nelson: Quantitative RT-PCR of AADAC, TGH.

Dr. Toshiyasu Kawahara: Assisting in statistical analysis, critical reading.

Dr. Ali Alsaghir: Assisting in performing apoB ELISA

Dr. Enhui Wei: Technical Support.

Dr. Lok Man John Law and Chao Chen: Analyzing HCV Infectivity titer.

Dr. Michael Houghton: Critical reading, academic support.

Characterization of VLDL and HCV production by hepatoma cells after the introduction of triacylglycerol hydrolase

Mahra Nourbakhsh[1*], Donna N. Douglas[1*¶], Christopher Hao Pu[1], Jamie T. Lewis[1], Toshiyasu Kawahara[1], Chelcey Buck[1], Ali Alsaghir[1], Enhui Wei[1], Lok Man John Law[5], Chao Chen[5], Randy Nelson[2], Michael Houghton[5], Richard Lehner[3,4], Norman M. Kneteman[1]

From the Departments of [1] Surgery, [2] Biochemistry, [3] Cell Biology, [4] Pediatrics, and [5]Med Microbiology & Immunology University of Alberta, Edmonton, Alberta, T6G 2E1, Canada

* D.N. Douglas and M. Nourbakhsh contributed equally to this work

Address correspondence to:

Donna N. Douglas, PhD

6-010A Katz Group-Rexall Centre, Department of Surgery, University of Alberta,

Edmonton, Alberta, T6G 2E1, Canada. Phone: 780-492-7921, FAX: 780-407-7374

E-mail: donnad@ualberta.ca

List of abbreviations:

CLD	cytosolic lipid droplet
LLD	luminal lipid droplet
VLDL	very low density lipoprotein
HCV	Hepatitis C virus
TG	triacylglycerol
DG	diacylglycerol
MG	monoacylglycerol
ORO	Oil Red O
MTP	microsomal triglyceride transfer protein
ApoB	apolipoprotein B-100
AADAC	arylacetamide deacetylase
GR148672X	trifluoro-2-[2-(3-methylphenyl)hydrazono]-1-(2-thienyl)butane-1,3-dione
ELISA	enzyme-linked immunosorbent assay
FP	fluorophosphonate
DMEM	Dulbecco's Modified Eagle Medium
FBS	fetal bovine serum
JFH	Japanese fulminant hepatitis
DNA	Deoxyribonucleic acid
RNA	ribonucleic acid
qRT-PCR	quantitative reverse transcriptase-polymerase chain reaction
OA	oleic acid
BSA	bovine serum albumin
PBS	phosphate buffered saline
ER	endoplasmic reticulum
TGH	triacylglycerol hydrolase
PDI	protein disulfide isomerase

Financial Support:

Financial support was provided by an operating grant from the Canadian Institute of Health Research (CIHR/IRSC) awarded to Drs. Kneteman, Douglas and Lehner, the National CIHR Research Training Program (NCRTP) in Hepatitis C awarded to Dr. Mahra Nourbakhsh, and a Canada Excellence in Research Chair (CERC) awarded to Dr. Michael Houghton.

Abstract

Background & Aims: Majority of triacylglycerol (TG) that is secreted by Very Low Density Lipoprotein (VLDL) originates from lipid droplets (LDs) in a process that requires lipolysis and re-esterification. A role for Triacylglycerol Hydrolase (TGH) in this process has been established. LDs are important for the hepatitis C virus (HCV) lifecycle and their expenditure by lipases may alter HCV replication, assembly and/or secretion. We have previously demonstrated that TGH is absent from the highly permissive JFH-1/Huh7.5 cell culture system for HCV infection. A role for TGH in the lipolytic mobilization of cellular TG stores for VLDL assembly and in the HCV lifecycle has yet to be demonstrated in this system and is relevant since TGH is highly expressed in human liver and is expected to impact both cellular LDs and VLDL assembly, both of which are suggested to be important for the HCV lifecycle.

Method: Huh7.5 cells stably expressing human TGH-cDNA (fused to EGFP, TGH-EGFP) were used to examine (i) the role of TGH in the lipolytic mobilization of cellular TG stores for VLDL assembly (ii) if TGH can restore defective lipolysis of cellular TG stores in infected cells due to AADAC deficiency, and (iii) if TGH has a role in the HCV lifecycle.

Results: TGH expression in Huh7.5 cells increased cellular lipolytic activity and mediated enhanced lipolysis of cellular TG stores, leading to the secretion of more VLDL-TG and ApoB. These alterations were abolished when cells were treated with specific inhibitor of TGH. We have previously demonstrated that AADAC deficiency in HCV infected cells contributes to defective lipolysis of cellular TG stores for output with VLDL. Surprisingly, this process remained defective when infection was established in TGH expressing cells, indicating that TGH cannot substitute for AADAC in this process. Finally, infected cells secreted more HCV RNA into the media when TGH was expressed, but the production of infectious HCV were similar between TGH expressing and wild-type cells.

Conclusions: TGH expression in Huh7.5 cells enhances the mobilization of TG for secretion with VLDL, but has little impact on HCV production.

Introduction

According to a report by the World Health Organization, an estimated 130-170 million individuals are chronically infected with Hepatitis C Virus (HCV) and more than 350,000 people die annually from HCV-related liver disease (1). HCV is a positive single-stranded RNA virus and is classified in the Hepacivirus genus within the Flaviviridae family. Its 9.6-kb genome encodes a polyprotein with about 3000 amino acids that is cleaved by host and viral proteases to ten structural (core, E1, E2) and non-structural (P7, NS2, NS3, NS4A, NS4B, NS5A and NS5B) proteins (2). The process of HCV assembly and export is not clearly known, but several findings suggest HCV adopts the Very Low Density Lipoprotein (VLDL) secretion pathway for egress while cellular lipid droplets (LDs) appear to be important for HCV assembly (3-5).

VLDL is a triacylglycerol (TG)-rich lipoprotein that is assembled and secreted exclusively by the liver in humans (6). VLDL structure consists of a core of hydrophobic lipids (essentially TG and to a lesser extent, cholesterol ester) surrounded by a layer of amphipathic lipids. The majority of its TG cargo (>70%) is derived from the lipolysis of cellular TG stores. A role for triacylglycerol hydrolase (TGH) in VLDL assembly has been established (7-10) and involves its ability to hydrolyze the TG present in cellular LDs so that the released fatty acids can contribute to the synthesis of TG that is ultimately loaded onto ApoB (11). Human TGH is a 60 kDa luminal serine hydrolase belonging to the carboxyl esterase (CES) family and phylogenetically classified in subclass CES1A (12, 13). It is highly expressed in hepatocytes but has been suggested to be absent from human hepatoma cells that have defective VLDL assembly (8, 14, 15) including Huh7.5 cells (Nourbakhsh et al. Journal of Hepatology, in press).

In this study, we have expressed human TGH tagged with EGFP in Huh7.5 cells to determine if TGH can act as a TG lipase in these cells, possibly affecting VLDL and HCV production.

Methods and Materials

Materials **-** Serum Triacylglycerol Determination Kit (Cat. No. TR0100), Iodixanol (OptiPrep Density Gradient Medium), fatty acid free-bovine serum albumin (BSA), oleic acid (OA), glycerol, protease inhibitor cocktail, G418, p-nitrophenol, p-nitrophenyl laurate and p-nitrophenyl acetate, were obtained from Sigma-Aldrich (Oakville, ON). ELISA kit for human Apolipoprotein B was from Mabtech (Cincinnati, OH). Biotinylated fluorophosphonate (FP-biotin) was obtained from Toronto Research Center (Toronto, ON). TGH-EGFP (16) plasmid and EGFP plasmid were kind gift from Dr. Richard Lehner (University of Alberta). Dulbecco's modified Eagles medium (DMEM), TRIzol, Platinum

Quantitative PCR SuperMix-UDG, penicillin-streptomycin mixture and Lipofectamine 2000 were purchased from Invitrogen (Burlington, ON). The antibodies were obtained from the following sources: mouse anti-core C7-50 monoclonal antibody was from Affinity BioReagents (Rockford, IL); goat anti human arylacetamide deacetylase (anti-AADAC) polyclonal antibody (sc-99249: clone K-12) were from Santa Cruz Biotech (Santa Cruz, CA); goat anti GFP was from Abcam (Cambridge, MA); rabbit anti human triacylglycerol hydrolase (anti-TGH) polyclonal antibody was obtained as described previously(17); mouse anti actin clone C4 (anti-actin) monoclonal antibody was from Millipore (Billerica, MA); mouse anti human protein disulfide isomerase (anti-PDI) monoclonal antibody was from Stressgen Biotechnologies (Victoria, BC); HRP-conjugated rabbit anti-goat IgG antibody was from Pierce Biotechnology Inc. (Rockford, IL); HRP-conjugated anti mouse IgG antibody was from MP Biomedical (Solon, OH); HRP-conjugated donkey anti rabbit IgG was from Jackson Immunoresearch (West Grove, PA); Alexa fluor 594 goat anti mouse IgG was from Invitrogen (Burlington, ON). Micro BCA Protein Assay Reagent Kit was obtained from Pierce Biotechnology (Rockford, IL). MEGAscript® T7 kit was obtained from Ambion/Applied Biosystems (Streetsville, ON). DAB substrate kit was from DAKO (Burlington, ON). ECL™ Western Blotting Detection Reagents and Hyperfilm™ ECL were from GE Healthcare Amersham (Milwaukee, WI). qScript cDNA SuperMix was from Quanta Biosciences (Gaithersburg, MD). All DNA primer synthesis was performed by IDT (Coralville, IA).

Cell Culture - Huh7.5 cells, a mutant line of Huh7 cells that support HCV replication with high efficiency(18), were generously provided by Dr. Charles M. Rice (Rockefeller University, NY). Primary human hepatocytes were obtained in site using procedures we have previously described(19). Cell cultures were maintained on Dulbecco's modified Eagle's medium (DMEM) containing 10% fetal bovine serum (FBS), 100 U/ml penicillin and 100 μg/ml streptomycin at 37ºC in humidified air containing 5% CO_2. Human hepatocytes were cultured on collagen dish and were subjected to the study not later than 24 hours after isolation.

Generation of naïve and infected cells used in experiments - HCV RNA was transcribed *in vitro* from pJFH-1 (provided by Dr. Charles M. Rice, Rockefeller University, NY) containing an HCV consensus clone (designated as JFH-1) derived from a Japanese patient with fulminant hepatitis(20, 21) according to the protocol published before(22). Transfected cultures were passaged at about 80% confluence (corresponding to approximately every 72 hours) and maintained in culture for 17-28 days. Viral stocks were generated from cell culture supernatants collected from transfected cells between 10-28 days post-transfection and the viral titer of viral stocks (expressed as focus-forming

units per milliliter of supernatant – ffu/ml) was determined essentially as described(23). The viral stocks were used to inoculate naïve cell cultures at a multiplicity of infection (MOI) of 0.01. These were maintained in culture for up to 14 days and were considered for "infected" cells to be used in experiments between days 8-14 post-inoculation. HCV infection in cell cultures were routinely monitored by qRT-PCR for HCV RNA in media and indirect immunofluorescence for HCV core protein in cells, essentially as described(22, 24). "Infected" cells were enrolled into experiments during the early peak of viral infection(25), as described previously. Infected cell culture during this period are characterized by > 10^7 IU of HCV RNA per µg of cellular RNA and had >95% of cells core-positive. "Naïve" cells used in experiments were derived from the same Huh7.5 cell stocks as their "Infected" counterparts and were cultured, passaged and maintained under identical conditions except they were not inoculated with viral stocks.

Indirect immunofluorescent detection of HCV core – Staining for HCV core was achieved using the same indirect immunofluorescence procedure described for HCV core (22). In brief, cells grown on coverslips were fixed and permeablized by incubation in cold methanol/acetone (1:1, v/v) fro 20 minutes at -20°C and were blocked in PBS + 1% BSA (w/v) + 2.5 mM EDTA for 1h at room temperature. Cells then were incubated for 1h at room temperature with mouse anti core anti body (1:300, v/v) followed by 1h in Alexa 594-Fluor anti mouse IgG (1:1000, v/v). Cells then were mounted with Perma Fluor mounting solution containing 1µg/ml DAPI.

Mass Secretion of TG from Preformed Cellular Storage Pools - Unless otherwise stated, cells at 60% confluency were incubated for a total of 14h in serum-free DMEM supplemented with 0.375 mM oleic acid (OA) complexed with 0.5% (w/v) fatty acid-free BSA (OA-BSA) to stimulate TG synthesis and increase cellular TG stores (OA group) or in DMEM supplemented with 10% FBS (FBS group). The preparation of an OA-BSA stock solution was as previously described (8). For the last 2h of this incubation, the media was replenished with fresh DMEM supplemented with OA-BSA. At the end of this incubation period (t = 0h), cellular and secreted lipids (present in media) were extracted from one half of the culture dishes for analysis of TG mass (see below). Thus the cellular deposition of newly synthesized TG stimulated by the OA supplement contributes to cellular TG mass at t=0h, and the newly synthesized TG that is found in the media at t=0h (while OA is still being supplied to cells) represents the pool of OA-stimulated TG that gets diverted to secretion rather than to storage. With the remaining half of the culture dishes, cells were washed and incubated for up to 8h with DMEM (without the OA supplement) ±10µM of GR148672X (A specific TGH inhibitor, GSKi) to allow for the

secretion of TG from preformed cellular storage pools. In some cases, during incubation media was replenished every 2h and fresh media was added.

Analysis of TG Mass - Briefly, lipids from cells (sonicated in 1 ml of phosphate buffered saline, PBS) and media were extracted with 4 ml of chloroform/methanol (2:1, v/v), dried under nitrogen, and resuspended in 20µl of ethanol for determination of TG content enzymatically using a Serum Triacylglycerol Determination Kit according to the supplied instructions.

Determination of levels of ApoB **-** Cells at 60% confluency were incubated for 14h in serum-free DMEM supplemented with OA-BSA (OA) or in DMEM + 10% FBS (FBS), then in DMEM (without OA) ±10µM GR148672X (GSKi) for 8h. Cells were washed and scraped in 2ml of PBS and were homogenized by sonication, and protein concentration was determined. Collected media were briefly centrifuged to remove cellular debris. Total ApoB in cells and media were measured by an ApoB ELISA (Mabtech) and was normalized to cell protein.

Density profile of ApoB **-** Iodixanol gradients were prepared as described by Nielsen et al. (26). Isopycnic linear density gradients were prepared from 6% (w/v) [1.7 ml of 60% (w/v) iodixanol, 0.34 ml of 0.5 M Tris-HCl, pH 8.0, 0.34 ml of 0.1 M EDTA, pH 8.0, and 14.6 ml 0.25 M sucrose] and 56.4% (w/v) [16.0 ml of 60% iodixanol (w/v), 0.34 ml of 0.5M Tris-HCl, pH 8.0, 0.34 ml of 0.1 M EDTA, pH 8.0, and 0.34 ml 0.25 M sucrose] iodixanol solutions in thin wall centrifuge tubes (14.89 mm, Beckman) using a two-chamber gradient maker. Media samples (1 ml) were applied to the top of 6 to 56% iodixanol gradients and centrifuged for 10 h in a Beckman Optima L100 XP ultracentrifuge at 41000 rpm and 4°C in an SW41 rotor. The gradient was harvested from the top and collected into 11 fractions (1 ml each). The density of each fraction was determined by measuring the weight of 200 µl. The ApoB concentration in each fraction was determined using an ELISA for human ApoB (Mabtech, Cincinnati, OH) according to the supplied protocol.

Determination of Lipolytic Activity and Activity-Based Protein Profiling – Lipolytic activity in cellular and microsomal preparations was estimated using a well-established procedure that is based on the production of p-nitrophenol from p-nitrophenyl acetate or p-nitrophenyl laurate (11). Activity-based protein profiling based on the reaction of FP-biotin with the catalytic serine residue in lipases and serine-hydrolases was performed as described previously (27). Briefly, Cells were lysed in 20 mM Tris, pH 7.0, 150 mM NaCl, 1mM EDTA adjusted to 1.5 mM (0.07%) Triton X-100. Cellular lysates (30 mg protein) were incubated with 100 µM FP-biotin (added from a 10 mM stock solution in dimethyl

sulfoxide) for 30 min at room temperature. Samples were then boiled in SDS-PAGE loading buffer and proteins resolved on 10% polyacrylamide gels under denaturing conditions. The proteins were transferred to a nitrocellulose membrane and proteins bound to FP-biotin were detected by probing with avidin-HRP (1:15000, v/v) followed by enhanced chemiluminescence (ECL) detection with Amersham Hyperfilm^{TM} ECL.

Immunoblot analysis - Cellular and microsomal proteins were separated on SDS-PAGE, transferred to nitrocellulose membranes and blocked with PBS containing 0.1% Tween 20 (v/v) and 5% non-fat dry milk powder (w/v). Membranes were then incubated for 1h at room temperature with appropriate dilutions of primary antibodies (1:5000 of anti-TGH, 1:500 anti-AADAC, 1:10000 anti-GFP, 1:1000 ant-core, 1:5000 anti-PDI and1:10000 anti-actin) followed by 1:10000 appropriate secondary HRP-conjugated IgG antibodies. All immunoreactive bands were detected using Amersham ECL^{TM} Western Blotting Detection Reagents with Amersham Hyperfilm^{TM} ECL.

Preparation of microsomal membranes - Cells from culture dishes were harvested into 20 mM Tris/HCl, pH7.5, containing 250 mM sucrose and 5 mM EDTA then homogenized with a Polytron. The microsomal membranes were isolated by ultracentrifugation of the post-mitochondrial supernatant (28).

Stable expression of TGH-EGFP and EGFP in Huh7.5 cells - For expression studies, naïve Huh7.5 cells were transfected with TGH-EGFP or EGFP vector using Lipofectamine 2000 according to the supplied protocol. Cells were then cultured for 10 days in G418 (1.6mg/ml). At day 10 the remaining cell colonies were trypsinized, picked and diluted to 1 cell/100μl of media and were cultured in 96 well plate, contains 400μg/ml G418. The expression of TGH or TGH-EGFP were serially tested using green fluorescence by microscopy and cell colonies with high levels of expression were expanded and subjected to assay for detection of lipase activity, following by immunoblot analysis for TGH and GFP expression.

Determination of HCV infectivity titer - Limiting dilution assays were used to quantify HCV infectivity between samples as median tissue culture infectious units per milliliter (TCID50/ml). The TCID50 is the dilution that infects 50% of replicate cell cultures and was determined essentially as described (29). Briefly, Huh 7.5 cells were seeded on poly-lysine coated 96 well plates (6 x 10^3 cells/well). At 24h post-seeding, cells were infected with 10 fold serially diluted cell culture supernatants (8 wells per dilution). Cell culture media was replaced with fresh media at 16h post-infection, then cells were fixed in methanol at 72h post-infection. HCV infected cells were detected by immunostaining using anti-NS5A antibody (9E10) with HRP conjugated sheep anti-mouse IgG secondary

antibody and subsequently visualized with a DAB substrate kit (DAKO). TCID50 was calculated, based on the NS5A positive wells, according to the method of Reed and Muench (30).

Quantitative RT-PCR of host mRNAs– Primer sequences were as follows hTGH-F, GTTTGGCTGGTTGATTCCAATG-3'; hTGH-R, 5'-CAAGGGGATAGGACTTCCACA-3'; hbetaActin-F, 5'-CCAACCGCGAGAAGATGA-3'; hbetaActin-R, 5'-TCCATCACGATGCCAGTG-3' hAADAC-F, 5'-CAAAATATG GTGTGAACCCTGA-3'; hAADAC-R, GAAGGGCAGGATAAATTAAAGA-3';. Total RNA was isolated using Trizol reagent and reverse transcribed with a mixture of random hexamers and oligo(dT) using qScript cDNA SuperMix according to the manufacturer's instructions. TGH (primers hTGH-F/hTGH-R), AADAC (primers hAADAC-F/hAADAC-R) and beta-actin (primers hbetaActin-F/hbetaActin-R) transcripts were detected by real-time PCR using a Qiagen RotorGene 3000 instrument. Reaction mixtures contained Platinum Quantitative PCR SuperMix-UDG with 400nM concentrations for each primer in a total volume of 20 ml. Following a 3 minute initial denaturation at 94°C, PCR amplification of TGH and AADAC proceeded for 40 PCR cycles of 95°C for 20 s, 56°C for 20 s then 72°C for 20 s. For beta-actin, samples were amplified for 35 cycles of 95°C for 20 s, 60°C for 20 s; 72°C for 20 s. Data analysis was performed with the Corbett Rotorgene software using the standard curves method. All TGH values were normalized to beta-actin.

Statistical analysis - The results were statistically analyzed by the Student *t* test of means and one-way ANOVA or non-parametric tests, Kruskal-Wallis and Mann Whitney U tests. *P* values less than 0.05 were considered to be significant. Calculations were performed using SPSS 20.0 software (Chicago, IL).

Other methods - Protein concentrations were determined by the Pierce Micro BCA Assay Kit.

Results

TGH deficiency in Huh7.5 cells leads to reduced lipase activity and is associated with a decrease in secretion of TG. To examine the possible role of TGH in the HCV life cycle, we used the highly permissive Huh7.5/JFH-1 cell culture system for HCV production. Similar to other hepatoma cell lines (8, 31), these cells do not express TGH and are deficient in mobilization (lipolysis/re-esterification) of TG from preformed stores for secretion with VLDL (Nourbakhsh et al. Journal of Hepatology, in press). Similar to what we have previously shown, TGH protein was not detected in cellular lysates and microsomes (where TGH is naturally present) obtained from Huh7.5 cells by immunoblot analysis (figure 1A) and TGH mRNA levels were negligible (Figure 1B). In addition,

microsomal lipolytic activity against an artificial substrate (p-nitrophenyl laurate) was significantly lower in Huh7.5 cells in comparison to human hepatocytes (HH), which is consistent with the absence of TGH (Figure 1C).

Similar to other hepatoma cells (8, 31), Huh7.5 cells have a strong dependency on exogenous oleic acid (OA) for VLDL-TG secretion and they are not able to secrete appreciable amounts of TG in the absence of exogenous OA (Nourbakhsh et al. Journal of Hepatology, in press). Therefore, to compare the TG secretion in Huh7.5 cells with human hepatocytes, we incubated the cells with OA to generate a large intracellular TG pool (Figure 1D). When the media still contained the OA supplement, Huh7.5 cells secreted ~46% less TG than HH ($P<0.005$, 0h). Upon removal of OA from cell culture, Huh7.5 cells secreted ~50% less TG than HH ($P<0.001$, 2-8h)). Human hepatocytes secreted more TG than lipid loaded Huh7.5 cells even without receiving the OA supplement (HH, FBS). This may have been due increased availability of TG stores in HH when compared with Huh7.5 cells (cellular, 0h). However, the attenuation of TG secretion in Huh7.5 cells occurred despite the presence of large intracellular TG stores (37.34 ± 2.09, 64.44 ± 2.43, 44.42 ± 3.92 μg TG/mg cell protein in Huh7.5 cells, HH supplemented with OA and HH with no OA supplementation respectively) still present at the end of the secretion period (Figure 1D cellular, 8h). This result indicates that Huh7.5 cells are deficient in mobilization of stored TG for secretion with VLDL and they secrete less TG, possibly due to TGH deficiency in these cells.

Functional expression of TGH in Huh7.5 and generation of TGH-EGFP cells: We stably transfected naïve Huh7.5 cells with human TGH cDNA expression vector (16). To easily track the TGH expression, an EGFP reporter was attached to the TGH (TGH-EGFP; see Figure 2A). Twelve G418-resistant colonies were evaluated for TGH-EGFP expression by EGFP fluorescence. Of these, one cellular clone (C2) was chosen for further studies. Immunoblot of microsomes prepared from C2 indicated the presence of a single protein with molecular mass of 87 kDa (molecular weight of TGH 60 kDa, GFP 27 kDa) that was recognized with both anti-human TGH and anti- GFP polyclonal antibodies (Figure 2B). In addition, TGH-EGFP mRNA was detected in C2 cells but was absent from wild-type (WT) when the primers were derived from the TGH and EGFP moieties (Figure 2C). A reticular pattern was observed for EGFP fluorescence in C2 cells (Figure 2D). This is consistent with the presence of an ER retention motif (HIEL, see Figure 2A) in TGH-EGFP. By contrast, a more diffuse pattern was observed for EGFP fluorescence in cells expressing only the EGFP motif.

Activity-dependent binding of FP-biotin to TGH has been demonstrated previously (32). The same approach was used to determine if FP-biotin can bind to TGH-EGFP expressed in C2 cells (Figure 2E). Reactions were also performed in the absence of FP-biotin to identify non-specific labeling of proteins due to binding of the streptavidin conjugate. FP-biotin labeled polypeptides consistent with the molecular mass of TGH-EGFP (87-kD) was observed with C2 cells, but were absent when wild-type or human hepatocytes were used. We have previously demonstrated that the FP-labeling in the 45-kDa range, which was observed with all cell lines, is due to endogenous AADAC (previous manuscript), the only other TG lipase suggested to play a role in VLDL assembly (33).

TGH-EGFP cells had ~3 fold increase in cellular lipolytic activity in comparison to wild type cells (Figure 2F). This was TGH-dependent since the increase in cellular lipolytic activity was prevented when the assay was performed in the presence of a specific inhibitor of TGH, GR148672X (GSKi).

In summary, we confirmed stable expression of functional TGH-EGFP in C2 cells (hereafter referred to as TGH-EGFP cells).

Expression of TGH-EGFP was associated with enhanced TG secretion. Expression of rat TGH into McArdleRH7777 cells was associated with enhanced mobilization of TG from lipid stores for secretion with VLDL (7, 8). Therefore, we compared the TG mass secretion from TGH-EGFP cells and WT cells after OA-stimulated expansion of cellular TG stores (Fig 3A). Prior to OA withdrawal from the culture media (i.e. prior to the secretion period), cellular TG levels were similar between TGH-EGFP cells and WT, indicating that TGH expression does not affect OA-stimulated expansion of cellular TG stores. After removal of OA from cell culture, TGH-EGFP cells secreted ~80% more TG into the media than wild type cells (secreted). Overall, 36% of the preformed TG stores present in TGH-EGFP cells were turned over during the secretion period whereas just 10% of these stores were turned over by WT cells (cellular, 8h vs. 0h). These changes were not observed when a TGH inhibitor (GSKi) was included in the culture media. This was likely due to inhibition of TGH-EGFP in the lumen of the ER since the addition of GSKi to cell cultures inhibited TGH-dependent lipolytic activity in microsomes (Figure 3B).

TGH-EGFP cells secrete more apoB into media. Unlike the majority of secretory proteins, apoB is not secreted as a free protein and without lipidation. In fact, if an inappropriate amount of lipidation occurs, apoB is destined for degradation by cellular machinery. Increased secretion of VLDL-TG is expected to be accompanied by an increase secretion of ApoB and/or an increase in ApoB buoyant density, due to the

addition of more TG. After all, it remains a possibility that TGH-EGFP secreted more TG during the OA withdrawal period simply by increasing the lipid status of pre-VLDLs, as opposed to making more ApoB containing particles.

Given TGH-EGFP secrete more TG, we examined if this was accompanied by increased apoB secretion (Figure 4A). TGH-EGFP secreted ~15% more apoB in comparison to wild type ($P<0.005$). This enhanced apoB secretion was TGH-dependent as TGH-EGFP cells incubated with GSKi secreted similar level of apoB to wild type. We also measured cellular apoB (Figure 4A, Cellular) and found that TGH-EGFP cells had more cellular apoB in comparison to wild type ($P<0.05$) indicating that either apoB synthesis was enhanced or apoB degradation was inhibited in these cells. The buoyant density of apoB containing lipoproteins inversely correlates with the amount of TG in their structure. Lipoproteins with higher TG levels have lower density. In order to examine if enhanced TG secretion in Huh-TGH cells altered density of apoB containing particles secreted into media, we separated these particles by isopycnic centrifugation over iodixanol gradient. We were not able to find any significant difference in the buoyant density of apoB containing particles in TGH-EGFP and wild- type cells. In both cells, the density peak of apoB containing lipoproteins was 1.03 g/ml (Figure 4B). This finding indicates that enhanced TG secretion in TGH-EGFP cells was associated with enhanced apoB secretion rather than secretion of VLDL with more TG.

HCV infected cells secrete less TG and have reduced AADAC expression. We have recently shown that HCV infected Huh7.5 cells have impaired mobilization of TG from cellular lipid stores and secrete VLDL with less TG. This was partially explained by AADAC-deficiency in these cells (Nourbakhsh et al. Journal of Hepatology, in press). A similar approach was used to examine the TG mass secretion from TGH-EGFP cells during the early peak of viral infection. After incubating cells for 14h with OA-BSA to stimulate cellular deposition of TG, cellular TG levels naïve and infected TGH-EGFP cells were similar (50.31 ± 3.85 μg/mg cell protein and 54.30 ± 5.67 μg/mg cell protein in naïve vs. infected cells, $p=0.582$). After 8h of OA withdrawal from the culture media, infected TGH-EGFP cells secreted about 50% less TG into media compared to naïve cells (Table 1, 8.12 ± 0.75 and 16.12 ± 1.83 μg TG/mg cell protein in infected and naïve TGH-EGFP cells respectively, $P<0.005$). In addition, naïve TGH-EGFP cells mobilized ~36% of preformed TG while infected cells mobilized only ~16% of their TG stores ($p<0.05$).

Naïve and infected TGH-EGFP cells secreted very similar amounts of apoB into media (1308.70 ± 239.76 and 1298.72 ± 17.70 ng apoB /mg cell protein in infected and naïve TGH-EGFP cells respectively). However, the buoyant density profile of ApoB secreted

into the media was quite different than the ApoB profile obtained with naïve cells (Fig 5A vs. Fig 4B), with less of the total ApoB appearing in the low density range. This is an indication that infected TGH-EGFP cells secrete VLDL particles with reduced TG content. This is similar to what we have demonstrated with infected WT (Huh7.5) cells (previous manuscript). Therefore, TGH expression did not restore defective lipidation of ApoB in these cells.

We examined the possibility TGH-EGFP had a lipase deficiency (other than TGH), to account for the reduced secretion of TG cells. Microsomal lipolytic activity was significantly reduced when TGH-EGFP cells were infected (Figure 5B). Therefore, we performed an ABPP assay to determine the esterase(s)/lipase(s) affected by HCV. Similar to what we have observed previously (Nourbakhsh et al. Journal of Hepatology, in press), reduced FP-labeling of AADAC was observed (Figure 5C) and this was due to reduced abundance of AADAC in these cells (Figure 5D). By contrast, TGH-EGFP labeling and abundance remained unchanged, as opposed to reduced AADAC activity. A transcriptional and/or post-transcriptional mechanism is suggested since AADAC mRNA was also reduced (Figure 5E).

The impact of TGH-EGFP expression on the HCV replication cycle in Huh7.5 cells. To investigate the role of TGH in HCV production, we inoculated the TGH-EGFP and wild-type cells with JFH-1 virus obtained from Huh7.5/JFH-1 electroporated culture. Seventy-two hours after the initial inoculation, WT cells had secreted significantly less HCV RNA into the media than TGH-EGFP cells (Figure 6A). This was not due to inhibition of RNA synthesis since similar levels of cellular HCV RNA were observed for WT and TGH-EGFP cells. However, an accumulation of intracellular HCV RNA may be difficult to observe since the amount of HCV RNA in cells was <1% of the HCV RNA found in media. No significant difference in the infectivity titer of HCV or in the buoyant density profile of HCV RNA that appeared in the media was observed for WT and TGH-EGFP cells (Figure 6B). Since we did not determine the infectivity titer of intracellular HCV, we cannot rule out the possibility that TGH impacts virion assembly/secretion.

Discussion

It has been estimated at least 70% of triacylglycerol that is secreted by hepatocytes through VLDL, originates from preformed cellular storage pool, whereas only 30% is derived from de novo triacylglycerol synthesis(34, 35). Recently it was shown that the lipidation of pre-VLDL requires mobilization of TG by lipolysis and re-esterification of preformed stores (8, 14, 16). Two ER lipases have been suggested as the enzymes that mediate the lipolytic process of TG mobilization; TGH and AADAC. We have recently

demonstrated that infected Huh7.5 cells are AADAC-deficient and we have demonstrated that this deficiency leads to impaired lipolysis of cellular TG stores and VLDL production. The role of TGH in mobilization of TG for secretion with VLDL has been investigated widely. It has been shown that a rat hepatoma (McArdleRH7777) cell line is deficient in TGH and this deficiency is associated with lower microsomal lipase activity and lower TG, ApoB secretion (8, 16). Introduction of rat TGH cDNA in McArdleRH7777 cell enhances the microsomal lipase activity, TG mobilization from preformed lipid stores and TG and apoB secretion(8, 16). These effects were obliterated when these cells were treated with a lipase inhibitor (7). In addition TGH knock down mice, secrete less TG and apoB secretion(10). Consistent with these results, our results show that Huh7.5 cells are TGH deficient and this deficiency is associated with less TG secretion. Introduction of TGH in Huh7.5 cells by stable transfection of these cells by TGH-EGFP vector, enhances the lipase activity, mobilization of TG from preformed lipid stores and TG and apoB secretion and these effects were obliterated when cells were treated with a specific human TGH inhibitor. This is very consistent with the defined role of TGH in mobilization of TG for secretion with VLDL.

Similar to what we had observed with WT Huh7.5 cells following infection with HCV, reduced mobilization of cellular TG stores for VLDL assembly was also observed when TGH-EGFP cells were infected with HCV and these infected cells also exhibited a deficiency for AADAC. Thus similar to infected Huh7.5 cells, it is likely that AADAC deficiency also contributed to reduced lipolytic mobilization of cellular TG stores for VLDL assembly by infected TGH-EGFP cells. The expression of TGH had only a minor impact on viral production since more HCV RNA was produced by TGH-EGFP cells, however this was not sufficient to impact the infectivity of secreted virions, since infectivity titers were similar for the HCV secreted by TGH-EGFP and WT cells.

Acknowledgements

The authors thank Zong Chao Ling and KMT Hepatech for RT-PCR analysis of HCV RNA, Dr. Charles Rice for providing key reagents that made this study possible (Huh7.5 cells, pJFH-1, and anti-NS5A 9E10).

Figure Legends

Figure 1. Deficiency of TGH in Huh7.5 cells associated with reduced cellular lipase activity and TG mobilization for secretion with VLDL

A. TGH expression levels were evaluated in cellular lysates and microsomes by immunoblot analysis. The same nitrocellulose membrane was stripped and re-probed with antibodies for the detection of PDI (**HH**, primary human hepatocytes). The immunoblots shown are representative of 4 independent experiments. **B.** TGH mRNA levels were determined by qRT-PCR and normalized to actin mRNA. Values are relative to Huh7.5 and represent Means ± SEM of N=4 independent experiments. **C.** Microsomal Lipolytic activity obtained from huh7.5 cells and human hepatocytes were estimated by the release of *p*-nitrophenol from p-nitrophenyl laurate. Data were normalized to cellular protein. Values are Means ± SEM for N=4 independent experiments. **D.** Huh7.5 cells or primary human hepatocytes were incubated for a total of 14h in DMEM supplemented with OA-BSA (OA) to increase cellular TG stores. Media were replaced with fresh DMEM supplemented with OA-BSA for the last 2h of incubation. Cells were washed and for half of the culture dishes, lipids were extracted for analysis of cellular TG levels prior to the withdrawal OA from the culture media (Cellular, 0h). With the remaining culture dishes, cells were incubated up to 8h in DMEM in the absence of extracellular OA to allow for secretion of TG (as VLDL-TG) from preformed cellular TG stores. During this incubation, the media was removed and replenished with fresh DMEM every 2h (time points 2-8h). After all media time points had been collected, lipids were extracted from cells for the analysis of cellular TG levels remaining at the end of the secretion period (Cellular, 8h) and TG mass secreted into the media while OA was still being supplied to cells (Secreted, 0h) and after OA had been withdrawn from the culture media (Secreted, 2-8h). HH that did not receive the OA supplement were included for comparison (FBS). These were cultured in DMEM containing 10% FBS (instead of OA-BSA) for 14h. For the last 2h of this incubation period, the media was replenished with fresh DMEM containing 10%FBS prior to the secretion period. Secreted and cellular values are Means ± SEM for N=4 independent experiments (Secreted: $*P_{0h}<0.005$,$*P_{2h}<0.05$, $*P_{4h}<0.00a$, $*P_{6h}<0.005$; $*P_{8h}<0.005$).

Figure 2. Functional expression of TGH in huh7.5 and generation of TGH-EGFP cells

A. Schematic structure of TGH-EGFP. **B.** TGH-EGFP expression was tested in microsomal lysates by immunoblot analysis using anti human TGH antibody and anti GFP antibody. The same nitrocellulose membranes were stripped and re-probed with antibodies for the detection of PDI as a loading control (**HH**, primary human hepatocytes;

WT, wild type Huh7.5 cells; **C2**, colony of Huh7.5 cells stably transfected with TGH-EGFP). The immunoblots shown are representative of 4 independent experiments. **C.** TGH or TGH-EGFP mRNA levels were determined by qRT-PCR and normalized to actin mRNA. Values are relative to C2 and represent Means ± SEM of N=4 independent experiments. **D.** Fluorescent microscopy for detection of GFP in Huh7.5 cells stably transfected with TGH-EGFP or EGFP. **E.** Cellular proteins from wild type Huh7.5 cells (**WT**) primary human hepatocyte (**HH**) and **C2** cells were labeled with FP-biotin (-/+ FP-biotin, as indicated) and visualized by chemiluminescent detection of bound streptavidin-HRP. Labeled proteins co-migrating with the expected molecular weights of TGH, TGH-EGFP and arylacetamide deacetylase (AADAC) are shown. These results are representative of 4 independent experiments. **F.** Lipolytic activity in cellular lysates obtained from wild type huh7.5 (**WT**) cells and human hepatocytes (**HH**) and **C2** cells by the release of *p*-nitrophenol from p-nitrophenyl laurate. Cellular lysates first incubated for 30 minutes at room temperature with 10μM specific TGH inhibitor (+GSKi) or equal volume of DMSO (-GSKi), then were applied to assay. Data were normalized to cellular protein. Values are Means ± SEM for N=4 independent experiments.

Figure 3. TG secretion from preformed stores in TGH-EGFP cells

A. Wild type Huh7.5 cells or Huh7.5 cells expressing were incubated for a total of 14h in DMEM supplemented with OA-BSA to increase cellular TG stores. Cells were washed and for half of the culture dishes, lipids were extracted for analysis of cellular TG levels prior to the withdrawal OA from the culture media (Cellular, 0h). With the remaining culture dishes, cells were incubated up to 8h in DMEM in the absence of extracellular OA with 10 μM TGH specific inhibitor (+GSKi) or equal volume of DMSO (-GSKi) to allow for secretion of TG (as VLDL-TG) from preformed cellular TG stores. After all media time points had been collected, lipids were extracted from cells for the analysis of cellular TG levels remaining at the end of the secretion period (Cellular, 8h) and TG mass secreted into the media after OA had been withdrawn from the culture media (Secreted). Secreted and cellular values are Means ± SEM for N=4 independent experiments. **B.** Lipolytic activity in microsomes obtained from wild type huh7.5 (**WT**) and Huh7.5 cells expressing TGH-EGFP **(TGH-EGFP)** utilized in **part A** experiment by the release of *p*-nitrophenol from p-nitrophenyl acetate.

Figure 4. Secretion of ApoB in TGH-EGFP Cells

A. Wild type (**WT**) and TGH-EGFP expressing Huh7.5 cells were incubated in DMEM supplemented with OA-BSA (OA) for 14h to increase cellular TG stores. Media was replaced with DMEM ± 10 μM TGH specific inhibitor (GSKi) for 8h to allow for secretion of VLDL-TG. Media and cell were collected and the level of apoB in media and cell lysate

were determined with an ApoB ELISA and were normalized to cell protein. Values represent Mean ± SEM of N=3 independent experiments. **B.** The media collected from the above experiment were subjected to density gradient ultracentrifugation using iodixanol. Fractions (1 ml) were collected from the top of the gradients and the levels of ApoB with an ApoB ELISA Kit. The density of each fraction in the gradient was determined by weighing 200 μl aliquots of each fraction. The profile is the representative of two separate experiments.

Figure 5. HCV infected TGH-EGFP cell are deficient in AADAC.

A. HCV infected TGH-EGFP cells were incubated in DMEM supplemented with OA-BSA for14h to increase cellular TG stores. Media was replaced with DMEM in for 8h to allow for secretion of VLDL-TG. Media were collected subjected to density gradient ultracentrifugation using iodixanol. Fractions (1 ml) were collected from the top of the gradients and the levels of ApoB with an ApoB ELISA Kit. The density of each fraction in the gradient was determined by weighing 200 μl aliquots of each fraction. The profile is the representative of two separate experiments. **B.** Lipolytic activity in cellular obtained from Naïve (-HCV) and Infected (+HCV) TGH-EGFP cells by the release of *p*-nitrophenol from p-nitrophenyl acetate. Values represent Mean ± SEM of N=3 independent experiments. **C.** Activity-based protein profiling of cellular proteins based on bound FP-biotin (+FP-biotin). Binding reactions were also performed without FP-biotin (-FP-biotin) to identify non-specific banding. TGH, triacylglycerol hydrolase; AADAC, arylacetamide deacetylase, HH, human hepatocytes). Results are representative of 3 experiments. **D.** AADAC expression was tested in cellular lysates obtained from infected TGH-EGFP cells by immunoblot analysis. The same nitrocellulose membranes were stripped and re-probed with antibodies for the detection of HCV core and Actin as a loading control (**HH**, primary human hepatocytes; **HepG2,** a hepatoma cell line deficient in AADAC and TGH). The immunoblots shown are representative of 3 independent experiments. **E.** AADAC mRNA levels (normalized to actin) in naïve and infected cells during the early peak of viral infection.

Figure 6. Impact of TGH-EGFP on HCV production

A. Viral RNA titers were determined after 72h post-infection of cells with JFH-1 (MOI=0.5). Tissue Culture Infection Dose ($TCID_{50}$) of media samples was measured as it was discussed in “methods and materials”. Values are Means ± SEM; N=4. **B.** Media were subjected to density gradient ultracentrifugation using iodixanol. Fractions (1 ml) were collected from the top of the gradients and the HCV RNA titer was measured in each fraction. The density of each fraction in the gradient was determined by weighing 200 μl aliquots of each fraction. The profile is the representative of two separate experiments.

Figure 1A, 1B and 1C.

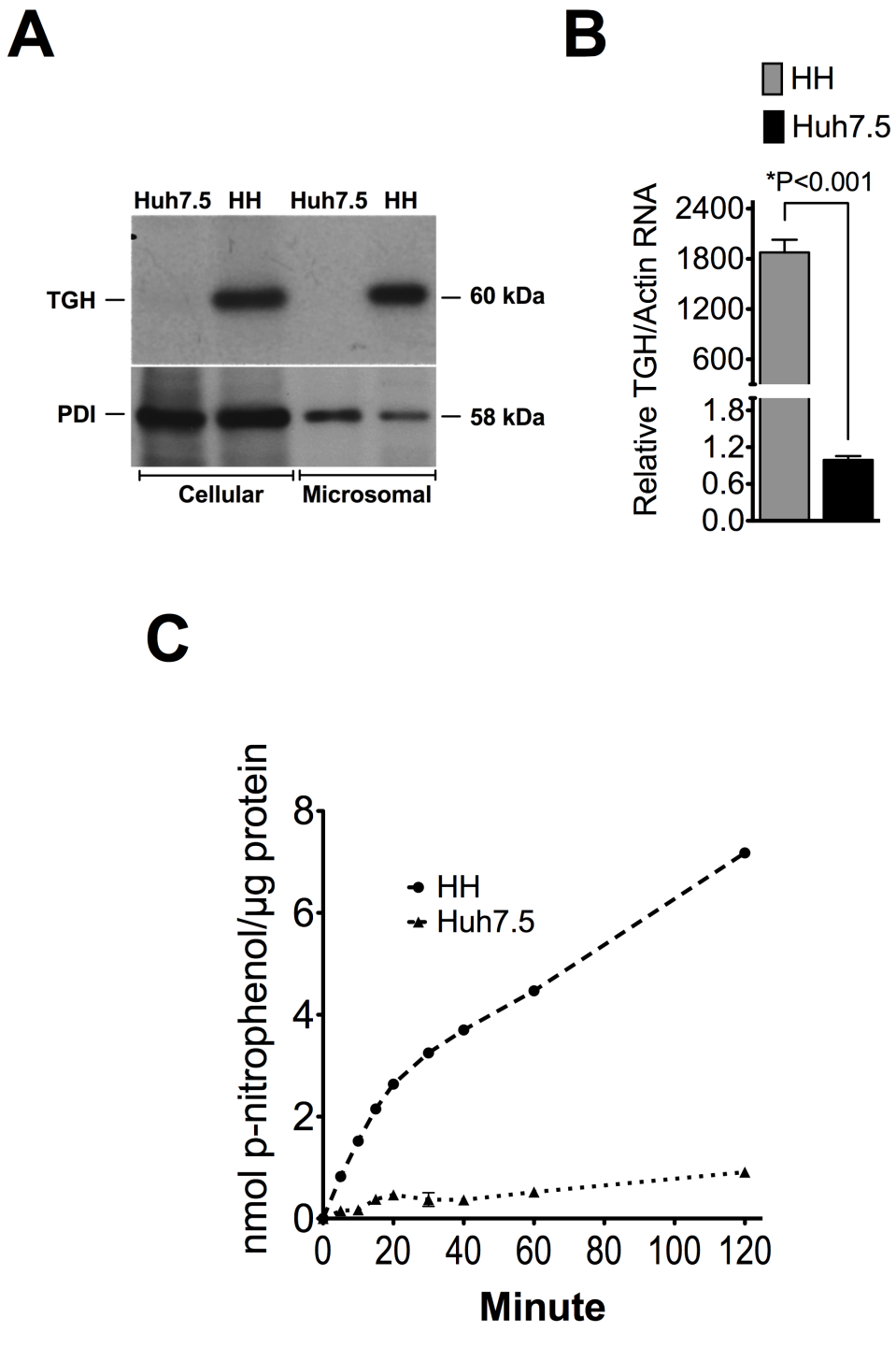

Figure 1D.

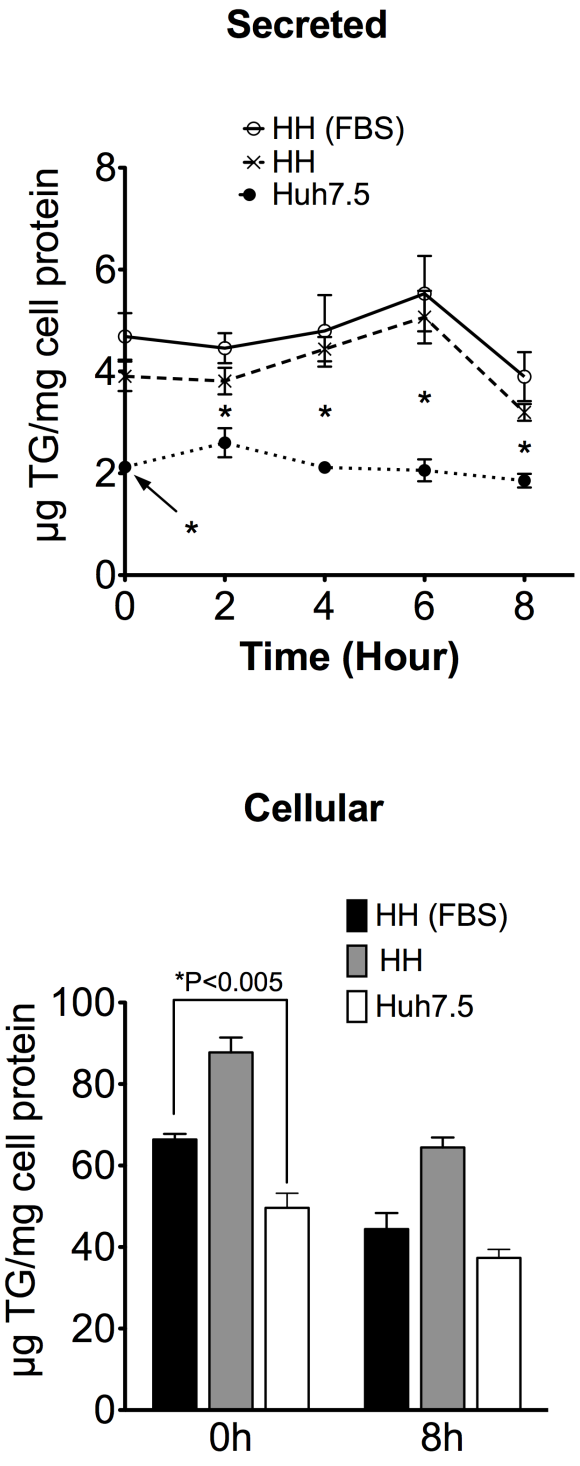
Secreted
HH (FBS)
HH
Huh7.5
µg TG/mg cell protein
0
2
4
6
8
Time (Hour)
Cellular
HH (FBS)
HH
Huh7.5
*P<0.005
µg TG/mg cell protein
0
20
40
60
80
100
0h
8h

Figure 2A, 2B, 2C and 2D.

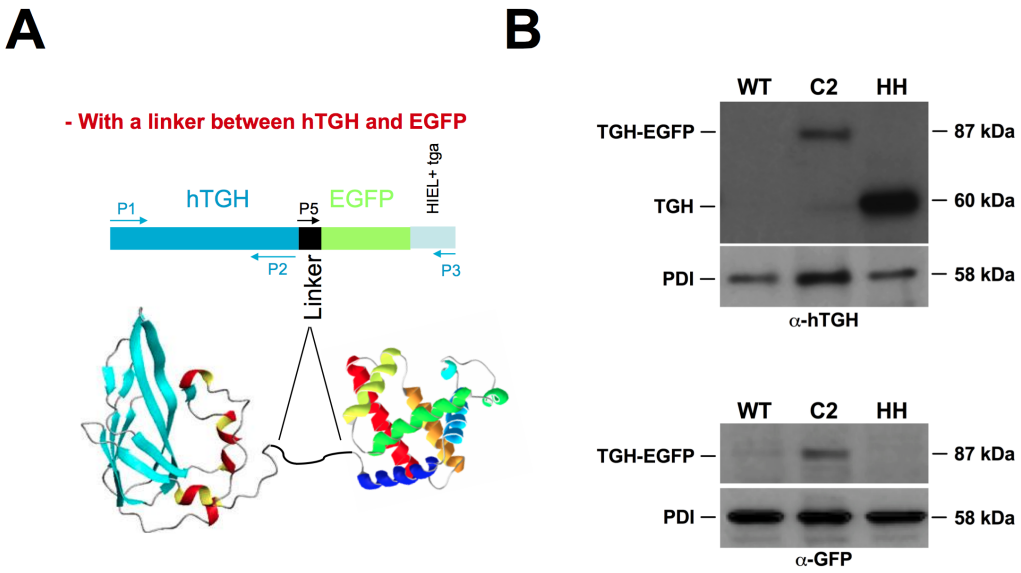

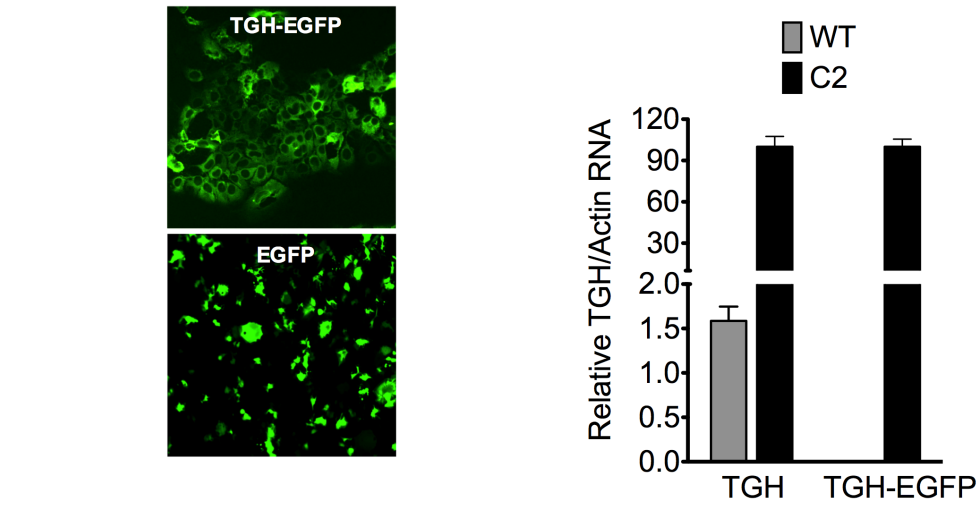

Figure 2E and 2F.

E

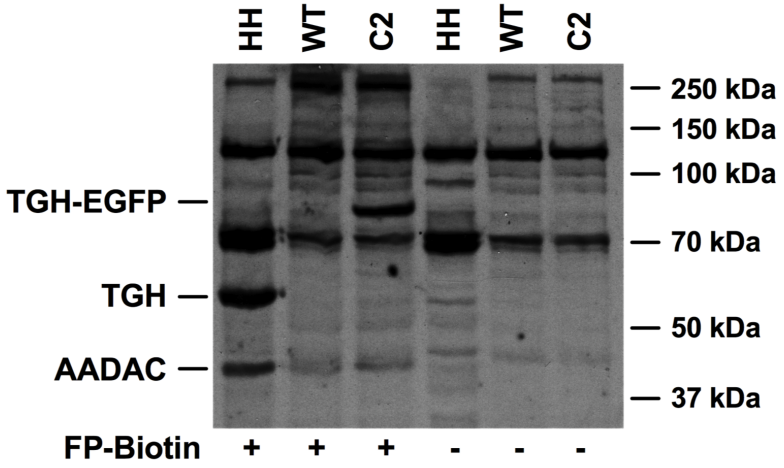

F

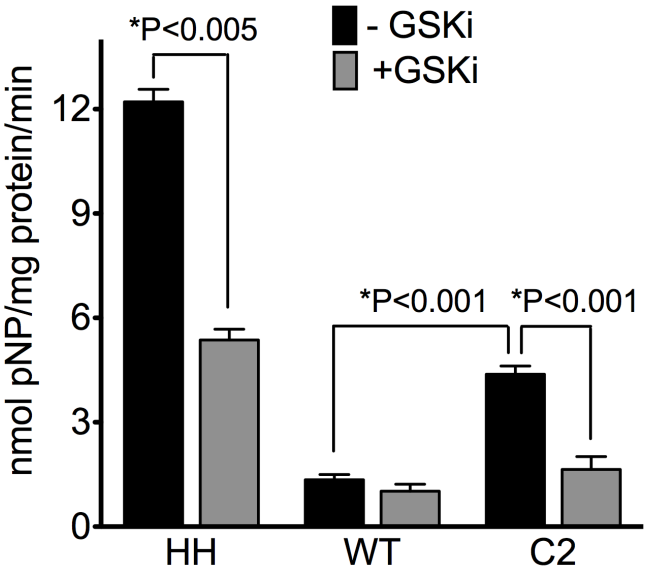

Figure 3.

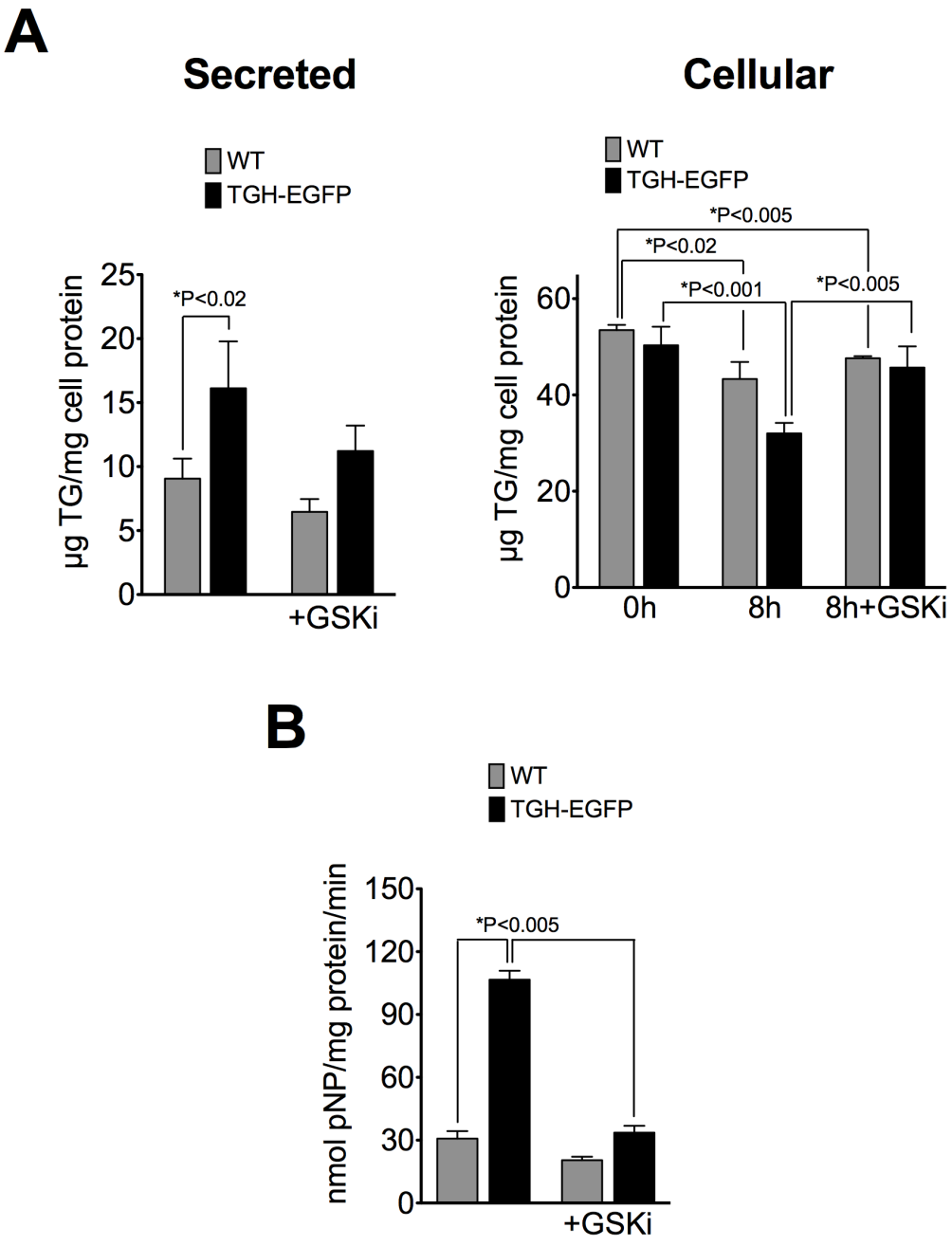
A
Secreted
WT
TGH-EGFP
µg TG/mg cell protein
25
20
15
10
5
0
*P<0.02
+GSKi
Cellular
WT
TGH-EGFP
*P<0.005
*P<0.02
*P<0.001
*P<0.005
µg TG/mg cell protein
60
40
20
0
0h
8h
8h+GSKi
B
WT
TGH-EGFP
nmol pNP/mg protein/min
150
120
90
60
30
0
*P<0.005
+GSKi

Figure 4.

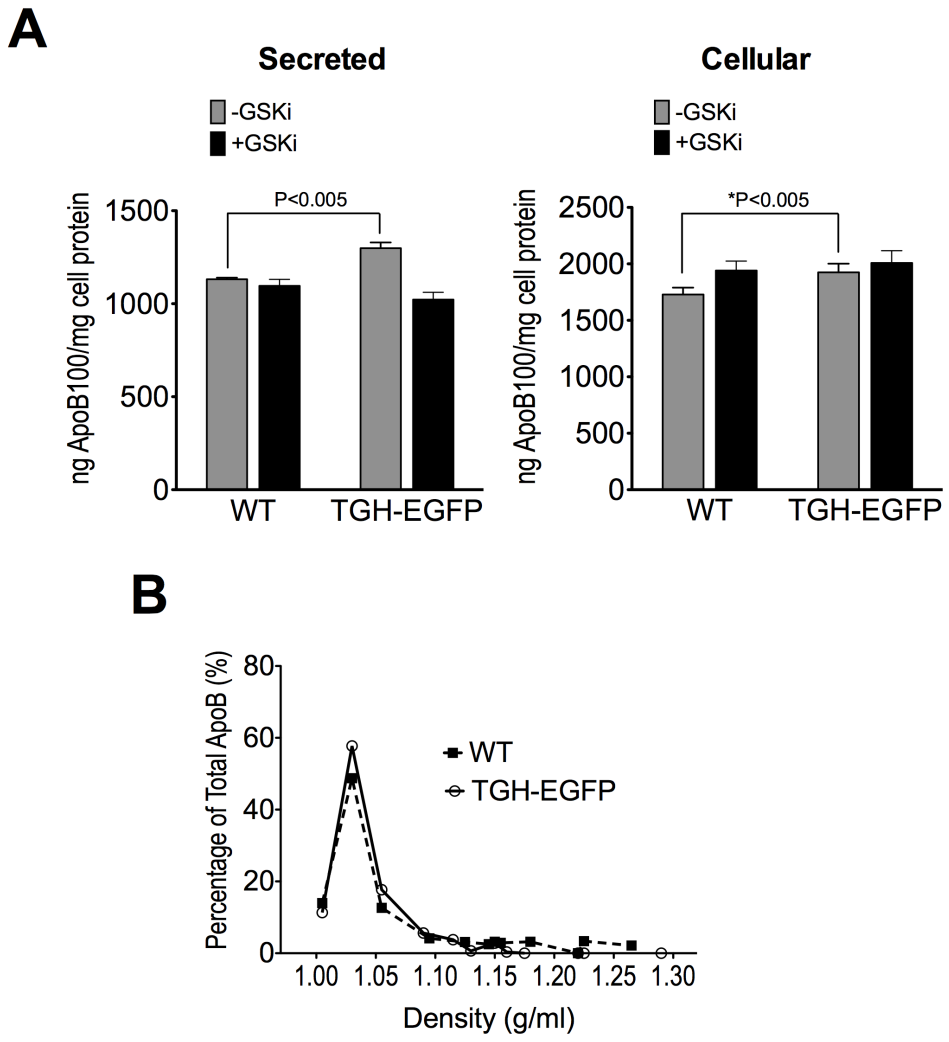
A
Secreted
Cellular
-GSKi
+GSKi
P<0.005
*P<0.005
ng ApoB100/mg cell protein
1500
1000
500
0
2500
2000
1500
1000
500
0
WT
TGH-EGFP
B
Percentage of Total ApoB (%)
80
60
40
20
0
WT
TGH-EGFP
1.00
1.05
1.10
1.15
1.20
1.25
1.30
Density (g/ml)

Figure 5A and 5B.

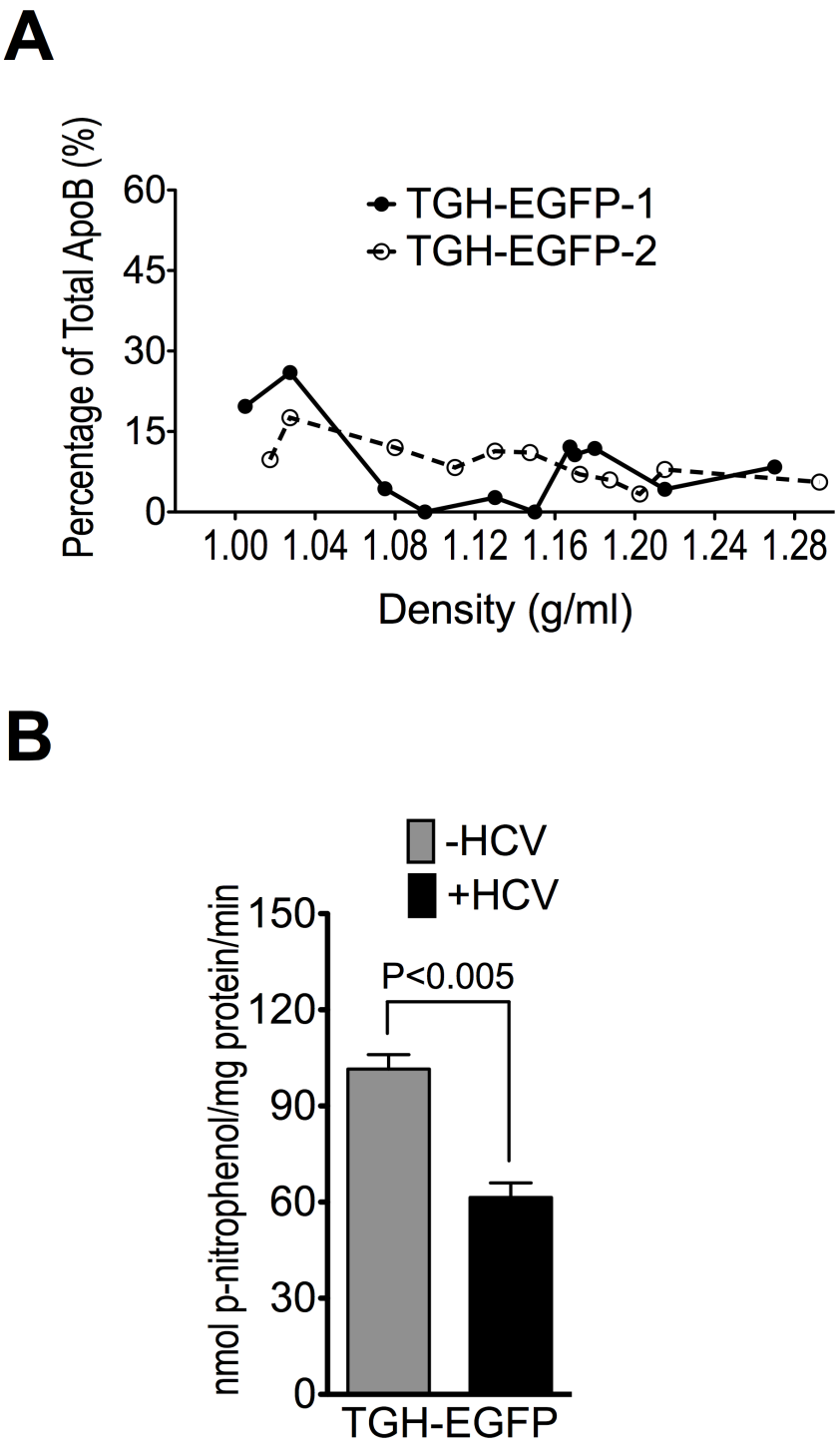

Figure 5C, 5D and 5E

C

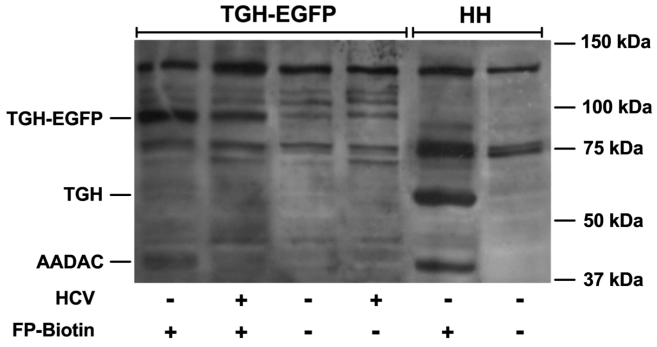

D

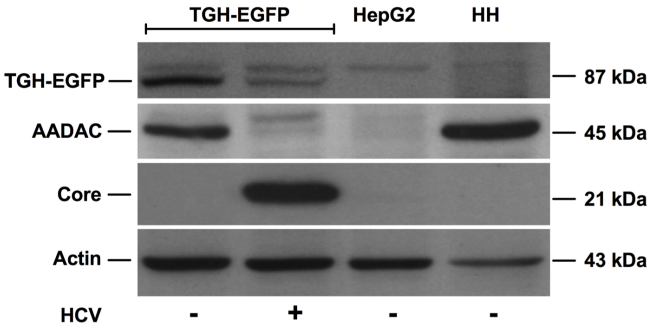

E

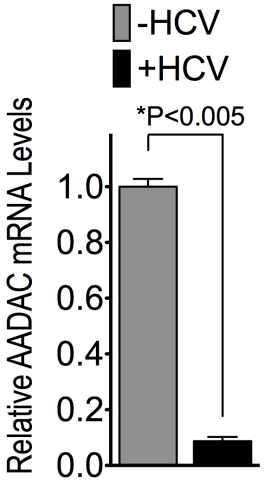

Figure 6.

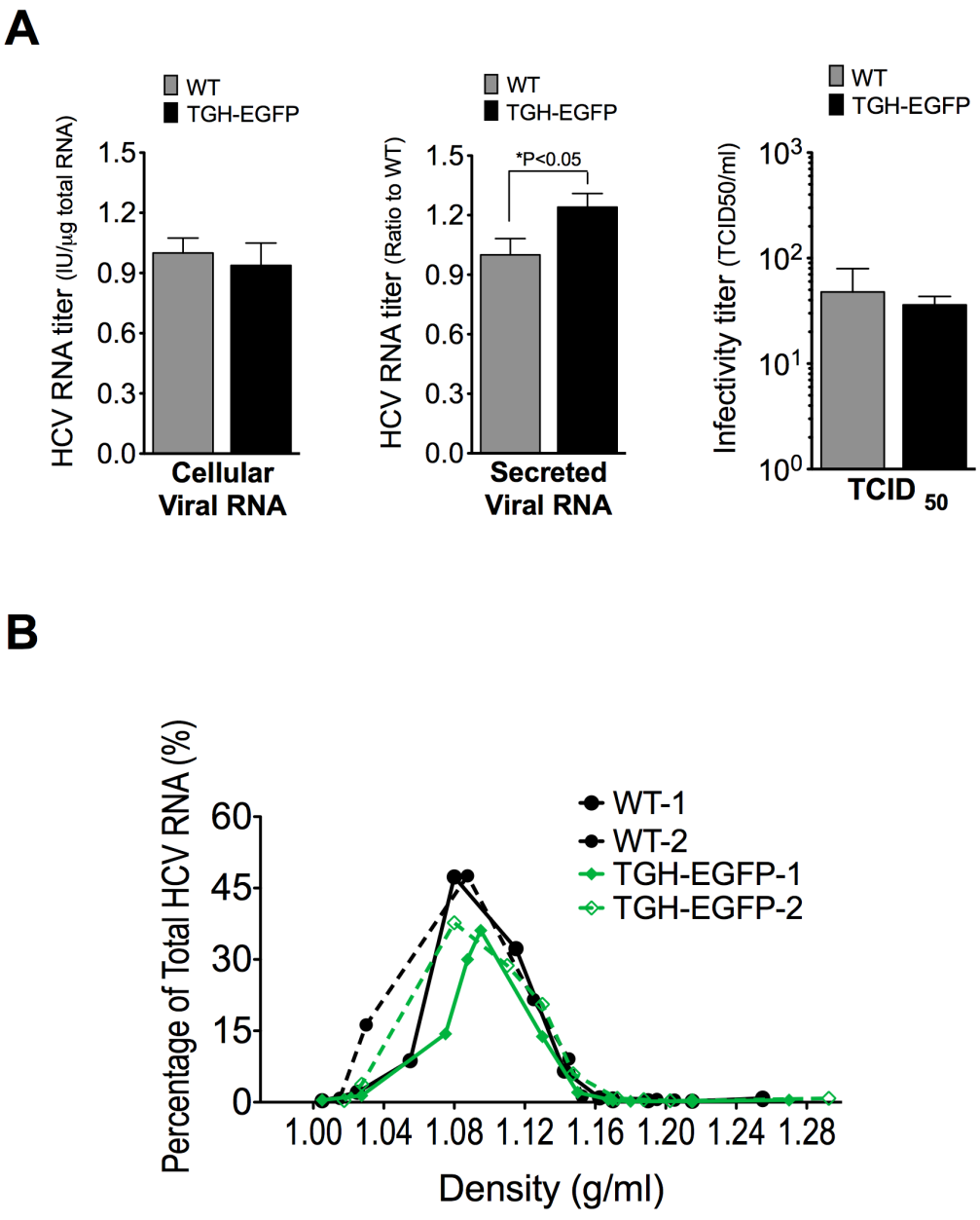
A
WT
TGH-EGFP
HCV RNA titer (IU/μg total RNA)
1.5
1.2
0.9
0.6
0.3
0.0
Cellular Viral RNA
WT
TGH-EGFP
HCV RNA titer (Ratio to WT)
*P<0.05
1.5
1.2
0.9
0.6
0.3
0.0
Secreted Viral RNA
WT
TGH-EGFP
Infectivity titer (TCID50/ml)
10^3
10^2
10^1
10^0
TCID 50
B
Percentage of Total HCV RNA (%)
60
45
30
15
0
WT-1
WT-2
TGH-EGFP-1
TGH-EGFP-2
1.00 1.04 1.08 1.12 1.16 1.20 1.24 1.28
Density (g/ml)

Table 1. TG mobilization and secretion in TGH-EGFP cells.

	Naïve	Infected	p-value
TG mobilized in 8h	36.36% ± 4.30%	16.24% ± 7%	0.049 *
TG secreted in 8h (µg/mg cell protein)	16.12 ± 1.83	8.12 ± 0.75	0.006 *

References

1. http://hcv.lanl.gov/content/index.

2. Lindenbach BD, Rice CM. Unravelling hepatitis C virus replication from genome to function. Nature. 2005;436(7053):933-8. Epub 2005/08/19.

3. Huang H, Sun F, Owen DM, Li W, Chen Y, Gale M, Jr., et al. Hepatitis C virus production by human hepatocytes dependent on assembly and secretion of very low-density lipoproteins. Proceedings of the National Academy of Sciences of the United States of America. 2007;104(14):5848-53. Epub 2007/03/23.

4. Icard V, Diaz O, Scholtes C, Perrin-Cocon L, Ramiere C, Bartenschlager R, et al. Secretion of hepatitis C virus envelope glycoproteins depends on assembly of apolipoprotein B positive lipoproteins. PloS one. 2009;4(1):e4233. Epub 2009/01/22.

5. Gastaminza P, Cheng G, Wieland S, Zhong J, Liao W, Chisari FV. Cellular determinants of hepatitis C virus assembly, maturation, degradation, and secretion. Journal of virology. 2008;82(5):2120-9. Epub 2007/12/14.

6. Salter AM, Brindley DN. The biochemistry of lipoproteins. J Inherit Metab Dis. 1988;11 Suppl 1:4-17. Epub 1988/01/01.

7. Gilham D, Ho S, Rasouli M, Martres P, Vance DE, Lehner R. Inhibitors of hepatic microsomal triacylglycerol hydrolase decrease very low density lipoprotein secretion. FASEB J. 2003;17(12):1685-7. Epub 2003/09/06.

8. Lehner R, Vance DE. Cloning and expression of a cDNA encoding a hepatic microsomal lipase that mobilizes stored triacylglycerol. The Biochemical journal. 1999;343 Pt 1:1-10. Epub 1999/09/24.

9. Wang H, Wei E, Quiroga AD, Sun X, Touret N, Lehner R. Altered lipid droplet dynamics in hepatocytes lacking triacylglycerol hydrolase expression. Mol Biol Cell. 2010;21(12):1991-2000. Epub 2010/04/23.

10. Wei E, Ben Ali Y, Lyon J, Wang H, Nelson R, Dolinsky VW, et al. Loss of TGH/Ces3 in mice decreases blood lipids, improves glucose tolerance, and increases energy expenditure. Cell Metab. 2010;11(3):183-93. Epub 2010/03/04.

11. Wang H, Gilham D, Lehner R. Proteomic and lipid characterization of apolipoprotein B-free luminal lipid droplets from mouse liver microsomes: implications for very low density lipoprotein assembly. The Journal of biological chemistry. 2007;282(45):33218-26. Epub 2007/09/13.

12. Alam M, Ho S, Vance DE, Lehner R. Heterologous expression, purification, and characterization of human triacylglycerol hydrolase. Protein Expr Purif. 2002;24(1):33-42. Epub 2002/01/29.

13. Satoh T, Hosokawa M. The mammalian carboxylesterases: from molecules to functions. Annu Rev Pharmacol Toxicol. 1998;38:257-88. Epub 1998/05/23.

14. Gibbons GF, Khurana R, Odwell A, Seelaender MC. Lipid balance in HepG2 cells: active synthesis and impaired mobilization. Journal of lipid research. 1994;35(10):1801-8. Epub 1994/10/01.

15. Boren J, Wettesten M, Rustaeus S, Andersson M, Olofsson SO. The assembly and secretion of apoB-100-containing lipoproteins. Biochem Soc Trans. 1993;21(2):487-93. Epub 1993/05/01.

16. Gilham D, Alam M, Gao W, Vance DE, Lehner R. Triacylglycerol hydrolase is localized to the endoplasmic reticulum by an unusual retrieval sequence where it participates in VLDL assembly without utilizing VLDL lipids as substrates. Mol Biol Cell. 2005;16(2):984-96. Epub 2004/12/17.

17. Wei E, Alam M, Sun F, Agellon LB, Vance DE, Lehner R. Apolipoprotein B and triacylglycerol secretion in human triacylglycerol hydrolase transgenic mice. Journal of lipid research. 2007;48(12):2597-606. Epub 2007/09/20.

18. Blight KJ, McKeating JA, Rice CM. Highly permissive cell lines for subgenomic and genomic hepatitis C virus RNA replication. Journal of virology. 2002;76(24):13001-14. Epub 2002/11/20.

19. Kawahara T, Toso C, Douglas DN, Nourbakhsh M, Lewis JT, Tyrrell DL, et al. Factors affecting hepatocyte isolation, engraftment, and replication in an in vivo model. Liver Transpl. 2010;16(8):974-82. Epub 2010/08/03.

20. Kato T, Date T, Miyamoto M, Furusaka A, Tokushige K, Mizokami M, et al. Efficient replication of the genotype 2a hepatitis C virus subgenomic replicon. Gastroenterology. 2003;125(6):1808-17. Epub 2004/01/16.

21. Kato T, Furusaka A, Miyamoto M, Date T, Yasui K, Hiramoto J, et al. Sequence analysis of hepatitis C virus isolated from a fulminant hepatitis patient. J Med Virol. 2001;64(3):334-9. Epub 2001/06/26.

22. Kato T, Date T, Murayama A, Morikawa K, Akazawa D, Wakita T. Cell culture and infection system for hepatitis C virus. Nat Protoc. 2006;1(5):2334-9. Epub 2007/04/05.

23. Zhong J, Gastaminza P, Cheng G, Kapadia S, Kato T, Burton DR, et al. Robust hepatitis C virus infection in vitro. Proceedings of the National Academy of Sciences of the United States of America. 2005;102(26):9294-9.

24. Kneteman NM, Asthana S, Lewis J, Dibben C, Douglas D, Nourbakhsh M, et al. Impact of calcineurin inhibitors with or without interferon on hepatitis C virus titers in a chimeric mouse model of hepatitis C virus infection. Liver Transpl. 2012;18(1):38-44. Epub 2011/08/13.

25. Zhong J, Gastaminza P, Chung J, Stamataki Z, Isogawa M, Cheng G, et al. Persistent hepatitis C virus infection in vitro: coevolution of virus and host. Journal of virology. 2006;80(22):11082-93. Epub 2006/09/08.

26. Nielsen SU, Bassendine MF, Burt AD, Martin C, Pumeechockchai W, Toms GL. Association between hepatitis C virus and very-low-density lipoprotein (VLDL)/LDL analyzed in iodixanol density gradients. Journal of virology. 2006;80(5):2418-28. Epub 2006/02/14.

27. Ko KW, Erickson B, Lehner R. Es-x/Ces1 prevents triacylglycerol accumulation in McArdle-RH7777 hepatocytes. Biochimica et biophysica acta. 2009;1791(12):1133-43. Epub 2009/08/05.

28. Lehner R, Kuksis A. Purification of an acyl-CoA hydrolase from rat intestinal microsomes. A candidate acyl-enzyme intermediate in glycerolipid acylation. The Journal of biological chemistry. 1993;268(33):24726-33. Epub 1993/11/25.

29. Lindenbach BD, Evans MJ, Syder AJ, Wolk B, Tellinghuisen TL, Liu CC, et al. Complete replication of hepatitis C virus in cell culture. Science. 2005;309(5734):623-6. Epub 2005/06/11.

30. Reed LJ, & Muench, H. . A simple method of estimating fifty percent endpoints. Am J Hygiene. 1938;27:493-7.

31. Lehner R, Cui Z, Vance DE. Subcellullar localization, developmental expression and characterization of a liver triacylglycerol hydrolase. The Biochemical journal. 1999;338 (Pt 3):761-8. Epub 1999/03/03.

32. Lo V, Erickson B, Thomason-Hughes M, Ko KW, Dolinsky VW, Nelson R, et al. Arylacetamide deacetylase attenuates fatty-acid-induced triacylglycerol accumulation in rat hepatoma cells. Journal of lipid research. 2010;51(2):368-77. Epub 2009/08/06.

33. Gibbons GF, Islam K, Pease RJ. Mobilisation of triacylglycerol stores. Biochimica et biophysica acta. 2000;1483(1):37-57. Epub 1999/12/22.

34. Wiggins D, Gibbons GF. The lipolysis/esterification cycle of hepatic triacylglycerol. Its role in the secretion of very-low-density lipoprotein and its response to hormones and sulphonylureas. The Biochemical journal. 1992;284 (Pt 2):457-62. Epub 1992/06/01.

35. Yang LY, Kuksis A, Myher JJ, Steiner G. Contribution of de novo fatty acid synthesis to very low density lipoprotein triacylglycerols: evidence from mass isotopomer distribution analysis of fatty acids synthesized from [2H6]ethanol. Journal of lipid research. 1996;37(2):262-74. Epub 1996/02/01.

Chapter 4: Conclusion

Hepatic steatosis is one of the common pathologies associated with chronic HCV infection (CHC) (1). Although presence of hepatic steatosis per se is a benign condition, it enhances the risk of non-alcoholic steatohepatitis (NASH), a disorder that intensifies the progression of fibrosis and may lead to premature cirrhosis. At least two types of steatosis have been defined in CHC; 1) the steatosis that occurs in genotype-3 which is positively correlated with HCV replication and is not related to metabolic factors (Viral Fat) and 2) steatosis in other genotypes that is related but not limited to metabolic factors (metabolic fat) (2). The etiology of viral fat in CHC is not perfectly known but in general, steatosis can develop when the production/absorption of lipids prevails over sequestration/secretion. Activation of de novo lipogenesis (in particular) has been widely studied as one of the possible mechanisms by which HCV induces steatosis (for review see the C. 3. 2. role of de novo fatty acid synthesis in HCV-related steatosis) but hepatocytes are the cells that have an extensive capability for the secretion of lipids (in particular TG) through VLDL pathway even in the presence of enhanced lipogenesis. Therefore it seems that in HCV-related steatosis, some aspects of VLDL secretory pathway might be impaired. Indeed, clinical data supports this hypothesis since steatosis is often presented in conjunction with hypobetalipoproteinemia (HBL) in CHC patients and both HBL and steatosis are resolved with anti-viral therapy (3-6).

Apart from being important for HCV assembly, lipid droplets (LDs) are the main source of TG that is assembled and secreted with VLDL. This is interesting because the VLDL secretory pathway has been suggested to be the means by which infectious HCV leaves the hepatocyte. As both LDs and VLDL are required for HCV production, we hypothesized that lipid droplets are sequestered from the normal role in VLDL assembly when cells are productively infected with HCV. Huh7.5/JFH-1 cell culture system was chosen to examine our hypothesis. Huh7.5 cells have a dependency on OA-induced expansion of cellular TG stores in order to secrete appreciable amount of TG in the absence of supplied fatty acids. Therefore in our experiments we primarily incubated the cells with OA to expand the cellular TG stores. Then OA was removed from cell culture and the expanded TG stores supplied VLDL secretion with the majority of its TG.

We found that after removal of OA, infected cell secreted significantly less TG and this correlated with an apparent accumulation of cellular TG stores. As VLDL is the only means by which TG is secreted from hepatocytes, the reduced TG secretion that was observed in infected cells was expected to be associated with a higher buoyant density of secreted VLDL and/or reduced number of VLDL particles produced (7). In fact, infected

cells produced VLDL particles with reduced TG content and secreted fewer VLDL particles. This study is the first to demonstrate impaired VLDL assembly/secretion in HCV infected cells.

We further investigated the VLDL secretory pathway by examining the expression and activity of MTP. MTP is believed to be involved in cotranslational lipidation of newly synthesized ApoB and has a key role in directing newly synthesized ApoB away from early proteasomal degradation (8-10). The impact of HCV on MTP expression and activity has been the focus of the study by several groups (11, 12). McPherson et. al. has shown that the level of MTP expression was reduced in the liver of HCV infected patients. In another study, HCV core transgenic mice had reduced MTP activity that was associated with accumulation of lipids in the liver (13). In our study, the protein abundance of MTP and its binding partner PDI was not altered in infected cells, but a modest reduction in MTP activity was observed which was not associated with enhanced proteasomal degradation of newly synthesized apoB. As MTP also functions in the smooth regions of the ER where lipoprotein particles containing ApoB have been shown to exhibit lower densities than those associated with the rough ER (10), reduced MTP activity may have contributed to the production ApoB-containing particles with reduced TG content.

Although the lipolysis of cellular TG stores represents a key regulatory step in the assembly and secretion of VLDL, very little is known about the lipases involved in this process. Reduced lipolysis of cellular TG stores for VLDL assembly by infected cells correlated with a significant reduction in the abundance of AADAC, one of just two ER-localized lipases that have been suggested to play a role in mobilization of cellular TG stores for VLDL assembly. The contribution of AADAC deficiency to impaired lipolysis of TG stores observed in infected cells was validated by two approaches. First, re-introduction of AADAC into HCV infected cells (that were AADAC deficient) improved the lipolytic mobilization of TG stores. Second, shRNA-mediated knockdown of endogenous AADAC in naïve cells led to defective lipolytic mobilization of TG stores and reduced secretion of VLDL-TG. The mechanism behind the observed AADAC deficiency in infected cells is not completely understood. We have established that the downregulation of AADAC in infected cells is temporally regulated, occurring in the more persistently infected cells present during the early peak of viral infection. AADAC deficiency was also observed in Huh7 cells bearing a stable HCV replicon based on the nonstructural HCV proteins. While this suggests that the nonstructural HCV proteins are sufficient for the downregulation of AADAC, it is not known which of the nonstructural proteins is involved or if on-going replication of the viral genome is responsible AADAC deficiency. In either

case, the absence of AADAC from the replicon cells is a strong indication that AADAC deficiency occurs after the initial translation of the viral genome has occurred.

At least one other group has reported HCV related impaired mobilization of TG stores (14). Harris et al. have shown that localization of HCV core protein to LDs in Huh7 cells expressing HCV core caused accumulation of cellular TG by inhibiting lipolysis and reducing turnover of TG in LDs. It was suggested that the attachment of the core protein to LDs sequestered TG from lipase-mediated hydrolysis. Our observation that AADAC expression restored TG lipolysis in infected cells would argue against sequestration of cellular TG stores by attachment of core protein to the surface of LDs.

Our study also revealed a role for AADAC in the replication cycle of HCV. Infection of AADAC knockdown cells resulted in a significant reduction in HCV production, as cellular and secreted HCV RNA and HCV infectivity titer of media were reduced in these cells. Further studies are required to determine which aspect of the HCV lifecycle is impaired by AADAC-deficiency. Given that AADAC is important for HCV production it was difficult to reconcile AADAC deficiency in HCV infected cells. However the AADAC deficiency was only observed during the early peak of HCV infection when >95% of cells were infected; AADAC deficiency was not observed at the earlier time points during the course of acute infection. It has been shown that during the early peak of HCV infection, variable cytopathic effects of HCV occur. This period is also characterized by fluctuating levels of viral RNA and during this period cells become more resistant to HCV infection (15). Therefore we suggested a model in which endogenous AADAC increases the efficiency of HCV production in early stages of HCV infection possibly by coupling early steps of replication/assembly events that is dependent on LD with maturation events that might be dependent on the VLDL secretory pathway through enhancing LD turnover. The AADAC deficiency, which occurs later in more persistently infected cells, might be related to the cellular reprogramming required for achieving viral resistance and therefore cellular survival. In addition to reduced virion production, the cellular consequences of AADAC deficiency included reduced mobilization of cellular TG stores and impaired VLDL production. These are established causes for the development of hepatic steatosis.

Dr. Lehner's lab has performed numerous experiments that demonstrate a role for TGH in the lipolysis of cellular TG stores for VLDL assembly. Unlike AADAC, TGH was absent from Huh7.5 cells altogether. The expression of TGH in Huh7 cells containing a HCV replicon has been described (16). The authors indicated that the presence of TGH in these cells represented an anomaly since similar replicon cellular clones did not express TGH. We did not observe any measurable TGH protein in HCV infected cells (or replicon

cells). Similar to the reports coming from Dr. Lehner's lab (17-21), the introduction of TGH to Huh7.5 cells increased lipolytic mobilization of TG from preformed lipid stores and TG secretion. Contrary to our expectations the introduction of TGH to Huh7.5 cells was not able to compensate for the reduced mobilization of preformed lipid stores that was related to AADAC deficiency in infected cells: During the early peak of infection, TGH-EGFP cells still displayed AADAC deficiency, still mobilized less TG from preformed cellular TG stores, and still secreted VLDL with reduced TG content. When HCV infection was established in TGH expressing cells, there was a modest increase in viral RNA secretion but these cultures still produced similar levels of infectious virions as wild-type cells.

In summary, these studies represent several novel findings. These include: (i) the lipolytic mobilization of cellular TG stores is impaired in hepatoma cells during HCV infection; (ii) infected hepatoma cells secrete fewer VLDL particles; (iii) infected cells secrete VLDL with reduced TG content; (iv) infected cells become AADAC deficient; (v) endogenous AADAC is expressed in Huh7.5 cells and has a role in the lipolysis of cellular TG stores and in the assembly of VLDL with more lipid content; (vi) AADAC deficiency is partially responsible for defective mobilization of cellular TG stores and VLDL assembly in infected cells; (vii) AADAC is important for the HCV lifecycle; and (viii) the ectopic expression of TGH is not sufficient to compensate for AADAC deficiency in infected cells and TGH cannot substitute for AADAC deficiency observed in infected cells.

Overall, these studies identified AADAC as a novel host factor important in the HCV lifecycle. The identification of AADAC provides an attractive potential new target for treating HCV infection.

Future Direction

The downregulation of AADAC in HCV infected cells during early peak of infection should be confirmed in an in vivo model. SCID/uPA mice model of HCV infection is a valuable animal model for this purpose(22). Also human liver biopsy from HCV infected patients can provide an alternative source for confirming our results. One of the difficulties of these in vivo models is that only small proportion of liver is infected by HCV. This can partially be overcome by immunohistochemistry approach or laser capture micro dissection of the infected area. In addition, the mechanism of this downregulation should be explored more. We showed that during early peak of infection, AADAC mRNA is downregulated. Therefore a transcriptional or a posttranscriptional mechanism is responsible for this downregulation. Therefore, there would be some benefit to examining AADAC mRNA stability during the course of HCV infection. In addition, transcriptional

studies can be performed with the 5'-proximal promoter of AADAC using a reporter system. Identification of cis and trans elements that are involved in regulating the AADAC promoter can be examined by way of ChIP (chromatin-immunopricipitation) assay and/or EMSA (electrophoretic mobility shift assay) and DNase foot-printing. These methods have been used for characterization of the human TGH promoter (23). Christopher Hao Pu in the Kneteman Lab is currently pursuing these studies.

We showed that AADAC is required for HCV production, but the mechanism remains unsolved. Infecting wild type and AADAC knockdown cells with HCVpp can confirm if the AADAC is required for HCV entry. By introducing a subgenomic replicon to AADAC knockdown cells we can investigate if AADAC is required for HCV replication. In addition, infectivity of HCV particles obtained from cells and media from AADAC knockdown and wild-type Huh7.5 cells should provide insight as to whether or not AADAC plays a role in HCV assembly and/or secretion.

While we have demonstrated that AADAC is also knocked down in stable replicon cells expressing NS3-NS5, it is not clear if any one of these viral proteins is sufficient to induce AADAC downregulation or if AADAC downregulation is instead an indirect consequence of these proteins or viral RNA replication. Expression studies with individual viral proteins can help to demonstrate if AADAC downregulation is a direct or indirect consequence of expression of viral proteins. It is also of interest to determine if infection with another unrelated virus, adenovirus for example, results in AADAC downregulation. This will help to determine if AADAC downregulation is specific to HCV infection.

Finally, we have shown that the downregulation of AADAC contributes to the reduced VLDL-TG secretion that was observed with infected cells. The introduction of TGH to these cells did not resolve this issue, despite TGH-dependent lipolysis of cellular TG stores and TGH-dependent VLDL-TG secretion. Importantly, factors other than AADAC and TGH appear to contribute to the unusual ApoB density profiles observed with infected cells. Given that ApoE is a host protein shown to be an integral component of infectious virions(24), it is tempting to speculate that acquisition of ApoE by HCV is responsible for the unusual ApoB density profile obtained from infected cells. The observation that ApoE deficiency leads to the production of poorly lipidated VLDL(25) supports this hypothesis. Below is a model derived from these observations and the hypothetical involvement of ApoE (Figure 1).

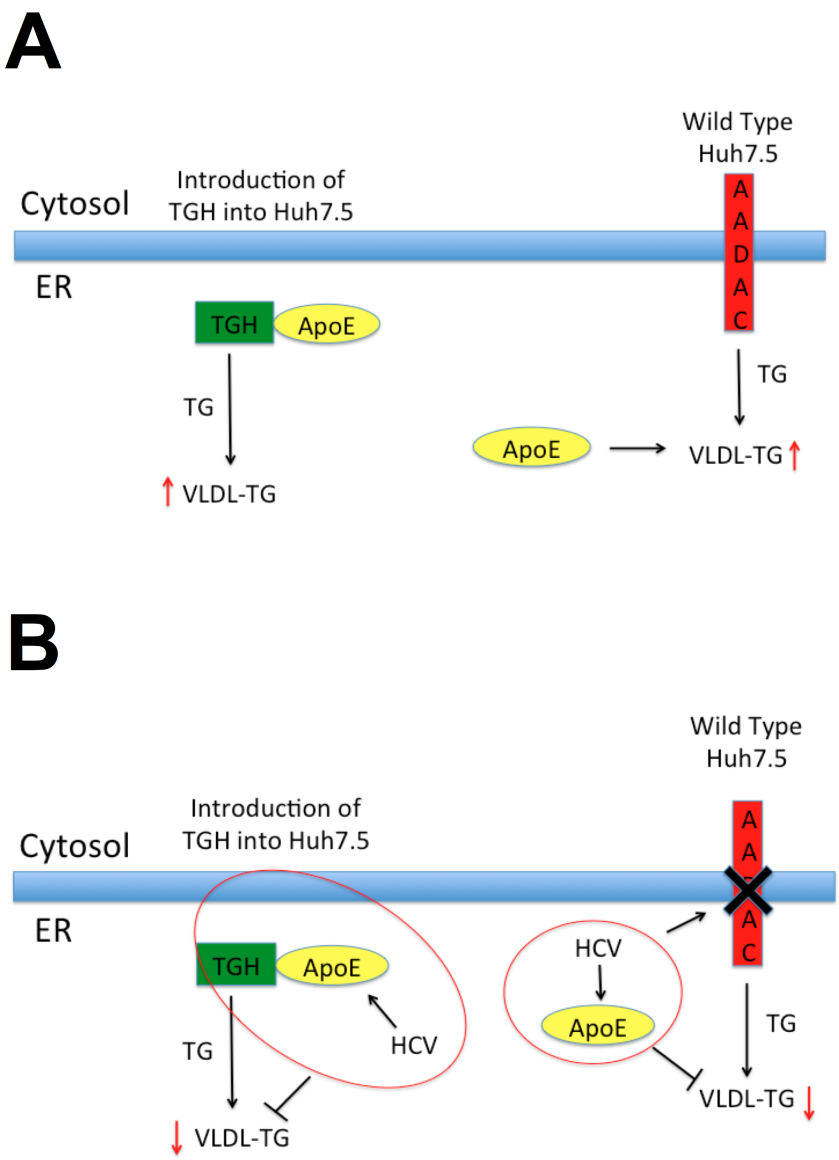

Figure 1. Hypothetical model for HCV-dependent modulation of VLDL assembly (with permission from Dr. Donna Douglas).

References

1. Asselah T, Rubbia-Brandt L, Marcellin P, Negro F. Steatosis in chronic hepatitis C: why does it really matter? Gut. 2006;55(1):123-30. Epub 2005/12/14.

2. Rubbia-Brandt L, Quadri R, Abid K, Giostra E, Male PJ, Mentha G, et al. Hepatocyte steatosis is a cytopathic effect of hepatitis C virus genotype 3. J Hepatol. 2000;33(1):106-15. Epub 2000/07/25.

3. Siagris D, Christofidou M, Theocharis GJ, Pagoni N, Papadimitriou C, Lekkou A, et al. Serum lipid pattern in chronic hepatitis C: histological and virological correlations. J Viral Hepat. 2006;13(1):56-61. Epub 2005/12/21.

4. Serfaty L, Andreani T, Giral P, Carbonell N, Chazouilleres O, Poupon R. Hepatitis C virus induced hypobetalipoproteinemia: a possible mechanism for steatosis in chronic hepatitis C. J Hepatol. 2001;34(3):428-34. Epub 2001/04/27.

5. Poynard T, Ratziu V, McHutchison J, Manns M, Goodman Z, Zeuzem S, et al. Effect of treatment with peginterferon or interferon alfa-2b and ribavirin on steatosis in patients infected with hepatitis C. Hepatology. 2003;38(1):75-85. Epub 2003/06/28.

6. Hofer H, Bankl HC, Wrba F, Steindl-Munda P, Peck-Radosavljevic M, Osterreicher C, et al. Hepatocellular fat accumulation and low serum cholesterol in patients infected with HCV-3a. Am J Gastroenterol. 2002;97(11):2880-5. Epub 2002/11/12.

7. Meex SJ, Andreo U, Sparks JD, Fisher EA. Huh-7 or HepG2 cells: which is the better model for studying human apolipoprotein-B100 assembly and secretion? Journal of lipid research. 2011;52(1):152-8. Epub 2010/10/20.

8. Benoist F, Nicodeme E, Grand-Perret T. Microsomal triacylglycerol transfer protein prevents presecretory degradation of apolipoprotein B-100. A dithiothreitol-sensitive protease is involved. Eur J Biochem. 1996;240(3):713-20. Epub 1996/09/15.

9. Benoist F, Grand-Perret T. Co-translational degradation of apolipoprotein B100 by the proteasome is prevented by microsomal triglyceride transfer protein. Synchronized translation studies on HepG2 cells treated with an inhibitor of microsomal triglyceride transfer protein. The Journal of biological chemistry. 1997;272(33):20435-42. Epub 1997/08/15.

10. Fisher EA, Ginsberg HN. Complexity in the secretory pathway: the assembly and secretion of apolipoprotein B-containing lipoproteins. The Journal of biological chemistry. 2002;277(20):17377-80.

11. McPherson S, Jonsson JR, Barrie HD, O'Rourke P, Clouston AD, Powell EE. Investigation of the role of SREBP-1c in the pathogenesis of HCV-related steatosis. J Hepatol. 2008;49(6):1046-54. Epub 2008/08/30.

12. Mirandola S, Realdon S, Iqbal J, Gerotto M, Dal Pero F, Bortoletto G, et al. Liver microsomal triglyceride transfer protein is involved in hepatitis C liver steatosis. Gastroenterology. 2006;130(6):1661-9. Epub 2006/05/16.

13. Perlemuter G, Sabile A, Letteron P, Vona G, Topilco A, Chretien Y, et al. Hepatitis C virus core protein inhibits microsomal triglyceride transfer protein activity and very low density lipoprotein secretion: a model of viral-related steatosis. FASEB J. 2002;16(2):185-94. Epub 2002/01/31.

14. Harris C, Herker E, Farese RV, Jr., Ott M. Hepatitis C virus core protein decreases lipid droplet turnover: a mechanism for core-induced steatosis. The Journal of biological chemistry. 2011;286(49):42615-25. Epub 2011/10/11.

15. Zhong J, Gastaminza P, Chung J, Stamataki Z, Isogawa M, Cheng G, et al. Persistent hepatitis C virus infection in vitro: coevolution of virus and host. Journal of virology. 2006;80(22):11082-93. Epub 2006/09/08.

16. Blais DR, Lyn RK, Joyce MA, Rouleau Y, Steenbergen R, Barsby N, et al. Activity-based protein profiling identifies a host enzyme, carboxylesterase 1, which is differentially active during hepatitis C virus replication. The Journal of biological chemistry. 2010;285(33):25602-12. Epub 2010/06/10.

17. Lehner R, Vance DE. Cloning and expression of a cDNA encoding a hepatic microsomal lipase that mobilizes stored triacylglycerol. The Biochemical journal. 1999;343 Pt 1:1-10. Epub 1999/09/24.

18. Wei E, Ben Ali Y, Lyon J, Wang H, Nelson R, Dolinsky VW, et al. Loss of TGH/Ces3 in mice decreases blood lipids, improves glucose tolerance, and increases energy expenditure. Cell Metab. 2010;11(3):183-93. Epub 2010/03/04.

19. Wei E, Alam M, Sun F, Agellon LB, Vance DE, Lehner R. Apolipoprotein B and triacylglycerol secretion in human triacylglycerol hydrolase transgenic mice. Journal of lipid research. 2007;48(12):2597-606. Epub 2007/09/20.

20. Wang H, Wei E, Quiroga AD, Sun X, Touret N, Lehner R. Altered lipid droplet dynamics in hepatocytes lacking triacylglycerol hydrolase expression. Mol Biol Cell. 2010;21(12):1991-2000. Epub 2010/04/23.

21. Gilham D, Ho S, Rasouli M, Martres P, Vance DE, Lehner R. Inhibitors of hepatic microsomal triacylglycerol hydrolase decrease very low density lipoprotein secretion. FASEB J. 2003;17(12):1685-7. Epub 2003/09/06.

22. Mercer DF, Schiller DE, Elliott JF, Douglas DN, Hao C, Rinfret A, et al. Hepatitis C virus replication in mice with chimeric human livers. Nat Med. 2001;7(8):927-33. Epub 2001/08/02.

23. Douglas DN, Dolinsky VW, Lehner R, Vance DE. A role for Sp1 in the transcriptional regulation of hepatic triacylglycerol hydrolase in the mouse. The Journal of biological chemistry. 2001;276(27):25621-30. Epub 2001/05/05.

24. Merz A, Long G, Hiet MS, Brugger B, Chlanda P, Andre P, et al. Biochemical and morphological properties of hepatitis C virus particles and determination of their lipidome. The Journal of biological chemistry. 2011;286(4):3018-32. Epub 2010/11/09.

25. Kuipers F, van Ree JM, Hofker MH, Wolters H, In't Veld G, Havinga R, et al. Altered lipid metabolism in apolipoprotein E-deficient mice does not affect cholesterol balance across the liver. Hepatology. 1996;24(1):241-7. Epub 1996/07/01.

Appendix

Cells and Cell Culture

Huh7.5 cells, a mutant line of Huh7 that support HCV replication in high efficiency (1), were generously provided by Dr. Charles Rice (Rockefeller University, NY). HepG2 cells were obtained from ATCC (Manassas, VA). Human hepatocytes were isolated in house from normal tissue peripheral to resected human liver using collagenase-based perfusion with Liberase HI solution and were purified on percoll density gradient (2). All the Huh 7.5 cells or derivatives (JFH-1 infected, over expressed TGH-EGFP, AADAC knock down and over expressed AADAC) and HepG2 were maintained in Dulbecco's modified Eagle's medium (DMEM) containing 10% fetal bovine serum (FBS), 100 U/ml penicillin and 100 μg/ml streptomycin at 37ºC in humidified air containing 5% CO_2, except where otherwise indicated. Cells were passaged at 70-80% confluency. Human hepatocytes were cultured on prepared collagen dish and were maintained similar to Huh7.5 cells. All the experiments were performed by human hepatocytes occurred within 24h after isolation.

Preparation of JFH-1 RNA

JFH1 RNA was prepared as it was discussed before (3). In the first step, plasmid JFH-1 (pJFH1) was linearized by *XbaI* restriction endonuclease. In the second step, the linearized pJFH1 was extracted form linearization reaction. In the third step, the single stranded sticky ends of linearized pJFH1 that were produced by *XbaI* were removed by Mung bean nuclease. In the fourth reaction pJFH1 was purified and extracted from Mung bean nuclease reaction. In the last step, JFH-1 RNA was prepared by in vitro transcription and was extracted from the reaction.

Linearization of pJFH1: pJFH1 was a kind gift from Dr. Takaji Wakita (National Institute of Infectious Disease, Tokyo, Japan). The pJFH1 (16 μg) was digested at 37°C fro 2h in the following reaction:

Reagent	Amount
pJFH1	16 μg
XbaI (100 U/μL)	1 μl (100 U)
10 × REACT® Buffer	5 μl
Nuclease Free water	up to 50 μl
Total Volume	50 μl

Table A. 1. Reagents required for linearization of pJFH1

The completion of digestion was tested by separation of 0.5 μl of digested samples, along with 1Kb Plus DNA Ladder, by electrophoresis through a 1% agarose gel (w/vol, in Tris-Acetate-EDTA Buffer, 40mM Tris-acetate, 1mM EDTA, pH=8.3). A single band with an approximate size of 13 Kb should be seen. Presence of a doublet b indicates incomplete digestion and the reaction should be continued for a longer period (overnight).

Extraction of Linearized pJFH1 by Phenol-Chloroform-Isoamyl Alcohol: 50 μl of TRIS-EDTA (TE buffer, 10mM Tris, 1mM EDTA, pH=8.0) was added to the above reaction and pJFH1 was extracted using equal volume (100μl) of phenol-chloroform-isoamyl alcohol (25:24:1, v/v/v) mixture. The mixture was shaken and centrifuged at 12,000g at room temperature for 15 minutes and aqueous phase was transferred into a new tube and mixed with 100 μl of chloroform. The mixture again was shaken and centrifuged for 5 minutes at 12,000g at room temperature and aqueous phase was separated and was mixed with1/10 volume of 3 M sodium acetate, 2.5 volume of 100% ethanol and 1/100 volume of glycogen (optional). The mixture was stored overnight at -20°C. Then it was centrifuged for 20 minutes at 12,000g at 4°C. The formed pellet was washed with 500 μl of 70% ethanol (prepared by nuclease free water) and centrifuged for 15 minutes at 12,000g at 4°C. The formed pellet was dried and re-suspended in 43 μl of RNase free water.

Removal of Sticky Ends by Mung Bean Nuclease: Linearized pJFH1was then treated with Mung bean nuclease to remove the sticky ends. For this purpose, 43 μl of pJFH1 was mixed with 2 μl (20 U) of Mung bean nuclease and 5 μl of 10 × Mung bean nuclease buffer and was incubated for 30 minutes in a heat block at 30°C. Mixture was then treated with 40 μg of proteinase K, 10 μl of 10% SDS in a 200 μl reaction at 50°C for 1h, to deactivate Mung Bean Nuclease.

Extraction of pJFH1 from Mung Bean Nuclease Reaction: The pJFH1 in the above reaction was extracted using equal volume of phenol-chloroform-isoamyl alcohol similar to previous extraction process and was re-suspended in 20 μl of nuclease free water. The size and complete digestion of pJFH1 was confirmed by electrophoresis thorough a 1% agarose gel as it was discussed above. After confirming the size and concentration of this plasmid it can be used as a template for generating JFH-1 RNA.

In Vitro Transcription Using T7-MEGAscript Kit: JFH1 RNA was generated using T7 MEGAscript kit as it is shown in table A. 2 and incubated for minimum of 3 hours at 37°C (alternatively it could be incubated overnight, if the RNA yield was low). At the end of reaction, 1 μl of DNase was added and the mixture incubated for 15 minutes to digest the

pJFH1 DNA template. The reaction was stopped by addition of 115 μl of nuclease free water and 15 μl of stop solution. 100 μl of water and RNA was added and JFH-1 RNA was purified with 750 μl of TRIzol LS (1:3 Vol/Vol).

Reagent	Amount
Linear pJFH1 template	2-4 μl (500 ng to 1 μg)
ATP Solution	2 μl
CTP Solution	2 μl
GTP Solution	2 μl
UTP Solution	2 μl
Reaction Buffer (10×)	2 μl
Enzyme Mix	2 μl
Nuclease Free Water	4-6 μl
Total Volume	20 μl

Table A. 2. Reagents required for in vitro transcription of JFH-1.

In summary, for each 250μl of mixture, 750 μl TRIzol LS and 200μl of chloroform (per 750 μl of TRIzol LS) were added and sample was shaken and incubated at room temperature for 10 minutes following by centrifugation at 12,000g for 15 minutes at 4°C. The top aqueous layer was transferred to a new tube and 500 μl 100% isopropyl alcohol was added and the sample was incubated overnight at -20°C. Then the mixture was centrifuged at 12,000g for 10 minutes at 4°C and the formed pellet was washed with 1ml (per 750 μl TRIzol LS) of 75% ethanol (prepared by nuclease free water). The mixture then was centrifuged at 7500g for 5 minutes at 4°C and the pellet was dried and re-suspended in 50 μl of nuclease free water. The quality and size of RNA was check by electrophoresis through 1% agarose gel.

Preparation of JFH-1 Infected Cells

HCV infection was generated either by electroporation of JFH-1 into naïve cells or inoculation of cells with JFH-1 virus obtained from cell culture generated by electroporation.

For electroporation, 7 million naive cells were washed with OptiMEM-I reduced-serum medium. Ten μg of JFH1 RNA was mixed with 400 μl of cytomix buffer (120mM KCl, 2mM EGTA, 25 mM HEPES, 5mM $MgCl_2$, 0.15 mM $CaCl_2$, 10 mM KH_2PO_4/K_2HPO_4, 2mM ATP and 5mM GSH, pH=7.6) and was transferred to a 0.4-cm gap width electroporation cuvette. The cells were electroporated with a Gene Pulser II apparatus in conditions of 260 V and 950 μF. Then cells were transferred to two 10 cm dishes and cultured.

For inoculation, cells were inoculated with HCV inoculum (10^4 ffu/ml) at MOI=0.01 or 0.5 depending on the experiment condition for 8h and then media was replaced with DMEM+10% FBS. The proportion of infected cells was determined by core immunofluorescence microscopy (see below). For each experiment, a naïve arm was prepared completely similar to infected arm with exception of mock electroporation or mock inoculation.

Indirect Immunofluorescence Detection of HCV Core Protein

Cells that were grown on coverslips were fixed in pre chilled acetone-methanol (1:1 v/v) for 10-20 minutes at -20°C and were blocked by immunofluorescence (IF) buffer (PBS, 1% BSA, 2.5 mM EDTA) for 1 hour at room temperature or alternatively at 4°C overnight. Cells were then incubated for 1 hour with mouse anti-core antibody (C7-50) diluted 1:300 (v/v) in IF buffer at room temperature, washed three times with PBS and were incubated 1h with appropriate fluorescent-conjugated anti mouse IgG at 1:1000 (vol/vol) dilution at room temperature. Cells then were washed twice with PBS and once with ddH_2O and the coverslip was mounted on glass slide using 10-15μl Perma-Fluor mounting solution contains DAPI (1μg/ml).

Dual Staining of Cells for Immunofluorescence Detection of Core and AADAC

JFH-1 infected Huh7.5 cells expressing AADAC, grown on coverslip, were fixed in pre chilled acetone-methanol (1:1, v/v) for 10-20 minutes at -20°C and were blocked by IF buffer (PBS + 1% BSA + 2.5 mM EDTA) for 1h at room temperature or alternatively at 4°C overnight. Cells were then incubated for 1h with mouse anti-core antibody diluted 1:300 (v/v) and 1:1000 goat anti-human AADAC in IF buffer at room temperature. Cells then were washed three times with PBS and were incubated 1h with Alexa Fluor 488-conjugated anti-mouse IgG and Alexa Fluor 594-conjugated anti-goat IgG at 1:1000 (v/v) dilution at room temperature. Coverslip was washed twice with PBS and once with ddH_2O and were mounted on glass slide using 10-15 μl Perma-Fluor mounting solution contains DAPI (1μg/ml).

Dual Staining of Cells for Immunofluorescence Detection of HCV Core and Lipid Droplets

For detection of lipid droplets, Oil Red O (ORO) staining was used. For this purpose, ORO stock solution was prepared by adding 500 mg of ORO to 100 ml of 100% isopropyl alcohol (0.5% ORO in 100% isopropyl alcohol). This solution was filtered through two layers of Whatman paper. For process of staining, ORO working solution (0.2% ORO in 40% Isopropyl Alcohol) was freshly prepared by mixing 20 ml of ORO stock solution with 30 ml of ddH_2O.

The dual staining was performed. In summary cells were fixed at 4% paraformaldehyde solution for 30 minutes at 4°C. Cells then were washed once with PBS and was permeabilized for 15 minutes at room temperature in 0.05% TX-100 in PBS, (vol/vol). Cells were then washed and blocked for 1 h in IF buffer (PBS + 1% BSA + 2.5mM EDTA) and then were incubated for 1h at room temperature with mouse anti-HCV core antibody 1:300 (v/v) in IF buffer. Cells were washed and incubated in 1 h with Alexa-Fluor 488 anti-mouse IgG 1:1000 (v/v) in immunofluorescent buffer at room temperature. Cells then were washed three times with PBS and were stained with 1ml of ORO working solution for 5 minutes and were washed extensively with ddH_2O until all the residues were cleared. Coverslip then were mounted using 10-15 μl Perma-Fluor mounting solution contains DAPI (1μg/ml).

Mass Secretion of TG from Preformed Cellular Storage Pools

Unless otherwise stated, 1.5 million cells (60% confluency) were incubated in 60 mm dishes for a total of 14h in 2 ml of serum-free DMEM supplemented with 0.375 mM oleic acid (OA) complexed with 0.5% (w/v) fatty acid-free BSA (OA-BSA) to stimulate TG synthesis and increase cellular TG stores. The preparation of an OA-BSA stock solution will be discussed separately. For the last 2h of this incubation, the media was replenished with fresh DMEM supplemented with OA-BSA. At the end of this incubation period (t = 0h), cellular and secreted lipids (present in media) were extracted from one half of the culture dishes for analysis of TG mass (see below). TG levels at this time represents the cellular TG levels before removal of OA and amount that is secreted represents the TG secreted in the presence of OA for two hours. With the remaining half of the culture dishes, cells were washed in PBS + 0.5% fatty acid free BSA (to remove the extra oleate) and incubated for up to 8h with DMEM (without the OA supplement) to allow for the secretion of TG from preformed cellular storage pools. In some cases, this incubation

was performed in the presence of a competitive inhibitor of acyl-CoA ligase, triacsin C (6 μM final), a lipase inhibitor, E600 (100 μM) in DMSO, a specific inhibitor of TGH, GR148672X (10μM). The concentration of DMSO was 0.1% (v/v) final. The media was collected and replenished every two hours. At the end of 8h cells were washed with PBS and TG cellular lipids were extracted (see below).

Extraction of lipids*:* Briefly, cells were scraped with cell scraper in 2 ml of PBS and were sonicated 3 times at power set at 4 for 5 seconds on ice. Lipid from cell lysate and media were extracted using 4 ml of chloroform/methanol (2:1, v/v). This mixture was vortexed for 20 seconds and then centrifuged for 10 minutes at 1300 g. The lower layer contains lipids was transferred to a new glass tube and dried under nitrogen in heat block at 37°C. The pellet formed at the bottom of the glass tube was resuspended in 20 μl of 100% ethanol for determination of TG content enzymatically using a Serum Triacylglycerol Determination Kit.

Measurement of TG: For measurement of TG, 160 μl of Glycerol reagent (provided by kit) was added to each tube and then was gently mixed. The mixture was incubated for 5 minutes at room temperature. A series of tube contains known amount of glycerol in 20 μl of 100% ethanol was used to generate standard curve. In addition, blank tubes contain the same 100% EtOH used for re-suspending the cell were also prepared. After 5 minutes 160 μl of the samples were plated in a 96 well plate and the plate was analyzed by spectrophotometer at 540 nm. The absorbance represents the amount of the free glycerol. Then 40 μl of TG reagent (provided by kit) contains lipoprotein lipase (LPL) was added to each well and the plate was incubated at room temperature for 30 minutes. The plate was analyzed at 540 nm. The absorbance represents the amount of free glycerol from previous reaction and the amount of the glycerol that was released for each molecule of TG by LPL. The amount of TG was calculated using the standard curve by subtracting the glycerol at final reading from glycerol at initial reading. Cellular and secreted TG in dish was normalized to cellular protein in dish.

Incorporation of OA into TG and PL

Cells were incubated for 4h with OA-BSA containing 2.5 μCi/ml of [9,10(n)-^{3}H]OA as radiolabeled tracer (pulse period) (4). Media was aspirated and cells were washed three times with PBS containing 0.5% fatty acid free BSA. Half of the cell cultures were harvested for lipid analysis (pulse). The remaining cell cultures were incubated for 4h with DMEM (without OA) before harvesting the cells for lipid analysis (chase). For lipid analysis, all cells were washed with ice-cold PBS, harvested in 2ml of the same buffer, and disrupted by sonication. Cellular lipids were extracted with chloroform/methanol (2:1,

v/v) as it was discussed above in the presence of nonradioactive lipid carriers (phoshatidylcholine [PC], and trioleoylglycerol). The chloroform phase containing lipids was dried under nitrogen, redissolved in 150 μl of chloroform, and applied to silica gel H thin-layer chromatography plates. The plates were developed in heptane/isopropyl ether/acetic acid (60:40:4, v/v/v) to separate neutral lipids from phospholipids. The lipid classes were visualized by exposure to iodine vapor, the bands were scraped, and the associated radioactivity was determined by scintillation counting. The data were normalized to cellular protein.

Analysis of LD morphology

OA was supplied to naïve and infected cells for 14h to expand cellular TG stores (as it was discussed before), and then cells were cultured up to 72 h in DMEM containing 6μM Triacsin C. LDs were observed by fluorescence microscopy after ORO staining. A total of 100 images (25 random cells per experiment, for 4 experiments) were captured for analysis of average area of individual LDs, number of LDs per cell, and total area of LDs per cell using Meta-Morph, version 7.5 software (Molecular Devices).

Determination of Levels of Newly Synthesized ApoB

The methods used to quantify the levels of newly synthesized (labeled) ApoB in cellular lysates and media were described previously(5). In brief, 1.5 million cells in 60 mm dish were incubated for 14h in serum-free DMEM supplemented with OA-BSA to increase intracellular TG stores, then in 2 ml of methionine/cysteine-free DMEM supplemented with 50 μCi/ml [^{35}S]-labeled methionine and cysteine ± 25 μM MG132 (proteasome inhibitor) for 2h. Cells were washed and scraped in 2ml of 1 × immunoprecipitation (IP) buffer (150 mM NaCl, 50 mM Tris/HCL, pH=7.4, 5 mM EDTA, 0.5% v/v Triton X-100, 0.1% w/v SDS) containing 1mM benzamidine and were homogenized by sonication, and protein concentration was determined. Collected media were briefly centrifuged to remove cellular debris and adjusted with 10 × IP buffer containing 1mM final concentration of benzamidine. Then 10 μl of goat anti-human ApoB IgG was added to 1 ml of cell sonicates or culture media and the mixture was incubated on a rotating rack for 12h at 4°C, after which 25 μl of protein A-Sepharose was added and the mixture was incubated on a rotating rack for additional 3h at 4°C. The beads were pelleted by brief centrifugation and were washed three times with excess 1 × IP buffer. Denaturing electrophoresis sample buffer was added, samples were boiled and underwent electrophoresis using 5% polyacrylamide gels. Gels were dried and exposed to Kodak BioMax MR Film for 4 weeks at -80ºC. Bands corresponding to labeled ApoB were quantified by densitometry using Bio-Rad Quantity One software.

Determination of Levels of Mass ApoB

1.5 million cells in 60 mm dish were incubated for 14h in 2 ml of serum-free DMEM supplemented with OA-BSA to increase intracellular TG stores. Media was removed and cells were washed once with PBS. Then 2 ml of DMEM was added and cells were incubated for 8h. At the end of this period media was collected and cells were washed and scraped in 2ml of PBS and were homogenized by sonication and protein concentration was determined. Then 100 μl of media or cells were subjected for detection of ApoB using Human ApoB ELISA Kit.

In brief high protein binding easy wash, 96 well plate was coated with 100 μl/well of monoclonal LDL antibody (provided by kit, mAb LDL20/17) with the concentration of 2μg/ml (dilution of 2:1000 v/v in PBS) and was incubated overnight at 4°C. The next day plate was washed twice with 200 μl/well of PBS and the plate was blocked by 200 μl/well of blocking buffer (PBS + 0.05% Tween 20 + 0.1% BSA) for 1h at room temperature. The plate then was washed once with 200 μl/well of washing buffer (PBS, 0.05% Tween 20) and 100-200μl of samples (cell lysates or media) was added to each well. A series of standard with known concentration of apoB (provided by kit) were also included. The plate was incubated at room temperature for 1h and then was washed 5 times with 200 μl/well of washing buffer and were incubated for 1h with 100 μl/well of monoclonal LDL antibody conjugated to biotin (1:1000, v/v in blocking buffer, provided by kit). After this period of incubation, plate was washed 5 times with 200 μl/well of washing buffer and incubated with 100 μl/well of Streptavidin-HRP (1:000, v/v in blocking buffer) for 1h followed by washing 5 times with 200 μl/well of washing buffer. Developing solution was prepared fresh by mixing 3.6 ml of 0.1M citric acid with 3.9 ml of 0.2M Na_2PO_4 in 7.5 ml of distilled water. pH was adjusted to 5.0 by using 1M citric acid and then 1 tablet of TMBD was added to solution. Solution was mixed, filtered by 0.22 micron filter and then 6 μl of 30% Hydrogen Peroxide was added to solution. 100 μl/well of the solution was added and plate was incubated at room temperature at dark for 15 minutes, and then reaction was stopped by adding 100μl/well of 1M sulfuric acid. Absorbance was measured at 450 nm and measured apoB was normalized to mg cell protein.

Density Profile of ApoB/HCV

Iodixanol gradients were prepared as described by Nielsen et al. (6). Isopycnic linear density gradients were prepared from 6% (w/v) (1.7 ml of 60% [w/v] iodixanol, 0.34 ml of 0.5 M Tris-HCl, pH 8.0, 0.34 ml of 0.1 M EDTA, pH 8.0, and 14.6 ml 0.25 M sucrose) and 56.4% (w/v) (16.0 ml of 60% iodixanol, 0.34 ml of 0.5M Tris-HCl, pH 8.0, 0.34 ml of 0.1 M

EDTA, pH 8.0, and 0.34 ml 0.25 M sucrose) iodixanol solutions in thin wall centrifuge tubes (14.89 mm, Beckman) using a two-chamber gradient maker (Jule Inc 17 ml gradient fomer). 5.2 ml of 6% solution was added to mixing chamber and 5.2 ml of 54.6% solution to storage chambers. Media samples (1 ml) were applied to the top of 6 to 56% iodixanol gradients and centrifuged for 10h in a Beckman Optima L100 XP ultracentrifuge at 41000 rpm and 4°C in an SW41 rotor. The gradient was harvested from the top and collected into 23 fractions (0.5 ml each) or 11 fractions (1 ml each). The density of each fraction was determined by measuring the weight of 200 ml. The ApoB concentration in each fraction was determined using Human ApoB/ApoE ELISA kit as it was discussed above. For HCV gradient density, Viral RNA was extracted from 30 μl of each fraction and subjected to qRT-PCR for detecting HCV titer.

Activity-Based Protein Profiling

Activity-based protein profiling based on the reaction of FP-biotin with the catalytic serine residue in lipases and serine-hydrolases was performed as described previously(7). Briefly, Cells were lysed in 20 mM Tris, pH 7.0, 150 mM NaCl, 1mM EDTA adjusted to 1.5 mM (0.07%) Triton X-100. Cellular lysates (30 μg protein) were incubated with 100 μM FP-biotin (added from a 10 mM stock solution in dimethyl sulfoxide) for 30 min at room temperature. In some cases lysate were incubated first for 30 min with 100μM of E600 or heat deactivated at 85°C for 10 minutes before addition of FP-biotin. Samples were then boiled in SDS-PAGE loading buffer and proteins were resolved on 10% polyacrylamide gels under denaturing conditions. The proteins were transferred to a nitrocellulose membrane and proteins bound to FP-biotin were detected by probing with avidin-HRP (1:15000, v/v) followed by enhanced chemiluminescence (ECL) detection with Amersham Hyperfilm^{TM} ECL.

Determination of Lipolytic Activity

Lipolytic activity in cellular and microsomal preparations was estimated using a well-established procedure that is based on the production of p-nitrophenol from p-nitrophenyl acetate or laurate. For p-nitrophenyl acetate procedure, 20 mM (200×) stock solution of p-nitrophenyl acetate was prepared in dichloromethane and was diluted to 100 μM in assay buffer (20 mM Tris, 150 mM NaCl, 0.01% TX-100, pH=8.0). One microgram of microsomes or 5 μg of cell lysate was added to a 96 well plate and then the volume was adjusted to 50 μl with assay buffer. A series of standards with known concentration of p-nitrophenol was prepared and subjected to the assay. Then 150 μl of diluted p-nitrophenyl acetate was added per well by multi channel pipet and the absorbance was measured at 405 nm every 5 minutes. The release of p-nitrophenol/min was calculated

and normalized to amount of protein that was subjected to the assay. The same procedure was used for p-nitrophenyl laurate but p-nitrophenyl laurate was diluted in an assay buffer contains 20μM Tris, 150 mM NaCl, 0.09% TX-100, pH=8.0.

MTP Activity Assay

MTP transfer activity was measured using the Roar MTP Activity Assay Kit according to the manufacturer's instructions and is based on MTP-mediated transfer of fluorescence between donor and acceptor particles. In brief, cells were sonicated in 200 µl of ice-cold homogenization buffer (10 mM Tris, 150mM NaCl, 1 mM EDTA, pH=7.4, 20 µg/ml leupeptin and 500µM PMSF). Cellular homogenate (100 µg protein) was combined with donor (5 µl) and acceptor (5 µl) vesicles in a total volume of 200 µl of assay buffer (provided by kit), then incubated at 37°C for 240 min. MTP activity was calculated by measuring fluorescence at the excitation wavelength of 465 nm and emission wavelength of 535 nm (Spectramax Gemini, Molecular Devices).

Immunoblot Analysis

Cellular and microsomal proteins were separated on SDS-PAGE, transferred to nitrocellulose membranes and blocked with PBS containing 0.1% Tween 20 (v/v) and 5% non-fat dry milk powder (w/v). Membranes were then incubated for 1h at room temperature with appropriate dilutions of primary antibodies (1:3000 of goat anti-human-MTP, 1:5000 mouse anti-human-PDI, 1:500 goat anti-human AADAC, 1:5000 rabbit anti-human TGH, 1:1000 mouse anti-core, 1:20000 mouse anti-NS5A, 1:15000 goat anti-GFP, or 1:10000 mouse anti-human actin) followed by 1:10000 appropriate secondary HRP-conjugated IgG antibodies. All immunoreactive bands were detected using Amersham ECL™ Western Blotting Detection Reagents with Amersham Hyperfilm™ ECL.

Quantitative RT-PCR of host mRNAs

Primer sequences were as follows:

Primer	Sequence
Fwd-hAADAC	5'-CAAAATATGGTGTGAACCCTGA-3'
Rev-hAADAC	5'-GAAGGGCAGGATAAATTAAAGA-3'
Fwd-hActin	5'-CCAACCGCGAGAAGATGA-3'
Rev-hActin	5'-TCCATCACGATGCCAGTG-3'

Table A. 3. List of primers used for quantitative RT-PCR of host mRNA.

Total RNA was isolated using Trizol LS reagent and reverse transcribed with a mixture of random hexamers and oligo(dT) using qScript cDNA SuperMix according to manufacturer's instructions. AADAC (primers hAADAC-Fwd/hAADAC-Rev) and beta-actin (primers hbetaActin-Fwd/hbetaActin-Rev) transcripts were detected by real-time PCR using a Qiagen RotorGene 3000 instrument. Reaction mixtures contained Platinum Quantitative PCR SuperMix-UDG with 400nM concentrations for each primer in a total volume of 20 ml. Following a 3 minute initial denaturation at 94°C, PCR amplification of AADAC proceeded for 40 PCR cycles of 95°C for 20 s, 56°C for 20 s then 72°C for 20 s. For beta-actin, samples were amplified for 35 cycles of 95°C for 20 s, 60°C for 20 s; 72°C for 20 s. Data analysis was performed with the Corbett Rotorgene software using the standard curves method. All AADAC values were normalized to beta-actin.

Titration of HCV growth curves

A recombinant HCV encoding for a secreted luciferase upon HCV replication (Bi-Gluc-J6/JFH) was kindly provided by Dr. Charles Rice (Rockefeller University, NY) and was used to monitor virus growth(8). Growth curves were set up in general by plating 8×10^3 cells per well in poly-L-lysine-coated 96-well plates 24h prior inoculation with 100 μl of a viral stock containing Bi-Gluc-J6/JFH at an MOI of 0.02. At time points, 6, 24, 48 and 72 hours post-infection, 10 μl supernatant was collected to measure the amount of secreted luciferase with the Renilla luciferase assay system. Briefly, 10 ml Renilla lysis buffer and 10 ml cell culture supernatant were mixed in a white polystyrene assay plate, followed by addition of 50 ml Renilla luciferase substrate to initiate the reaction. The resultant luminescence was measured with the Enspire 2300 Multilabel Reader (PerkinElmer).

Determination of HCV Infectivity Titer

Limiting dilution assays were used to quantify HCV infectivity between samples as median tissue culture infectious units per milliliter (TCID50/ml). The TCID50 is the dilution that infects 50% of replicate cell cultures and was determined essentially as described(9). Briefly, Huh 7.5 cells were seeded on poly-lysine coated 96 well plates (6×10^3 cells/well). At 24h post-seeding, cells were infected with 10 fold serially diluted cell culture supernatants (8 wells per dilution). Cell culture media was replaced with fresh media at 16h post-infection, then cells fixed in methanol at 72h post-infection. HCV infected cells were detected by immunostaining using anti-NS5A antibody (9E10) with HRP conjugated sheep anti-mouse IgG secondary antibody and subsequently visualized with a DAB substrate kit (DAKO). TCID50 was calculated, based on the NS5A positive wells, according to the method of Reed and Muench(10).

Generation of stable short hairpin RNA (shRNA)-expressing Huh7.5 cells

MISSION® Lentiviral Transduction Particles expressing shRNAs targeting human arylacetamide deacetylase (AADAC) and a non-targeting (NT) shRNA that does not target any known human transcripts (5'-CAACAAGATGAAGAGCACCAA-3') were used to generate stable shRNA-expressing Huh7.5 cells. The following sequences in AADAC were targeted: AADAC-1 (5′-GCCATGCTTTCCAGACAACAT-3′), AADAC-2 (5′-GCTCCCTGAGAGGTTTATAAA-3′), AADAC-3 (5′-GCCATGCTTTCCAGACAACAT-3′), AADAC-4 (5'-CGTATCAACCAAC TACAGATT-3'), and AADAC-5 (5'-CTGTGGGATTTCATTTCAATT-3'). Huh7.5 cells were transduced at a MOI of 5 with shRNA-expressing lentiviruses and Polybrene (8 μg/ml). After 48-h incubation with lentiviruses, fresh medium containing puromycin (10 μg/ml) was applied. After 3 weeks of drug selection, target protein knockdown was evaluated by immunoblot analysis. Stable knockdown cell lines were routinely maintained in medium containing puromycin (2 μg/ml).

References

1. Blight KJ, McKeating JA, Rice CM. Highly permissive cell lines for subgenomic and genomic hepatitis C virus RNA replication. Journal of virology. 2002;76(24):13001-14. Epub 2002/11/20.

2. Kawahara T, Toso C, Douglas DN, Nourbakhsh M, Lewis JT, Tyrrell DL, et al. Factors affecting hepatocyte isolation, engraftment, and replication in an in vivo model. Liver Transpl. 2010;16(8):974-82. Epub 2010/08/03.

3. Kato T, Date T, Murayama A, Morikawa K, Akazawa D, Wakita T. Cell culture and infection system for hepatitis C virus. Nat Protoc. 2006;1(5):2334-9. Epub 2007/04/05.

4. Lo V, Erickson B, Thomason-Hughes M, Ko KW, Dolinsky VW, Nelson R, et al. Arylacetamide deacetylase attenuates fatty-acid-induced triacylglycerol accumulation in rat hepatoma cells. Journal of lipid research. 2010;51(2):368-77. Epub 2009/08/06.

5. Gilham D, Ho S, Rasouli M, Martres P, Vance DE, Lehner R. Inhibitors of hepatic microsomal triacylglycerol hydrolase decrease very low density lipoprotein secretion. FASEB J. 2003;17(12):1685-7. Epub 2003/09/06.

6. Nielsen SU, Bassendine MF, Burt AD, Martin C, Pumeechockchai W, Toms GL. Association between hepatitis C virus and very-low-density lipoprotein (VLDL)/LDL analyzed in iodixanol density gradients. Journal of virology. 2006;80(5):2418-28. Epub 2006/02/14.

7. Ko KW, Erickson B, Lehner R. Es-x/Ces1 prevents triacylglycerol accumulation in McArdle-RH7777 hepatocytes. Biochimica et biophysica acta. 2009;1791(12):1133-43. Epub 2009/08/05.

8. Reyes-del Valle J, de la Fuente C, Turner MA, Springfeld C, Apte-Sengupta S, Frenzke ME, et al. Broadly neutralizing immune responses against hepatitis C virus induced by vectored measles viruses and a recombinant envelope protein booster. Journal of virology. 2012;86(21):11558-66. Epub 2012/08/17.

9. Lindenbach BD, Evans MJ, Syder AJ, Wolk B, Tellinghuisen TL, Liu CC, et al. Complete replication of hepatitis C virus in cell culture. Science. 2005;309(5734):623-6. Epub 2005/06/11.

10. Reed LJ, & Muench, H. . A simple method of estimating fifty percent endpoints. Am J Hygiene. 1938;27:493-7.